PALLADIUM-CATALYZED FUNCTIONALIZATION OF 4-ALKYLPYRIDINES: PYRIDLYIC DEHYDROGENATION & MECHANISTIC INVESTIGATION OF PYRIDYLIC ALLYLATION

NOUR WASFY

A THESIS SUBMITTED TO THE FACULTY OF GRADUATE STUDIES

IN PARTIAL FULFILLMENT OF THE REQUIREMENTS

FOR THE DEGREE OF MASTER OF SCIENCE

GRADUATE PROGRAM IN CHEMISTRY

YORK UNIVERSITY

TORONTO, ONTARIO

July 2020

Abstract

Pyridines are important frameworks in drug development, valued for their ubiquitous presence in biologically active compounds. As such, we have taken a keen interest in developing mild methods for pyridylic functionalization suited for drug discovery. By implementing a soft enolization approach we are able to effect pyridylic functionalization under mild conditions not achieved by traditional pyridylic activation strategies. Employing alkylidene dihydropyridines (ADHPs) as intermediates in palladium-catalysis, the group developed a mild and practical pyridylic allylation method with broad functional group tolerance. In this report, we extend this reactivity to induce pyridylic dehydrogenation as a direct and reliable approach to accessing 4-alkenylpyridines. Optimizing this dehydrogenation pathway we are able to form vinyl pyridines in good-to-excellent yields and with broad functional group tolerance. A thorough investigation of the functional group compatibility of the method is presented through substrate scope studies and functional group compatibility screen. Additionally, we detail mechanistic investigation of the allylation analogue conducted to aid our efforts in achieving an enantioselective variant of the transformation. Mechanistic probes revealed that the allylation proceeds by a pyridylic anion nucleophile and through outer-sphere reductive elimination, establishing a new pK_a threshold for soft nucleophiles in transition-metal catalyzed allylations.

Acknowledgment

I would like to give a special thanks to my family, my parents, Moataz and Zolfa; siblings, Ahmed, Noura, Sondoce and Mohamed; and beautiful nieces, Karmen and Dareen. I would not have made it this far without all the love, support and joy you bring to my life. Mom and dad, I am forever indebted to you, for fighting a long battle to bring us to Canada for a better education and better life.

Art, a supervisor, mentor and friend. I am truly thankful to have been a part of your group, I couldn't have asked for a better supervisor. Thank you for your patience, for always supporting me and giving me confidence in my abilities as a chemist. I deeply appreciate all the opportunities you have given me, and I hope I do justice to everything you've taught me in my chemistry career. Apart from science, you have helped me grow tremendously as a person, I appreciate all the conversations we've had, and I am glad we have crossed paths. I won't forget where I came from.

I would like to thank Dr. Howard Hunter for all of his NMR help, without whom, some of my experiments wouldn't have been possible. Thank you for going out of your way to help me and for always making time to troubleshoot problems. It was certainly a pleasure having you around, Howard.

Dr. Ryan Hili and Dr. Gino Lavoie, it was an honour to have you on my committee. Thank you for taking the time to discuss my project during the research evaluations, I am grateful for all the constructive input you have given me.

I want to give a special thanks to Dr. Arturo Orellana, Dr. Ryan Hili, Dr. Chris Caputo, and Dr. Gino Lavoie for helping me figure out the next step of my career.

To all the friends I made at York, my Masters study is a lot more memorable because of you. Hao, Anmol, Ashik, Brandon, Brian, Izzy, Andrei and Faizan, you have been like a second family to me. Lab work is always more enjoyable with you around. I will always remember the times we've spent together.

Lastly, to my very close friend, Maryan Mohaiadin, thank you for always being there to listen to me vent. Our adventures together helped me keep my sanity through the frustrations of research.

Table of Contents

List of Schemes

List of Tables

List of Figures

List of Symbols and Abbreviations

α	1,2 relative position
β	1,3 relative position
Δ	reflux
Ac	acetyl
ACS	American Chemical Society
ADHP	alkylidene dihydropyridine
Alloc-Cl	allyl chloroformate
BHT	butylated hydroxytoluene
Cat.	catalytic
COSY	(^{1}H-^{1}H)-homonuclear correlation spectroscopy
DBA	dibenzylideneacetone
DCM	dichloromethane
DDQ	2,3-dichloro-5,6-dicyano-1,4-benzoquinone
DMF	dimethylformamide
E1cB	elimination Unimolecular conjugate Base
ee	enantiomeric excess
Et	ethyl
Equiv.	equivalents
FDA	Food and Drug Administration
HMBC	heteronuclear multiple bond correlation
HWE	Horner-Wadsworth-Emmons

Hz	hertz
J	coupling constant
KHMDS	potassium bis(trimethylsilyl)amide
LDA	lithium diisopropylamide
LiHMDS	lithium bis(trimethylsilyl)amide
Ln	ligand(s) (n = number of ligands)
Me	methyl
MeCN	acetonitrile
MW	molecular weight
n-Bu	*n*-butyl
NMR	nuclear magnetic resonance
NOE	nuclear Overhauser effect
OTf	triflate
Ph	phenyl
pK_a	acid dissociation constant
ppm	parts per million
r.t.	room temperature
S_N2	substitution nucleophilic bimolecular
THF	tetrahydrofuran
TLC	thin layer chromatography
TMS	trimethylsilyl

Chapter 1: Introduction

1.1 Importance of Pyridines in Drug Discovery

Pyridines are privileged structural motifs in the modern drug discovery process. The pyridine fragment serves to modulate the lipophilicity, polarity, aqueous solubility and hydrogen bond capacity of drug candidates, potentially improving their pharmacological and physiochemical properties.[1] This is reflected in their ubiquitous presence in natural products, biologically active compounds and marketed drugs. To illustrate, ten small molecules featuring a pyridine skeleton were listed in the top 200 most prescribed pharmaceutical products in 2018.[2] In fact, a study showed that 59% of all unique small-molecule drugs that are US FDA approved contain a nitrogen heterocycle and that pyridine is the most widely incorporated aromatic heterocycle in these drugs.[3,4] Alkylpyridines bearing a stereogenic centre at the pyridylic or homopyridylic positions are featured in many drug candidates including the GPR40 agonist AM-3189,[5] and the phosphodiesterase IV inhibitor CDP-840[6] and some naturally occurring compounds such as Simplakidine A[7] (**Figure 1**). As a result, lateral functionalization of pyridines has garnered increased attention in organic methodology development.

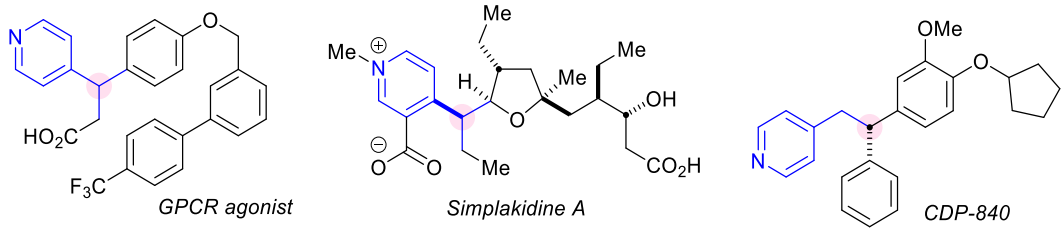

Figure 1. Examples of drug candidates featuring a stereogenic centre at the pyridylic and homopyridylic positions.

1.2 The Chasm Between Needs of the Industry and Academic Development

The drug discovery process relies heavily on organic synthesis to explore novel and diverse chemical space which is needed to access small molecule drugs.[8] Being able to diversify compounds systematically allows a wider exploration of chemical space which should eventually translate into identifying better drug candidates. Compound diversification is greatly reliant on organic chemistry developments since it enhances the synthetic toolbox of the medicinal

chemist. Although there are thousands of methods being reported every year by academic researchers, it is usually the case that they deliver molecules that are not considered "drug like".[9] Most methodology generate compounds that are too lipophilic,[10,11] have high MW,[12] are poor in functional group content, lack 3-dimentionality,[13] or require reagents that are not scalable or sustainable, including precious transition-metals such as Rh or Ir.[14] Additionally, many methodologies target functionalization of aromatic compounds and are not applicable to hetero-aromatics, which, as we have shown, are more prevalent in drug development.[8] To support the pharmaceutical sector, we need to develop chemistry that can be scalable,[15,16] tolerate polar functionality,[17] incorporate heterocyclic fragments, and introduce new stereogenic centres.[18] In an effort to bridge the gap between industrial chemistry and academia, industrial scientists have highlighted the properties that a drug-like compound should possess and called upon academic research to support molecular discovery. In addition to these methodology development guidelines, a perfect opportunity lies in increasing industry-academia collaborations, which can mediate better understanding of the needs of the industry by the academic community.[19]

1.3 Vinylpyridines: Utility & Synthesis

Conjugate addition of nucleophiles onto alkenes activated with electron withdrawing groups is a fundamental transformation and one of the most reliable methods for selective C-C bond formation.[20] Although this 1,4-addition is often associated with activating groups such as carbonyls, nitriles and nitro groups, aza-arenes with an embedded imine moiety (C=N) are electronically homologous to carbonyl compounds and promote the same reactivity.[21] As such, interest has increased in utilizing aza-arenes with a built-in imine functionality in catalytic enantioselective transformations normally associated with carbonyl compounds.[22] Vinylpyridines have emerged as valuable synthons that can be exploited to access synthetically elaborate molecules.[23] For instance, a nickel-catalyzed Grignard addition onto a vinylpyridine was a key connection to accessing phosphodiesterase IV inhibitor CDP-840 (**Figure 2**), which was investigated by Merck and Celltech as a potential drug treatment for Asthma that entered phase II clinical trials.[6]

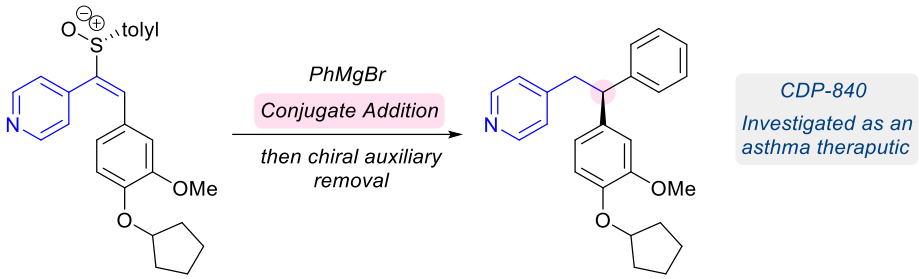

Figure 2. Synthesis of CDP-840 utilizing conjugate addition onto 4-alkenylpyridine as a key disconnection.

Generally, methods to access the vinylpyridine framework follow an addition-elimination sequence including Wittig olefination,[24] and Grignard addition onto pyridinecarboxaldehydes followed by dehydration[25] (**Scheme 1a**). The highly basic and nucleophilic intermediates (phosphonium ylides and Grignard reagents) generated in these reactions limit their functional group tolerance. Alternatively, Heck coupling can be used to elaborate the β-position of simple vinylpyridine substrates (**Scheme 1b**), however, the scope of this transformation is limited since only aryl and vinyl partners are viable.[26] Although there is a wealth of reactions developed to directly oxidize carbonyls to their corresponding α,β-unsaturated analogues using transition metals, these transformations lack for alkylpyridine systems.[27,28] Recently, Newhouse reported the first transition metal-catalyzed dehydrogenation of 2-alkylpyridines utilizing a Ni-PMe_3 catalyst system, $Zn(TMP)_2$ as base and a bromothiophene as a stoichiometric oxidant (**Scheme 1c**).[29] Although they have shown applicability of this method to various aza-heterocycles, their substrate scope is devoid of many useful reactive functionality as a result of the strong base used. Additionally, the stoichiometric oxidant employed generates a high MW by-product, 2-methylthiophene, which is not atom-economical. As a result, alternative methods for one-step dehydrogenations of alkylpyridines that are mild and sustainable should be investigated since they would enable efficient late-stage functionalization of complex substrates.

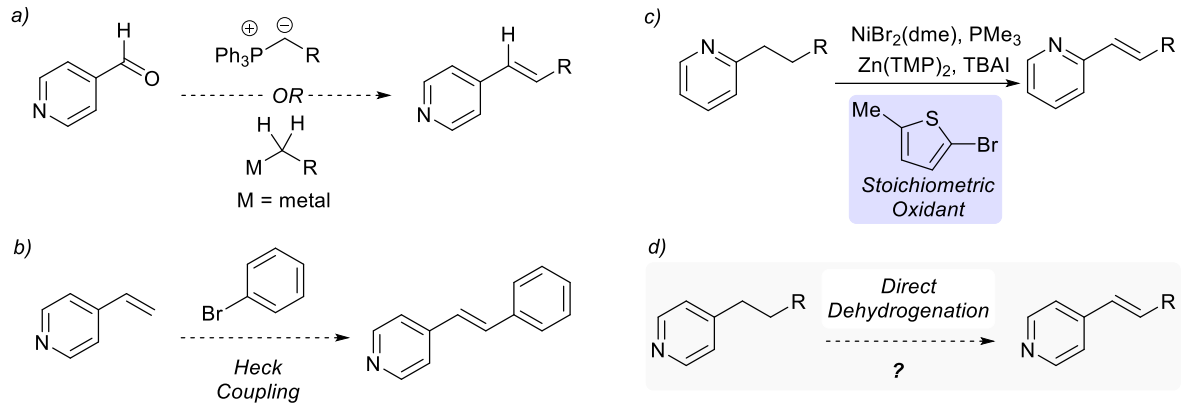

Scheme 1. Methods to synthesize vinylpyridines: Grignard addition-dehydration and Wittig olefination (a), Heck coupling (b), Newhouse's dehydrogenation of 2-alkylpyridines (c), and the possibility for direct dehydrogenation of 4-alkylpyridines (d).

1.4 π-Allylpalladium: a Reliable Oxidant for Installing *α,β*-Unsaturation

In the late 20th century, Pd(II) emerged as a versatile tool to install α,β-unsaturation in carbonyl-containing compounds.[30] Prominently, the Saegusa–Ito oxidation, developed in 1978, transforms silyl enol ethers to their corresponding α,β-unsaturated ketones using stoichiometric amounts of $Pd(OAc)_2$ or catalytic $Pd(OAc)_2$ and a stoichiometric oxidant such as DDQ.[31] Although this method can prove costly because of the non-catalytic amounts of palladium needed, it provides a reliable platform for dehydrogenations especially in the realm of complex natural product synthesis (**Scheme 2a**).[32] Tsuji later demonstrated that π-allylpalladium(II) is a more reliable oxidant that can be employed catalytically, proving more efficient than Saegusa's system (**Scheme 2b**).[33] This method conveniently generates the π-allylpalladium(II) oxidant through reaction of Pd(0) and an allylic electrophile, and functionalizes enol derivatives of carbonyls to their α,β-unsaturated analogues. Mechanistically, the reaction proceeds through oxidative addition of Pd(0) across an allylic electrophile generating π-allylpalladium(II) **A**, which is the active oxidant (**Scheme 2c**). The Pd(II) catalyst then intercepts the nucleophilic enolate in an inner-sphere fashion forming π-allylpalladium(II)-enolate complex **B**, which can then undergo β-hydride elimination, forging the new C=C bond and releasing π-allylpalladium(II)hydride **C**. After alkene dissociation, reductive elimination of propene gas regenerates the Pd(0) species and turns over the catalytic cycle. Tsuji demonstrated dehydrogenation of aldehydes, ketones, esters and lactones using this protocol in

the 1980s. More recently, Newhouse has expanded this chemistry to include dehydrogenation of nitriles, amides and carboxylic acids.[28]

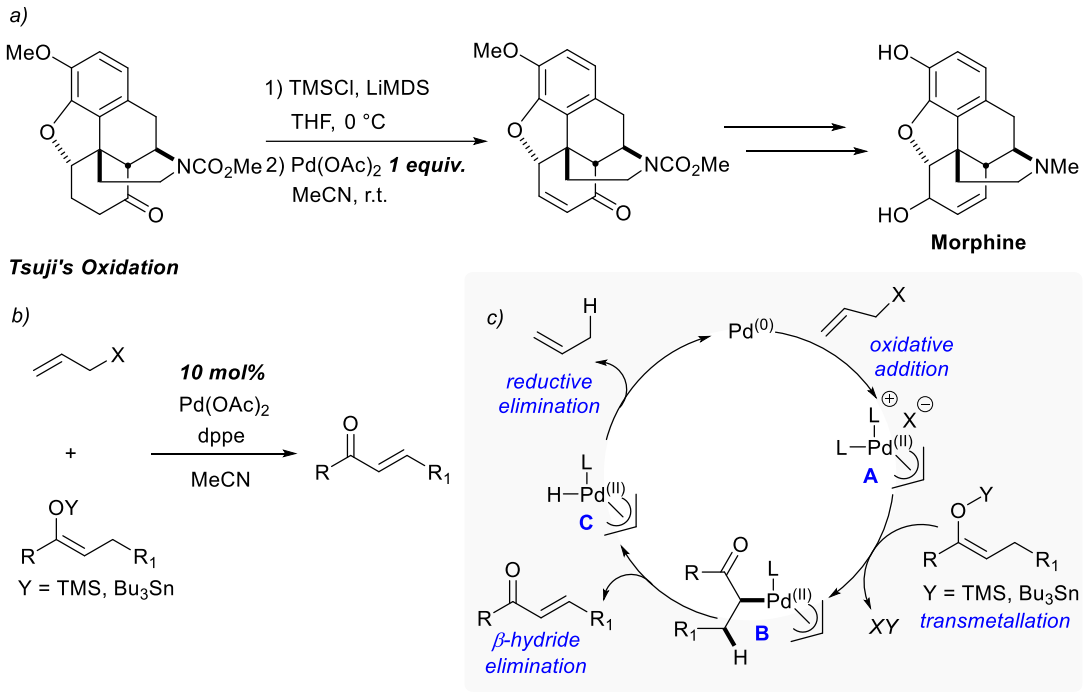

Scheme 2. a) Utility of the Saegusa-Ito oxidation in natural product synthesis: preparation of Morphine, b) overview of the Tsuji dehydrogenation, c) and the general mechanism of the reaction.

1.5 Transition-Metal Catalyzed Pyridylic Allylation

Pyridines are especially valuable fragments in medicinal chemistry, therefore, selective pyridylic functionalization has become of special interest for methodology development since it allows elaboration of simple pyridine frameworks to more complex systems. Allylic substitution of alkylpyridines is attractive since it effects selective combination of two sp^3 carbons. Increasing the 3-dimentionality of drug-like compounds by incorporating more sp^3 containing fragments increases their likelihood of progression from the preclinical stage to successful phase III clinical trials.[18] In addition, allylation introduces at least one new stereogenic centre, which can help drug candidates become more target-selective.[34] Further, the alkene moiety can be easily diversified through known chemistry, enabling the delivery of high-value small molecules.[35] To achieve allylation at the pyridylic position, it is possible to use a simple aza-enolate alkylation approach, which entails pyridylic deprotonation using a strong base such as LDA followed by alkylation using

allyl bromide.[36] Although this is an effective strategy it holds two major drawbacks i) the stereochemistry of the new stereogenic centre cannot be controlled, and ii) selective pyridylic allylation is not possible in the presence of other acidic and enolizable functionality. Therefore, transition-metal catalyzed allylation has emerged to combat these challenges and contributions to this field have increased in the past few years.[37-42]

1.6 Challenges in Pyridylic Functionalization

A major obstacle in pyridylic functionalization is the high pK_a of the pyridylic position (>30).[43] Different strategies have been developed to activate the pyridylic position for allylation (**Scheme 3**). A common approach involves activation of the pyridine nitrogen with a Lewis acid, which acidifies the pyridylic position for deprotonation (**Scheme 3A**).[37-39] This strategy, however, requires the use of stoichiometric amounts of strong Lewis acids such as BF_3•OEt_2, and super stoichiometric amounts of bases such as *n*-BuLi and LiHMDS, which significantly limits its functional group tolerance.[37,38] A notable exception is Sawamura's method, which avoids the use of harsh reagents and employs the palladium cross-coupling catalyst itself as Lewis acid and the alkoxide by-product (pK_a = 16) generated from the coupling reaction as base.[39] Another activation technique involves the installation of an aryl group to activate the pyridylic position allowing deprotonation using Li-, Na- or K-HMDS bases (**Scheme 3B**).[40] However, this is limited to benzylpyridines and cannot be used for alkylpyridine substrates. Further, no positional selectivity can be achieved using this method. Lastly, by introducing a carboxylate group at the desired pyridylic site, allylation can be promoted through decarboxylative or pre-decarboxylative allylation pathways (**Scheme 3C**).[41,42] Although these reactions proceed under mild conditions, the required pre-formation of the pyridine carboxylate substrate is not very practical. It should be noted that these methods either display no positional selectivity or are selective of the 2-pyridylic site, and none have reported selective functionalization of 4-alkylpyridines.

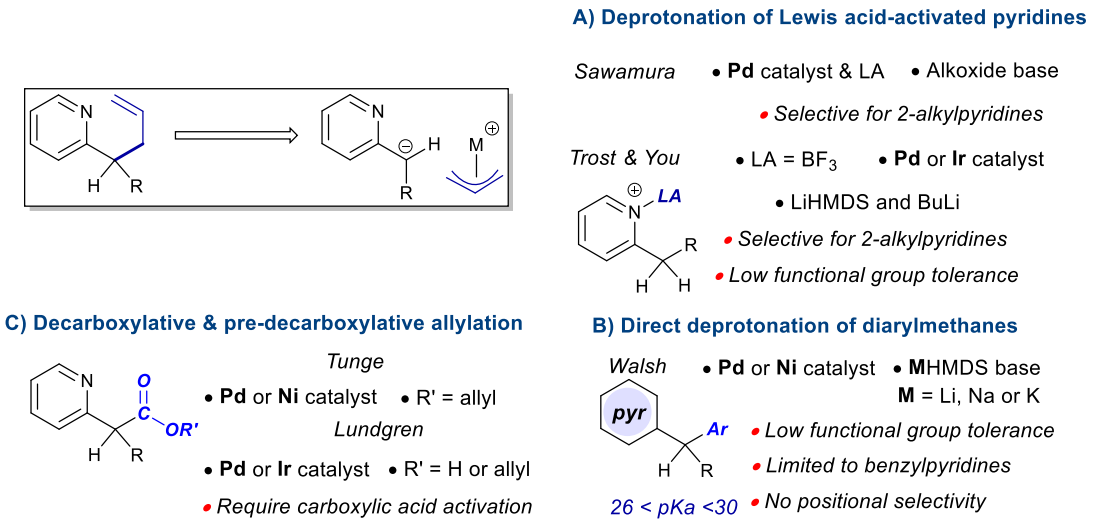

Scheme 3. Approaches towards pyridylic allylation – use and limitations.

1.7 Palladium-Catalyzed Allylation of 4-Alkylpyridines

Driven by the importance of pyridines and the obvious need for developing mild and reliable methodology to functionalize pyridine compounds, we have established a conceptually new mechanistic entry for lateral pyridylic functionalizations. Treating 4-alkylpyridines with allyl chloroformate and triethylamine allows access to alkylidene dihydropyridines (ADHPs) that can later be utilized in decarboxylative coupling chemistry using palladium catalysis (**Scheme 4**).[44] By adopting this soft enolization approach to activate the pyridylic position, we were able to achieve pyridylic allylation under mild conditions without requiring the use of aggressive reagents such as strong Lewis acids and bases, and with high functional group tolerance.[45] Treating these ADHPs with a Pd-Xantphos catalyst system induces pyridylic allylation in excellent yields. Mechanistically, we envisioned that this reaction operates through first oxidative addition of Pd(0) across the allylic site generating a cationic π-allylpalladium(II) (**Scheme 4**, intermediate **I**) and a carbamate that can spontaneously decarboxylate to release a pyridylic anion. Since it was previously established that anions with pK_a values higher than 32 undergo reductive elimination through an inner-sphere pathway,[40] it is reasonable that the pyridylic anion (pK_a~35) first binds to the Pd(II) species (**Scheme 4**, intermediate **II**) before reductively eliminating to form the new C-C bond. We found that the reaction enjoys a wide range of functional group compatibility and can proceed even in the presence of electrophilic and acidic functionality including aldehydes,

ketones and carbamates. Additionally, the allylation method is selective for 4-alkylpyridines even in substrates bearing multiple pyridylic sites, marking the first method ever to exhibit this positional selectivity.

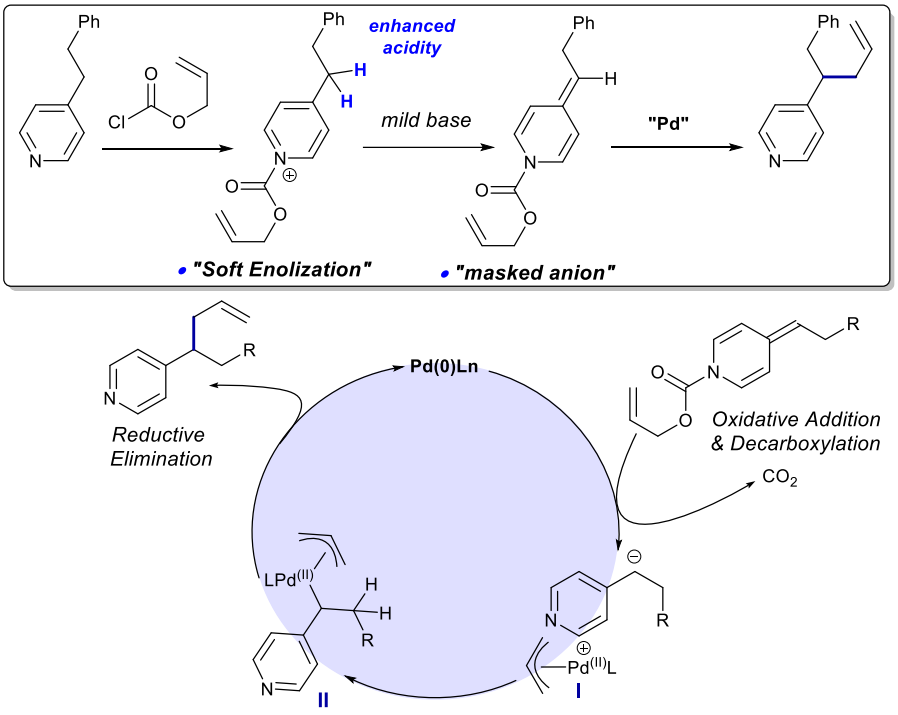

Scheme 4. General overview of Orellana's pyridylic allylation and its proposed mechanism.

Chapter 2: Palladium-Catalyzed Decarboxylative Dehydrogenation of 4-Alkylpyridines

π-Allylpalladium(II) is a well-documented oxidant known for its ability to dehydrogenate carbonyl compounds to their α,β-unsaturated variants. As shown in **scheme 4**, this complex is a key intermediate in our palladium-catalyzed pyridylic allylation reaction. We wanted to exploit the oxidation ability of this intermediate to reroute the reaction to become a dehydrogenation rather than an allylation process (**Scheme 5**). This should proceed in a manner similar to Tsuji's dehydrogenation whereby the π-allylpalladium(II) complex, which is generated by oxidative addition across the ADHP, is intercepted by a pyridylic aza-enolate (**Scheme 5**, complex **II**). β-Hydride elimination forms the alkenylpyridine product and a π-allylpalladium(II)hydride (**Scheme 5**, complex **III**), reductive elimination of propene regenerates the Pd(0) catalyst and turns over the cycle. Since the allylation reaction displays selectivity for the 4-pyridylic site and enjoys wide functional group tolerance, we hoped this would be carried to the dehydrogenation analogue which can allow it to become a practical means to directly dehydrogenate 4-alkylpyridines to their 4-alkenyl counterparts under mild conditions. Our goal for this project was to find conditions that would favor the formation of the alkenyl product in good yields, and to explore the scope and limitations of the reaction. This chapter details optimization studies of the palladium-catalyzed pyridylic dehydrogenation of 4-alkylpyridines, and reaction scope and limitations in the form of substrate scope studies and a functional group compatibility screen.[16]

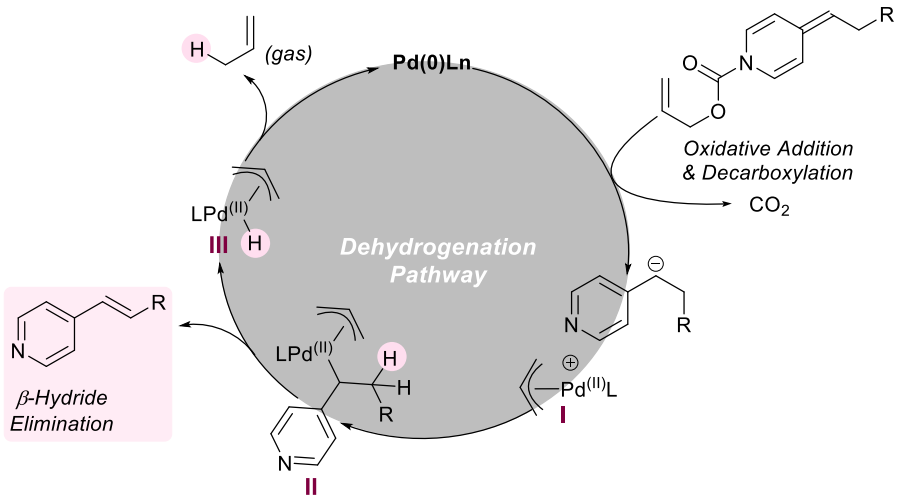

Scheme 5: Proposed catalytic cycle for the palladium-catalyzed dehydrogenation of 4-alkylpyridines.

2.1 Optimization Studies

Exposing ADHPs to Pd(0) can potentially form two products, the product arising from pyridylic allylation and that resulting from β-hydride elimination. Previous ligand screening of the palladium coupling step was conducted to investigate how ligand structure affects product distribution (**Scheme 6**). Testing various phosphines revealed that generally sterically demanding monodentate ligands or bidentate ligands with large bite angles favor the reductive elimination pathway (**Scheme 6**, entries 1, 2, 5, 6, 9-13). Bidentate ligands with a small bite angle gave significant amounts of the dehydrogenation product but as a mixture with the undesired allylated pyridine (**Scheme 6**, entries 7-8). As **scheme 6** details, selective dehydrogenation could not be established in the presence of phosphine ligands. Exclusive formation of the alkenylpyridine was accomplished by using a phosphine-free catalyst system (**Scheme 6**, entry 14). This is consistent with Tsuji's findings as he previously demonstrated that "ligandless" or phosphine-free $Pd_2(dba)_3$ is an effective catalyst in π-allylpalladium(II) catalyzed dehydrogenations.[33a] The efficiency of this ligandless system in dehydrogenations is probably a result of the palladium centre being electron deficient and bearing empty coordination sites, which allows it to easily engage in agostic interactions leading to β-hydride elimination.

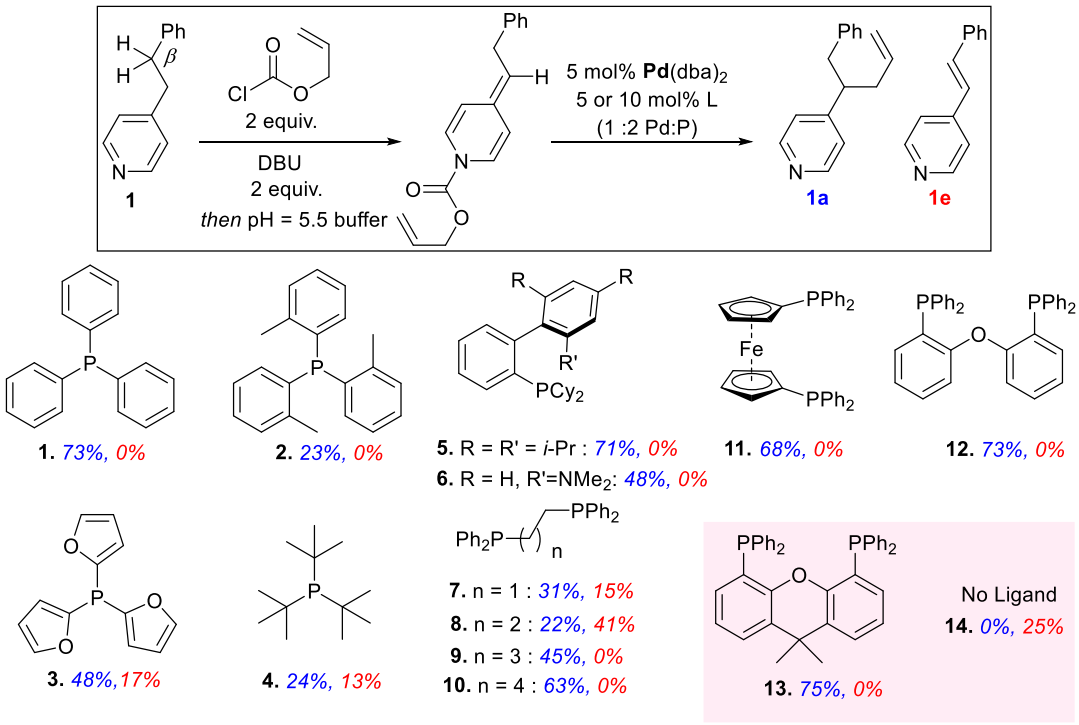

Scheme 6. Exploring the effect of ligand structure on product distribution in the palladium-catalyzed functionalization of 4-alkylpyridines (results obtained from Faizan Rasheed).

Having established our catalyst system to be phosphine-free Pd(0), we planned to proceed with our optimization by conducting solvent and temperature screens. As shown in **table 1**, we found that subjecting ADHP **1'** to 2.5 mol% $Pd_2(dba)_3$ (5 mol% Pd) and heating at 50 °C, toluene, dioxane and THF stood out as the best solvent choices (**Table 1**, entries 3-5) promoting full conversion of the ADHP, providing clean crude mixtures and generating the dehydrogenation product in good quantitative NMR yields. It was surprising that the yields of product were not higher since aza-stillbene **1e** appeared to be the sole product of the reaction, at least by crude ^{1}H NMR. We were confident that the synthesis of the ADHP is high yielding because allylation of pyridine **1** proceeding through the same ADHP **1'** takes place in 92% yield (over two steps). Throughout our studies we found that ADHPs are fairly stable intermediates that can even survive mildly acidic aqueous work-up. Although we have no clear indication of their half-life, they decompose on standing. Therefore, it is possible that the ADHP may be undergoing non-metal induced decomposition during the reaction, and that this might be contributing to yield loss. We wondered if by increasing the catalyst loading we could increase the rate of dehydrogenation,

which would translate to less thermal decomposition of the intermediate ADHP. Indeed, employing 3.5 mol% $Pd_2(dba)_3$ (7 mol% Pd) induced an average of 7% yield increase (**Table 1**, entries 6-8). Further increase in catalyst loading did not prove useful and gave the same yield as that using 3.5 mol% (**Table 1**, entry 9). In addition, it was reasoned that lowering the reaction temperature can help decrease the rate of ADHP decomposition, however, conducting the reaction using 3.5 mol% $Pd_2(dba)_3$ (7 mol% Pd) at 40 °C resulted in incomplete conversion of **1'** (**Table 1**, entries 10-12).

Table 1. Optimization of the palladium-catalyzed dehydrogenation of 4-alkylpyridines.

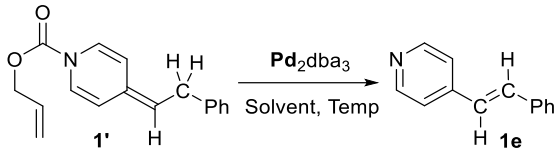

entry	solvent	Pd_2dba_3	temperature	yield
1	1,2-DCE	2.5%	50	33
2	MeCN	2.5%	50	49
3	Toluene	2.5%	50	74
4	Dioxane	2.5%	50	76
5	THF	2.5%	50	83
6	Toluene	3.5%	50	80
7	Dioxane	3.5%	50	83
8	*THF*	*3.5%*	*50*	*88*
9	Dioxane	5%	50	83
10	Toluene	3.5%	40	*Incomplete Conversion*
11	Dioxane	3.5%	40	
12	THF	3.5%	40	

Finally, since vinylpyridines are known to undergo radical decomposition,[46] we wondered if product decomposition rather than intermediate decomposition was responsible for low product yields. To probe this, we conducted two dehydrogenation reactions side by side, one employing stoichiometric amounts of butylated hydroxytoluene (BHT), a radical inhibitor, and the other without any radical suppressants. Both reactions provided comparable yields of product indicating that the alkenylpyridine displays stability against radical processes during the reaction time (**Figure 3**). At this point, we were satisfied with the optimization results obtained and

decided to use 3.5 mol% $Pd_2(dba)_3$ in THF at 50 °C (**Table 1**, entry 8) in the dehydrogenation step for further reaction development. We then proceeded to obtain the isolated yield of product using these conditions.

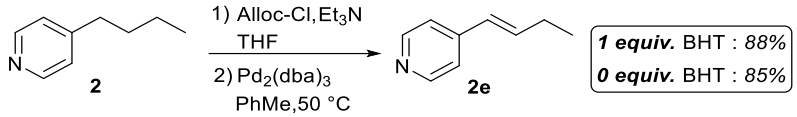

Figure 3. Investigating potential product loss through radical decomposition pathways.

In some cases, purification of the alkene product using column chromatography proved inefficient since side products with similar R_f values co-eluted in some fractions resulting in yield loss. We therefore wanted to develop an alternative protocol, complementary to flash chromatography, for product isolation that is both practical and would not result in significant loss of product. Since the problematic side products are minor, we considered recrystallization as a better strategy for purification. After completion of the reaction, we decided to convert the alkenylpyridine product to the corresponding pyridinium hydrochloride salt which serves to i) easily separate it from non-basic reaction components including dibenzylideneacetone (DBA) and ii) solidify the product for recrystallization. Employing this protocol, product **1e** was obtained cleanly in 88% isolated yield after recrystallization from DCM.

2.2 Substrate Synthesis

To expedite our substrate scope studies we relied on a number of key strategies to prepare a library of functionalized 4-alkylpyridines including 4-picoline alkylation, Horner-Wadsworth-Emmons (HWE) reaction, Sonogashira coupling, hydrogenation and functional group interconversions. As illustrated in **figure 4**, alkylation of 4-picoline allowed us quick access to substrates bearing aryl (**1** & **6**), alkyl (**2** & **5**), vinyl (**3**), silyl ether (**7**) and acetal (**8**) functionality. Gratifyingly, we can synthesize cyano-functionalized substrate **9** in good yield using this method, which can be further elaborated to other useful structures (refer to **Scheme 8**).

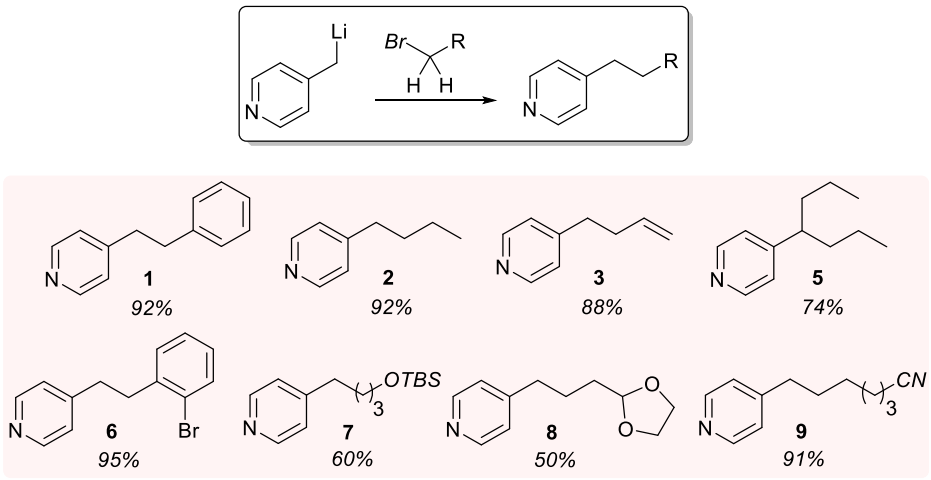

Figure 4. Preparation of functionalized 4-alkylpyridines through alkylation of 4-picoline.

Alkyne **4** was synthesized through an alkylation-Sonogashira coupling sequence (**Scheme 7**). Benzylation of 4-picoline using 4-bromobenzyl bromide formed **4.1** in excellent yield. Sonogashira coupling of **4.1** and 1-hexyne using diisopropylamine as base, and a copper (I) iodide and bis(triphenylphosphine)palladium(II) dichloride catalytic system afforded substrate **4** in 83% yield.

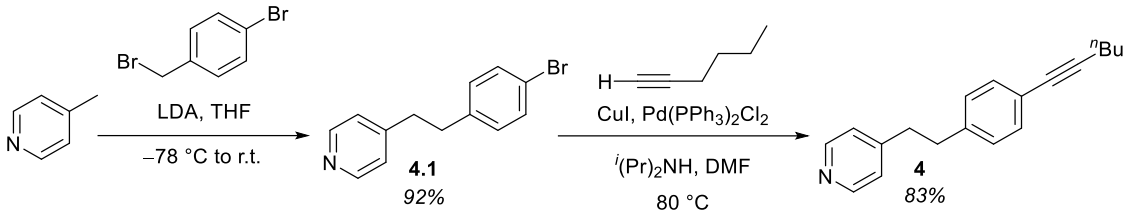

Scheme 7. Synthesis of alkyne tethered 4-alkylpyridine substrate through an alkylation-Sonogashira coupling sequence.

Hydrolysis of pyridine **9** followed by esterification provided substrate **10**, bearing a tethered methyl carboxylate functionality (**Scheme 8A**). Weinreb amide **11** was prepared through an HWE-hydrogenation-amide formation sequence (**Scheme 8B**). Reaction of 4-pyridine carboxaldehyde with the anion of ethyl 4-(diethylphosphono)crotonate formed the expected *E,E*-diene **11.1** in good yield. Transfer hydrogenation gave access to ester **11.2**, which was transformed to the Weinreb amide through trimethylaluminum mediated transamidation. In this reaction, pre-mixing of trimethylaluminum and *N,O*-dimethylhydroxylamine hydrochloride is required to generate the active dimethylaluminum amide complex.[47]

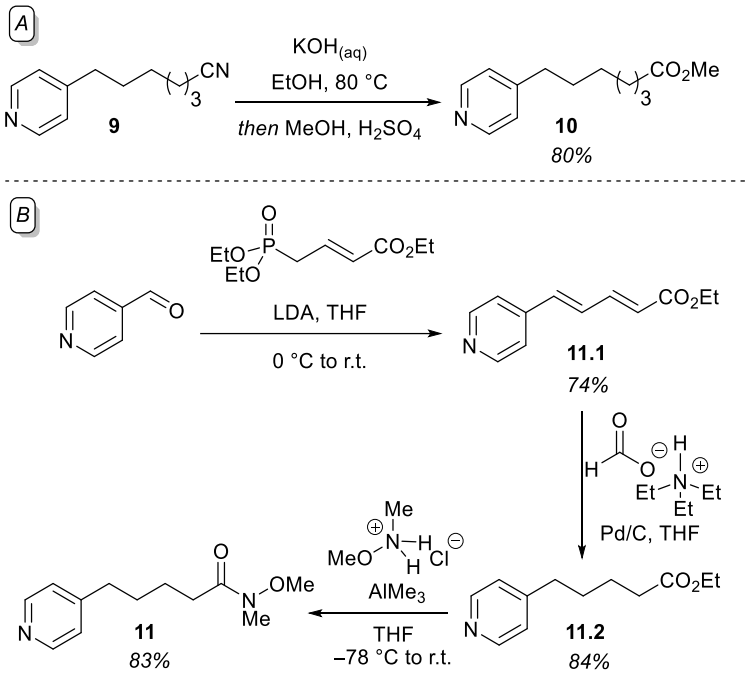

Scheme 8. Preparation of substrates bearing tethered A) ester and B) Weinreb amide functionality.

Knochel's direct alkylation of 3-substitued pyridines proved very efficient in preparing substrates with polar groups at the 3-position.[48] This strategy entails activation of the pyridine with BF_3•OEt_2 as a Lewis acid, followed by Grignard attack at the 4-position, forming the substituted dihydropyridine intermediate. Oxidation with chloranil rearomatizes the system and furnishes the 3,4-disubstituted pyridine. 3-Cyano-4-butylpyridine (**12.1**) and methyl 4-butylnicotinate (**13**) were synthesized using this method in good yields (**Scheme 9A**). Nitrile **12.1** was further transformed to the corresponding amide **12** through a Ritter reaction using *tert*-butyl acetate as the cation source which generates isobutylene *in situ* through acid mediated elimination (**Scheme 9B**).

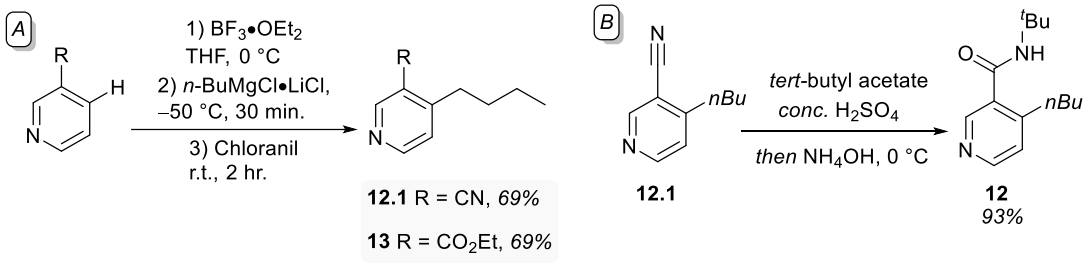

Scheme 9. A) Preparation of 3-substituted-4-alkylpyridines using Knochel's direct alkylation method, B) Ritter reaction for accessing amide-substituted 4-alkylpyridine.

To investigate the regioselectivity of our dehydrogenation method, we wanted to build a system containing separate 2- and 4-alkylpyridine scaffolds and decided to connect the two fragments through a phenyl linker. Benzylation of 4-picoline using ethyl-4-bromomethylbenzoate installed the first pyridine ring and formed **15.1** in moderate yield (**Scheme 10**). Lithium borohydride reduction followed by bromination formed **15.3**, setting the stage to connect the final 2-alkylpyridine fragment. Reaction of benzyl bromide **15.3** and the lithium anion of 2-picoline completed the synthesis, producing bipyridine **15** in good yield.

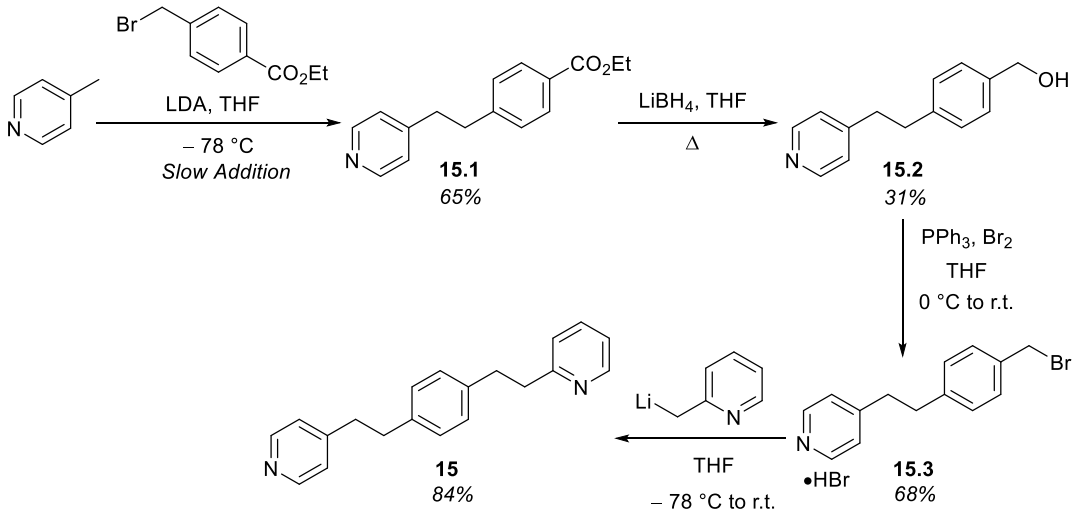

Scheme 10. Synthesis of a system bearing 2- and 4-alkylpyridines designed to probe the regioselectivity of our dehydrogenation method.

2.3 Substrate Scope Studies

We were pleased to find that our dehydrogenation method displays a wide range of functional group tolerance (**Table 2**). Oxidation of 4-butylpyridine provided 4-(1-butenyl)pyridine **2e** in 86% yield. The presence of terminal alkenes and internal alkynes did not interfere with the dehydrogenation and gave products **3e** and **4e,** bearing extended conjugation, in 73% and 63% yield respectively. It is also possible to oxidize tertiary pyridylic centres, dehydrogenation of 4-(heptan-4-yl)pyridine **5** proceeded in 82% yield forming a 5.9:1 *E:Z* mixture of diastereomers. Aryl bromides were found to be innocuous, showing no signs of oxidative addition across the C(sp^2)-Br bond, indicating that this dehydrogenation is orthogonal to traditional cross-coupling reactions (**6e**, 94%). Acid-sensitive groups including TBS-ether and acetal remained intact throughout the reaction and their dehydrogenation products **7e** and **8e** were formed in 89% and 77% yield respectively. We were pleased to find that the dehydrogenation displayed pyridylic chemoselectivity in the presence of functionality with acidic α-protons, including nitriles (**9e**, 74%, pK_a 32), esters (**10e**, 81%, pK_a 30), and amides (**11e**, 82%, pK_a 35). The presence of strongly coordinating groups at the 3-position hinders the catalytic cycle, likely due to chelation to palladium as shown in **table 2**. Using DMF as solvent and heating to 80 °C alleviated this problem, likely through stabilization of the metal centre with the strongly coordinating DMF, allowing formation of products **12e** in 69% yield and **13e** in 71% yield.

Table 2. Substrate scope of the palladium-catalyzed decarboxylative dehydrogenation of 4-alkylpyridines.

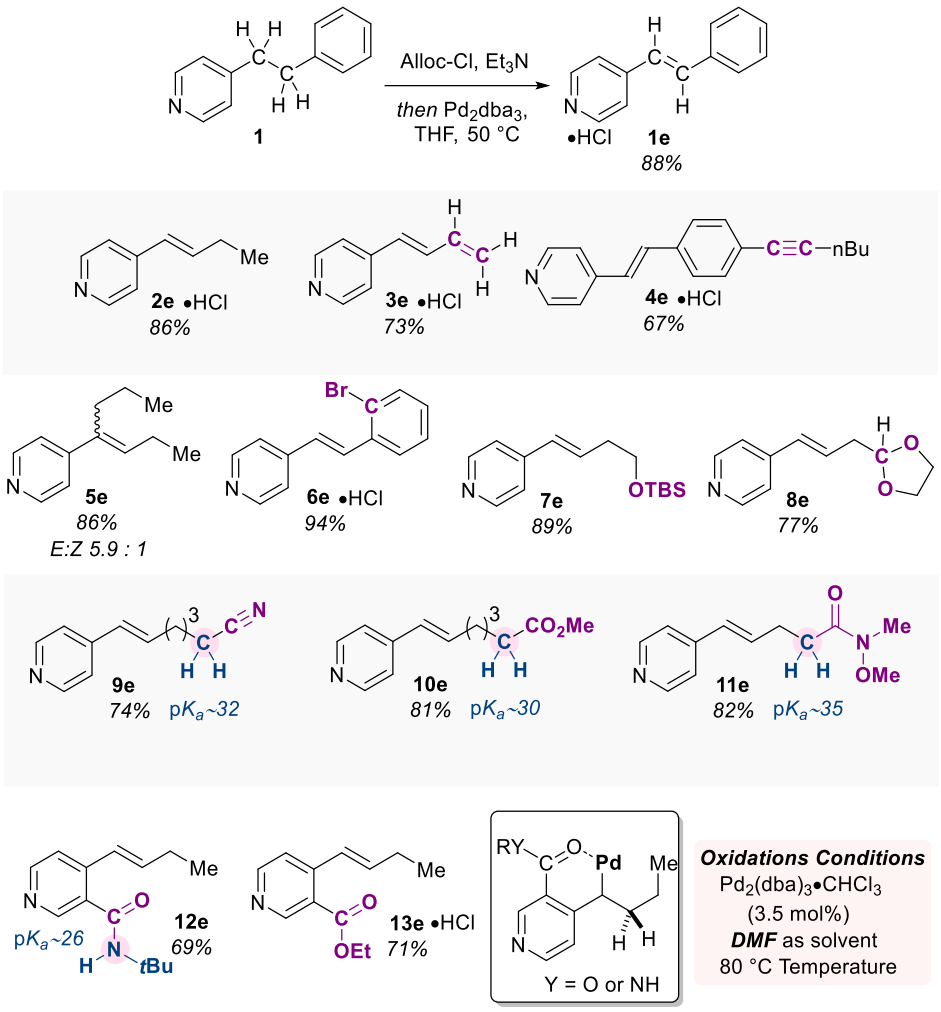

It should be noted that the reaction displays *E*-selectivity providing *trans*-alkenes as the sole product of dehydrogenation. This is not surprising since the *E*-isomer is the kinetic and thermodynamic product of the reaction (**Scheme 11**). It is unclear if the reaction is reversible since we never observed the alkene with *Z*-geometry. It is therefore more likely that the reaction proceeds through the lowest energy route where the palladium-aza-enolate complex adopts the lowest energy conformation before undergoing β-hydride elimination, which eventually leads to the observed *trans*-isomer. The *E*-geometry in the products was confirmed through the alkene signature in the NMR spectra showing coupling constants between 15.6 – 16.4 Hz, typical of *trans*-substituted alkenes.

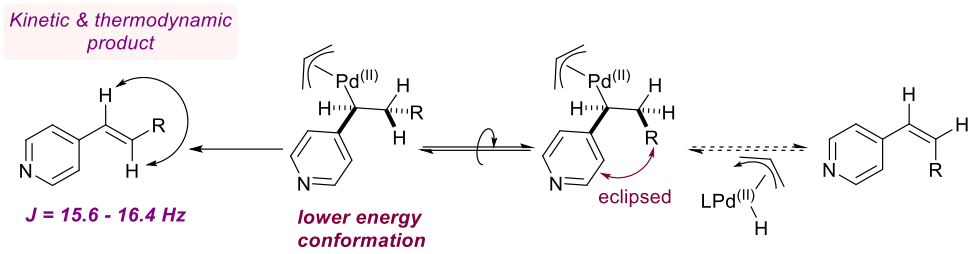

Scheme 11. The palladium-catalyzed dehydrogenation of 4-alkylpyridines displays *E*-selectivity.

Previous studies of the allylation of monosubstituted alkylpyridines revealed that ADHPs only form with systems bearing alkyl groups at the 4-position (**Scheme 12**). Although 2-, 3-, and 4-alkylpyridines can all react with allyl chloroformate to form the respective pyridinium salts, only the 4-alkylpyridine system can be deprotonated to the ADHP (**Scheme 12A**). As can be expected, since the pyridylic position of the 3-alkylpyridinium salt is not activated by the pyridine nitrogen, deprotonation forms a localized anion and therefore cannot be achieved using triethylamine as base (**Scheme 12B**). It is in unclear why the 2-alkylpyridiunium salt cannot be converted to the ADHP. It may be that the allyloxy carbonyl group is orthogonal to the pyridine ring thereby limiting its pyridylic acidification. Another possible reason is developing allylic strain between the alkene and the carbamate fragment during deprotonation, which raises the activation barrier of the transformation (**Scheme 12C**). As a result, using this method, we can selectively allylate the 4-pyridylic position in systems bearing multiple pyridylic sites and we expected this selectivity to extend to our dehydrogenation method. Indeed, dehydrogenation of tetrahydroisoquinoline, which bears 3- and 4-pyridylic sites, occurred exclusively at the 4-position (**14e**, **Scheme 12**). It is notable that over-oxidation to the quinoline did not take place, further illustrating the mildness of our dehydrogenation method. In addition, subjecting a system composed of tethered 2- and 4-alkylpyridines (**15e**, **Scheme 12**) to our dehydrogenation conditions installed the unsaturation exclusively at the pyridylic site of the 4-substitued ring, exemplifying that dehydrogenation can take place at the less acidic heterobenzylic position.

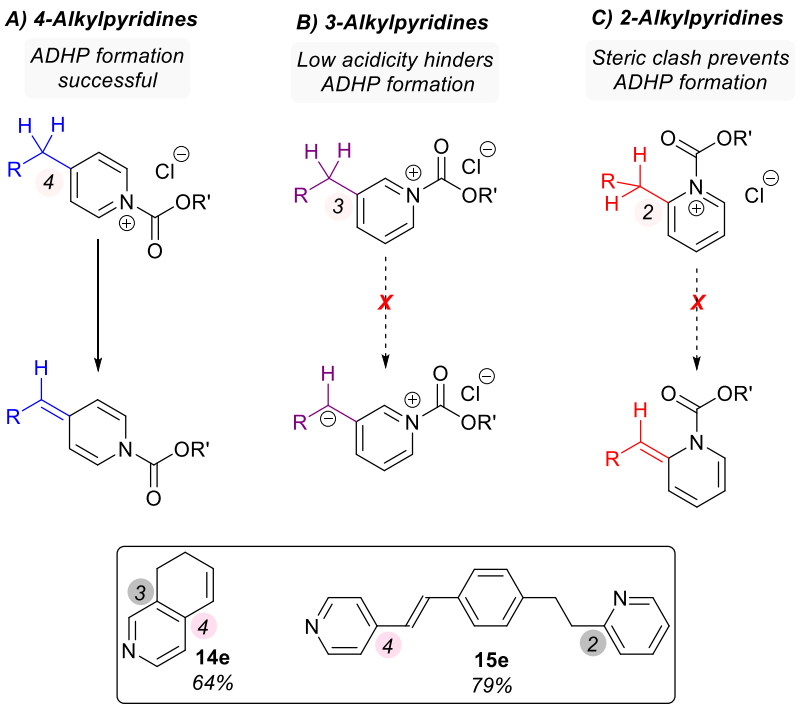

Scheme 12. ADHP formation is limited to 4-alkylpyridines resulting in selective dehydrogenation at the 4-pyridylic site.

2.4 Functional Group Compatibility Screen

To further test the robustness of this reaction, we conducted a functional group compatibility screen whereby the performance of the dehydrogenation is assessed in the presence of additives bearing a variety of useful functionality.[15-17] The information obtained from this screen is two-fold, it informs on i) the tolerance of the reaction to additives and ii) the stability of additives to reaction conditions. This study is conducted by preparing a 1:1 mixture of the additive and 4-phenethylpyridine **1**, and subjecting this mixture to standard enolization and dehydrogenation conditions. Quantitative ^{1}H NMR is then used to measure the yield of product, recovery of the additive, and ADHP consumption. Deviation of ADHP consumption and product yield from that obtained in the control experiment (without additive) should reflect interference of the additive with the dehydrogenation sequence.

We found that aryl bromides do not hinder the reaction, even those activated by electron withdrawing groups such as additives **F2**, **F9**-**F11** (**Table 3**). Strongly electrophilic functionality, which can engage in other reactions with organometallic nucleophiles, including aldehydes (**F3**),

ketones (**F4**), Michael acceptors (**F5**), and esters (**F2**, **F6**, **F7**) appeared innocuous, displaying high additive recovery and good product yield. Alkyl chlorides were also found to be compatible with our system (**F6**).

Table 3. Functional group compatibility screen of the palladium-catalyzed pyridylic dehydrogenation.

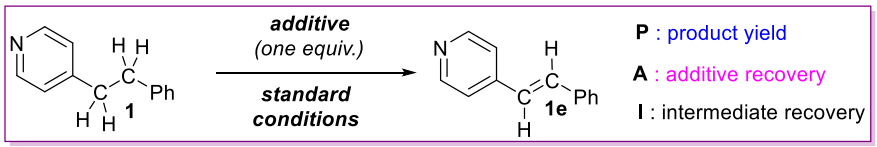

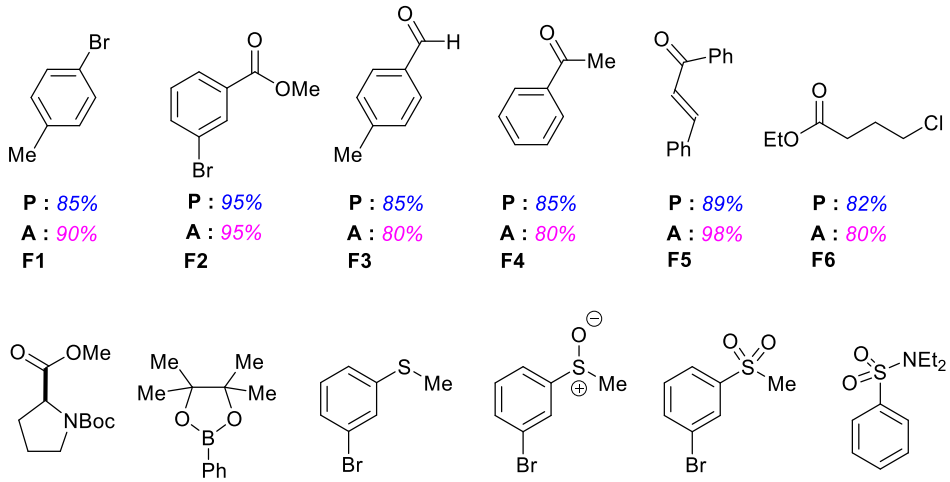

P : *85%* **A** : *90%* **F1**

P : *95%* **A** : *95%* **F2**

P : *85%* **A** : *80%* **F3**

P : *85%* **A** : *80%* **F4**

P : *89%* **A** : *98%* **F5**

P : *82%* **A** : *80%* **F6**

P : *80%* **A** : *>99%* **F7**

P : *71%* **A** : *82%* **F8**

P : *79%* **A** : *94%* **F9**

P : *67%* **A** : *97%* **F10**

P : *70%* **A** : *98%* **F11**

P : *58%* **A** : *97%* **F12**

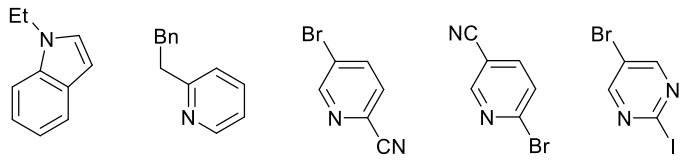

P : *79%* **A** : *94%* **F13**

P : *80%* **A** : *>99%* **F14**

P : *70%* **A** : *93%* **F15**

P : *42%* **A** : *90%* **I** : *23%* **F16**

P : *0%* **A** : *87%* **I** : *67%* **F17**

The presence of an arylboronic ester **F8**, which can be problematic because of possible transmetallation, is tolerated and we found that the dehydrogenation pathway is favored with the vinylpyridine forming in 71% yield and minimal formation of the cross-coupling product (<10%). Thioethers (**F9**), sulfoxides (**F10**), sulfones (**F11**) and sulfonamides (**F12**), which are commonly found in drug candidates and also are known for being potential poison for palladium,[49] are tolerated with the unsaturated pyridine being formed in good yields.

Nucleophilic groups such as indoles (**F13**) and 2-alkylpyridines (**F14**-**F16**), which can potentially react with the electrophilic allyl chloroformate,[39,50] did not interfere with either the dearomatization or the dehydrogenation steps observing excellent recovery and formation of the product in good yield. Finally, we wanted to further challenge our system with building blocks commonly used in medicinal chemistry (**F15**-**F17**). We found that 5-bromo-2-cyanopyridine (**F15**) is well tolerated. Its positional isomer **F16** bearing a more reactive C(sp^2)-Br bond, activated by the pyridine ring and cyano group, reduced the yield of product and prevented the full consumption of the ADHP. The reaction shut down completely in the presence of a strongly activated C(sp^2)-I bond (**F17**).

2.4 Conclusion

We developed a mild palladium-catalyzed dehydrogenation of 4-alkylpyridines that exploits alkylidene dihydropyridines as substrates. This approach takes advantage of soft enolization for pyridylic activation thereby eliminating the use of harsh reagents including strong bases and oxidants. We found that employing a simple phosphine-free $Pd_2(dba)_3$ catalyst effects dehydrogenation in good to excellent yield. Functional group compatibility screen and substrate scope studies demonstrated that the reaction tolerates a wide range of functional groups including acidic and electrophilic functionality. Additionally, fragments commonly used in medicinal chemistry such as sulfoxides, sulfones, activated aryl bromides, and boronic esters were compatible with our oxidation, making this a suitable pyridylic dehydrogenation method for use in drug discovery.

Chapter 3: Mechanistic Investigation of the Palladium-Catalyzed Allylation of 4-Alkylpyridines

Considering the potential utility of our allylation reaction in drug discovery, we wanted to develop an asymmetric variant of the transformation. We initially approached the enantioselective studies using the mechanistic proposal outlined in **scheme 13**. It has been generally accepted that nucleophiles with pK_a below 25 are considered "soft" and undergo palladium-catalyzed transformations outside the coordination sphere of the metal.[51] In 2013, Walsh showed that diarylmethanes (pK_a~32) undergo reductive elimination in an outer-sphere fashion, which updated the pK_a limit of soft nucleophiles and raised it to 32.[40] Depending on their substitution pattern, the pK_a of 4-alkylpyridines can vary significantly and it generally spans from 26 to 35. It seemed reasonable that simple 4-alkylpyridine systems such as 4-phenethylpyridine (pK_a~35) proceed through an inner-sphere reductive elimination mechanism since their pK_a lies above the established soft-anion threshold. Additionally, the fact that we observed β-hydride elimination in some entries of the ligand screen (**Scheme 6**), which used 4-phenethylpyridine as substrate, strongly suggests that the reaction proceeds through binding of the nucleophile to the metal centre, further supporting an inner-sphere pathway.

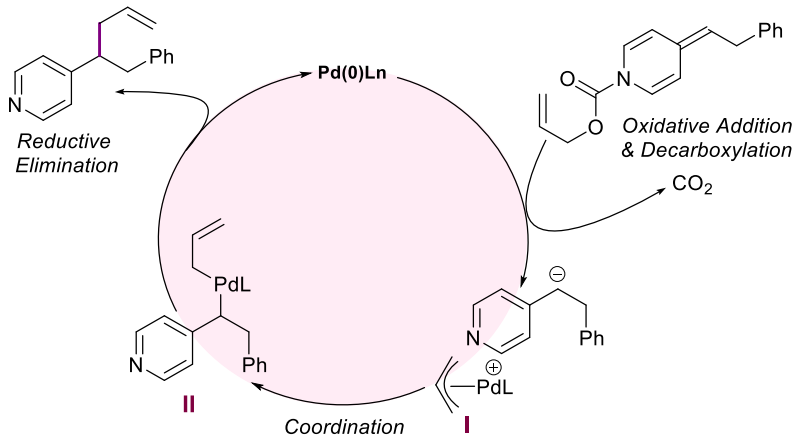

Scheme 13: Proposed mechanism for the palladium-catalyzed allylation of 4-alkylpyridines involving pyridylic anions behaving as hard nucleophiles.

Embarking this journey, we were confident that by screening ligand scaffolds previously successful in enantioselective allylations we would readily observe positive results. Since we initially viewed our allylation as an inner-sphere process, we expected that achieving high levels of stereoinduction would not be extremely challenging. In an inner-sphere process chiral

information is easily transferred to the prochiral nucleophile since it directly binds to the metal carrying the chiral ligand (**Scheme 14**). This is opposite to an outer-sphere process, where the ligand has to extend beyond the plane of the allyl fragment to relay the stereochemical information (**Scheme 14**).[51]

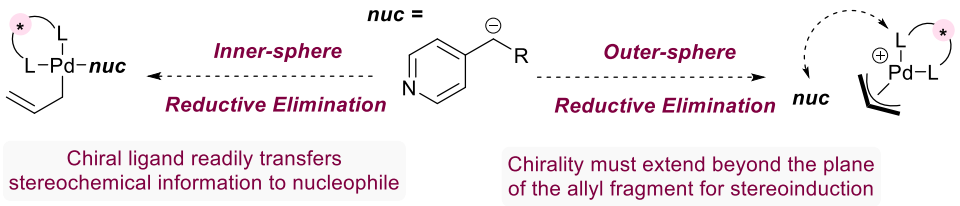

Scheme 14. Stereoinduction requirements for inner-sphere and outer-sphere processes for enantioselective transformations.

Our work began by screening a variety of optically-pure bidentate ligand scaffolds known to induce high levels of enantioselectivity in similar transformations. It was very surprising to find that most ligands imparted almost no stereoinduction (**Scheme 15**) with ligands **L1** through **L6** providing essentially racemic products. Interestingly, the reaction failed when Trost ligand **L7** was used (**Scheme 15**), presumably a result of the deprotonation of the ligand backbone by the generated high pK_a pyridylic anion. Methylation of the amide nitrogens on this ligand provided the allylation product in 88% yield but still with very poor enantiomeric excess (**Scheme 15**, ligand **L8**). Phosphoramidites are an invaluable class of ligands used in asymmetric Cu and Ir allylation chemistry[52,53] and have even shown impressive results in Sawamura's Pd-catalyzed pyridylic allylation.[39] We found that in our system, phosphoramidite ligand **L9** (**Scheme 15**) showed the most promise, forming the allylation product with 32% *ee*, the highest enantiomeric excess observed in the screen. In view of these unexpected results from the ligand screen, we began questioning our understanding of the mechanism of this reaction and decided to embark on a mechanistic investigation with the long-term goal of exploiting insights in an enantioselective version.

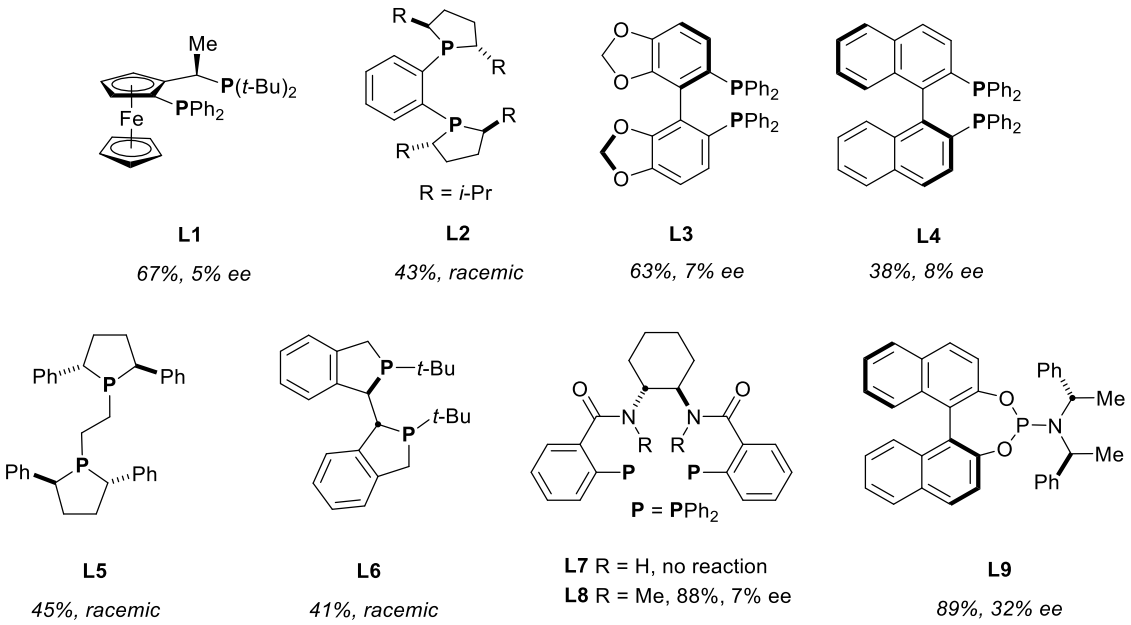

L1
67%, 5% ee

L2
43%, racemic

L3
63%, 7% ee

L4
38%, 8% ee

L5
45%, racemic

L6
41%, racemic

L7 R = H, no reaction
L8 R = Me, 88%, 7% ee

L9
89%, 32% ee

Scheme 15. Pyridylic allylation with chiral ligands led to essentially racemic products in most cases. Data obtained from Faizan Rasheed and Jiaqi Shi.

3.1 Possible Mechanistic Scenarios for the Palladium-Catalyzed Allylation of 4-Alkylpyridines

Originally, we envisaged that the allylation reaction proceeds as in **scheme 13** whereby oxidative addition and decarboxylation generate the allylating agent (**Scheme 13**, complex **I**) and a pyridylic anion. Considering the highly reactive nature of the anionic species, we imagined that it is very likely that it attacks the electrophilic palladium complex and turns over the cycle. In 2007, Tunge showed the decarboxylative allylation of 2-pyridyl cinnamyl esters, which proceeds by N-allylation and decarboxylation, followed by a [3,3]-aza-Cope rearrangement as shown in **scheme 16A**.[41] A similar mechanistic pathway can be envisioned in our system, whereby oxidative addition and decarboxylation lead to N-allylation instead of pyridylic allylation. Two sequential [3,3]-sigmatropic rearrangements rearomatize the ring and form the pyridylic allylation product (**Scheme 16B**). In this sequence of events, enantioselectivity should not be possible since the pyridylic bond-forming step does not occur at the chiral metal centre. Having observed enantio-induction with some of the optically active ligands screened (**Scheme 15**), this mechanistic sequence seems very unlikely.

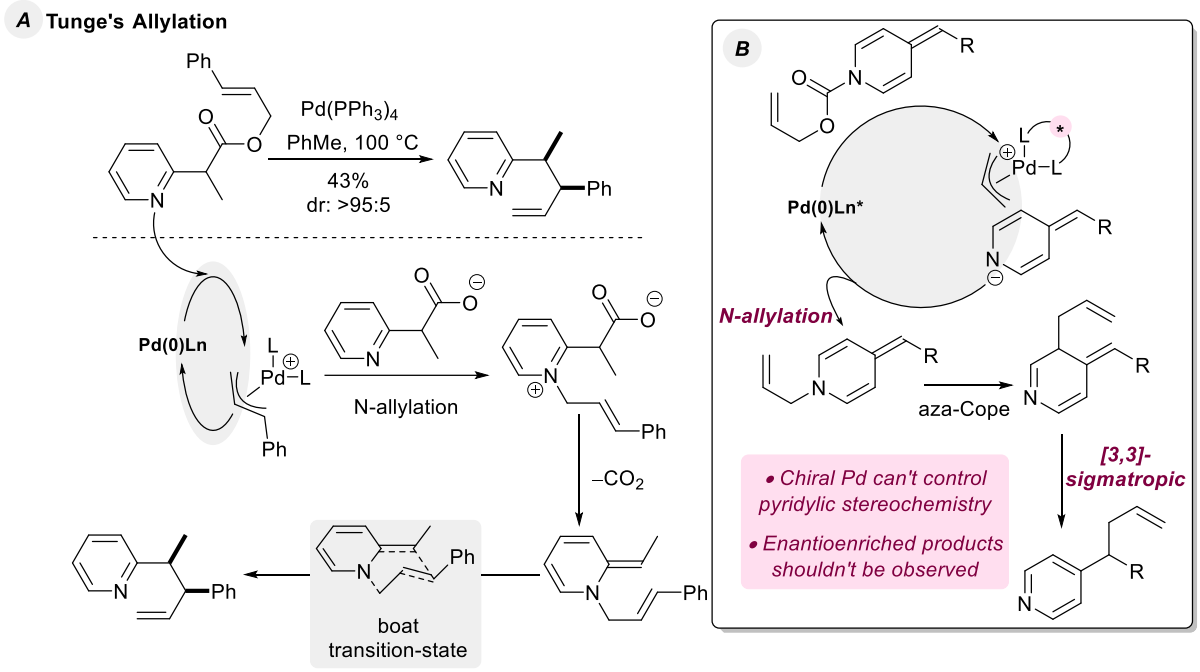

Scheme 16: A) Mechanism of Tunge's decarboxylative allylation of 2-pyridyl cinnamyl esters, and B) a mechanistic proposal for the palladium-catalyzed allylation of 4-alkylpyridines involving N-allylation followed by two sequential sigmatropic rearrangements.

Examining transition-metal catalyzed pyridylic allylation methods that rely on pyridylic deprotonation for functionalization,[37,38,40] it is clear that their functional group compatibility is limited, as can be expected in the presence of a highly basic species that is introduced in super stoichiometric amounts at the outset of the reaction. In stark contrast, our palladium-catalyzed allylation of 4-alkylpyridines displays very broad functional group tolerance, which is at first glance inconsistent with the presence of a strongly basic pyridylic anion, as proposed in **scheme 13**. In addition, our inability to achieve high enantio-discrimination using ligands previously successful in stereoinduction in inner-sphere processes casts doubts on the presence of "hard" pyridylic anions. We therefore began considering alternative catalytic cycles that do not invoke the formation of highly basic nucleophiles. Lundgren recently showed Ir and Pd catalyzed pre-decarboxylative allylation of aryl acetic acids, which proceed through allylation of the active methylene compounds followed by proto-decarboxylation (**Scheme 17**).[42] This process is mechanistically distinct from regular decarboxylative coupling pathways since the bond forming

event takes places prior to the release of CO_2, thereby avoiding the generation of highly basic benzylic anions.[54]

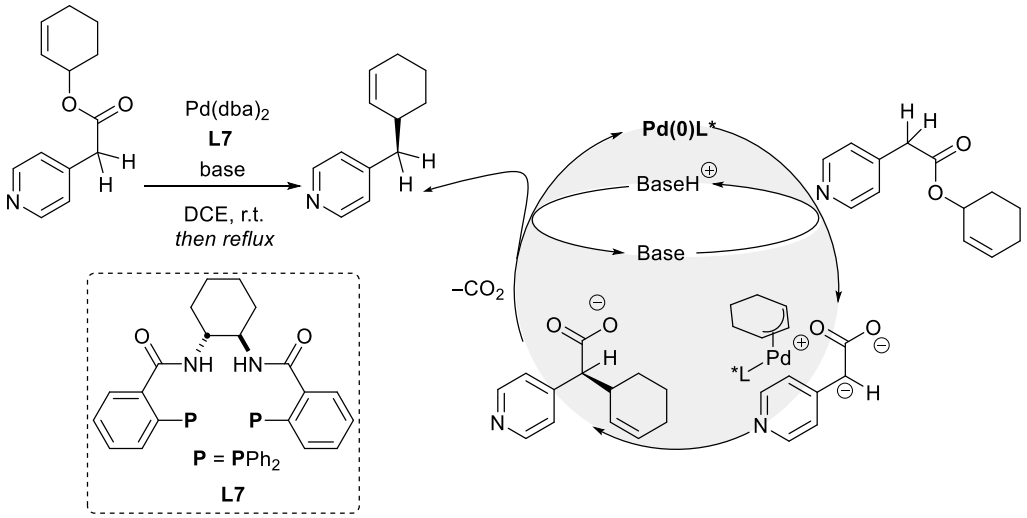

Scheme 17. Lundgren's enantioselective palladium catalyzed pre-decarboxylative allylation of aryl acetic acids.

A conceptually similar pre-decarboxylative coupling pathway can be envisioned in our system. Ionization of ADHP can generate a dihydropyridine bound carboxylate and allylpalladium(II) as an ion pair. Pyridylic attack onto the electrophilic allyl group followed by decarboxylation forms the coupled product (**Scheme 18**). Verifying this pathway experimentally would be extremely challenging since carbamic acid derivatives are inherently unstable,[55] therefore isolating these intermediates would not be a trivial task.[56] However, deactivation of Trost ligand **L7** in our system weakens this proposal. Since we found that protection of the amide nitrogen of the Trost ligand is necessary to avoid catalyst inactivity, it is likely that the amide backbone is deprotonated by a pyridylic nucleophile. This deprotonation is more likely to occur by a strongly basic species rather than through proto-decarboxylation and therefore is inconsistent with the presence of a carboxylate group during the bond forming event (**Scheme 18**). Nevertheless, this mechanistic proposal cannot be dismissed since we do not have strong evidence to disprove it.

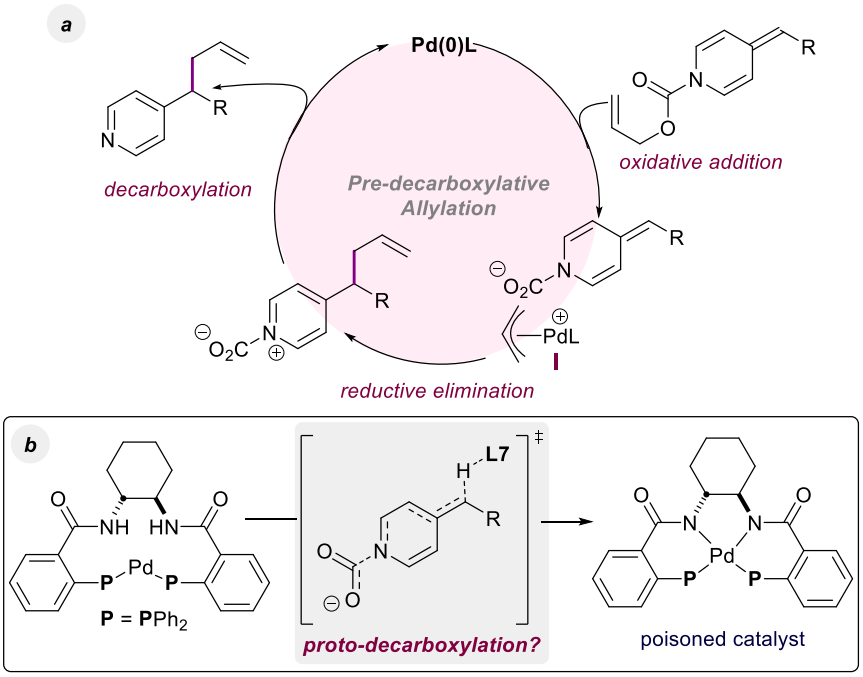

Scheme 18. a) A pre-decarboxylative allylation mechanistic proposal for the palladium-catalyzed allylation of 4-alkylpyridines, and b) the possibility of proto-decarboxylation deactivating a Pd-Trost ligand catalyst system.

Another possible catalytic cycle involves alkylidene dihydropyridines themselves being the primary nucleophiles in the reaction rather than pyridylic anions (**Scheme 19**). In this scenario, oxidative addition onto an ADHP initiates the allylation cycles by generating π-allylpalladium(II) complex **I**. This complex can then be intercepted by another molecule of ADHP, forming a new C-C bond and producing an allylated pyridinium salt **IV** bearing a highly activated allylic carbamate fragment and Pd(0). Oxidative addition onto the allylic electrophile, followed by decarboxylation releases the coupled product and regenerates the π-allylpalladium(II) active catalyst. As shown in **scheme 19**, to initiate this pathway, a catalytic amount of the pyridylic anion has to be released. In order for the π-allylpalladium(II) complex to be intercepted by an ADHP rather than a more nucleophilic pyridylic anion, the initially formed pyridylic anion-Pd(II) ion pair have to be solvent-separated. In addition, facile oxidative addition across the allylated pyridinium salt **IV** must take place in order for the cycle to be maintained and prevent oxidative addition across ADHPs, which would divert the cycle into that shown in **scheme 13**.

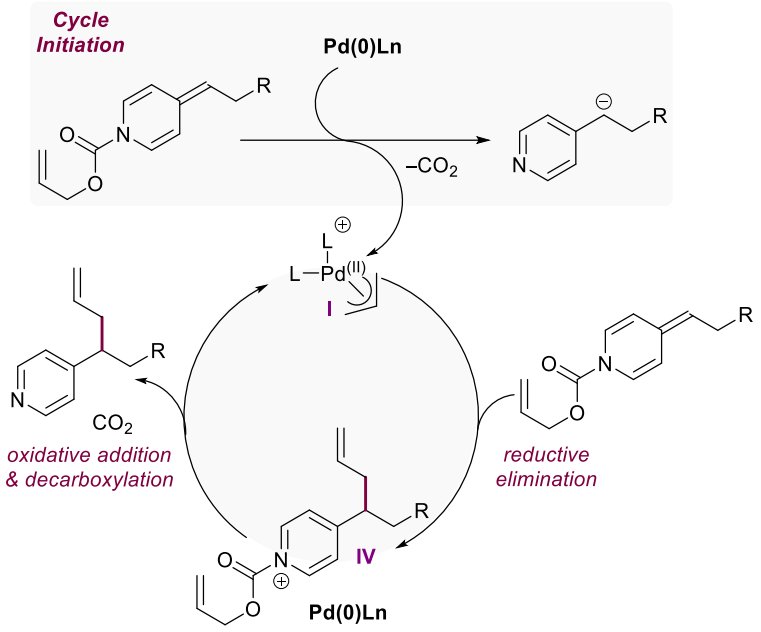

Scheme 19. An alternative mechanistic route for the palladium-catalyzed pyridylic allylation involving alkylidene dihydropyridines acting as primary nucleophiles.

As shown above, our allylation reaction could be proceeding through a number of different routes. Observing stereoinduction with some optically pure ligands eliminated the pathway involving N-allylation and subsequent sigmatropic rearrangements. Possible mechanistic routes can be split into two categories, one where a highly nucleophilic pyridylic anion is present and another involving a less basic ADHP in the bond forming step. In order to differentiate the two, we planned to investigate the nature of the ion pair, separated or tight, since it will inform on the possibility of a cycle dominated by ADHPs acting as primary nucleophiles, as proposed in **scheme 19**. In addition, we aimed to probe the mode of reductive elimination, because not only will it help us distinguish between the proposed cycles but also will aid in our enantioselective development. If reductive elimination is an inner-sphere process, then the presence of hard nucleophiles would be supported and would support the generation of pyridylic anions. On the other hand, if outer-sphere reductive elimination is observed, more support would be lent to pathways involving ADHP nucleophiles, including the pre-decarboxylative route. Being able to differentiate these mechanisms will grant us better understanding of the reaction and will allow us to better cater to the enantioselective development including choosing the proper class of ligands for the transformation.

3.2 Probing the Nature of Ion-Pairs in the Catalytic-Cycle

Investigating the nature of the ion pair is one of our primary interests since it will inform on the validity of ADHPs behaving as primary nucleophiles. Tight ions pairs cannot initiate a catalytic cycle in which ADHPs are primary nucleophiles since it will result in reductive elimination through the more nucleophilic pyridylic anion. Therefore, determining the nature of the ion pair can aid in assessing the plausibility of the catalytic cycle shown in **scheme 19**. To conduct this investigation, we planned a cross-over experiment where two different pyridines are activated using chloroformates bearing distinct allyl substituents (**Scheme 20**). Subjecting this ADHP mixture to Pd(0), oxidative addition and decarboxylation are expected to take place generating two separate ion pairs, each with differentiated pyridylic anions and π-allylpalladium(II) complexes. If the ion pairs are tightly bound inside the solvent cage, we should expect reductive elimination to take place generating the non-cross over intramolecular-coupled products. Alternatively, if the ions can escape the solvent cage, cross-over would take place and four different allylation products will form, the intramolecular and intermolecular-coupled pyridines.

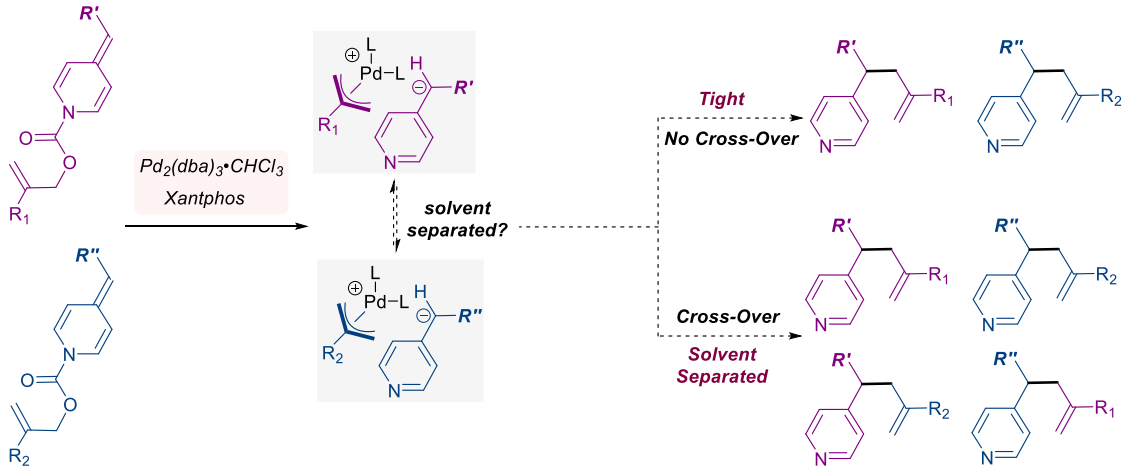

Scheme 20. Approach towards probing the nature of the ion pair generated during the allylation reaction.

We attempted this cross-over experiment using an ADHP activated with allyl chloroformate and another formed using 2-methallyl chloroformate (not shown), however, we found that the rate of reaction of both differed, probably a result of the different steric and electronic effects caused by the additional methyl group. This rate difference made our results slightly difficult to interpret, therefore, we elected to use 2-methallyl chloroformate and its deuterated equivalent in order to

avoid any difference in reactivity. Deuterated methallyl alcohol was synthesized by first alkylation of diethyl malonate using iodomethane d_3 (≥99.5 atom % D) forming the mono-methylated (d_3) product in 73% yield (**scheme 21**). Base mediated di-ester hydrolysis proceeded quantitatively generating the d_3-methylated malonic acid which was directly subjected to the Doebner-modification of Knoevenagel condensation forming 2-methylacrylic acid-d_3.[57] This reaction proceeds through enolization of the malonic acid which facilitates nucleophilic attack onto an iminium ion generated through condensation of diethylamine with paraformaldehyde (**Scheme 21**). Protonation of the amine turns it into a good leaving group and allows malonate decarboxylation to induce an E1cB sequence forming the α,β-unsaturated product. Lithium aluminium hydride mediated 1,2-reduction proceeded cleanly forming the deuterated methallyl alcohol **16** albeit in low yield.

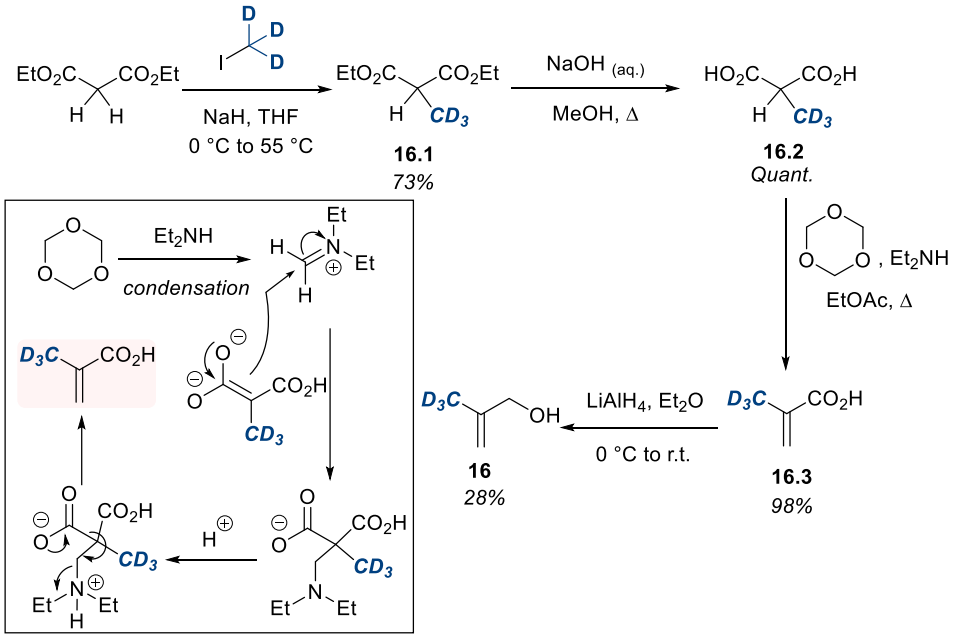

Scheme 21. Synthesis of methallyl alcholol d_3 utilizing ethyl malonate as starting material.

Before conducting the cross-over experiment, we prepared allylation products of 4-phenethylpyridine **1** and 4-pentylpyridine **17** using methallyl chloroformate and methallyl chloroformate-d^3 as shown in **scheme 22**. These were prepared as standards for the cross-over experiment in order to obtain their spectroscopic data as reference.

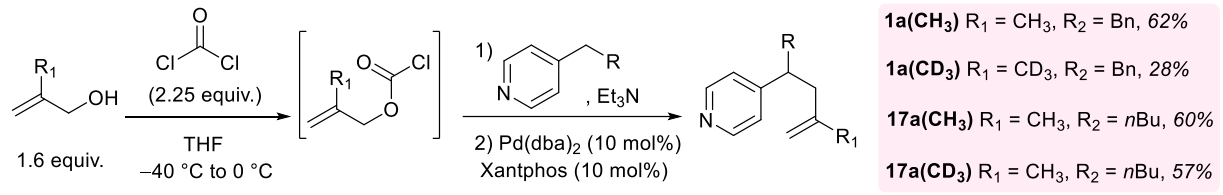

Scheme 22. Preparation of allylation products using methallyl and d_3-methallyl chloroformates as standards for the cross-over experiment.

To set up the cross-over experiment, chloroformates of methallyl and deuterated methallyl alcohols were synthesized separately by subjecting them to excess phosgene (used as a DCM solution) at low temperatures (−40 °C) as shown in **scheme 22**. Each was then introduced to the appropriate pyridine (**Scheme 23**) to afford ADHPs **1'(CH₃)** and **17'(CD₃)**. Exposing a 1:1 mixture of these ADHPs to standard allylation conditions provided a complex crude mixture. The two sets of products (**1a(CH₃)** + **1a(CD₃)** and (**17a(CH₃)** + **17a(CD₃)**) were separated using flash chromatography. The ratio of deuterated to methylated products was determined using either quantitative ^{1}H or ^{2}H NMR. We found that a mixture of all four possible coupled pyridines was obtained in approximately 1.75:1 ratio of non-crossover to crossover products (**Scheme 23**). It is worth noting that the overall yield for this reaction is consistent with the yields obtained for the synthesis of the individual standards (**Scheme 22**)

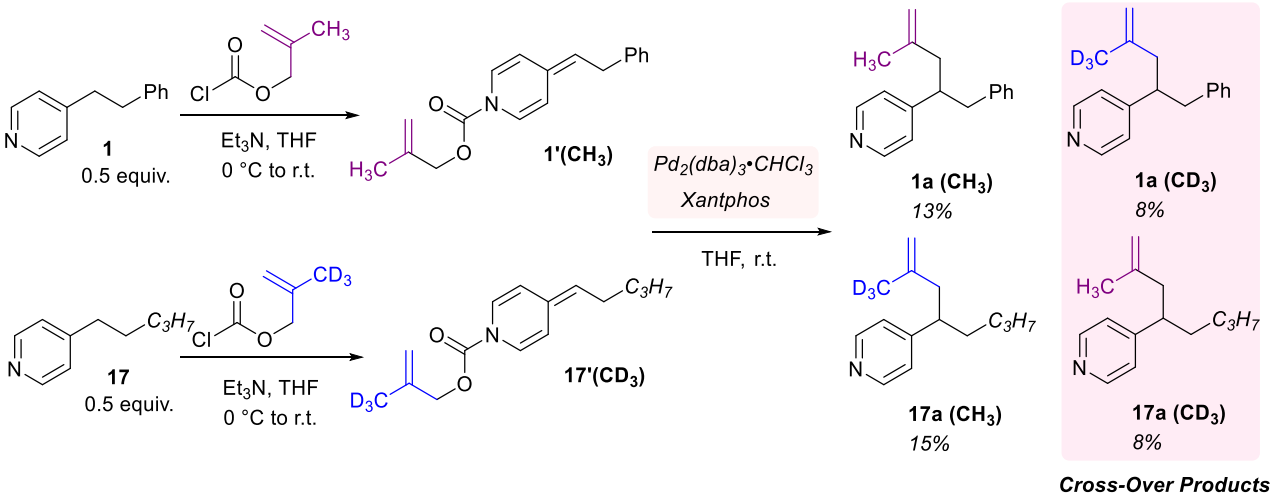

Scheme 23. Establishing the nature of the ion pair generated in the allylation of 4-alkylpyridines.

These cross-over results establish the presence of solvent-separated ion pairs in the reaction, supporting the possibility of ADHPs assuming a nucleophile role in the sequence. As can be

inferred from the product distribution obtained, the domination of non-crossover product suggests that the rate of reductive elimination is faster than the rate of ion pair separation, which may indicate that pyridylic anions and ADHPs are both active nucleophiles throughout the reaction.

3.3 Investigating the Mode of Reductive Elimination[1]

At the outset of our enantioselective studies we had envisaged that the allylation reaction proceeds through an inner-sphere reductive elimination of a "hard" pyridylic anion. Failure of optically pure ligands to impart high enantioselectivity led us to question our understanding of the reductive elimination step. Therefore, we wanted to directly validate the mode of reductive elimination since it will dictate the class of ligands required to provide more enantioenriched products. A common strategy for exploring the mechanism of the reductive elimination step is through the use of a stereochemical probe.[40a,51] In allylation reactions, the overall change in stereochemistry at the allylic site allows differentiation between the two modes of reductive elimination. To illustrate, consider a typical palladium-mediated allylation of a cyclohexenyl electrophile shown in **scheme 24**. Oxidative addition across the allylic electrophile proceeds through an S_N2 pathway, forming the π-allylPd(II) complex **I** with inversion in configuration at the allylic position. If inner-sphere reductive elimination takes place, the nucleophile first bonds to the metal centre (**Scheme 24** – complex **II**) then undergoes reductive elimination with an overall inversion in configuration. Alternatively, in an outer-sphere process, the incoming nucleophile directly attacks the allyl group in an S_N2 fashion displacing the metal and reducing it in the process. This results in overall retention in configuration at the allylic position. Therefore, by investigation the stereochemical outcome of the reaction we can deduce the mode of reductive elimination.

[1] *The work in this section was conducted in collaboration with Isabelle Hunter. Although we both have conducted extensive experimentation to investigate the mode of reductive elimination, the final stereochemical probe results were obtained from Isabelle Hunter.*

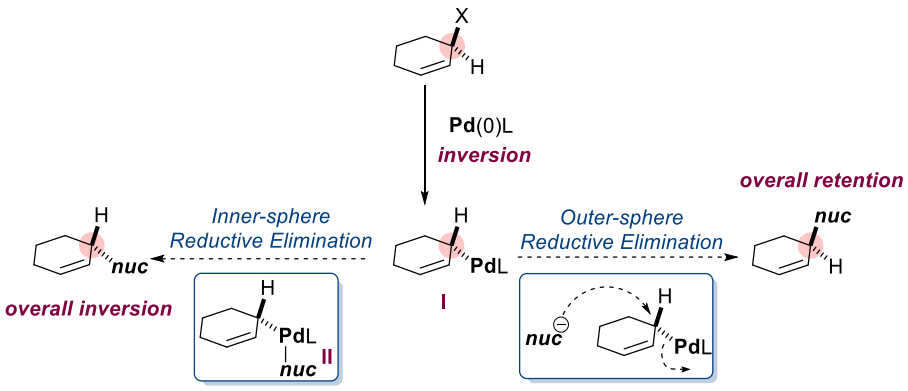

Scheme 24. General overview of inner-sphere and outer-sphere reduction elimination processes in allylation reactions. Allyl-palladium intermediates are shown as σ-complex to clearly demonstrate stereochemical change in the allylic system.

To keep track of the change in allylic stereochemistry, we aimed to synthesize ADHP **17''** as a single *cis*-diastereomer. Depending on the mode of reductive elimination, one of two diastereomeric allylation products will form (**Scheme 25**). Subjecting ADHP **17''** to our standard allylation conditions should induce oxidative addition with inversion in stereochemistry as shown in **scheme 25**, generating an allyl system bearing phenyl and palladium(II) substituents with an anti-relationship. If inner-sphere reductive elimination takes place, we should observe an overall inversion in stereochemistry and obtain *trans*-diastereoselectivity. On the other hand, if the *cis*-diastereomer is observed then an outer-sphere reductive elimination occurred, with a net retention in stereochemistry.

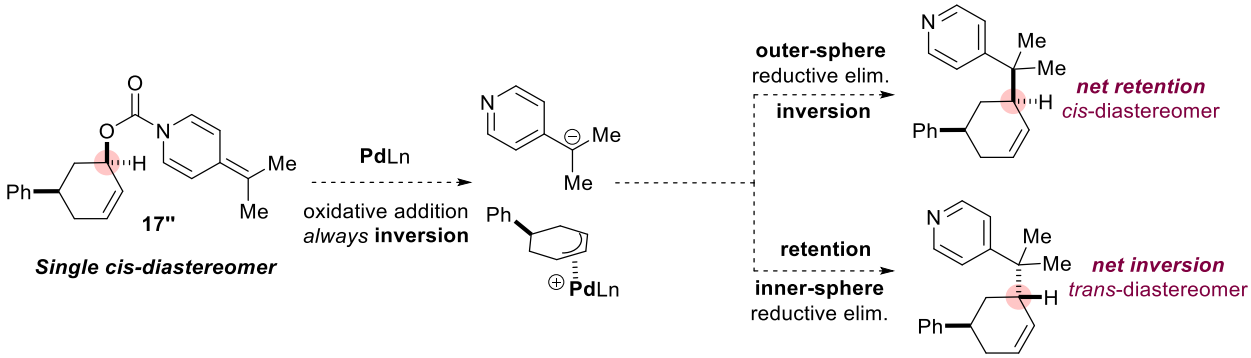

Scheme 25. Approach for probing the mode of reductive elimination of our pyridylic allylation reaction.

We attempted the synthesis of ADHP **17''** through first accessing the corresponding chloroformate of *cis*-5-phenylcyclohex-2-enol **16**, which was prepared according to known

procedure utilizing 5-phenyl-1,3-cyclohexanedione as starting material (**Scheme 26A**).[58] Formation of the vinylogous isobutyl ester followed by 1,4-reduction using lithium aluminium hydride provided access to cyclohexenone **18.1**. Luche reduction of the enone exclusively formed the *cis*-diastereomer of 5-phenylcyclohexenol which was confirmed through observing NOE correlations between protons at the 1 and 5 positions (**Scheme 26A**). We then attempted to synthesize chloroformate **18'** through phosgenation of the cyclohexenyl alcohol, unfortunately, this system is prone to decomposition and forms 5-phenylcyclohexenyl chloride as side product (**Scheme 26B**).[59] After many attempts and even under rigorous temperature control, we could not access the ADHP cleanly. Therefore, we resorted to an alternative sequence for this synthesis (**Scheme 26C**). Enolization of pyridine **19** using phenyl chloroformate and triethylamine formed ADHP **19'**, phenoxide substitution was then undertaken using KHMDS deprotonated 5-phenylcyclohexenol providing ADHP **19''**. We found that ADHP **19''** readily hydrolyses in water, therefore, to remove the potassium phenoxide by-product, the crude mixture was triturated using toluene.

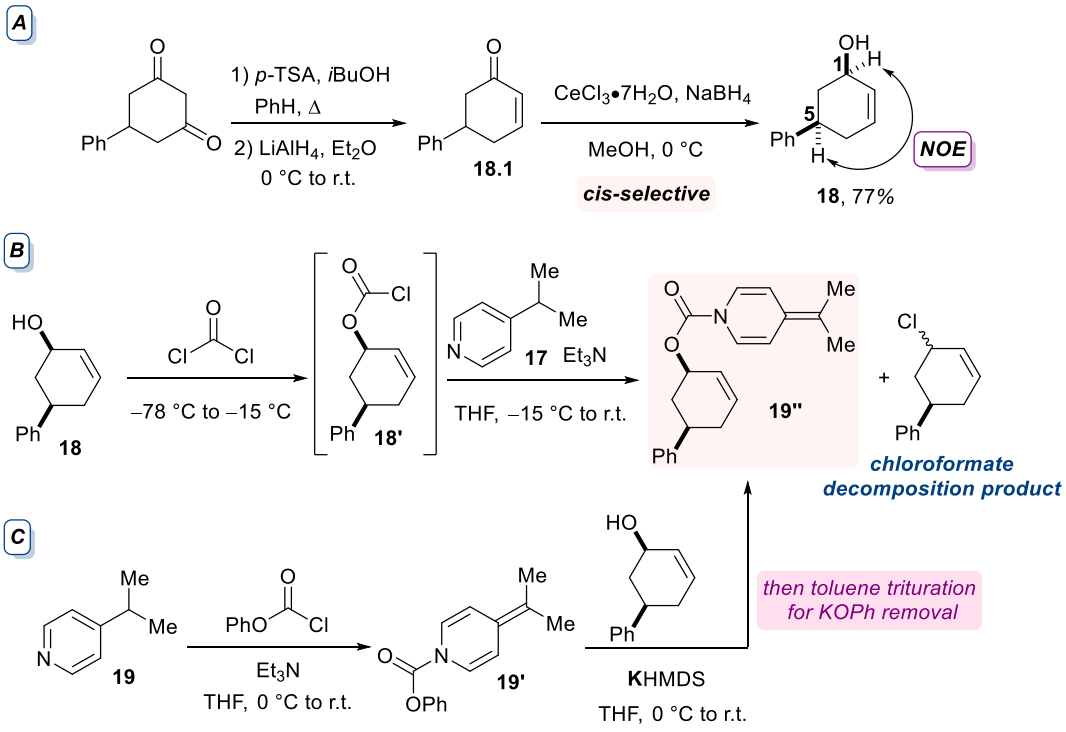

Scheme 26. Synthesis of stereochemical probe ADHP **17''**.

We found that allylation of the stereochemical probe ADHP **19''** using the standard Pd-Xantphos system proceeded with an overall retention of stereochemistry at the allyl position forming the *syn*-diastereomer of the substitution product as confirmed by the NOE interaction of the methyne protons highlighted in **scheme 27**. The exclusive formation of this diastereomer reveals that the reaction undergoes an outer-sphere reductive elimination pathway. This is remarkable because if pyridylic anions are involved in this reaction, as suggested by prior experiments (c.f. **Scheme 15**, **L7** vs. **L8**), this would raise the pKa boundary for palladium-catalyzed outer-sphere allylation beyond the current limit of 32.

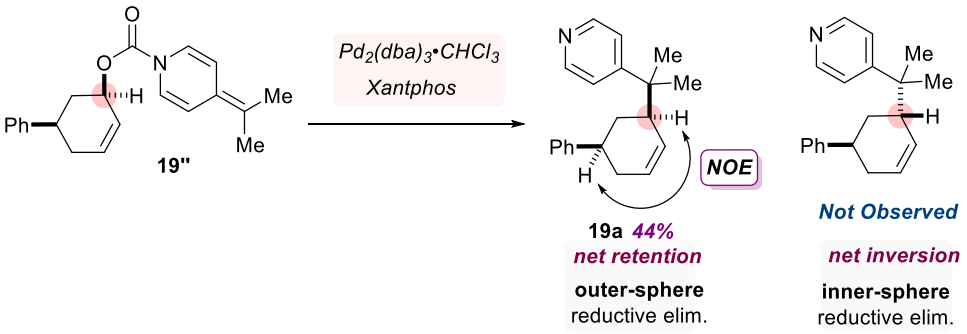

Scheme 27. 4-Alkylpyridines undergo outer-sphere reductive elimination in our palladium-catalyzed allylation reaction. Results obtained from Isabelle Hunter.

3.4 Investigating the Nature of the Nucleophile

Establishing that the allylation proceeds through a solvent-separated ion pair and undergoes reductive elimination through an outer-sphere pathway provides more support to a mechanism operating by simple ADHP nucleophiles or through a pre-decarboxylative route. Since it remains unclear if pyridylic anions are involved in our reaction, we aimed to validate if ADHPs are sufficiently nucleophilic to participate in pyridylic allylations. To do this, we prepared [(Xantphos)Pd(π-allyl)]OTf complex **C1** through a ligand exchange-anion metathesis sequence (**Scheme 28A**).[60] We then synthesized an ADHP activated using ethyl chloroformate, which is incapable of ionizing due to the absence of oxidative addition sites previously available in ADHPs activated by allyl chloroformate, and subjected it to stoichiometric amounts of complex **C1** (**Scheme 28B**). We rationalized that by supressing the ionization pathway, any allylation that would take place would reflect the ability of ADHP **1''** to act as a nucleophile towards π-

allylpalladium(II) species. It is worth mentioning that we chose [(Xantphos)Pd(π-allyl)]OTf as reagent because it closely mimics our reaction system, which is free of any coordinating spectator ions. In addition, DCM was used as solvent because complex **C1** proved insoluble in THF. We found that reaction of ADHP **1''** with complex **C1** in a 1:1 ratio produced **1a** in 88% yield after hydrolytic workup, showing that indeed ADHPs are competent nucleophiles. It is important to note that despite being stoichiometric in palladium, we found that the rate of this reaction is slower than that of the parent allylation process, requiring more time for the full consumption of the ADHP.

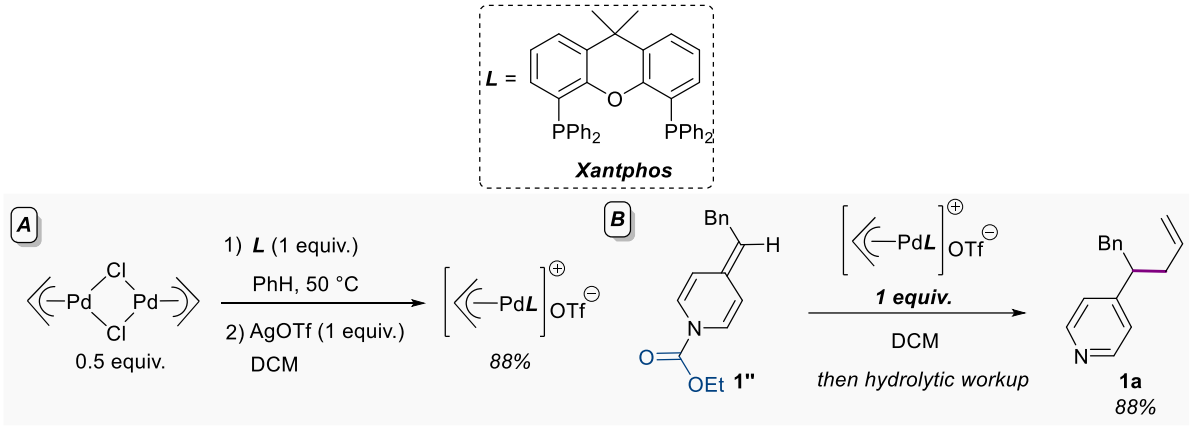

Scheme 28. A – Preparation of [(Xantphos)Pd(π-allyl)]OTf complex **C1**. B – Testing the nucleophilicity of the non-ionizable ADHP **1''** through a stoichiometric reaction with complex **C1**.

It is therefore clear that ADHPs can behave as nucleophiles towards allylic electrophiles. However, the slow rate of the stoichiometric allylpalladium reaction raised questions about the ability of ADHPs to initiate and maintain a catalytic allylation cycle. To test the competence of ADHPs in initiating a catalytic system, we planned to subject allyl chloroformate activated ADHP **1'** to 1 mol% (a standard catalyst loading) of complex **C1**. Using complex **C1** as a catalyst prevents formation of pyridylic anions in the initiation stage and forces the reaction to proceed through a cationic manifold in which ADHP attacks the allylpalladium complex, at least in the first cycle, to achieve allylation. Treating ADHP **1'** to 1 mol% of complex **C1** formed the allylated pyridine **1a** in 92% yield (**Scheme 29**). Although this demonstrates that the reaction can be sustained in the absence of pyridylic anions formed in the initiation stage, it doesn't fully support an anion free

mechanism since formation of Pd(0) can divert the cycle to an anionic pathway through reaction with a molecule of ADHP as seen in **scheme 29B**.

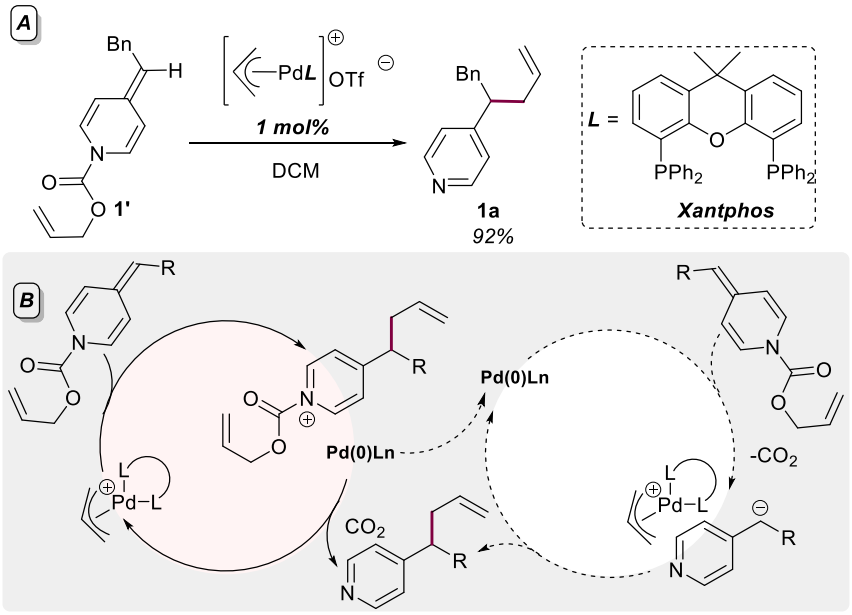

Scheme 29. Establishing the ability of ADHPs to initiate and sustain allylation in a catalytic setting.

It is reasonable to expect that pyridylic anions should be more nucleophilic than neutral ADHPs. Therefore, we resorted to qualitative rate comparisons to probe the different reactivity patterns of both nucleophiles. By treating a mixture of equal amounts of an ADHP incapable of ionizing, prepared using ethyl chloroformate, and an ionizable, allyl chloroformate activated ADHP with our standard catalytic conditions for allylation we can investigate if an ADHP can outcompete a pyridylic anion in the presence of a π-allylpalladium(II) electrophile (**Scheme 30**). The design of this experiment forces cycle initiation to proceed through selective ionization of ADHP **6'** which forms the allylating π-allylpalladium(II) electrophile **I** and releases the anion of pyridine **6**. The electrophile generated can be intercepted by pyridylic anion **6''**, ADHP **6'** or ADHP **1'**. We expected that if a mixture of allylation products **1a** and **6a** is observed, it will indicate that ADHPs are competent nucleophiles even in the presence of the more reactive pyridylic anions. Alternatively, if **6a** is the sole product it will validate that ADHPs are not sufficiently nucleophilic to engage in allylation when in competition with pyridylic anions. As predicted, we found that after hydrolytic workup, allylation took place to provide pyridine **6a** exclusively in 73% yield (**Scheme 30**), with no sign of reaction of ADHP **1''** which was recovered in 76%.

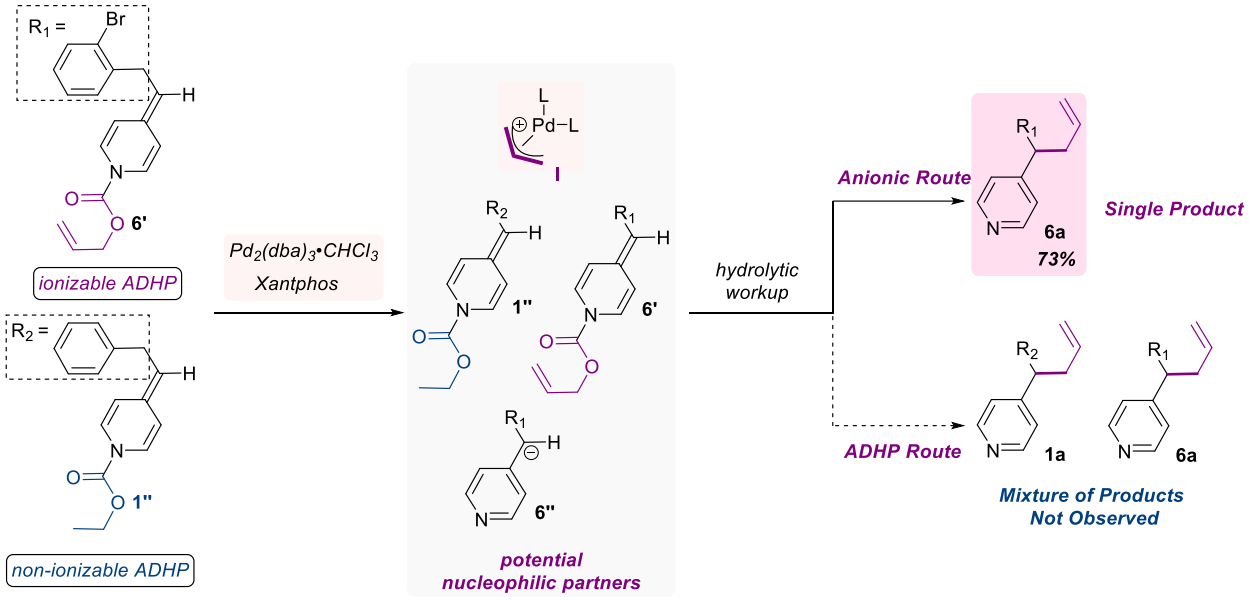

Scheme 30. Cross-over experiment between ionizable and non-ionizable ADHPs to probe the relative rates of allylation of a neutral ADHP and a pyridylic anion.

To further dismiss the likelihood that an ADHP is an active nucleophile in the reaction, we conducted a head-to-head comparison between the kinetic profiles of allylation using standard catalytic conditions ($Pd_2(dba)_3$-Xantphos) and that using complex **C1** as catalyst. Reaction progress was recorded by monitoring ADHP consumption and product formation through quantitative ^1H NMR spectroscopy. To construct the kinetic profiles, a 50mg batch of 4-phenethylpyridine **1** was enolized using our standard conditions to obtain a stock of ADHP **1'**. Two portions of the ADHP were withdrawn, each constituting one fifth of the total crude mass. Each of the 2 portions were dissolved in 0.79 mL of CD_2Cl_2 and transferred to NMR tubes. Stock solutions of each catalytic system were prepared in CD_2Cl_2 with equal concentrations of [0.01 M] – 0.21 mL of the appropriate complex was introduced, and the solution was quickly mixed and immediately placed in the NMR spectrometer. The reactions were monitored for approximately 6.5 hours, recording a scan every minute with relaxation delay set to 60 seconds. The collected scans were analyzed using Bruker Dynamics Center 2.5.5 to obtain the decay of the intermediate and rise of the allylated product and the data points were plotted using Excel to generate the graphs shown in **scheme 31**.

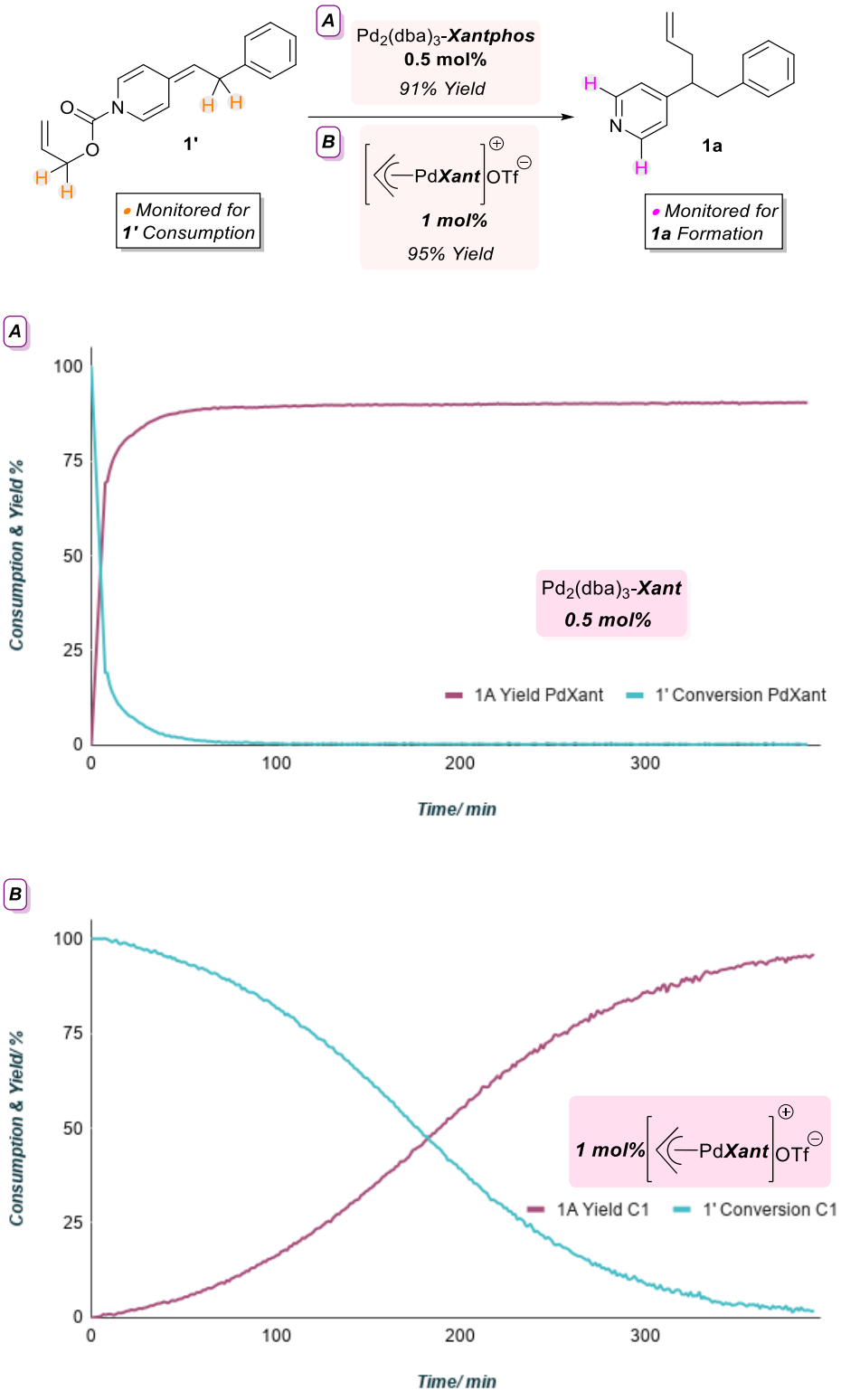

Scheme 31. A) Reaction profile for allylation using standard catalytic conditions ($Pd_2(dba)_3$ and Xantphos), B) reaction profile for allylation using complex **C1** as catalyst.

As shown in **scheme 31**, the two experiments have varying reaction progress whereby the Pd-Xantphos system exhibits fast kinetics with the product rise plateauing around 50 minutes (**Scheme 31A**). On the other hand, the [(Xantphos)Pd(π-allyl)]OTf complex showed slow and steady growth of product and reached completion after 6 hours (**Scheme 31B**). If allylation proceeds through ADHP attack as in **scheme 19**, the kinetic profile of the standard Pd-Xantphos system (**Scheme 31A**) should resemble that of complex **C1** (**Scheme 31B**). This divergent behaviour of reactions supports the mechanism outlined in **scheme 13**, and indicates that in competition with a pyridylic anion, it is unlikely that an ADHP is an active nucleophile in our allylation reaction.

3.5 Conclusions & Future Work

Our mechanistic investigation allowed us to establish a fundamental understanding of how the allylation reaction proceeds. Currently, we believe that the mechanism of the allylation most likely proceeds as in **scheme 32** whereby Pd(0) oxidatively adds across the allylic site of an ADHP, decarboxylation forms a solvent-separated ion pair of the π-allylpalladium(II) complex and pyridylic anion. In an outer-sphere fashion, the pyridylic nucleophile directly attacks the allyl group displacing Pd(II), reducing it in the process and turning over the catalytic cycle. Our allylation demonstrated exceptional functional group compatibility not witnessed in other pyridylic allylations that rely on stoichiometric pyridylic deprotonation. We believe that the catalytic generation of the reactive anion accompanied with fast rate of reductive elimination prevents unwanted side reactions with reactive functionality. In the future, we plan to investigate the rate order with respect to palladium. A possible mechanistic pathway is one that is bimetallic in nature, where two palladium species could be working in concert to form the coupled product. These investigations are currently ongoing in the group.

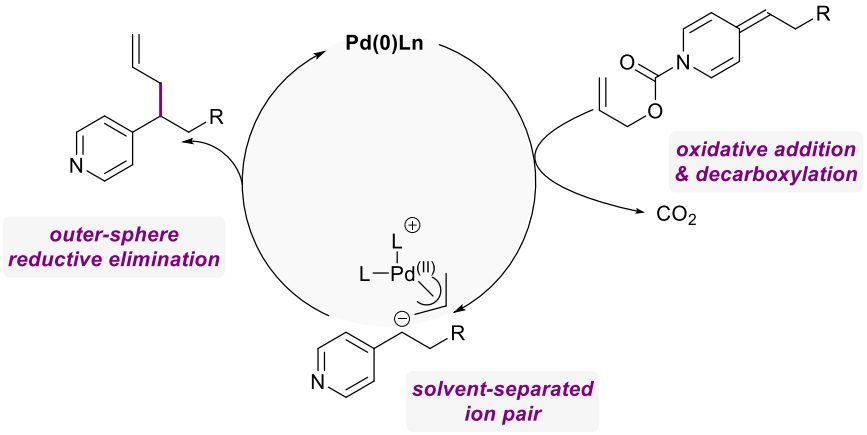

Scheme 32. Refined mechanism for the palladium-catalyzed allylation of 4-alkylpyridines.

Going into this mechanistic study, we had hoped to find clues into why we could not achieve stereochemically controlled allylation. Indeed, the kinetic investigations inspired a new direction for the enantioselective studies. Since we know that the active nucleophile is a high energy pyridylic anion, according to Hammond's postulate, it is reasonable to expect the bond forming reductive elimination transition state to closely resemble the pyridylic nucleophile (that is, it has a low activation barrier). In asymmetric allylation, this would translate into having both diastereomeric reductive elimination transition states easily accessible (**Scheme 33a**), and therefore we should not see significant differentiation between the two enantiomeric products, which is mainly what we observe. We wonder if by employing a lower energy nucleophile we can induce enantioselecivity by effectively raising the activation barrier for both diastereomeric transition states, which should result in enhanced enantioselectivity (**Scheme 33b**). Therefore, we plan to examine reactions of ADHPs with chiral π-allylPd(II) complexes and explore the impact of this strategy on the stereochemical outcome of the reaction.

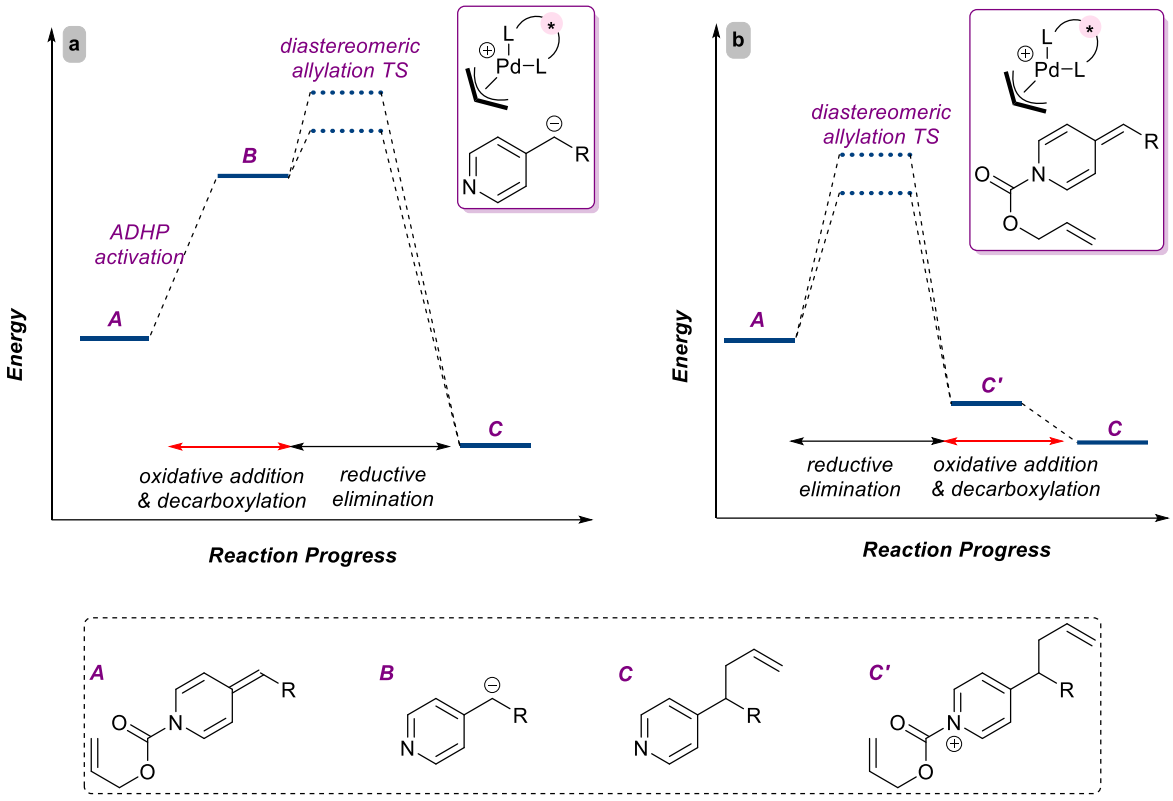

Scheme 33. Predicted reaction energy profiles for asymmetric allylation using pyridylic anions vs. neutral ADHPs.

CHAPTER 4: CONCLUSIONS

Driven by the importance of pyridines in drug discovery and the need for developing mild and scalable reactions to functionalize heterocycles, the Orellana group started a campaign for lateral pyridylic functionalization using a soft enolization approach for hetero-benzylic activation. Reacting pyridines with allyl chloroformate and triethylamine provides access to alkylidene dihydropyridines capable of engaging in palladium-catalyzed decarboxylative coupling. Optimizing this reaction, the group was able to induce pyridylic allylation and developed a mild and valuable method for this transformation. We extended this work and developed the first palladium-catalyzed dehydrogenation of 4-alkylpyridines as a reliable strategy to access 4-alkenylpyridines. We found that dehydrogenation can be effected by subjecting alkylidene dihydropyridines to a simple ligandless palladium (0) catalytic system. Substrate scope studies and functional group compatibility screen showed that our dehydrogenation tolerated a wide range of functional groups including electrophilic and acidic functionality. Our method is selective of the 4-position even in systems bearing multiple pyridylic sites.

Since our allylation method can provide a handle into reliably accessing complex molecules we wanted to pursue an enantioselective variant of the reaction. Unfortunately, screening chiral ligands showed that stereochemical discrimination is a challenge. Therefore, we conducted a mechanistic study to gain a clearer understanding of how the reaction proceeds so we can adjust our strategy towards stereochemical control. Through mechanistic probes, we found that the reaction proceeds through Pd(0) induced oxidative addition and decarboxylation generating a solvent-separated pyridylic anion- π-allylPd(II) ion pair. In an outer-sphere fashion, the pyridylic anion attacks the electrophilic allyl group forming the coupled product and regenerating the Pd(0) species. Our mechanistic study provided insights into possible explanations behind the low enantioselectivity obtained and inspired a new strategy to harness stereochemical control.

CHAPTER 5: EXPERIMENTAL

5.1 General Experimental

All reactions were conducted in flame- or oven-dried glassware under an atmosphere of argon using anhydrous solvents unless specified otherwise. Tetrahydrofuran (THF), diethylether (Et_2O), dichloromethane (DCM) and toluene were dried using an INERT® PureSolv solvent purification system. Commercial reagents were used as received. Thin-layer chromatography was performed on SiliCycle® silica gel 60 F254 plates. Visualization was carried out using UV light (254 nm) and/or $KMnO_4$, $(NH_4)_2Ce(NO_3)_6$, vanillin, or anisaldehyde stains. Flash column chromatography[61] was carried out using SiliCycle® Silia*Flash*® silica gel (230-400 mesh, 40- 63 µ, 60 Å pore size). Hexanes (ACS grade) and ethyl acetate (ACS grade) were used as received. ^{1}H-NMR and ^{13}C-NMR spectra were recorded on a Bruker 400 AV, Bruker DRX 600 or Bruker 300 AV spectrometer in chloroform-d (99.8 % deuterated). Spectra recorded using chloroform were calibrated to 7.26 ppm ^{1}H and 77.16 ppm ^{13}C. ^{31}P-NMR spectra were obtained at 122 MHz and chemical shifts are reported relative to an 85% H_3PO_4 external standard. Chemical shifts (δ) are reported in ppm and multiplicities are indicated by s (singlet), d (doublet), t (triplet), q (quartet), p (quintet), sext (sextet), sept (septet), dd (doublet of doublets), dt (doublet of triplets), td (triplet of doublets), qd (quartet of doublets), ddd (doublet of doublet of doublets), tdd (triplet of doublet of doublets), dddd (doublet of doublet of doublet of doublets),[62] m (multiplet) and br (broad). Coupling constants *J* are reported in Hertz (Hz). Infrared (IR) spectra were recorded as thin films (neat) using AlphaPlatinum ATR, Bruker, diamond crystal FT-IR instrument.

5.2 Pyridylic Dehydrogenation: Preparation of Substrates – Procedures and Structural Data

Procedure 1: *Alkylation of 4-methylpyridine*

A flame-dried round-bottomed flask equipped with a stir bar was charged with freshly distilled diisopropylamine (1.1 equiv.) in THF and cooled to −78 °C. To this solution, *n*-BuLi (1.0 equiv., 1.6 M in hexanes) was added dropwise and the mixture was stirred for 15 min to form LDA. A solution of 4-methylpyridine (1.0 equiv.) in THF was introduced at the same temperature. The deprotonated picoline was transferred via cannula to a round-bottomed flask containing the electrophile (1.0 equiv.) in THF. The reaction was kept at −78 °C for 1 h and then allowed to warm slowly to room temperature overnight. The reaction was quenched with water, and the aqueous layer was extracted three times with EtOAc. The combined organics were then washed with brine, dried using $MgSO_4$ and concentrated *in vacuo*. Unless otherwise stated, the product was purified by the following method. The crude mixture was dissolved in minimal DCM and was treated with pentane. The resulting suspension was filtered through a cotton plug and the filtrate was concentrated *in vacuo* to obtain the desired product.

Procedure 2: *Alkylation of pyridines by Knochel's method*[48]

A flame-dried round-bottomed flask equipped with a stir bar was charged with the appropriate pyridine (1.0 equiv.) as a solution in THF and cooled to 0 °C. BF_3•OEt_2 (1.1 equiv.) was added dropwise and the mixture was stirred for 15 min. The reaction mixture was then cooled to −50 °C and a THF solution of the required alkyl Grignard reagent (1.3 equiv.) was added. After 30 min, chloranil (2.0 equiv.) was added, the mixture was warmed up to room temperature and stirred for 2 additional hours. The reaction was quenched with $NH_4OH_{(aq.)}$ (1.0 mL/mmol of pyridine), filtered through a pad of Celite® and extracted thrice with diethyl ether. The combined organics were washed with brine and dried with $MgSO_4$. The product was concentrated *in vacuo* and purified using flash column chromatography.

4-(2-Phenylethyl)pyridine (**1**, CAS 2116-64-5)

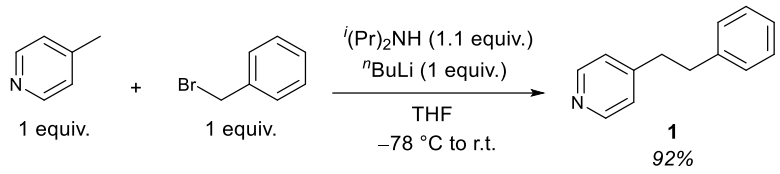

Substrate **1** was synthesized according to procedure 1 using 4-picoline (0.52 g, 5.6 mmol, 1.0 equiv.) and benzyl bromide (0.96 g, 5.6 mmol, 1.0 equiv.). The product was obtained as a yellow solid (0.94 g, 5.1 mmol) in 92% yield. Spectral data obtained is consistent with that previously reported.[63]

Data for **1**

^{1}H-NMR (400 MHz, $CDCl_3$)

δ 8.48 (d, *J* = 5.6 Hz, 2 H), 7.30-7.19 (m, 3 H), 7.15 (d, *J* = 7.6 Hz, 2 H), 7.08 (d, *J* = 5.6 Hz, 2 H), 2.93 (m, 4 H).

^{13}C-NMR (76 MHz, $CDCl_3$)

δ 150.4, 149.7, 140.6, 128.4, 128.3, 126.2, 123.9, 37.0, 36.5.

4-Butylpyridine (**2**, CAS 5335-75-1)

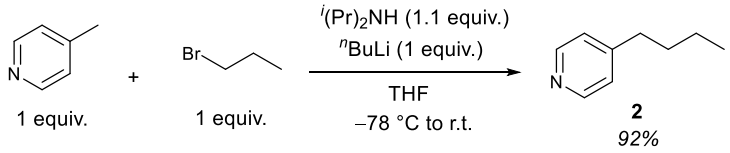

Substrate **2** was synthesized according to procedure 1 using 4-picoline (1.5 g, 16 mmol, 1.0 equiv.) and 1-bromopropane as the electrophile (2.0 g, 16 mmol, 1.0 equiv.). The product was purified by flash chromatography and obtained as a yellow oil (2.0 g, 15 mmol) in 92% yield. Spectral data is consistent with that previously reported.[64]

Chromatography: 30% EtOAc in hexane (R_f = 0.30).

Data for **2**

^{1}H-NMR (400 MHz, $CDCl_3$)

δ 8.48 (d, *J* = 6.1 Hz, 2H), 7.10 (d, *J* = 6.1 Hz, 2H), 2.60 (t, *J* = 7.7 Hz, 2H), 1.61 (p, *J* = 7.7 Hz, 2H), 1.36-1.27 (m, 2H), 0.93 (t, *J* = 7.3 Hz, 3H).

^{13}C-NMR (101 MHz, $CDCl_3$)

δ 151.8, 149.7, 124.0, 35.1, 32.5, 22.4, 14.0.

4-(But-3-en-1-yl)pyridine (**3**, CAS 45814-04-8)

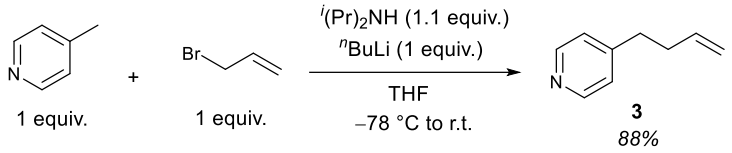

Substrate **3** was synthesized according to procedure 1 using 4-picoline (0.98 g, 11 mmol, 1.0 equiv.) and allyl bromide (1.3 g, 11 mmol, 1.0 equiv.). The product was obtained as a yellow oil (1.2 g, 9.3 mmol) in 88% yield. Spectral data is consistent with that previously reported.[65]

Data for **3**

^{1}H-NMR (400 MHz, $CDCl_3$)

δ 8.51 (d, *J* = 5.6 Hz, 2 H), 7.13 (d, *J* = 5.6 Hz, 2 H),
5.84 (dddd, *J* = 17.2, 10.0, 6.8, 6.8 Hz, 1 H), 5.06-4.99 (m, 2 H),
2.75-2.71 (m, 2 H), 2.44-2.38 (m, 2 H).

^{13}C-NMR (101 MHz, $CDCl_3$)

δ 150.1, 149.2, 136.5, 123.5, 115.2, 34.0, 33.7.

4-(4-(hex-1-yn-1-yl)phenethyl)pyridine (**4**)

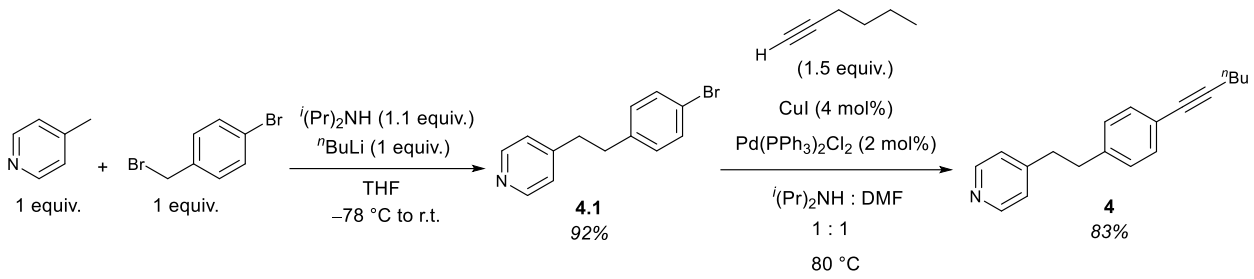

*Synthesis of 4-(4-bromophenethyl)pyridine **4.1** (CAS 1083087-58-4) :* **4.1** was synthesized according to procedure 1 using 4-picoline (0.15 g, 1.6 mmol, 1.0 equiv.) and 4-bromobenzyl bromide as the electrophile (0.40 g, 1.6 mmol, 1.0 equiv.). The crude mass was purified by flash chromatography to afford **4.1** as a white solid (0.37 g, 1.4 mmol) in 87% yield. Spectral data is consistent with that reported in the literature.[66]

Chromatography: 80% EtOAc in hexane (R_f = 0.30).

Data for **4.1**

^{1}H-NMR (400 MHz, $CDCl_3$)

δ 8.49 (d, *J* = 6.1 Hz, 2H), 7.39 (d, *J* = 8.4 Hz, 2H), 7.05 (d, *J* = 6.1 Hz, 2H), 7.00 (d, *J* = 8.4 Hz, 2H), 2.89 (m, 4H).

^{13}C-NMR (101 MHz, $CDCl_3$)

δ 150.1, 150.0, 139.7, 131.7, 130.3, 124.0, 120.2, 37.0, 36.1.

4-(4-(hex-1-yn-1-yl)phenethyl)pyridine (**4**)

Sonogoshira Coupling: An oven-dried sealable vial equipped with a stir bar was charged with CuI (18 mg, 0.08 mmol, 4 mol%), $Pd(PPh_3)_2Cl_2$ (30 mg, 0.04 mmol, 2 mol%) and arylbromide **4.1** (0.55 g, 2.1 mmol). DMF (5 mL) and $^{i}(Pr)_2NH$ (5 mL) were added and then 1-hexyne (0.36 mL, 3.2 mmol, 1.5 equiv.) was introduced. The vial was then sealed and heated to 80 °C. After an overnight reaction, a second batch of catalyst was introduced [CuI (18 mg, 0.08 mmol, 4 mol%), $Pd(PPh_3)_2Cl_2$ (30 mg, 0.04 mmol, 2 mol%)] to promote the complete conversion of the arylbromide. Once complete, the mixture was diluted with EtOAc and washed with distilled H_2O thrice. The organic phase was dried with brine and $MgSO_4$ then concentrated *in vacuo* to afford the crude product. After purification with flash chromatography, the coupled product **4** was obtained as a brown oil (0.45 g, 1.7 mmol) in 83% yield.

Chromatography: 20% EtOAc : 5% Et_3N : 75% Hexanes (R_f. = 0.35).

Data for **4**

^{1}H-NMR (300 MHz, $CDCl_3$)
δ 8.47 (d, *J* = 6.1 Hz, 2H), 7.30 (d, *J* = 8.2 Hz, 2H), 7.09 – 7.00 (m, 4H),
2.90 (m, 4H), 2.40 (t, *J* = 7.0 Hz, 2H), 1.67–1.39 (m, 4H), 0.95 (t, *J* = 7.2 Hz, 3H).

^{13}C-NMR (101 MHz, $CDCl_3$)
δ 150.3, 149.9, 140.2, 131.8, 128.4, 124.1, 122.1, 90.3, 80.5, 37.0, 36.5, 31.0,
22.2, 19.2, 13.8.

IR Alpha-Platinum ATR, Bruker, diamond crystal
υ = 2956.1, 2929.9, 2228.4, 1599.6 cm^{-1}

HRMS ESI
Calculated mass for $(M+H)^+$ of $C_{19}H_{21}N$ is 264.1748 found 264.1725.

4-(heptan-4-yl)pyridine (**5**)

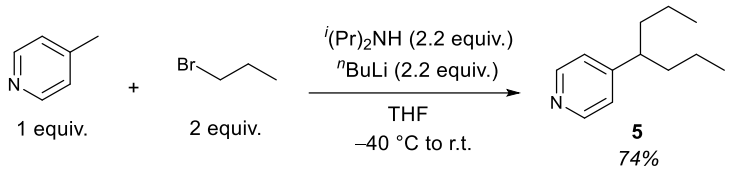

A flame-dried round-bottomed flask equipped with a stir bar was charged with freshly distilled diisopropylamine (2.2 equiv.) in THF and cooled to −40 °C. To this solution, *n*-BuLi (2.2 equiv., 1.6 M in hexanes) was added dropwise and the mixture was stirred for 15 min to form LDA. A solution of 4-methylpyridine (1.0 equiv.) in THF was introduced and allowed to stir for 1 hr at the same temperature. A solution of bromopropane (2.0 equiv.) in THF was added and the mixture was stirred at −40 °C for 1 hr then at room temperature overnight. The reaction was then quenched with water, and the aqueous layer was extracted three times with EtOAc. The combined organics were washed with brine, dried using $MgSO_4$ and concentrated *in vacuo*. The product was purified by flash chromatography and obtained as a yellow oil (0.28 g, 1.59 mmol) in 74% yield.

Chromatography: 20% EtOAc in hexane (R_f = 0.25).

Data for **5**

^{1}H-NMR (400 MHz, $CDCl_3$)
δ 8.48 (d, *J* = 6.1 Hz, 2H), 7.06 (d, *J* = 6.1 Hz, 2H), 2.51 (m, 1H),
1.66–1.44 (m, 4H), 1.22–1.05 (m, 4H), 0.84 (t, *J* = 7.3 Hz, 6H).

^{13}C-NMR (101 MHz, $CDCl_3$)
δ 155.5, 149.8, 123.4, 45.2, 38.6, 20.7, 14.2.

IR Alpha-Platinum ATR, Bruker, diamond crystal
υ = 2956.2, 2928.7, 1597.5 cm^{-1}

HRMS ESI
Calculated mass for $(M+H)^+$ of $C_{12}H_{19}N$ is 178.1590 found 178.1608.

4-(2-Bromophenethyl)pyridine (**6**)

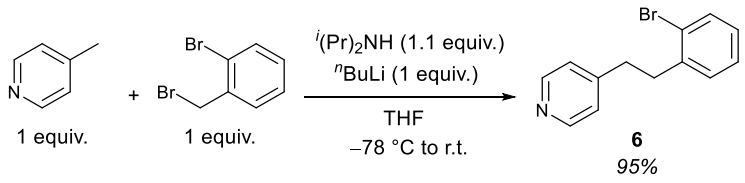

Substrate **6** was synthesized according to procedure 1 using 4-picoline (0.36 g, 3.9 mmol, 1.0 equiv.) and 2-bromobenzyl bromide (0.98 g, 3.9 mmol, 1.0 equiv.). The product was obtained as a yellow oil (0.97 g, 3.7 mmol) in 95% yield.

Data for **6**

^{1}H-NMR (400 MHz, $CDCl_3$)

δ 8.49 (d, *J* = 6.0 Hz, 2 H), 7.55 (d, *J* = 8.0 Hz, 1 H), 7.22-7.19 (m, 1 H), 7.13-7.06 (m, 4 H), 3.06-3.02 (m, 2 H), 2.93-2.89 (m, 2 H).

^{13}C-NMR (101 MHz, $CDCl_3$)

δ 149.8, 149.5, 139.6, 132.6, 130.2, 127.8, 127.3, 124.1, 123.6, 36.8, 35.0.

IR Alpha-Platinum ATR, Bruker, diamond crystal

υ = 3066, 3023, 2930, 1599, 1559 cm^{-1}

HRMS ESI

Calculated mass for $(M+H)^+$ of $C_{13}H_{12}BrN$ is 262.0226 found 262.0223.

4-(4-((*tert*-Butyldimethylsilyl)oxy)butyl)pyridine (**7**)

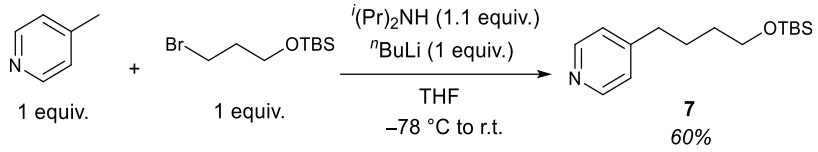

Substrate **7** was synthesized according to procedure 1 using 4-picoline (0.85 g, 9.1 mmol, 1.0 equiv.) and (3-bromopropoxy)-*tert*-butyldimethylsilane (2.3 g, 9.1 mmol, 1.0 equiv.). The product was purified by flash chromatography and obtained as a yellow oil (1.6 g, 5.5 mmol) in 60% yield.

Chromatography: 40% EtOAc in hexane (R_f. = 0.56).

Data for **7**

^{1}H-NMR (400 MHz, $CDCl_3$)

δ 8.48 (d, *J* = 5.6 Hz, 2 H), 7.10 (d, *J* = 5.6 Hz, 2 H), 3.62 (t, *J* = 6.4 Hz, 2 H), 2.62 (t, *J* = 7.6 Hz, 2 H), 1.78-1.66 (m, 2 H), 1.57-1.52 (m, 2 H), 0.91 (s, 9 H), 0.06 (s, 6 H).

^{13}C-NMR (76 MHz, $CDCl_3$)

δ 151.2, 149.4, 123.6, 62.4, 34.7, 31.9, 26.3, 25.7, 18.1, -5.5.

IR Alpha-Platinum ATR, Bruker, diamond crystal

υ = 2894, 2857, 1602 cm^{-1}

HRMS ESI

Calculated mass for $(M+H)^+$ of $C_{15}H_{27}NOSi$ is 266.1935 found 266.1928.

4-(3-(1,3-Dioxolan-2-yl)propyl)pyridine (**8**, CAS 639089-29-5)

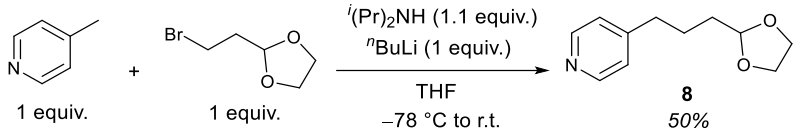

Substrate **8** was synthesized according to procedure 1 using 4-picoline (1.1 g, 11 mmol, 1.0 equiv.) and 2-(2-bromoethyl)-1,3-dioxolane (2.1 g, 13 mmol, 1.1 equiv.). The product was purified by flash chromatography and obtained as a yellow oil (1.1 g, 5.7 mmol) in 50% yield. Spectral data is consistent with that previously reported.[67]

Chromatography: 100% EtOAc (R_f. = 0.50).

Data for **8**

^{1}H-NMR (400 MHz, $CDCl_3$)

δ 8.48 (d, *J* = 5.6 Hz, 2 H), 7.11 (d, *J* = 5.6 Hz, 2 H), 4.87 (t, *J* = 4.4 Hz, 1 H), 3.99-3.93 (m, 2 H), 3.92-3.81 (m, 2 H), 2.65 (t, *J* = 7.2 Hz, 2 H), 1.79-1.68 (m, 4 H).

^{13}C-NMR (101 MHz, $CDCl_3$)

δ 151.1, 149.8, 123.9, 104.2, 65.0, 35.0, 33.3, 24.6.

4-Pyridineheptanenitrile (**9**, CAS 154939-07-8)

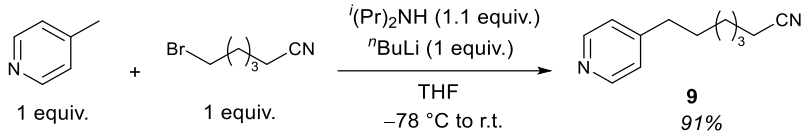

Substrate **9** was synthesized according to procedure 1 using 4-picoline (0.50 g, 5.4 mmol, 1.0 equiv.) and 6-bromohexanenitrile (0.95 g, 5.4 mmol, 1.0 equiv.). The product was obtained as a yellow oil (0.92 g, 4.9 mmol) in 91% yield. Spectral data is consistent with that previously reported.[68]

Data for **9**

^{1}H-NMR (400 MHz, $CDCl_3$)

δ 8.49 (dd, *J* = 5.3 Hz, 2 H), 7.09 (d, *J* = 5.3 Hz, 2 H),
2.61 (t, *J* = 7.4 Hz, 2 H), 2.34 (t, *J* = 7.4 Hz, 2 H), 1.69-1.62 (m, 4 H),
1.53-1.45 (m, 2 H), 1.40-1.37 (m, 2 H).

^{13}C-NMR (101 MHz, $CDCl_3$)

δ 151.1, 149.5, 123.7, 119.6, 34.9, 29.8, 28.2, 28.1, 25.1, 17.0.

Methyl 7-(pyridin-4-yl)heptanoate (**10**, CAS 100618-77-7)

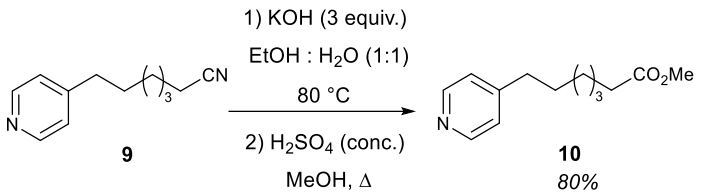

*Hydrolysis of **9**:* A solution of nitrile **9** (0.96 g, 5.1 mmol, 1.0 equiv.) and potassium hydroxide (0.86 g, 15 mmol, 3.0 equiv.) was made in a water : ethanol mixture (1 : 1, 50 mL) then heated to 80 °C. The progress of the reaction was monitored by ^{1}H NMR spectroscopy. Once complete, the pH of the mixture was adjusted to 5 using 1M $HCl_{(aq)}$. The solution was then concentrated *in vacuo* and the residue was triturated with water to remove the KCl salt. The resulting solid was dried under vacuum and then taken up in methanol (50 mL) in a round-bottomed flask equipped with a stir bar. A few drops of fuming sulfuric acid were added and the reaction mixture was heated under reflux overnight. The mixture was then diluted with distilled H_2O and the aqueous layer was extracted thrice with EtOAc. The combined organics were dried using brine and $MgSO_4$ then concentrated *in vacuo*. The crude mixture was purified by flash chromatography to afford **10** (1.0 g, 4.6 mmol) as a yellow oil in 90% yield.

Chromatography: 60% EtOAc in hexanes (R_f = 0.31).

Data for **10**

^{1}H-NMR (400 MHz, $CDCl_3$)

δ 8.50 (d, *J* = 4.9 Hz, 2H), 7.12 (d, *J* = 4.9 Hz, 2H), 3.69 (s, 3H),
2.62 (t, *J* = 7.7 Hz, 2H), 2.33 (t, *J* = 7.7 Hz, 2H), 1.65 (m, 4H), 1.37 (m, 4H).

^{13}C-NMR (101 MHz, $CDCl_3$)

δ 174.3, 151.6, 149.8, 124.0, 51.7, 35.3, 34.1, 30.2, 29.0, 28.9, 24.9.

N-methoxy-N-methyl-5-(pyridin-4-yl)pentanamide (**11**, CAS 1400304-19-9)

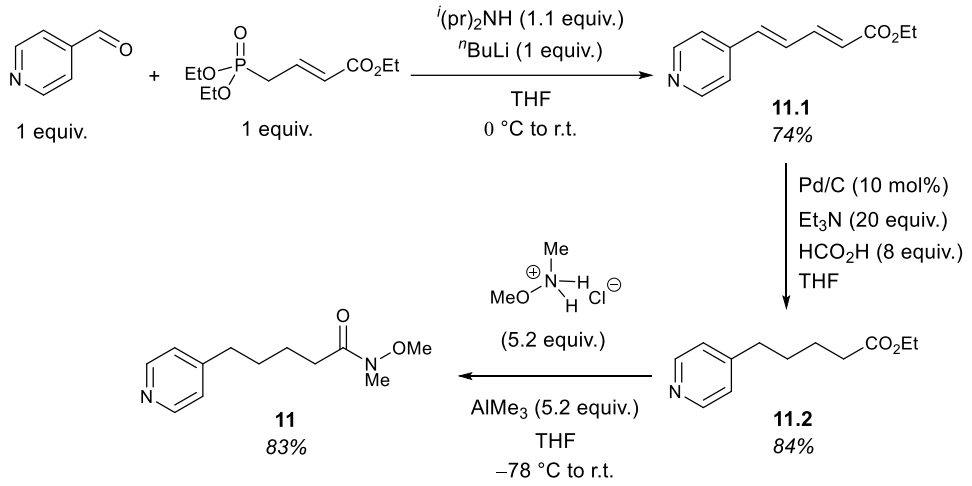

*Horner-Wadsworth-Emmons Reaction (**11.1**, CAS 344553-96-4):* A flame-dried round-bottomed flask equipped with a stir bar was charged with freshly distilled diisopropylamine (0.57 mL, 4.1 mmol, 1.0 equiv.) in THF (12 mL) and cooled to 0 °C. To this solution, *n*-BuLi (2.6 mL, 1.0 equiv., 1.6 M in hexanes) was added dropwise and the mixture was stirred for 15 min to form LDA. A solution of triethyl-*trans*-4-phosphonocrotonate (1.0 g, 4.1 mmol, 1.0 equiv.) in THF (12 mL) was introduced and the mixture was stirred for 30 min at the same temperature. 4-Pyridinecarboxaldehyde (0.44 g, 4.1 mmol, 1.0 equiv.) in THF (12 mL) was then added dropwise and the solution was warmed to room temperature and stirred overnight. The reaction was quenched with water, and the aqueous layer was extracted three times with EtOAc. The combined organics were then washed with brine, dried using $MgSO_4$ and concentrated *in vacuo*. The crude mass was purified using flash chromatography to afford **11.1** as a white solid (0.61 g, 3.0 mmol) in 74% yield. Spectral data is consistent with that previously reported.[69]

Chromatography: 50% - 70% EtOAc in hexane (R_f = 0.31 in 70% EtOAc : 30% hexane).

Data for **11.1**

^{1}H-NMR (300 MHz, $CDCl_3$)

δ 8.59 (d, *J* = 6.2 Hz, 2H), 7.42 (dd, *J* = 15.3, 11.0 Hz, 1H),
7.30 (d, *J* = 6.2 Hz, 2H), 7.03 (dd, J = 15.6, 11.0 Hz, 1H),
6.81 (d, *J* = 15.6 Hz, 1H), 6.08 (d, *J* = 15.3 Hz, 1H), 4.24 (q, *J* = 7.1 Hz, 2H),
1.32 (t, *J* = 7.1 Hz, 3H).

^{13}C-NMR (75 MHz, $CDCl_3$)

δ 166.7, 150.6, 143.3, 143.2, 137.2, 130.5, 124.3, 121.2, 60.8, 14.4.

N-methoxy-N-methyl-5-(pyridin-4-yl)pentanamide (**11**, CAS 1400304-19-9)

*Hydrogenation of **11.1**:* A round-bottomed flask equipped with a stir bar was charged with THF solution (12 mL) of α,β-unsaturated ester **11.1** (0.62 g, 3.0 mmol, 1.0 equiv.), triethylamine (8.4 mL, 60 mmol, 20 equiv.), 5% w/w Pd/C (0.64 g, 0.30 mmol, 10 mol%) and formic acid (0.91 mL, 24 mmol, 8.0 equiv.) and the mixture was left to stir overnight. The reaction mixture was then diluted with EtOAc and filtered through a pad of Celite®. The filtrate was concentrated *in vacuo* and the crude product was purified using flash chromatography to afford **11.2** (CAS 78775-05-0) as a light yellow oil (0.52 g, 2.5 mmol) in 84% yield. Spectral data is consistent with that reported in the literature.[69]

Chromatography: 50% - 80% EtOAc in hexane (R_f = 0.23 in 70% EtOAc : 30% hexane).

Data for **11.2**

^{1}H-NMR (300 MHz, $CDCl_3$)

δ 8.49 (d, *J* = 6.1 Hz, 2H), 7.14 (d, *J* = 6.1 Hz, 2H), 4.13 (q, *J* = 7.1 Hz, 2H), 2.72–2.57 (m, 2H), 2.38–2.26 (m, 2H), 1.70-1.65 (m, 4H), 1.25 (t, *J* = 7.1 Hz, 3H).

^{13}C-NMR (75 MHz, $CDCl_3$)

δ 173.5, 152.0, 149.1, 124.2, 60.5, 35.1, 34.1, 29.8, 24.6, 14.4.

N-methoxy-N-methyl-5-(pyridin-4-yl)pentanamide (**11**, CAS 1400304-19-9)

*Synthesis of **11**:* A flame-dried round-bottomed flask equipped with a stir bar was charged with *N,O*-dimethylhydroxylamine hydrochloride (1.27 g, 13.0 mmol, 5.20 equiv.) and THF (8 mL) and cooled to −78 °C. Trimethylaluminium (6.51 mL, 2.00 M in hexanes, 5.20 equiv.) was then added dropwise and the mixture was stirred for 45 min at the same temperature. A THF solution (8 mL) of **11.2** (0.52 g, 2.5 mmol, 1.0 equiv.) was introduced dropwise and the mixture was slowly warmed to room temperature. After an overnight reaction, the mixture was cooled to 0 °C and slowly quenched with saturated $NH_4Cl_{(aq)}$. The aqueous layer was extracted thrice with EtOAc and the combined organics were dried using brine and $MgSO_4$ then concentrated *in vacuo*. The crude mass was purified using flash chromatography to afford **11** (0.46 g, 2.1 mmol) as a yellow oil in 83% yield. Spectral data is consistent with that previously reported.[69]

Chromatography: 50% EtOAc : 5% Et_3N : 45% hexanes (R_f = 0.24).

Data for **11**

^{1}H-NMR (300 MHz, $CDCl_3$)

δ 8.48 (d, *J* = 6.1 Hz, 2H), 7.11 (d, *J* = 6.1 Hz, 2H), 3.67 (s, 3H), 3.17 (s, 3H), 2.64 (m, 2H), 2.45 (m, 2H), 1.76–1.61 (m, 4H).

^{13}C-NMR (75 MHz, CDCl3)

δ 174.3, 151.3, 149.8, 124.0, 61.4, 35.2, 32.3, 31.7, 30.1, 24.3.

***N*-(*tert*-Butyl)-4-butylnicotinamide** (**12**, CAS 331969-16-5)

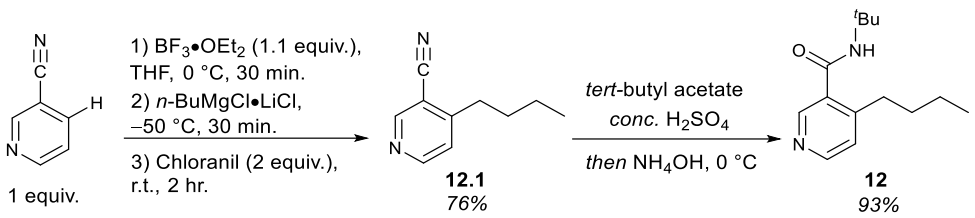

*Alkylation of 3-cyanopyridine (**12.1**):* **12.1** was synthesized according to procedure 2 using 3-cyanopyridine (0.78 g, 7.5 mmol, 1.0 equiv.) and *n*-BuMgBr (4.9 mL, 9.7 mmol, 2.0 M, 1.3 equiv.). The product was purified by flash chromatography and obtained as a colorless oil (0.91 g, 5.7 mmol) in 76% yield.

Chromatography: 20% EtOAc in hexanes (R_f. = 0.40).

Data for **12.1**

^{1}H-NMR (400 MHz, $CDCl_3$)
δ 8.77 (s, 1 H), 8.64 (d, *J* = 5.2 Hz, 1 H), 7.26 (d, *J* = 5.2 Hz, 1 H),
2.82 (t, *J* = 7.6 Hz, 2 H), 1.70-1.62 (m, 2 H), 1.44-1.35 (m, 2 H),
0.97 (t, *J* = 7.2 Hz, 3 H).

^{13}C-NMR (101 MHz, $CDCl_3$)
δ 155.6, 153.1, 152.7, 124.1, 116.1, 110.6, 34.0, 32.1, 22.4, 13.9.

IR Alpha-Platinum ATR, Bruker, diamond crystal
υ = 2958, 2932, 2872, 2228, 1589, 1553 cm^{-1}

HRMS ESI
Calculated mass for $(M+H)^+$ of $C_{10}H_{12}N_2$ is 161.1073 found 161.1077.

***N*-(*tert*-Butyl)-4-butylnicotinamide** (**12**, CAS 331969-16-5)

*Ritter reaction using **12.1**:* To a round-bottomed flask containing a solution of 3-cyano-4-butylpyridine (0.40 g, 2.5 mmol, 1.0 equiv.) in *tert*-butyl acetate (5 mL) was added concentrated H_2SO_4 (1 mL), and the mixture was stirred at room temperature overnight. The solution was then diluted with water and carefully neutralized by adding NH_4OH (3 mL) at 0 °C. The aqueous phase was extracted three times with a 1:1 mixture of hexane-EtOAc and the combined organics were washed with brine, dried with $MgSO_4$, filtered, and concentrated *in vacuo*. The residue was purified using flash column chromatography on silica gel to afford the product as a white solid (0.54 g, 2.3 mmol) in 93% yield. Spectral data is consistent with that previously reported.[70]

Chromatography: 70%-90% EtOAc in hexanes (R_f. = 0.34).

Data for **12**

^{1}H-NMR (400 MHz, $CDCl_3$)

δ 8.50 (s, 1 H), 8.48 (d, *J* = 5.2 Hz, 1 H), 7.14 (d, *J* = 5.2 Hz, 1 H), 5.64 (br, 1 H), 2.76 (t, *J* = 7.6 Hz, 2 H), 1.59 (p, *J* = 7.6 Hz, 2 H), 1.47 (s, 9 H), 1.37 (sext, *J* = 8.0 Hz, 2 H), 0.93 (t, *J* = 7.2 Hz, 3 H).

^{13}C-NMR (101 MHz, $CDCl_3$)

δ 167.4, 150.7, 150.3, 147.5, 133.8, 124.9, 52.4, 32.9, 32.5, 29.0, 22.9, 14.1.

Ethyl 4-butylnicotinate (**13**)

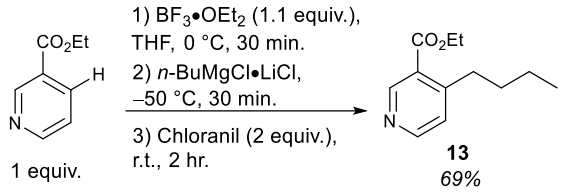

Substrate **13** was prepared according to procedure 2 using 3-ethyl nicotinate (0.76 g, 5.0 mmol, 1.0 equiv.) and *n*-BuMgCl•LiCl (11 mL, 7.9 mmol, 1.6 equiv., 0.70 M in THF). The product was purified by flash chromatography and obtained as a colorless oil (0.71 g, 3.5 mmol) in 69% yield.

Chromatography: 3.33% Et_3N in hexanes (R_f. = 0.20).

Data for **13**

^{1}H-NMR (400 MHz, $CDCl_3$)

δ 9.03 (s, 1 H), 8.56 (d, *J* = 5.1 Hz, 1 H), 7.17 (d, *J* = 5.1 Hz, 1 H), 4.39 (q, *J* = 7.2 Hz, 2 H), 2.97 (t, *J* = 7.8 Hz, 2 H), 1.63-1.55 (m, 2 H), 1.45-1.36 (m, 5 H), 0.94 (t, *J* = 7.2 Hz, 3 H).

^{13}C-NMR (101 MHz, $CDCl_3$)

δ 166.3, 153.7, 152.1, 151.7, 126.1, 125.4, 61.3, 33.6, 33.0, 22.8, 14.3, 14.0.

IR Alpha-Platinum ATR, Bruker, diamond crystal

υ = 2959, 2932, 2872, 1719, 1590, 1556 cm^{-1}

HRMS ESI

Calculated mass for $(M+H)^+$ of $C_{12}H_{17}NO_2$ is 208.1332 found 208.1326.

2-(4-(2-(Pyridin-4-yl)ethyl)phenethyl)pyridine (**15**)

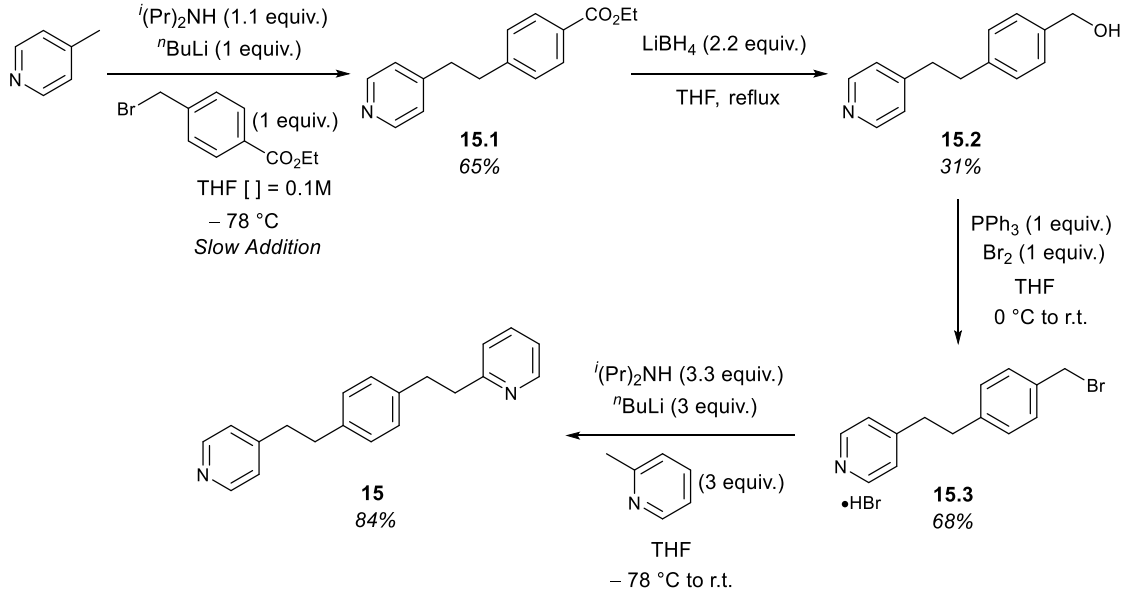

*Synthesis of **15.1*** (CAS: 1802629-62-4) – **15.1** was synthesized according to procedure 1 using 4-picoline (0.80 g, 8.6 mmol, 1.0 equiv.) and ethyl-4-bromomethylbenzoate as the electrophile (2.1 g, 8.6 mmol, 1.0 equiv.). The crude mass was purified by flash chromatography to afford **15.1** as a white solid (1.4 g, 5.6 mmol) in 65% yield. Spectral data is consistent with that reported in the literature.[71]

Chromatography: 80% EtOAc in hexanes (R_f. = 0.46).

Data for **15.1**

^{1}H-NMR (400 MHz, $CDCl_3$)

δ 8.48 (d, *J* = 5.2 Hz, 2 H), 7.95 (d, *J* = 8.4 Hz, 2 H),
7.20 (d, *J* = 8.4 Hz, 2 H), 7.05 (d, *J* = 5.2 Hz, 2 H), 4.36 (q, *J* = 7.2 Hz, 2 H),
3.01-2.91 (m, 4 H), 1.39 (t, *J* =7.2 Hz, 3 H).

^{13}C-NMR (101 MHz, $CDCl_3$)

δ 166.6, 150.0, 149.9, 146.0, 129.9, 128.8, 128.6, 124.0, 61.0, 36.7, 36.6, 14.5.

2-(4-(2-(Pyridin-4-yl)ethyl)phenethyl)pyridine (**15**)

*Reduction of **15.1*** – A flame-dried round-bottomed flask equipped with a stir bar was charged with a solution of ester **15.1** (1.4 g, 5.6 mmol, 1.0 equiv.) in dry THF (50 mL). $LiBH_4$ (0.15 g, 6.7 mmol, 1.2 equiv.) was then added and the reaction was heated to reflux and left to stir overnight. A second portion of $LiBH_4$ (0.15 g, 6.7 mmol, 1.2 equiv.) was added, and after 2 h the reaction was quenched with a saturated solution of $NaHCO_3$ and extracted with EtOAc three times. The combined organics were washed with brine, dried using $MgSO_4$ and concentrated *in vacuo*. The crude mixture was purified by flash chromatography to afford **15.2** as a white solid (0.36 g, 1.7 mmol) in 31% yield.

Chromatography: 100% EtOAc (R_f. = 0.34).

Data for **15.2**

^{1}H-NMR (400 MHz, $CDCl_3$)

δ 8.46 (dd, *J* = 4.8, 1.6 Hz, 2 H), 7.29 (d, *J* = 8.0 Hz, 2 H),
7.14 (d, *J* = 8.0 Hz, 2 H), 7.05 (dd, *J* = 4.8, 1.6 Hz, 2 H), 4.67 (s, 2 H),
2.94-2.91 (m, 4 H), 1.97 (br, 1 H).

^{13}C-NMR (101 MHz, $CDCl_3$)

δ 150.6, 149.8, 140.2, 139.1, 128.8, 127.4, 124.1, 65.2, 37.2, 36.4.

IR Alpha-Platinum ATR, Bruker, diamond crystal

υ = 3158, 2879, 1603, 1558 cm^{-1}

HRMS ESI

Calculated mass for $(M+H)^+$ of $C_{14}H_{15}NO$ is 214.1226 found 214.1216.

2-(4-(2-(Pyridin-4-yl)ethyl)phenethyl)pyridine (**15**)

*Bromination of **15.2*** – A flame-dried round-bottomed flask equipped with a stir bar was charged with triphenylphosphine (0.32 g, 1.2 mmol, 1.0 equiv.) and dry THF (5 mL), and cooled to 0 °C. Bromine (0.060 mL, 1.2 mmol, 1.0 equiv.) was then added dropwise and the mixture was left to stir for 20 min. A solution of alcohol **15.2** (0.26 g, 1.2 mmol, 1.0 equiv.) in THF (7 mL) was introduced and the reaction mixture was allowed to warm to room temperature overnight. The pyridinium salt (**15.3**) precipitated out of the mixture and was isolated as a white solid after vacuum filtration (0.29 g, 0.83 mmol) in 68% yield. This salt was used in the next step without further purification.

Data for **15.3**

^{1}H-NMR (400 MHz, $CDCl_3$)

δ 8.64 (d, *J* = 6.8 Hz, 2 H), 7.62 (d, *J* = 6.8 Hz, 2 H), 7.33 (d, *J* = 8.0 Hz, 2 H), 7.06 (d, *J* = 8.0 Hz, 2 H), 4.67 (s, 2 H), 3.23 (t, *J* = 7.4 Hz, 2 H), 3.06 (t, *J* = 7.4 Hz, 2 H).

^{13}C-NMR (101 MHz, $CDCl_3$)

δ 162.8, 140.2, 138.6, 137.0, 129.8, 128.9, 127.1, 37.9, 35.6, 33.0.

IR Alpha-Platinum ATR, Bruker, diamond crystal

υ = 3370, 3091, 3052, 1634, 1594 cm^{-1}

HRMS ESI

Calculated mass for $(M+H)^+$ of $C_{14}H_{15}Br_2N$ is 355.9644 found $(C_{14}H_{15}BrN+H-HBr)^+$ 276.0400.

2-(4-(2-(Pyridin-4-yl)ethyl)phenethyl)pyridine (**15**)

*Alkylation of **15.3** using 2-methylpyridine* – **15** was synthesized according to procedure 1 using 2-picoline (0.23 g, 2.5 mmol, 3.0 equiv.) and **15.3** (0.30 g, 0.82 mmol, 1.0 equiv.) as the electrophile. The product was purified using flash chromatography and obtained as a white solid (0.20 g, 0.69 mmol) in 84% yield.

Chromatography: 3% MeOH in EtOAc (R_f. = 0.44).

Data for **15**

^{1}H-NMR (400 MHz, $CDCl_3$)

δ 8.56 (d, *J* = 4.4 Hz, 1 H), 8.48 (dd, *J* = 4.4, 1.6 Hz, 2 H),
7.56 (td, *J* = 7.6, 1.6 Hz, 1 H), 7.13-7.04 (m, 8 H), 3.10-3.01 (m, 4 H),
2.89 (br, 4 H).

^{13}C-NMR (101 MHz, $CDCl_3$)

δ 161.4, 150.7, 149.8, 149.5, 139.6, 138.4, 136.4, 128.7, 128.5, 124.1, 123.1, 121.3, 40.4, 37.2, 36.2, 35.7.

IR Alpha-Platinum ATR, Bruker, diamond crystal

υ = 2922, 2856, 1587, 1566 cm^{-1}

HRMS ESI

Calculated mass for $(M+H)^+$ of $C_{20}H_{20}N_2$ is 289.1699 found 289.1688.

5.3 Pyridylic Dehydrogenation: Summary of Reaction Optimization

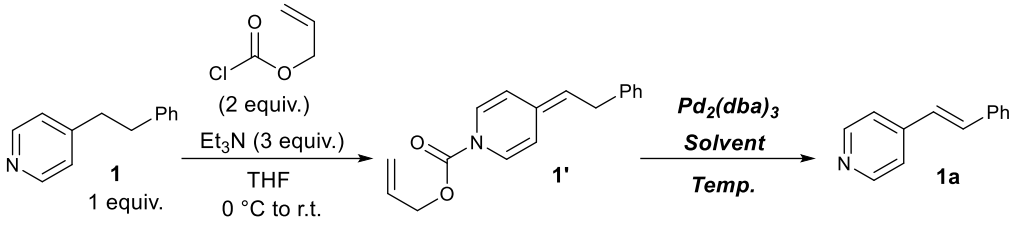

	Solvent	Cat. loading (mol%)	Temp. (°C)	Yield (%)
1	1,2-DCE	2.5	50	33
2	MeCN	2.5	50	49
3	Toluene	2.5	50	74
4	1,4-Dioxane	2.5	50	76
5	THF	2.5	50	83
6	Toluene	3.5	50	80
7	1,4-Dioxane	3.5	50	83
8	1,4-Dioxane	5	50	83
9	***THF***	***3.5***	***50***	***88***
10	Toluene	3.5	40	*Incomplete Conversion*
11	1,4-Dioxane	3.5	40	*Incomplete Conversion*
12	THF	3.5	40	*Incomplete Conversion*
13	1,4-Dioxane	5	40	83

Reactions performed on 0.55 mmol scale, 12 hr. Yields were determined by quantitative ^{1}H NMR using 1,4-bis(trichloromethyl)benzene as an internal standard.

5.4 Pyridylic Dehydrogenation: Substrate Scope – Procedure and Structural Data

Procedure 3: General procedure for Pd-catalyzed dehydrogenation of 4-alkylpyridines

Synthesis of the ADHP intermediate: Triethylamine (3.0 equiv.) was added to a solution of the appropriate pyridine (1.0 equiv.) in dry THF (0.1 M) in a flame-dried round-bottomed flask equipped with a stir bar. The resulting solution was cooled to 0 °C and allyl chloroformate (2.0 equiv.) was added dropwise. The ice bath was then removed and the resulting suspension was stirred for 30 min. The mixture was then concentrated in vacuo and the resulting crude mass was suspended in diethyl ether and filtered through a plug of cotton to remove the triethylammonium chloride salt. The filtrate was concentrated in vacuo to afford the desired ADHP which was used in the next step without further purification.

Palladium-catalyzed decarboxylative dehydrogenation: A flame-dried round-bottomed flask equipped with a stir bar was charged with $Pd_2(dba)_3 \bullet CHCl_3$ (3.5 mol%). A solution of the ADHP in dry THF (0.1 M) was then added to the flask containing the catalyst and the mixture was stirred at 50 °C for 12 hr. The reaction mixture was then concentrated in vacuo and purification was done either by:

1) Recrystallization: after concentration, the crude mass was dissolved in Et_2O (0.3 M) and then equipped with a stir bar and cooled to 0 °C. Anhydrous HCl (1.5 equiv., 4 M in dioxane) was then added dropwise and the mixture was stirred for 15 minutes at the same temperature. The pyridinium salt was then collected using vacuum filtration and then dissolved in DCM, filtering off the palladium residue. The DCM solution was concentrated until saturation and the product was left to recrystallize overnight by slow evaporation. The pure crystals were then collected by filtration from the mother liquor, washed with Et_2O twice and dried *in vacuo*.
2) Flash chromatography: after concentration, the crude mass was directly subjected to flash chromatography, eluting with the indicated solvent mixture to afford the desired product.

4-(2-Phenylethyl)pyridine Dehydrogenation Product (**1e**, CAS 19337-93-0)

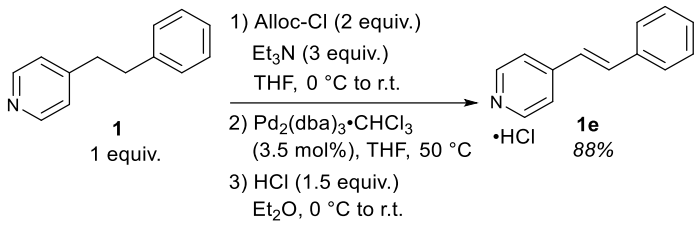

Using procedure 3, pyridine **1** (0.20 g, 1.1 mmol, 1.0 equiv.) provided product **1e** (0.21 g, 0.97 mmol) in 88% yield as a yellow solid after recrystallization.

Data for **1e**

^{1}H-NMR (400 MHz, $CDCl_3$)

δ 8.67 (d, *J* = 6.2 Hz, 2H), 7.90 (d, *J* = 6.2 Hz, 2H), 7.68–7.60 (m, 3H), 7.51–7.42 (m, 3H), 7.16 (d, *J* = 16.2 Hz, 1H).

^{13}C-NMR (101 MHz, DMSO)

δ 153.5, 141.4, 140.0, 135.3, 130.2, 129.0, 128.0, 123.9, 123.3.

4-Butylpyridine Dehydrogenation Product (2e)

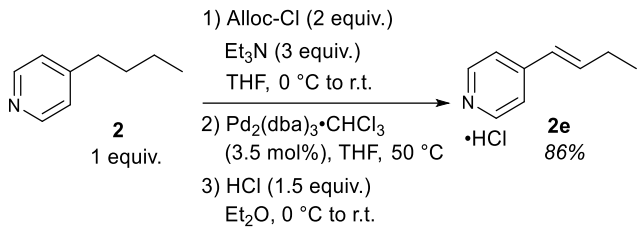

Using procedure 3, pyridine **2** (0.20 g, 1.5 mmol, 1.0 equiv.) provided product **2e** (0.22 g, 1.3 mmol) in 86% yield as a beige solid after recrystallization.

Data for **2e**

^{1}H-NMR (300 MHz, $CDCl_3$)

δ 8.64 (d, *J* = 6.3 Hz, 2H), 7.75 (d, *J* = 6.3 Hz, 2H),

6.95 (dt, *J* = 15.9, 6.5 Hz, 1H), 6.50 (d, *J* = 15.9 Hz, 1H), 2.48–2.30 (m, 2H),

1.14 (t, *J* = 7.4 Hz, 3H).

^{13}C-NMR (75 MHz, $CDCl_3$)

δ 154.9, 147.7, 140.6, 124.9, 123.0, 26.7, 12.6.

IR Alpha-Platinum ATR, Bruker, diamond crystal

υ = 3057.1, 2965.2, 1622.9, 1601.3 cm^{-1}

HRMS ESI

Calculated mass for (M+H)+ of $C_9H_{12}ClN$ is 170.0731 found ($C_9H_{12}ClN$+H-HCl)+ 134.0962.

4-(But-3-en-1-yl)pyridine Dehydrogenation Product (3e)

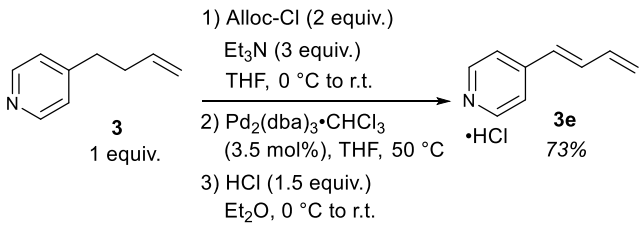

Using procedure 3, pyridine **3** (0.10 g, 0.75 mmol, 1.0 equiv.) provided product **3e** (92 mg, 0.55 mmol) in 73% yield as a yellow solid after recrystallization.

Data for **3e**

^{1}H-NMR (300 MHz, $CDCl_3$, **3e**−HCl)

δ 8.53 (d, *J* = 6.1 Hz, 2H), 7.25 (d, *J* = 6.1 Hz, 2H),

6.95 (dd, *J* = 15.7, 10.5 Hz, 1H), 6.59–6.49 (m, 1H), 6.48 (d, *J* = 15.7 Hz, 1H), 5.46 (d, *J* = 16.3 Hz, 1H), 5.33 (d, *J* = 10.2 Hz, 1H).

^{13}C-NMR (101 MHz, $CDCl_3$, **3e**−HCl)

δ 150.3, 144.5, 136.5, 134.0, 130.2, 120.9, 120.8.

IR Alpha-Platinum ATR, Bruker, diamond crystal

υ = 3087.7, 2981.5, 1602.9, 1587.6 cm^{-1}

HRMS ESI

Calculated mass for (M+H)+ of $C_9H_{10}ClN$ is 168.0575 found ($C_9H_{10}ClN$+H-HCl)+ 132.0805.

4-(heptan-4-yl)pyridine Dehydrogenation Product (**4e**)

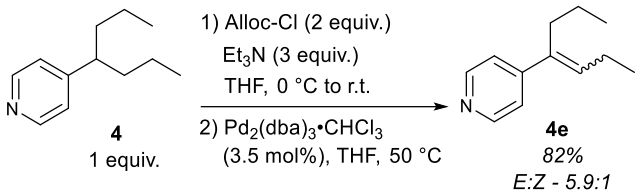

Using procedure 3, pyridine **4** (0.15 g, 0.84 mmol, 1.0 equiv.) provided product **4e** (0.10 g, 0.69 mmol) in 82% yield as a yellow oil.

Chromatography: 15% EtOAc in hexanes (R_f. = 0.33 & 0.29).

Data for **4e**

^{1}H-NMR (400 MHz, $CDCl_3$)

δ 8.54 (d, *J* = 6.1 Hz, 0.32H), 8.50 (d, *J* = 6.3 Hz, 2H), 7.23 (d, *J* = 6.3 Hz, 2H), 7.06 (d, *J* = 6.1 Hz, 0.32H), 5.87 (t, *J* = 7.3 Hz, 1H), 5.51 (t, *J* = 7.5 Hz, 0.17H), 2.50–2.41 (m, 2H), 2.29 (m, 0.34H), 2.24 (p, *J* = 7.4 Hz, 2H), 1.99–1.84 (m, 0.34H), 1.44–1.21 (m, 2.34H), 1.07 (t, *J* = 7.5 Hz, 3H), 0.97–0.81 (m, 4H).

^{13}C-NMR (101 MHz, $CDCl_3$)

δ 150.6, 149.8, 149.7, 137.9, 137.3, 134.0, 131.0, 123.7, 121.0, 40.5, 30.8, 22.3, 22.0, 21.9, 21.2, 14.6, 14.2, 13.9, 13.6.

IR Alpha-Platinum ATR, Bruker, diamond crystal

υ = 3068.7, 2959.4, 1593.8 cm^{-1}

HRMS ESI

Calculated mass for $(M+H)^+$ of $C_{11}H_{17}N$ is 176.1434, found 176.1416.

4-(4-(hex-1-yn-1-yl)phenethyl)pyridine Dehydrogenation Product (5e)

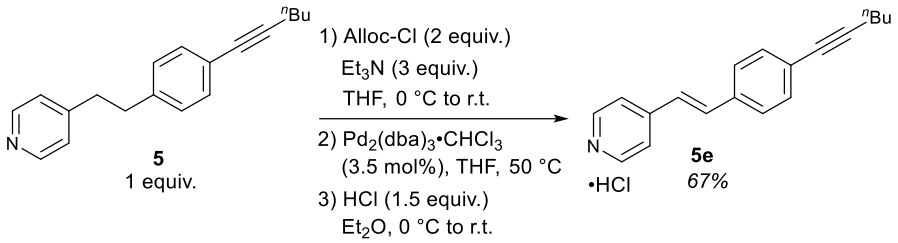

Using procedure 3, pyridine **5** (0.10 g, 0.38 mmol, 1.0 equiv.) provided product **5e** (66 mg, 0.26 mmol) in 67% yield as a yellow solid. The following modification to the procedure was adapted: following reaction completion, the reaction mixture was diluted with EtOAc and washed with saturated $NaHCO_{3(aq.)}$. The aqueous layer was extracted twice more with EtOAc and the combined organics were dried using brine and $MgSO_4$ then concentrated *in vacuo*. The crude product was turned into the corresponding HCl salt and purified by recrystallized according to procedure 3.

Data for **5e**

^{1}H-NMR (300 MHz, DMSO)

δ 8.81 (d, *J* = 6.0 Hz, 2H), 8.12 (d, *J* = 6.0 Hz, 2H), 7.94 (d, *J* = 16.3 Hz, 1H), 7.71 (d, *J* = 8.3 Hz, 2H), 7.53 (d, *J* = 16.3 Hz, 1H), 7.48 (d, *J* = 8.3 Hz, 2H), 2.45 (t, *J* = 7.0 Hz, 2H), 1.62–1.37 (m, 4H), 0.92 (t, *J* = 7.1 Hz, 3H).

^{13}C-NMR (101 MHz, $CDCl_3$)

δ 154.2, 141.1, 140.8, 133.5, 132.4, 128.2, 127.0, 123.4, 123.0, 94.1, 80.3, 30.8, 22.1, 19.3, 13.7.

IR Alpha-Platinum ATR, Bruker, diamond crystal

υ = 3090.3, 2955.3, 2160.3, 1621.0, 1597.0 cm^{-1}

HRMS ESI

Calculated mass for $(M+H)^+$ of $C_{19}H_{20}ClN$ is 298.1357 found ($C_{19}H_{20}ClN$+H-HCl)+ 262.1587.

4-(2-Bromophenethyl)pyridine Dehydrogenation Product (**6e**)

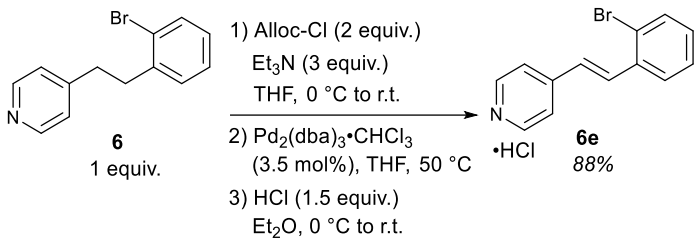

Using procedure 3, pyridine **6** (0.20 g, 0.76 mmol, 1.0 equiv.) provided product **6e** (0.21 g, 0.71 mmol) in 94% yield as a yellow solid.

Data for **6e**

^{1}H-NMR (300 MHz, $CDCl_3$, **6e**−HCl)

δ 8.61 (d, *J* = 6.2 Hz, 2H), 7.67 (d, *J* = 16.3 Hz, 1H),

7.65 (m, 2H), 7.40 (d, *J* = 6.2 Hz, 2H), 7.34 (td, *J* = 7.7, 1.2 Hz, 1H),

7.18 (td, *J* = 7.7, 1.5 Hz, 1H), 6.95 (d, *J* = 16.3 Hz, 1H).

^{13}C-NMR (75 MHz, $CDCl_3$, **6e**−HCl)

δ 150.4, 144.3, 136.2, 133.4, 132.0, 130.0, 128.9, 127.8, 127.2, 124.7, 121.2.

IR Alpha-Platinum ATR, Bruker, diamond crystal

υ = 3021.0, 2924.3, 1592.1 cm^{-1}

HRMS ESI

Calculated mass for $(M+H)^+$ of $C_{13}H_{12}BrClN$ is 295.98742 found ($C_{13}H_{12}BrClN$+H-HCl)+ 260.0066.

4-(4-((*tert*-Butyldimethylsilyl)oxy)butyl)pyridine Dehydrogenation Product (7e)

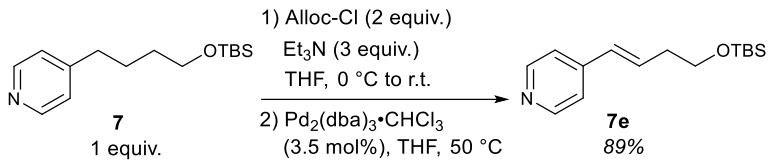

Using procedure 3, pyridine **7** (91 mg, 0.34 mmol, 1.0 equiv.) provided product **7e** (80 mg, 0.30 mmol) in 89% yield as a yellow oil.

Chromatography: 25% EtOAc in hexanes (R_f. = 0.25).

Data for **7e**

^{1}H-NMR (300 MHz, $CDCl_3$)

δ 8.51 (d, *J* = 6.2 Hz, 2H), 7.20 (d, *J* = 6.2 Hz, 2H),

6.49 (dt, *J* = 16.0, 6.5 Hz, 1H), 6.37 (d, *J* = 16.0 Hz, 1H), 3.75 (t, *J* = 6.5 Hz, 2H),

2.46 (qd, *J* = 6.5, 1.0 Hz, 2H), 0.90 (s, 9H), 0.06 (s, 6H).

^{13}C-NMR (75 MHz, $CDCl_3$)

δ 150.2, 145.1, 132.9, 129.7, 120.7, 62.5, 36.7, 26.1, 18.5, -5.1.

IR Alpha-Platinum ATR, Bruker, diamond crystal

υ = 3050.1, 2952.7, 1651.1, 1598.8 cm^{-1}

HRMS ESI

Calculated mass for $(M+H)^+$ of $C_{15}H_{25}NOSi$ is 264.1747 found 264.1741.

4-(3-(1,3-Dioxolan-2-yl)propyl)pyridine Dehydrogenation Product (**8e**, CAS 639089-50-2)

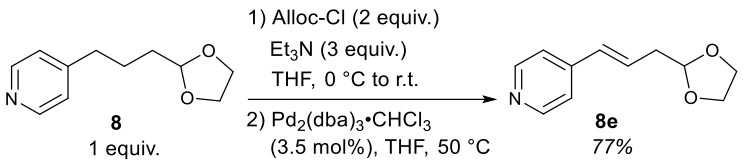

Using procedure 3, pyridine **8** (0.10 g, 0.52 mmol, 1.0 equiv.) provided product **8e** (77 mg, 0.40 mmol) in 77% yield as a yellow oil. Spectral data is consistent with that previously reported.[72]

Chromatography: 20% EtOAc : 5% Et_3N : 75% hexanes (R_f. = 0.18).

Data for **8e**

^{1}H-NMR (300 MHz, $CDCl_3$)

δ 8.51 (br d, *J* = 6.2 Hz, 2H), 7.22 (d, *J* = 6.2 Hz, 2H), 6.55–6.37 (m, 2H), 5.00 (t, *J* = 4.5 Hz, 1H), 4.07–3.82 (m, 4H), 2.63 (m, 2H).

^{13}C-NMR (101 MHz, $CDCl_3$)

δ 150.1, 144.7, 131.1, 129.2, 120.9, 103.4, 65.2, 37.9.

4-Pyridineheptanenitrile Dehydrogenation Product (**9e**)

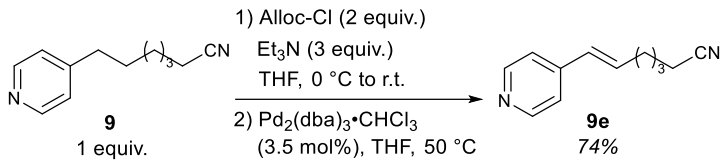

Using procedure 3, pyridine **9** (0.10 g, 0.53 mmol, 1.0 equiv.) provided product **9e** (74 mg, 0.39 mmol) in 74% yield as a yellow oil.

Chromatography: 35% EtOAc : 5% Et_3N : 60% hexanes (R_f. = 0.25).

Data for **9e**

^{1}H-NMR (400 MHz, $CDCl_3$)

δ 8.51 (d, *J* = 6.2 Hz, 2H), 7.20 (d, *J* = 6.2 Hz, 2H),

6.43 (dt, *J* = 15.9, 6.5 Hz, 1H), 6.35 (d, *J* = 15.9 Hz, 1H), 2.39 (t, *J* = 6.7 Hz, 2H),

2.31 (q, *J* = 6.5 Hz, 2H), 1.78 – 1.65 (m, 4H).

^{13}C-NMR (101 MHz, $CDCl_3$)

δ 150.2, 144.8, 134.6, 128.9, 120.7, 119.6, 32.2, 28.0, 25.0, 17.2.

IR Alpha-Platinum ATR, Bruker, diamond crystal

υ = 3087.7, 2934.6, 2245.8, 1650.9, 1593.8 cm^{-1}

HRMS ESI

Calculated mass for $(M+H)^+$ of $C_{12}H_{15}N_2$ is 187.1230 found 187.1221.

Methyl 7-(pyridin-4-yl)heptanoate Dehydrogenation Product (10e)

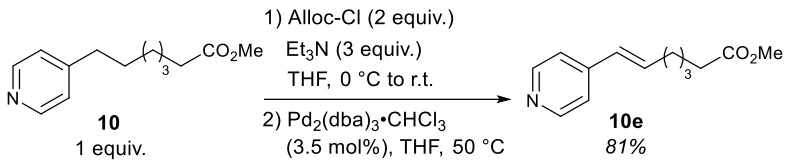

Using procedure 3, pyridine **10** (0.10 g, 0.38 mmol, 1.0 equiv.) provided product **10e** (81 mg, 0.31 mmol) in 81% yield as a yellow oil.

Chromatography: 13% EtOAc : 5% Et_3N : 82% hexanes (R_f. = 0.22).

Data for **10e**

^{1}H-NMR (400 MHz, $CDCl_3$)

δ 8.50 (d, *J* = 6.2 Hz, 2H), 7.19 (d, *J* = 6.2 Hz, 2H),
6.45 (dt, *J* = 15.9, 6.8 Hz, 1H), 6.32 (d, *J* = 15.9 Hz, 1H), 3.67 (s, 3H),
2.35 (t, *J* = 7.4 Hz, 2H), 2.27 (q, *J* = 7.3 Hz, 2H), 1.76–1.64 (m, 2H),
1.60–1.48 (m, 2H).

^{13}C-NMR (101 MHz, $CDCl_3$)

δ 174.1, 150.1, 145.1, 135.6, 128.3, 120.7, 51.7, 34.0, 32.8, 28.5, 24.6.

IR Alpha-Platinum ATR, Bruker, diamond crystal

υ = 3023.4, 2946.9, 1732.1, 1650.4, 1593.7 cm^{-1}

HRMS ESI

Calculated mass for $(M+H)^+$ of $C_{13}H_{18}NO_2$ is 220.1332 found 220.1322.

N-methoxy-N-methyl-5-(pyridin-4-yl)pentanamide Dehydrogenation Product (11e)

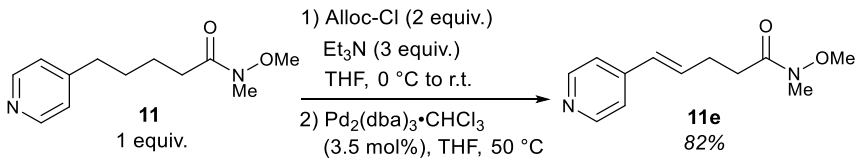

Using procedure 3, pyridine **11** (0.14 g, 0.65 mmol, 1.0 equiv.) provided product **11e** (0.12 g, 0.53 mmol) in 82% yield as a yellow oil.

Chromatography: 90% EtOAc : 10% toluene (R_f. = 0.43 in 5% Et_3N in EtOAc).

Data for **11e**

^{1}H-NMR (300 MHz, $CDCl_3$)

δ 8.50 (d, *J* = 6.2 Hz, 2H), 7.20 (d, *J* = 6.2 Hz, 2H),

6.52 (dt, *J* = 15.9, 6.3 Hz, 1H), 6.38 (d, *J* = 15.9 Hz, 1H), 3.69 (s, 3H),

3.20 (s, 3H), 2.60 (m, 4H).

^{13}C-NMR (75 MHz, $CDCl_3$)

δ 173.5, 150.2, 144.9, 134.7, 128.7, 120.8, 61.4, 32.4, 31.3, 28.0.

IR Alpha-Platinum ATR, Bruker, diamond crystal

υ = 3026.8, 2966.2, 1652.7, 1593.8 cm^{-1}

HRMS ESI

Calculated mass for $(M+H)^+$ of $C_{12}H_{16}N_2O_2$ is 221.128454 found 221.1265.

***N*-(*tert*-Butyl)-4-butylnicotinamide Dehydrogenation Product (12e)**

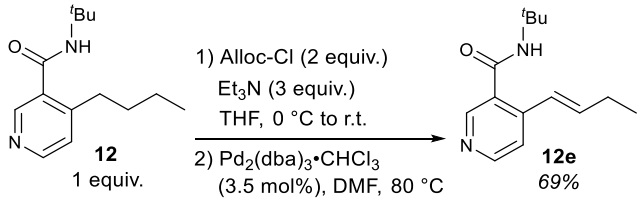

Using procedure 3 and using DMF at 80 °C in the dehydrogenation step, pyridine **12** (0.20 g, 0.85 mmol, 1.0 equiv.) provided product **12e** (0.14 g, 0.59 mmol) in 69% yield as a yellow solid.

Chromatography: 30% EtOAc : 5% Et_3N : 65% hexanes (R_f. = 0.25).

Data for **12e**

^{1}H-NMR (300 MHz, $CDCl_3$)

δ 8.57 (s, 1H), 8.49 (d, *J* = 5.3 Hz, 1H), 7.34 (d, *J* = 5.3 Hz, 1H),
6.64 (d, *J* = 15.9 Hz, 1H), 6.48 (dt, *J* = 15.9, 6.2 Hz, 1H), 5.66 (s, 1H),
2.36–2.20 (m, 2H), 1.47 (s, 9H), 1.11 (t, *J* = 7.4 Hz, 3H).

^{13}C-NMR (75 MHz, $CDCl_3$)

δ 166.8, 150.5, 148.5, 143.3, 139.9, 131.5, 124.3, 120.0, 52.4, 28.9, 26.4, 13.1.

IR Alpha-Platinum ATR, Bruker, diamond crystal

υ = 3238.0, 3064.1, 2967.0, 1628.7, 1583.3 cm^{-1}

HRMS ESI

Calculated mass for $(M+H)^+$ of $C_{14}H_{20}N_2O$ is 233.1648 found 233.1628.

Ethyl 4-butylnicotinate Dehydrogenation Product (13e)

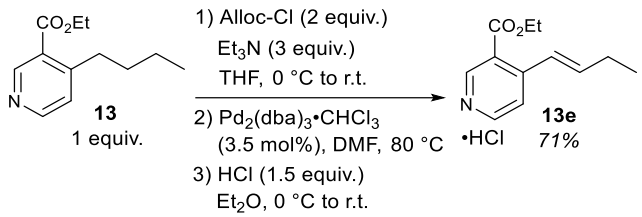

Using procedure 3 and using DMF at 80 °C in the dehydrogenation step, pyridine **13** (0.20 g, 0.97 mmol, 1.0 equiv.) provided product **13e** (0.17 g, 0.69 mmol) in 71% yield as a white solid. Product purification was done by first subjecting the crude mass to flash chromatography. The obtained product was then converted to its corresponding HCl salt according to procedure 3 and washed with Et_2O thrice to remove residual dibenzylideneacetone. This protocol delivered pure **13e**.

Chromatography: 4% Et_3N in hexanes (R_f. = 0.29 in 5% Et_3N in hexanes).

Data for **13e**

^{1}H-NMR (300 MHz, $CDCl_3$)

δ 9.16 (s, 1H), 8.65 (d, *J* = 5.9 Hz, 1H), 8.01 (d, *J* = 5.9 Hz, 1H),
7.57 (d, *J* = 15.9 Hz, 1H), 6.94 (dt, *J* = 15.9, 6.6 Hz, 1H), 4.46 (q, *J* = 7.1 Hz, 2H),
2.53–2.37 (m, 2H), 1.44 (t, *J* = 7.1 Hz, 3H), 1.19 (t, *J* = 7.4 Hz, 3H).

^{13}C-NMR (75 MHz, $CDCl_3$)

δ 162.3, 156.1, 149.7, 143.5, 141.4, 125.6, 123.7, 123.6, 63.1, 27.2, 14.2, 12.5.

IR Alpha-Platinum ATR, Bruker, diamond crystal

υ = 3040.4, 2966.4, 1723.4, 1622.5, 1591.9 cm^{-1}

HRMS ESI

Calculated mass for $(M+H)^+$ of $C_{12}H_{16}ClNO_2$ is 242.0942 found ($C_{12}H_{16}ClNO_2$+H-HCl)+ 206.1159.

5,6,7,8-Terahydroisoquinoline Dehydrogenation Product (**14e**, CAS 24334-24-5)

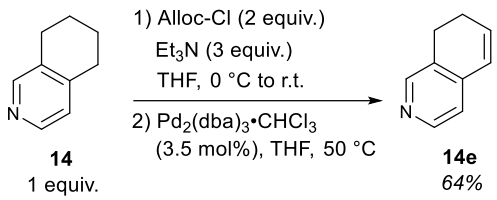

14
1 equiv.

14e
64%

Using procedure 3, pyridine **14** (0.10 g, 0.75 mmol, 1.0 equiv.) provided product **14e** (63 mg, 0.48 mmol) in 64% yield as a yellow oil.

Chromatography: 60% EtOAc in toluene (R_f. = 0.33).

Data for **14e**

^{1}H-NMR (300 MHz, $CDCl_3$)

δ 8.38 (d, *J* = 4.9 Hz, 1H), 8.32 (s, 1H), 6.89 (d, *J* = 4.9 Hz, 1H), 6.43 (dt, *J* = 9.6, 1.9 Hz, 1H), 6.26 (dt, *J* = 9.6, 4.4 Hz, 1H), 2.79 (t, *J* = 8.2 Hz, 2H), 2.38 (tdd, *J* = 8.2, 4.4, 1.9 Hz, 2H).

^{13}C-NMR (101 MHz, $CDCl_3$)

δ 148.7, 148.2, 140.9, 134.3, 129.8, 126.1, 119.9, 23.7, 23.1.

2-(4-(2-(Pyridin-4-yl)ethyl)phenethyl)pyridine Dehydrogenation Product (15e)

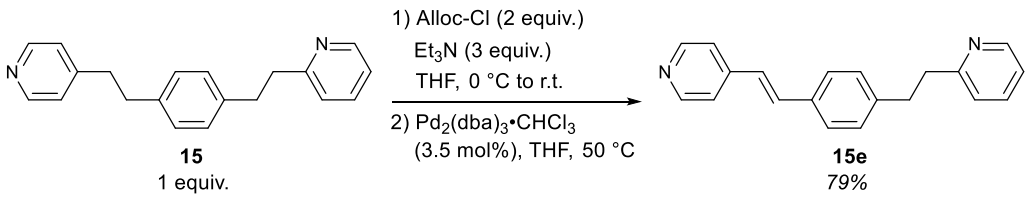

Using procedure 3, pyridine **15** (76 mg, 0.26 mmol, 1.0 equiv.) provided product **15e** (59 mg, 0.21 mmol) in 79% yield as a white solid.

Chromatography: 40% EtOAc : 5% Et_3N : 55% hexanes (R_f. = 0.29).

Data for **15e**

^{1}H-NMR (400 MHz, $CDCl_3$)

δ 8.57 (m, 3H), 7.57 (td, *J* = 7.6, 1.9 Hz, 1H), 7.45 (d, *J* = 8.2 Hz, 2H), 7.35 (d, *J* = 6.1 Hz, 2H), 7.27 (d, *J* = 16.4 Hz, 1H), 7.22 (d, *J* = 8.0 Hz, 2H), 7.12 (dd, *J* = 7.6, 4.9 Hz, 1H), 7.08 (d, *J* = 7.8 Hz, 1H), 6.97 (d, *J* = 16.4 Hz, 1H), 3.10 (m, 4H).

^{13}C-NMR (101 MHz, $CDCl_3$)

δ 161.4, 150.7, 149.9, 145.2, 143.0, 136.8, 134.4, 133.5, 129.5, 127.5, 125.7, 123.5, 121.7, 121.2, 40.5, 36.2.

IR Alpha-Platinum ATR, Bruker, diamond crystal

υ = 3068.9, 2960.8, 1633.2, 1589.6 cm^{-1}

HRMS ESI

Calculated mass for $(M+H)^+$ of $C_{20}H_{18}N_2$ is 287.1543 found 287.1530.

2-(4-(2-(Pyridin-4-yl)ethyl)phenethyl)pyridine coupled product (15e)

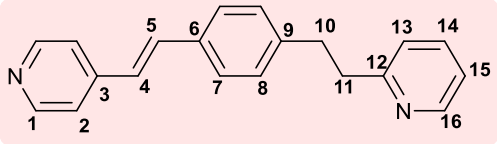

Carbon No.	^{13}C δ (ppm)[a]	^{1}H δ (ppm) (mult; *J* (Hz))[b,c]	HMBC Correlations
1	150.7	H-1: part of the multiplet at 8.57 (m, 3H)	2
2	121.2	H-2: 7.35 (d, *J* = 6.1 Hz, 2H)	1, 4
3	145.2	--	1, 4, 5
4	125.7	H-4: 7.27 (d, *J* = 16.4 Hz, 1H)	2
5	133.5	H-5: 6.97 (d, *J* = 16.4 Hz, 1H)	7
6	134.4	--	8, 4
7	127.5	H-7: 7.45 (d, *J* = 8.2 Hz, 2H)	5
8	129.5	H-8: 7.22 (d, *J* = 8.0 Hz, 2H),	10
9	143.0	--	7
10	36.2	H-10: part of the multiplet at 3.10 (m, 4H)	13
11	40.5	H-11: part of the multiplet at 3.10 (m, 4H)	8
12	161.4	--	10, 14, 15
13	123.5	H-13: 7.08 (d, *J* = 7.8 Hz, 1H)	11, 15
14	136.8	H-14: 7.57 (td, *J* = 7.6, 1.9 Hz, 1H)	16
15	121.7	H-15: 7.12 (dd, *J* = 7.6, 4.9 Hz, 1H)	13
16	149.9	H-16: part of the multiplet at 8.57 (m, 3H)	13, 14

[a] Recorded at 101 MHz. [b] Recorded at 400 MHz.
[b] Assignments based on HSQC-DEPT and HMBC data.
[c] Only those correlations which could be unambiguously assigned are reported.

5.5 Pyridylic Dehydrogenation: Functional Group Compatibility Screen

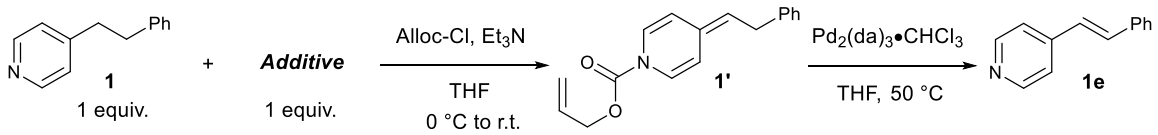

Entry	Additive	1e Yield (%)	Additive Recovery (%)	Entry	Additive	1e Yield (%)	Additive Recovery (%)
1	none	88	--	**8**	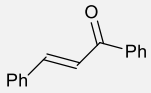	89	98
2	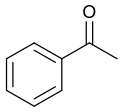	87	89	**9**	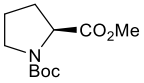	80	>99
3[a]	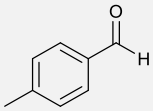	85	80	**10**	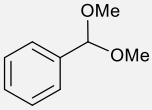	77	82
4	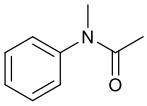	81	98	**11**	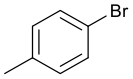	85	90
5	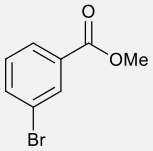	95	95	**12**	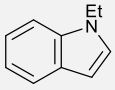	79	94
6	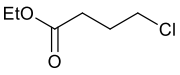	82	80	**13**	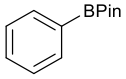	71	82
7	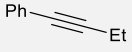	84	80	**14**	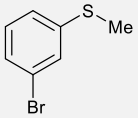	79	94

Reactions performed on 0.55 mmol scale according to general procedure 3 with an additional 1 equivalent of an additive. Yields were determined by quantitative ^{1}H NMR either using 1,4-bis(trichloromethyl)benzene, 1,3,5-trimethoxybenzene or 1,4-dimethoxybenzene as an internal standard. [a] dehydrogenation was run at 70 °C.

Functional Group Compatibility Screen Continued.

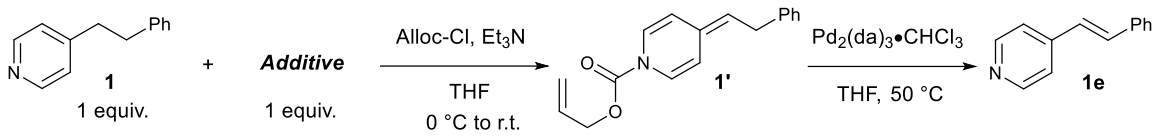

Entry	Additive	1e Yield (%)	Additive Recovery (%)	Entry	Additive	1e Yield (%)	Additive Recovery (%)
15	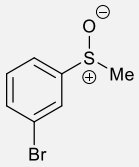	67	97	**18**	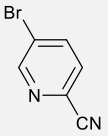	70	93
16	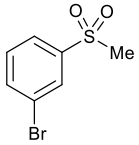	70	98	**19**[a,b]	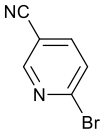	53	98
17	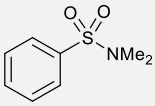	58	97	**20**[c]	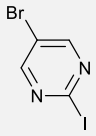	0	87

Reactions performed on 0.55 mmol scale according to general procedure 3 with an additional 1 equivalent of an additive. Yields were determined by quantitative ^{1}H NMR either using 1,4-bis(trichloromethyl)benzene, 1,3,5-trimethoxybenzene or 1,4-dimethoxybenzene as an internal standard. [a] dehydrogenation was run at 70 °C, [b] 22% of ADHP **1'** was recovered, [c] 67% of ADHP **1'** was recovered.

5.6 Pyridylic Allylation: Cross-over Experiment

Methallyl alcohol-*d3* (**16**)

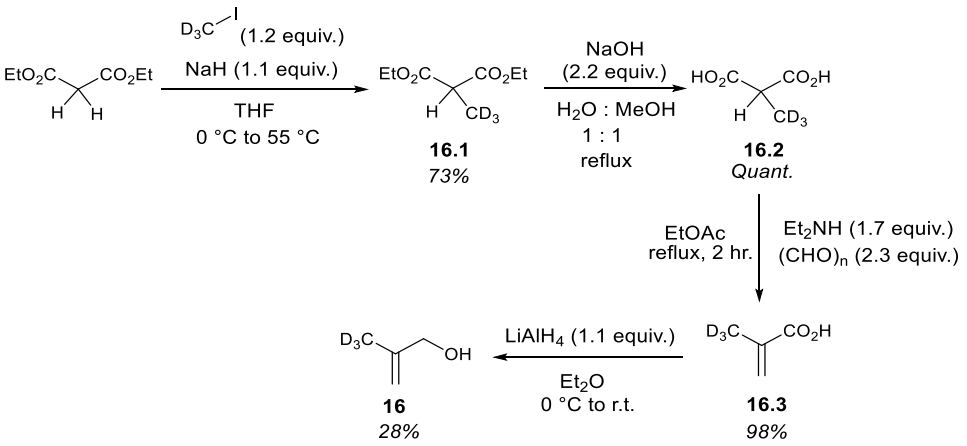

Alkylation of diethylmalonate (**16.1**, CAS: 54840-57-2) – An oven-dried 50 mL vial equipped with a stir bar was brought inside a glove box and charged with dry NaH (380 mg, 15.8 mmol, 1.10 equiv.). It was then brought out, kept under an atmosphere of argon and anhydrous THF (24 mL) was introduced to form a suspension of NaH. The vial was cooled to 0 °C and then a solution of diethylmalonate (2.30 g, 14.4 mmol, 1.00 equiv.) in THF (24 mL) was added slowly. The clear solution was stirred at ambient temperature for 1 h, and then cooled again to 0 °C. Methyl iodide-d3 was then added dropwise and the mixture was allowed to warm up to ambient temperature. The solution was stirred for two hours at room temperature and heated to 55 °C overnight. The solution was cooled to room temperature then quenched with saturated aqueous ammonium chloride. The aqueous layer was extracted with EtOAc three times and the combined organics were dried with $MgSO_4$, concentrated *in vacuo* and purified using flash chromatography to deliver the product as a colorless oil (1.86 g, 10.5 mmol) in 73% yield. Spectral data is consistent with that reported in the literature.[73]

Chromatography: 100% hexanes – 4% EtOAc in hexanes (R_f. = 0.3 in 10% EtOAc in hexanes).

Data for **16.1**

^{1}H-NMR (400 MHz, $CDCl_3$)

δ 4.20 (m, 4 H), 3.4 (s, 1H), 1.2 (t, *J* = 8.0 Hz, 6 H).

^{13}C-NMR (76 MHz, $CDCl_3$)

δ 170.2, 61.3, 46.0, 14.0.

Methallyl alcohol-*d3* (16)

Ester Hydrolysis (**16.2**, CAS: 42522-59-8) – Sodium hydroxide pellets (0.94 g, 24 mmol, 2.2 equiv.) were added to a solution of *d3*-methyl diethylmalonate (1.9 g, 11 mmol, 1.0 equiv.) in a 1:1 MeOH:H_2O (30 mL), and the resulting mixture was refluxed for 4 hours. After being cooled to ambient temperature, the mixture was diluted with distilled water and the aqueous layer was extracted once with EtOAc. The aqueous layer was then acidified to pH = 1 using 1M HCl, and then extracted thrice with EtOAc. The combined organics were dried with $MgSO_4$ then concentrated *in vacuo* to provide the diacid **18.2** as a white solid (1.3 g, 11 mmol) in quantitative yield which was used in the next step without further purification.

Formation of the α,β-Unsaturated Acid (**16.3**)[74] – A solution of the crude *d3*-methyl malonic acid (1.3 g, 11 mmol, 1.0 equiv.) in EtOAc (43 mL) was cooled to 0 °C. Diethylamine (1.9 mL, 18 mmol, 1.7 equiv.) was added dropwise to form a white suspension. Paraformaldehyde (0.72 g, 24 mmol, 2.3 equiv.) was added and the mixture was refluxed for two hours, then cooled to 0 °C and quenched with 1M HCl. The aqueous layer was extracted thrice with Et_2O and the combined organics were washed with brine, dried with $MgSO_4$ then concentrated *in vacuo* to provide the α,β-unsaturated acid as a yellow oil (0.87 g, 9.8 mmol) in 93% yield. This material was used in the next step without further purification.

$LiAlH_4$ Reduction – A flame-dried round-bottomed flask equipped with a stir bar was charged with the α,β-unsaturated acid (0.94 g, 9.9 mmol, 1.0 equiv.) in diethyl ether (15 mL) and cooled to 0 °C. A solution of Lithium Aluminum Hydride (1.4 g, 11 mmol, 1.1 equiv.) in diethyl ether (15 mL) was added dropwise and the mixture was allowed to stir for 4 hours at room temperature. Once complete, the mixture was cooled to 0 °C and quenched with distilled H_2O (1.5 mL) followed by 1M $NaOH_{(aq.)}$ (1.5 mL) and distilled H_2O (4.5 mL). The mixture was then transferred to a separatory funnel and Rochelle's salt was added. The aqueous layer was extracted thrice with Et_2O and the combined organics were given a brine wash, dried with $MgSO_4$ then concentrated by distillation under atmospheric pressure using a Vigreux column. The crude product was purified using flash chromatography and the pure product obtained after atmospheric distillation as a 2.5 M solution in diethyl ether (2.8 mmol) in 28% yield.

Chromatography: 40% Et_2O in Pentane (R_f. = 0.42).

Data for **16**

^{1}H-NMR (300 MHz, $CDCl_3$)

δ 4.98 (q, *J* = 1.4 Hz, 1 H), 4.87 (s, 1 H), 4.05 (dt, *J* = 6.3, 1.4 Hz, 2 H).

^{2}H-NMR (46 MHz, $CDCl_3$)

δ 1.73.

^{13}C-NMR (151 MHz, $CDCl_3$)

δ 144.5, 110.0, 67.0, 18.3 (m).

HRMS DART

Calculated mass for $(M+H)^+$ of $C_4H_6D_3O$ is 75.0764,found $(C_4H_6D_3O-H)^+$ 75.0778.

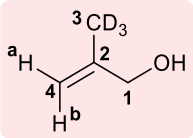

Carbon No.	**^{13}C δ (ppm)**	**^{1}H δ (ppm) (mult; *J* (Hz))** [a, b]	**HMBC Correlations**
1	67.0	H-1 : 4.05 (dt, *J* = 6.3, 1.2 Hz, 2 H)	H-4a, H-4b
2	144.5	--	H-1
3	18.3 (m)	--	H-1, H-4a
4	110.0	4.98 (q, *J* = 1.5 Hz, 1 H), 4.87 (s, 1 H)	H-1

[a] Recorded at 600 MHz.

[b] Only those correlations which could be unambiguously assigned are reported.

Cross-over Experiment.

Part A: Synthesis of Reference Compounds.

Procedure 4: General procedure for allylation of 4-alkylpyridines using methallyl chloroformate

Synthesis of methallyl chloroformate: A flame-dried round-bottomed flask equipped with a stir bar was cooled to −40 °C and charged with phosgene solution (15% in toluene, 2.24 equiv.). A solution of methallyl alcohol (1.6 equiv.) in THF (1.4 M) was then introduced dropwise and the temperature was maintained at −40 °C for one hour, then warmed to 0 °C for 10 minutes. The solution was then purged for 20 minutes with a stream of argon into a 1M aqueous sodium hydroxide trap to quench the excess phosgene. The resulting solution of methallyl chloroformate was maintained at 0 °C and used in the next step without isolation.

Synthesis of the ADHP intermediate: Triethylamine (3.0 equiv.) was added to a solution of the appropriate pyridine (1.0 equiv.) in dry THF (0.1 M) in a flame-dried flask equipped with a stir bar. The resulting solution was cooled to 0 °C and methallyl chloroformate (1.6 equiv.) was added dropwise. The mixture was allowed to stir for 45 min then concentrated in vacuo (on a rotary evaporator inside a fumehood). The resulting crude mass was suspended in diethyl ether and filtered through a plug of cotton to remove the triethylammonium chloride salt. The filtrate was concentrated in vacuo to afford an oil which was used in the next step without further purification.

Palladium-catalyzed decarboxylative allylation: An oven-dried round-bottomed flask equipped with a stir bar was charged with Xantphos (10 mol%) and $Pd(dba)_2$ (10 mol%). Dry THF was added and the resulting solution was allowed to stir for 10 min at room temperature under an atmosphere of argon. A solution of the ADHP in dry THF was then added to the flask containing the catalyst and the mixture was stirred at room temperature overnight. The mixture was then concentrated *in vacuo* and purified using flash chromatography, eluting with the indicated solvent mixture to afford the desired product.

4-(2-Phenylethyl)pyridine coupled product 1a (CH_3)

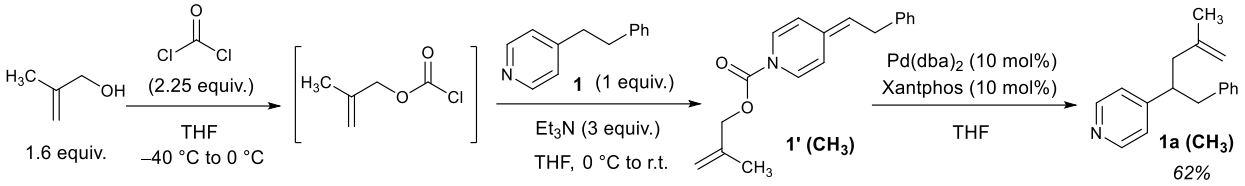

Using procedure 4, pyridine **1** (0.10 g, 0.55 mmol, 1.0 equiv.) provided product **1a (CH_3)** (80 mg, 0.34 mmol) in 62% yield as a colorless oil.

Chromatography: 25% EtOAc in Hexanes (R_f. = 0.28).

Data for **1a (CH_3)**

^{1}H-NMR (400 MHz, $CDCl_3$)

δ 8.46 (d, *J* = 6 Hz, 2 H), 7.23-7.13 (m, 3 H), 7.02-6.95 (m, 4 H), 4.73 (s, 1 H), 4.63 (s, 1 H), 3.11-2.96 (m, 2 H), 2.78 (dd, *J* = 8.8, 13.2 Hz, 1 H), 2.51-2.35 (m, 2 H), 1.59 (s, 3 H).

^{13}C-NMR (101 MHz, $CDCl_3$)

δ 153.7, 149.7, 142.7, 139.6, 129.1, 128.3, 126.3, 123.4, 113.1, 45.6, 43.6, 42.6, 22.4.

IR Alpha-Platinum ATR, Bruker, diamond crystal

υ = 3026, 2931, 1649, 1597 cm^{-1}

HRMS DART

Calculated mass for $(M+H)^+$ of $C_{17}H_{20}N$ is 238.1590, found 238.1590.

4-(2-Phenylethyl)pyridine coupled product 1a (CD_3)

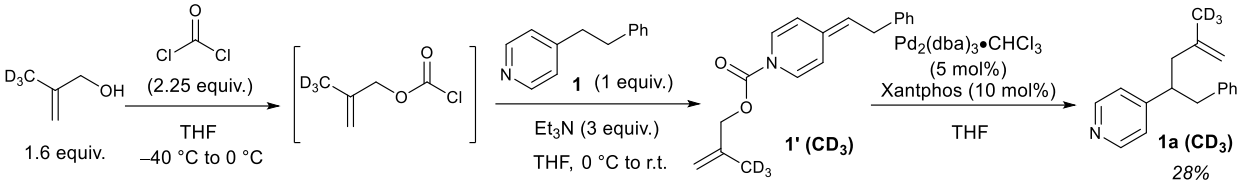

Following procedure 5 and using *d3*-methallyl alcohol (66 mg, 0.87 mmol, 1.6 equiv.), pyridine **1** (0.10 g, 0.55 mmol, 1.0 equiv.) provided product **1a (CD_3)** (37 mg, 0.15 mmol) in 28% yield as a colorless oil.

Chromatography: 100% Hexanes – 30% EtOAc in Hexanes (R_f. = 0.28 in 25% EtOAc in Hexanes).

Data for **1a (CD_3)**

^{1}H-NMR (400 MHz, $CDCl_3$)

δ 8.44 (d, *J* = 6 Hz, 2 H), 7.21-7.14 (m, 3 H), 7.00-6.95 (m, 4 H), 4.71 (s, 1 H), 4.61 (s, 1 H), 3.07-2.95 (m, 2 H), 2.80 (dd, *J* = 8.6, 13.4 Hz, 1 H), 2.46-2.33 (m, 2 H).

^{2}H-NMR (61 MHz, $CDCl_3$)

δ 1.62 (s, 3 D).

^{13}C-NMR (151 MHz, $CDCl_3$)

δ 153.7, 149.7, 142.7, 139.6, 129.2, 128.4, 126.3, 123.4, 113.1, 45.7, 43.6, 42.6, 21.6 (sept, *J* = 18.1 Hz).

IR Alpha-Platinum ATR, Bruker, diamond crystal

υ = 3068, 2928, 2266, 1643, 1597 cm^{-1}

HRMS DART

Calculated mass for $(M+H)^+$ of $C_{17}H_{17}D_3N$ is 241.17786, found 241.17808.

4-Phenetylpyridine coupled product 1a (CD_3)

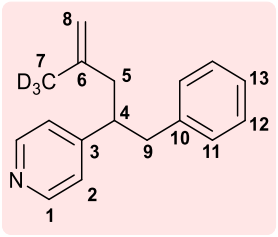

Carbon No.	^{13}C δ (ppm)[a]	^{1}H δ (ppm) (mult: *J* (Hz))[a, b]	HMBC Correlation
1	149.7	H-1: 8.44 (d, J = 6 Hz, 2 H)	H-2
2	123.4	Part of the multiplet at : 7.00-6.95 (m, 4 H)	H-1, H-4
3	153.7	--	H-1, H-4, H-5, H9
4	45.7	Part of the multiplet at: 3.07-2.95 (m, 2 H)	H-1, H-2, H-5, H-8, H-9
5	43.6	H-5: 2.46-2.33 (m, 2 H)	H4, H-8, H-9
6	142.7	--	H-4, H-5, H-8
7	21.6 (sept, *J* = 18.1 Hz)	--	H-5, H-8
8	113.1	H-8: 4.71 (s, 1 H), 4.61 (s, 1 H)	H-5
9	42.6	Part of the multiplet at: 3.07-2.95 (m, 2 H), 2.80 (dd, *J* = 8.6, 13.4 Hz, 1 H)	H-4, H-5, H-11
10	139.6	--	H-4, H-9, H-12
11	129.2	Part of the multiplet at : 7.00-6.95 (m, 4 H)	H-9, H-12, H-13
12	128.4	Part of the multiplet at: 7.21-7.14 (m, 3 H)	H-13
13	126.3	Part of the multiplet at: 7.21-7.14 (m, 3 H)	H-11, H-12

[a] Recorded at 151 MHz.

[b] Only those correlations which could be unambiguously assigned are reported.

4-Pentylpyridine coupled product 17a (CH_3)

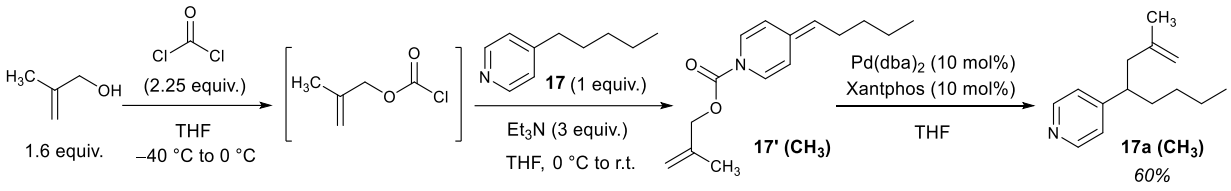

Using procedure 5, pyridine **17** (0.10 g, 0.67 mmol, 1.0 equiv.) provided product **17a (CH_3)** (82 mg, 0.40 mmol) in 60% yield as a colorless oil.

Chromatography: 13% EtOAc in Hexanes (R_f. = 0.31).

Data for **17a (CH_3)**

^{1}H-NMR (400 MHz, $CDCl_3$)

δ 8.49 (d, *J* = 6 Hz, 2 H), 7.07 (d, *J* = 6 Hz, 2 H), 4.66 (s, 1 H), 4.55 (s, 1 H), 2.69 (m, 1 H), 2.36-2.21 (m, 2 H), 1.65-1.45 (m, 5 H), 1.35-1.05 (m, 4 H), 0.82 (t, *J* = 6.9 Hz, 3 H).

^{13}C-NMR (101 MHz, $CDCl_3$)

δ 154.9, 149.8, 143.1, 123.4, 112.7, 44.9, 43.6, 35.5, 29.7, 22.8, 22.5, 14.1.

IR Alpha-Platinum ATR, Bruker, diamond crystal

υ = 3070, 2929, 1598 cm^{-1}

HRMS DART

Calculated mass for $(M+H)^+$ of $C_{14}H_{22}N$ is 204.1747, found 204.1748.

4-Pentylpyridine coupled product 17a (CD_3)

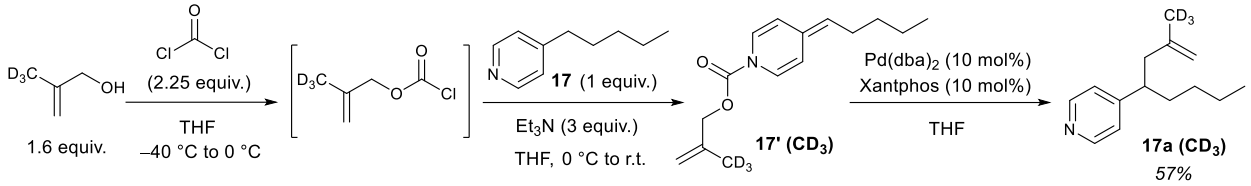

Following procedure 5 and using *d3*-methallyl alcohol (81 mg, 1.1 mmol, 1.6 equiv.), pyridine **17** (0.10 mg, 0.67 mmol, 1.0 equiv.) provided product **17a (CD_3)** (79 mg, 0.38 mmol) in 57% yield as a colorless oil.

Chromatography: 15% EtOAc in Hexanes (R_f. = 0.35).

Data for **17a (CD_3)**

^{1}H-NMR (300 MHz, $CDCl_3$)

δ 8.49 (d, *J* = 6 Hz, 2 H), 7.07 (d, *J* = 6 Hz, 2 H), 4.70 (s, 1 H),
4.52 (s, 1 H), 2.70 (m, 1 H), 2.39-2.23 (m, 2 H), 1.70-1.41 (m, 2 H),
1.35-1.05 (m, 4 H), 0.82 (t, *J* = 6.9 Hz, 3 H).

^{2}H-NMR (46 MHz, $CDCl_3$)

δ 1.62 (s, 3 D).

^{13}C-NMR (151 MHz, $CDCl_3$)

δ 154.9, 149.8, 143.0, 123.3, 112.7, 44.8, 43.6, 35.5, 29.7, 22.7,
21.8 (sept, *J* = 19.6 Hz), 14.0.

IR Alpha-Platinum ATR, Bruker, diamond crystal

υ = 3071, 2929, 2226, 1597 cm^{-1}

HRMS DART

Calculated mass for $(M+H)^+$ of $C_{14}H_{19}D_3N$ is 207.1935, found 207.1940.

4-Pentylpyridine coupled product 17a (CD_3)

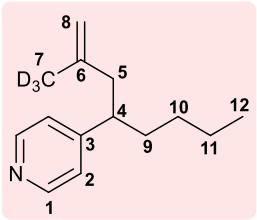

Carbon No.	^{13}C δ (ppm)[a]	^{1}H δ (ppm) (mult: *J* (Hz))[a, b]	HMBC Correlation
1	149.8	H-1: 8.49 (d, *J* = 6 Hz, 2 H)	H-2
2	123.3	H-2: 7.07 (d, *J* = 6 Hz, 2 H)	H-1, H-4
3	154.9	--	H-4, H-5, H9
4	43.6	2.70 (m, 1 H)	H-1, H-2, H-5, H-5
5	44.8	2.39-2.23 (m, 2 H)	H4, H-8
6	143.0	--	H-4, H-5, H-8
7	21.8 (sept, *J* = 19.6 Hz)	--	H-5, H-8
8	112.7	4.70 (d, *J* = 21.3 Hz, 1 H), 4.52 (d, *J* = 21.3 Hz, 1 H)	H-5
9	35.5	1.70-1.41 (m, 2 H)	H-4, H-5, H-10, H-11
10	29.7	Part of the multiplet at: 1.35-1.05 (m, 4 H)	H-4, H-9, H-11, H-12
11	22.7	Part of the multiplet at: 1.35-1.05 (m, 4 H)	H-9, H-10, H-12
12	14.0	0.82 (t, *J* = 6.9 Hz, 3 H)	H-10, H-11

[a] Recorded at 151 MHz.

[b] Only those correlations which could be unambiguously assigned are reported.

Cross-Over Experiment.

Part B: Cross-Over Experiment Procedure and Analysis.

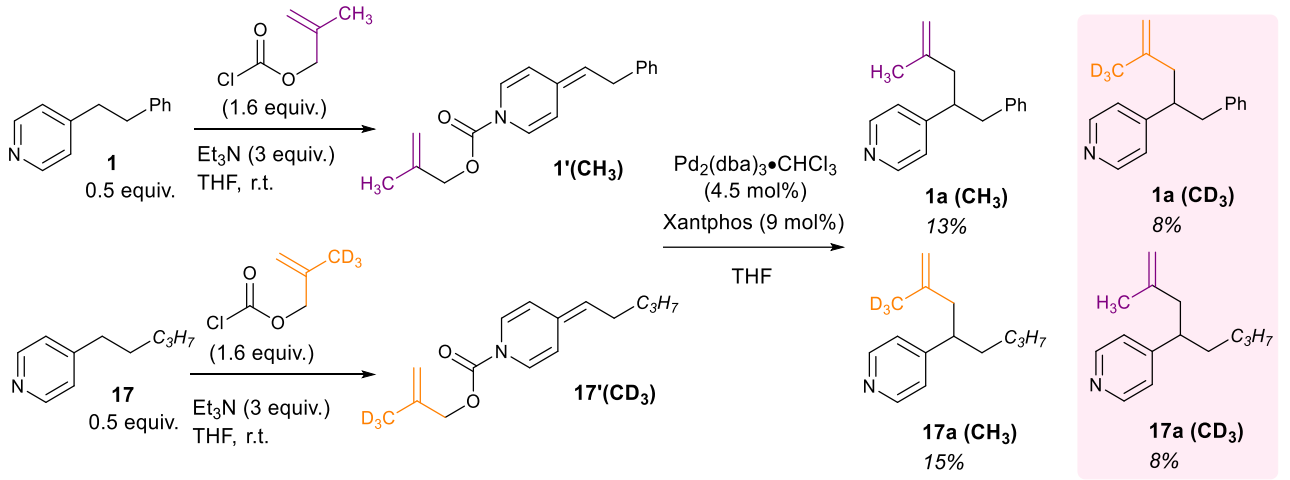

*ADHP **1'(CH$_3$)** Formation* – Using procedure 5, pyridine **1** (0.12 mg, 0.67 mmol, 1.0 equiv.) was reacted with triethylamine (0.28 mL, 2.0 mmol, 3.0 equiv.) and methallyl chloroformate (1.1 mmol, 1.6 equiv.) to provide alkylidene dihydropyridine **1'(CH$_3$)** as a bright yellow oil.

*ADHP **17'(CD$_3$)** Formation* – Using procedure 5, pyridine **17** (0.10 mg, 0.67 mmol, 1.0 equiv.) was reacted with triethylamine (0.28 mL, 2.0 mmol, 3.0 equiv.) and *d3*-methallyl chloroformate (1.1 mmol, 1.6 equiv.) to provide alkylidene dihydropyridine **17'(CD$_3$)** as a pink oil.

Cross-Over Experiment – A flame-dried round bottomed flask equipped with a stir bar was charged with $Pd_2(dba)_3$•$CHCl_3$ (64 mg, 0.067 mmol, 4.5 mol%), Xantphos (78 mg, 0.13 mmol, 10 mol%) and dry THF (6 mL) and the mixture was stirred for 15 min. ADHP intermediates **1'(CH$_3$)** and **17'(CD$_3$)** were then added as a solution in THF (7 mL) and the mixture was left to stir overnight. The solution was then concentrated *in vacuo* and using flash chromatography two sets of products were separated: (**1a(CH$_3$)** + **1a(CD$_3$)** and (**17a(CH$_3$)** + **17a(CD$_3$)**). The ratio of deuterated to methylated products was determined using quantitative ^{1}H NMR for **1a (CH$_3$) + 1a (CD$_3$)** using the CH_3 peak of **1a (CH$_3$)** as the internal standard and quantitative ^{2}H NMR for **17a (CH$_3$) + 17a (CD$_3$)** using CD_3CN as an internal standard.

Determining Product Ratio – The product set **1a (CH_3)** + **1a (CD_3)** was isolated with a total mass of 64.6 mg (0.27 mmol). ^{1}H NMR was used to determine the molar ratio of the products; the CH_3 singlet of **1a (CH_3)** at 1.68 ppm was calibrated to 3 H and compared to the total integration of the multiplet at 6.92 ppm (which accounts for 2 phenyl protons and 2 pyridine protons for each of the compounds). This established the product ratio to be 1 : 0.69 of **1a (CH_3)** : **1a (CD_3)**; **1a (CH_3)** (37.9 mg, 0.16 mmol) and **1a (CD_3)** (26.5 mg, 0.11 mmol).

The product set **17a (CH_3)** + **17a (CD_3)** was isolated with a total mass of 63.8 mg (0.21 mmol). Quantitative ^{2}H NMR was performed using known amounts of CD_3CN as an internal standard which revealed the mixture contains 40.9 mg (0.20 mmol) of **17a (CD_3)**. By considering the total isolated mass and the mass of **17a (CD_3)** obtained through quantitative ^{2}H NMR, it was deduced that **17a (CH_3)** was present in 22.9 mg (0.11 mmol). The products **17a (CH_3)** + **17a (CD_3)**, therefore, existed in a 1 : 0.41 molar ratio.

5.7 Pyridylic Allylation: Stereochemical Probe

***cis*-5-Phenyl-2-cyclohexen-1-ol** (**18**, CAS 26114-87-4)

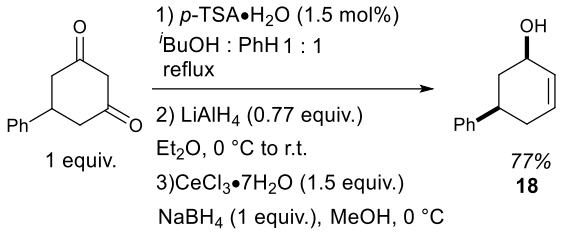

A round-bottomed flask equipped with a stir bar was charged with 5-phenyl-1,3-cyclohexanedione (0.20 g, 1.1 mmol, 1.0 equiv.), *p*-toluic acid (2.0 mg, 0.016 mmol, 0.015 equiv.) and a benzene : isobutylalcohol mixture (1 : 1, 4.7 mL). The flask was fitted with a Dean-Stark trap and heated to reflux for 3 h. The solution was then cooled to room temperature and concentrated under reduced pressure to afford a viscous oil which was dissolved in diethyl ether (8 mL) and washed with 2M NaOH three times. The organic layer was washed with brine, dried over $MgSO_4$ and concentrated under reduced pressure. The resulting oil was dissolved in anhydrous diethyl ether (12 mL) and transferred to a flame-dried round-bottomed flask. The solution was cooled to 0°C, $LiAlH_4$ (31 mg, 0.82 mmol, 0.77 equiv.) was added portion-wise and the resulting mixture was stirred at room temperature for 2 h. The reaction was quenched with 10% aq. HCl, extracted with diethyl ether, washed with brine, dried over $MgSO_4$ and concentrated under reduced pressure. The resulting oil was then dissolved in methanol (16 mL), $CeCl_3•7H_2O$ (0.39 g, 1.6 mmol, 1.5 equiv.) was added, and then $NaBH_4$ was added portion-wise (40 mg, 1.1 mmol, 1.0 equiv.). This reaction mixture was stirred for 3 h at 0°C, then concentrated under reduced pressure and washed with 1 M HCl (3x) and brine. It was then dried over $MgSO_4$ and concentrated *in vacuo*. Purification by chromatography furnished *cis*-5-phenyl-2-cyclohexen-1-ol (0.14 g, 0.85 mmol) as a white solid in 77% yield. Spectral data is consistent with that reported in the literature.[58]

Chromatography: 20% EtOAc in Hexanes (R_f. = 0.40).

Data for **18**

^{1}H-NMR (300 MHz, $CDCl_3$)

δ 7.33-7.29 (m, 2 H), 7.23-7.18 (m, 3 H), 5.84-5.81 (m, 1 H), 5.77-5.73 (m, 1 H), 4.47 (br, 1 H), 2.96-2.83 (m, 1 H), 2.37-2.21 (m, 2 H), 2.19-2.04 (m, 1 H), 1.78-1.68 (m, 1 H), 1.58 (d, *J* = 5.1Hz, 1 H).

^{13}C-NMR (101 MHz, $CDCl_3$)

δ 145.6, 131.1, 128.7, 128.6, 126.8, 126.4, 68.6, 39.6, 39.3, 33.8.

***cis*-5-Phenyl-2-cyclohexen-1-ol** (**18**, CAS 26114-87-4)

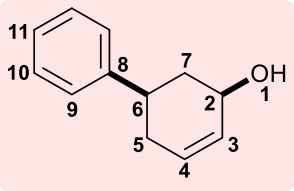

Proton	**^{1}H** δ (ppm) (mult: *J* (Hz))[a, b,c,d]	**COSY Correlation**
H-1	1.58 (d, *J* = 5.1Hz, 1H)	H-2, H-7a, H-7b
H-2	4.47 (s, 1H)	H-1, H-5a H-7a, H-7b
H-3	5.77-5.73 (m, 1H)	H-4
H-4	5.84-5.81 (m, 1H)	H-4, H-5b, H-7b
H-5	H-5a: 2.19-2.04 (m, 1H) H-5b: part of the m at 2.37-2.21	H-2, H-4, H-6, H-7a, H-7b
H-6	2.96-2.83 (m, 1H)	H-5a, H-5b, H-7a, H-7b
H-7	H-7a: 1.78-1.68 (m, 1H) H-7b: part of the m at 2.37-2.21	H-1, H-2, H-4, H-5a, H-5b, H-6
H-9	Part of the m at 7.23-7.18	H-10, H-11
H-10	7.33-7.29 (m, 2H)	H-9, H-11
H-11	Part of the m at 7.23-7.18	H-9, H-19

[a] Recorded at 600 MHz. [b] Assignments based on HSQC-DEPT and HMBC data

[c] Methylene protons are designated H-Xa and H-Xb arbitrarily

[d] Only those correlations which could be unambiguously assigned are reported.

***cis*-5-Phenyl-2-cyclohexen-1-ol** (**18**, CAS 26114-87-4)

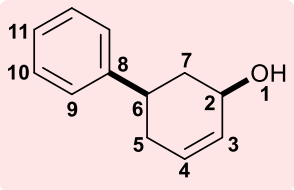

Proton No.	**^{1}H** δ (ppm) (mult: *J* (Hz))[a, b,c,d]	**NOESY Correlation**
H-1	1.58 (d, *J* = 5.1Hz, 1H)	H-2
H-2	4.47 (s, 1H)	H-1, H-6, H-7a, H-7b
H-3	5.77-5.73 (m, 1H)	H-4, H-7a
H-4	5.84-5.81 (m, 1H)	H-3, H-5a, H-5b, H-7b
H-5	H-5a: 2.19-2.04 (m, 1H) H-5b: part of the m at 2.37-2.21	H-2, H-4, H-6, H-7a, H-7b, H-9
H-6	2.96-2.83 (m, 1H)	H-2, H-5a, H-5b, H-7a, H-7b, H-9
H-7	H-7a: 1.78-1.68 (m, 1H) H-7b: part of the m at 2.37-2.21	H-2, H-3, H-4, H-5a, H-5b, H-6, H-9
H-9	Part of the m at 7.23-7.18	H-5a, H-5b, H-7a, H-7b, H-10, H-11
H-10	7.33-7.29 (m, 2H)	H-9, H-11
H-11	Part of the m at 7.23-7.18	H-9, H-10

[a] Recorded at 600 MHz. [b] Assignments based on HSQC-DEPT and HMBC data

[c] Methylene protons are designated H-Xa and H-Xb arbitrarily

[d] Only those correlations which could be unambiguously assigned are reported.

Stereochemical Probe.

4-Isopropylpyridine coupled product (19a)

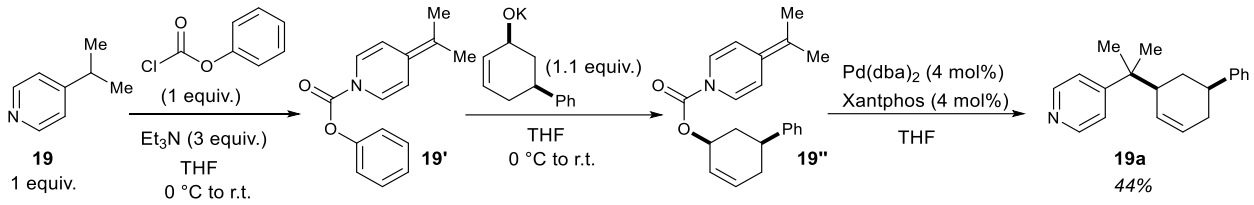

*ADHP **19'** Formation* – Using procedure 4, pyridine **19** (0.34 g, 2.8 mmol, 1.0 equiv.) was reacted with triethylamine (1.2 mL, 8.4 mmol, 3.0 equiv.) and phenyl chloroformate (0.44 g, 2.8 mmol, 1.0 equiv.) to provide ADHP **19'** as a white solid.

*ADHP **19"** Formation* – A flame-dried round bottomed flask equipped with a stir bar was charged with *cis*-5-phenyl-2-cyclohexen-1-ol (0.52 mg, 3.0 mmol, 1.1 equiv.) and dry THF (30 mL) and cooled to 0 °C under an argon atmosphere. KHMDS (6.2 mL, 3.3 mmol, 1.1 equiv., 0.50 M in toluene) was then added dropwise and the mixture was allowed to stir at 0°C for 30 minutes. This potassium alkoxide was added dropwise to another flame-dried flask containing a solution of intermediate **19'** in dry THF (27 mL) at 0°C and the mixture was allowed to warm to room temperature over 1.5 hours. The solution was then *in vacuo* and the resulting crude mass was suspended in toluene and filtered through a plug of cotton to remove the phenyl alkoxide salt. The filtrate was concentrated *in vacuo* to afford ADHP **19''** as a yellow oil which was used in the next step without further purification.

Palladium-catalyzed decarboxylative allyation – Using procedure 4, ADHP **19"** was mixed with Xantphos (4.0 mol%) and $Pd(dba)_2$ (4.0 mol%) in dry THF (27 mL) and allowed to stir at room temperature overnight. This afforded product **19a** (70 mg, 1.2 mmol) as a yellow solid in 44% yield.

Chromatography: 25% EtOAc in Hexane (R_f = 0.30).

Data for **19a**

^{1}H-NMR (600 MHz, $CDCl_3$)
δ 8.50 (d, *J* = 6.0 Hz, 2 H), 7.28 (t, *J* = 7.5 Hz, 2 H), 7.25 (d, *J* = 4.7 Hz, 2 H), 7.19-7.15 (m, 3 H), 5.81-5.77 (m, 1 H), 5.48 (d, *J* = 10.4 Hz, 1 H), 2.83-2.77 (m, 1 H), 2.76-2.64 (m, 1 H), 2.19-2.03 (m, 2 H), 1.69-1.68 (m, 1 H), 1.43 (q, *J* = 12.4 Hz, 1 H), 1.30 (s, 3 H), 1.26 (s, 3 H).

^{13}C-NMR (151 MHz, $CDCl_3$)
δ 158.5, 149.6, 146.8, 128.7, 128.4, 127.8, 126.8, 126.2, 121.6, 47.4, 40.8, 40.4, 33.6, 32.1, 24.8, 24.2.

IR Alpha-Platinum ATR, Bruker, diamond crystal
υ = 2893, 1592, 1442, 1148, 822, 760, 699, 578 cm^{-1}

HRMS DART
Calculated mass for $(M+H)^+$ of $C_{20}H_{24}N$ is 278.1903, found 278.1910.

4-Isopropylpyridine coupled product (19a)

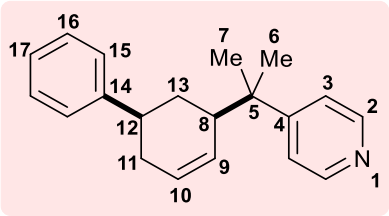

Proton No.	^{1}H δ (ppm) (mult: *J* (Hz))[a, b,c]	COSY Correlation
H-2	8.50 (d, *J* = 6.0 Hz, 2H)	H-3
H-3	7.25 (d, *J* = 4.7 Hz, 2H)	H-2
H-6	1.30 (s, 1H)	H-7
H-7	1.26 (s, 1H)	H-6
H-8	2.76-2.64 (m, 1H)	H-10, H-11, H-13a, H-13b
H-9	5.48 (d, *J* = 10.4 Hz, 1H)	H-10
H-10	5.81-5.77 (m, 1H)	H-9, H-11
H-11	2.19-2.03 (m, 2H)	H-10, H-12
H-12	2.83-2.77 (m, 1H)	H-11, H-13b
H-13	H-13a : 1.69-1.68 (m, 1H) H-13b : 1.43 (q, *J* = 12.4 Hz, 1H)	H-8
H-15	part of the multiplet at: 7.19-7.15 (m, 3 H)	H-17, H-16
H-16	7.28 (t, *J* = 7.5 Hz, 2H)	H-17, H-15
H-17	Part of the multiplet at: 7.19-7.15 (m, 3 H)	H-16, H-15

[a] Recorded at 600 MHz. [b] Methylene protons are designated H-Xa and H-Xb arbitrarily

[c] Only those correlations which could be unambiguously assigned are reported.

4-Isopropylpyridine coupled product (19a)

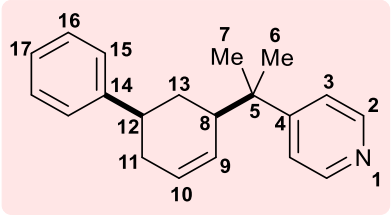

Carbon No.	^{13}C δ (ppm)[a]	^{1}H δ (ppm) (mult: *J* (Hz))[a, b,c,d]	HMBC Correlation
2	149.6	H-2 : 8.50 (d, *J* = 6.0 Hz, 2H)	H-3
3	121.6	H-3 : 7.25 (d, 4.7 Hz, 2H)	H-16, H-15, H-6, H-7
4	158.5	--	H-2, H-6, H-7
5	40.4	--	H-2, H-3, H-6, H-7
6	24.2	H-6 : 1.30 (s, 1H)	H-7
7	24.8	H-7 : 1.26 (s, 1H)	H-6
8	47.4	H-8 : 2.76-2.64 (m, 1H)	H-10, H-12, H-13a, H-13b, H-6, H-7
9	127.8	H-9 : 5.48 (d, *J* = 10.4 Hz, 1H)	H-13a, H-13b
10	128.7	H-10 : 5.81-5.77 (m, 1H)	H-11
11	33.6	H-11 : 2.19-2.03 (m, 2H)	H-10, H-12, H-13a, H-13b
12	40.8	H-12 : 2.83-2.77 (m, 1H)	H-15, H-10, H-8, H-11, H-13a, H-13b
13	29.7	H-13a : 1.69-1.68 (m, 1H) H-13b : 1.43 (q, *J* = 12.4 Hz, 1H)	H-9, H-12, H-11
14	146.8	--	H-16, H-15, H-12, H-13a, H-13b
15	126.8	Part of the multiplet at: 7.19-7.15 (m, 3 H)	H-16, H-17, H-12
16	128.4	H-16: 7.28 (t, *J* = 7.5 Hz, 2H)	H-17
17	126.2	Part of the multiplet at: 7.19-7.15 (m, 3 H)	H-16, H-15

[a] Recorded at 600 MHz. [b] Assignments based on HSQC-DEPT and HMBC data

[c] Methylene protons are designated H-Xa and H-Xb arbitrarily

[d] Only those correlations which could be unambiguously assigned are reported.

4-Isopropylpyridine coupled product (19a)

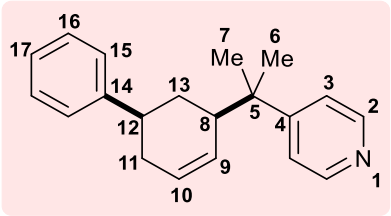

Proton No.	^{1}H δ (ppm) (mult: *J* (Hz))[a, b,c,d]	NOESY Correlation
H-3	7.25 (d, *J* = 4.7 Hz, 2H)	H-6, H-7, H-8
H-6	1.30 (s, 1H)	H-8, H-3, H-9
H-7	1.26 (s, 1H)	H-8, H-3, H-9
H-8	2.76-2.64 (m, 1H)	H-6, H-7, H-13a, H-13b
H-9	5.48 (d, *J* = 10.4 Hz, 1H)	H-6, H-7
H-10	5.81-5.77 (m, 1H)	H-11
H-11	2.19-2.03 (m, 2H)	H-10, H-12, H-15
H-12	2.83-2.77 (m, 1H)	H-13a, H-13b, H-11
H-13	H-13a : 1.69-1.68 (m, 1H) H-13b : 1.43 (q, *J* = 12.4 Hz, 1H)	H-8, H-15
H-15	Part of the multiplet at: 7.19-7.15 (m, 3 H)	H-13, H-11, H-12

[a] Recorded at 600 MHz. [b] Assignments based on HSQC and HMBC data

[c] Methylene protons are designated H-Xa and H-Xb arbitrarily

[d] Only those correlations which could be unambiguously assigned are reported.

5.8 Pyridylic Allylation: Allylation Using [(Xantphos)Pd(η3-allyl)]OTf

[(Xantphos)Pd(η3-allyl)]OTf (**C1**)

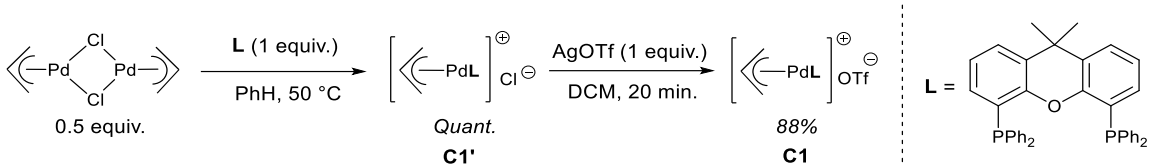

A flame-dried round-bottomed flask equipped with a stir bar was charged with $[Pd(\eta^3\text{-allyl})Cl]_2$ (0.10 g, 0.27 mmol, 0.50 equiv.) and benzene (7.5 mL). Xantphos (0.32 g, 0.55 mmol, 1.0 equiv.) was suspended in benzene (7.5 mL) in a second round-bottomed flask. Both flasks were heated to 50 °C until the solids dissolved, then the solution of palladium in benzene was transferred via cannula to the flask containing xantphos. After stirring for 30 min at 50 °C, the resulting suspension was allowed to cool to ambient temperature, and the precipitate was isolated by filtration in air. The precipitate was washed two times with 15 mL of Et_2O and dried *in vacuo* to give [(Xantphos)Pd(allyl)Cl] **C1'** (0.42 mg, 0.55 mmol) as an orange solid in quantitative yield. 0.3 g of the complex was then taken inside a glovebox, dissolved in DCM (24 mL) and transferred to a 50 mL vial equipped with a stir bar. To it was added AgOTf (0.10 g, 0.39 mmol, 1.0 equiv.) and the mixture was stirred for 20 min. The suspension was then filtered through Celite® and concentrated *in vacuo.* The crude product was recrystallized by dissolving the crude complex in a minimum amount of DCM, then layering it with Et_2O and cooling to −35 °C overnight. The pure complex was isolated by filtration, and was washed with Et_2O twice and obtained as a yellow solid (0.30 g, 0.35 mmol) in 88% yield. Spectral data is consistent with that reported in the literature.[60]

Data for **C1**

^{1}H-NMR (300 MHz, CD_2Cl_2)

δ 7.67 (dd, *J* = 7.7, 1.2 Hz, 2 H), 7.45-7.33 (m, 12 H), 7.20-7.11 (m, 10 H), 6.58 (t, *J* = 7.8 Hz, 2 H), 6.58 (sept, *J* = 7.2 Hz, 1 H), 3.75 (d, *J* = 6.9 Hz, 2 H), 3.42 (m, 2 H), 1.65 (br, 3 H), 1.54 (s, 3 H).

^{13}C-NMR (101 MHz, CD_2Cl_2)

δ 155.6 (t, *J* = 3.5 Hz), 134.8, 133.3 (t, *J* = 6 Hz), 132.9 (t, *J* = 6 Hz), 132.7, 132.5, 131.4 (d, *J* = 6 Hz), 129.8 (m), 129.5 (t, *J* = 6 Hz), 129.0, 125.4 (t, *J* = 4 Hz), 123.1, 122.5 (t, *J* = 5.1 Hz), 118.3, 117.9 (m), 79.9 (t, *J* = 15.2 Hz), 36.6, 30.2, 25.8.

^{31}P-NMR (122 MHz, CD_2Cl_2)

δ 4.27.

Stoichiometric Allylation Using Complex C1.

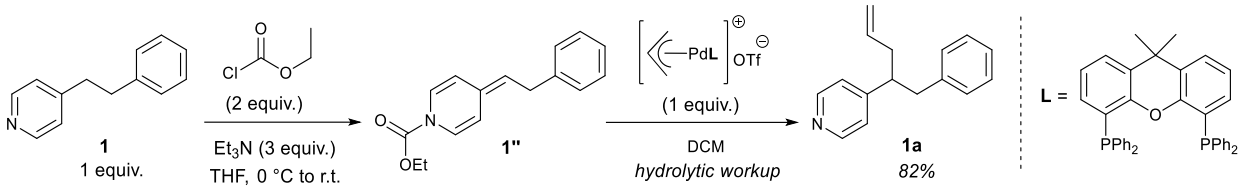

Using procedure 4, pyridine **1** (11 mg, 0.060 mmol, 1.0 equiv.) was reacted with triethylamine (24 µL, 0.17 mmol, 3.0 equiv.) and ethyl chloroformate (11 µL, 0.12 mmol, 2.0 equiv.) to provide alkylidene dihydropyridine **1''** as a bright yellow oil which was used without further purification. A 5 mL oven-dried scintillation vial was brought inside the glovebox and charged with Complex **C1** (48 mg, 0.060 mmol, 1.0 equiv.) and then brought out and kept under an inert atmosphere of argon. The complex was then dissolved in DCM (0.7 mL) and to it was added alkylidene dihydropyridine **1''** in DCM (0.5 mL). After an overnight reaction, the mixture was concentrated *in vacuo* then stirred in aqueous saturated sodium bicarbonate. The aqueous solution was extracted with EtOAc (3x) and the combined organics were washed with brine, dried over $MgSO_4$ and concentrated *in vacuo*. The yield of the product was determined using quantitative ^{1}H NMR using 1,4-bis(trichloromethyl)benzene as an internal standard.

Catalytic Allylation Using Complex C1.

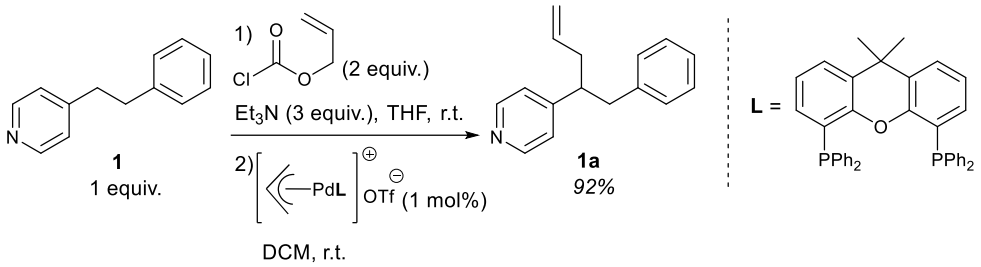

Using procedure 4 and using Complex **C1** as catalyst (4.8 mg, 0.060 mmol, 1.0 mol%), pyridine 1 (0.10 g, 0.55 mmol, 1.0 equiv.) provided product **1a** (0.11 g, 0.51 mmol) in 92% yield as a clear oil.

Chromatography: 30% EtOAc in hexane (R_f. = 0.30).

Data for **1a**

^{1}H-NMR (400 MHz, $CDCl_3$)

δ 8.45 (d, *J* = 5.6 Hz, 2 H), 7.24-7.13 (m, 3 H), 7.01-7.00 (m, 4 H),
5.63 (dddd, *J* =17.2, 10.4, 6.8, 6.8 Hz, 1 H), 4.97 (d, *J* = 17.2 Hz, 1 H),
4.96 (d, *J* = 10.4 Hz, 1 H), 2.99 (dd, *J* = 12.4, 6.8 Hz, 1 H),
2.97-2.89 (m, 1 H), 2.83 (dd, *J* = 12.4, 7.4 Hz, 1 H), 2.50-2.36 (m, 2 H).

^{13}C-NMR (101 MHz, $CDCl_3$)

δ 153.5, 149.8, 139.5, 135.8, 129.2, 128.4, 126.3, 123.5, 117.2, 47.4, 42.1,
39.4.

IR Alpha-Platinum ATR, Bruker, diamond crystal

υ = 3064, 3026, 2923, 1640, 1597, 1557, 1495, 1453, 1413, 910 cm^{-1}

HRMS ESI

Calculated mass for $(M+H)^+$ of $C_{13}H_{17}N$ is 224.1434, found 224.1424.

5.9 Pyridylic Allylation: Anionic vs. Neutral Cross-Over Experiment

Competition cross-over experiment between neutral ADHP 1" and a pyridylic anion of 6.

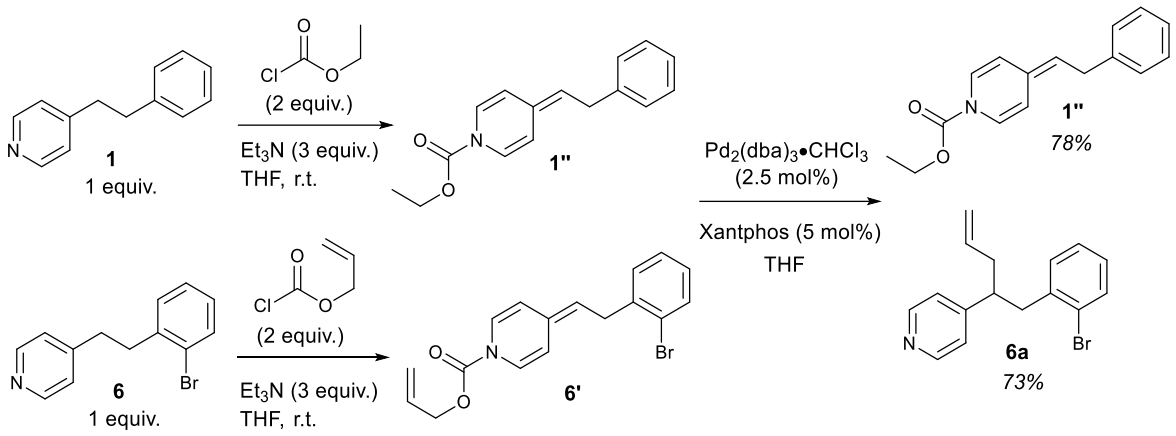

*ADHP **1" Formation*** – Using procedure 4, pyridine **1** (0.15 mg, 0.82 mmol, 1.0 equiv.) was reacted with triethylamine (0.34 mL, 2.5 mmol, 3.0 equiv.) and ethyl chloroformate (0.16 mL, 1.6 mmol, 2.0 equiv.) to provide alkylidene dihydropyridine **1''** as a bright yellow oil which was used without further purification.

*ADHP **6' Formation*** – Using procedure 4, pyridine **6** (0.22 g, 0.82 mmol, 1.0 equiv.) was reacted with triethylamine (0.34 mL, 2.5 mmol, 3.0 equiv.) and allyl chloroformate (0.17 mL, 1.6 mmol, 2.0 equiv.) to provide ADHP **6'** as a bright yellow oil which was used without further purification.

Cross-Over Experiment – A flame-dried round bottomed flask equipped with a stir bar was charged with $Pd_2(dba)_3$•$CHCl_3$ (21 mg, 0.020 mmol, 2.5 mol%), Xantphos (24 mg, 0.040 mmol, 5.0 mol%) and dry THF (3 mL) and the mixture was stirred for 15 min. ADHP intermediates **1''** and **6'** were then added as a solution in THF (7 mL) and the mixture was left to stir overnight. The solution was then diluted with EtOAc and washed with a saturated aqueous solution of sodium bicarbonate, the aqueous layer was extracted twice more with EtOAc and the combined organics were washed with brine, dried over $MgSO_4$ and concentrated *in vacuo*. Product yield and ADHP recovery were determined using quantitative ^{1}H NMR using 1,4-bis(trichloromethyl)benzene as an internal standard.

5.10 Pyridylic Allylation: NMR Reaction Progress Experiments

*ADHP **1'** Formation* – Using procedure 4, pyridine **1** (50 mg, 0.27 mmol, 1.0 equiv.) was reacted with triethylamine (0.11 mL, 0.82 mmol, 3.0 equiv.) and allyl chloroformate (0.060 mL, 0.55 mmol, 2.0 equiv.) to provide alkylidene dihydropyridine **1'** as a bright yellow oil which was used without further purification.

Preparation of Pd-Xantphos Stock Solution – A flame-dried 5mL scintillation vial was charged with $Pd_2(dba)_3 \bullet CHCl_3$ (5 mg, 0.005 mmol), Xantphos (9 mg, 0.02 mmol) and CD_2Cl_2 (3.9 mL) and the solution was stirred for 15 min before use.

*Preparation of Complex **C1** Stock Solution* – A flame-dried 5 mL scintillation vial was brought inside the glovebox and charged with complex 33 (8 mg, 0.01 mmol) then brought outside and kept under an atmosphere of argon. CD_2Cl_2 (3.7 mL) was then added and the solution was stirred for 15 min before use.

NMR Reaction Progress Experiment – An oven-dried NMR tube was charged with AHDP **1'** (14 mg, 0.050 mmol) in CD_2Cl_2 (0.79 mL). 0.21 mL of the appropriate complex was introduced and the mixture was quickly mixed and immediately placed in the NMR. The reaction was monitored for approximately 6.5 hours, recording a scan every minute with relaxation delay set to 60 seconds. The collected scans were then analyzed using Bruker Dynamics Center 2.5.5 to obtain the decay of the intermediate and rise of the allylated product.

NMR Reaction Progress Experiment – Pd-Xantphos Catalytic System

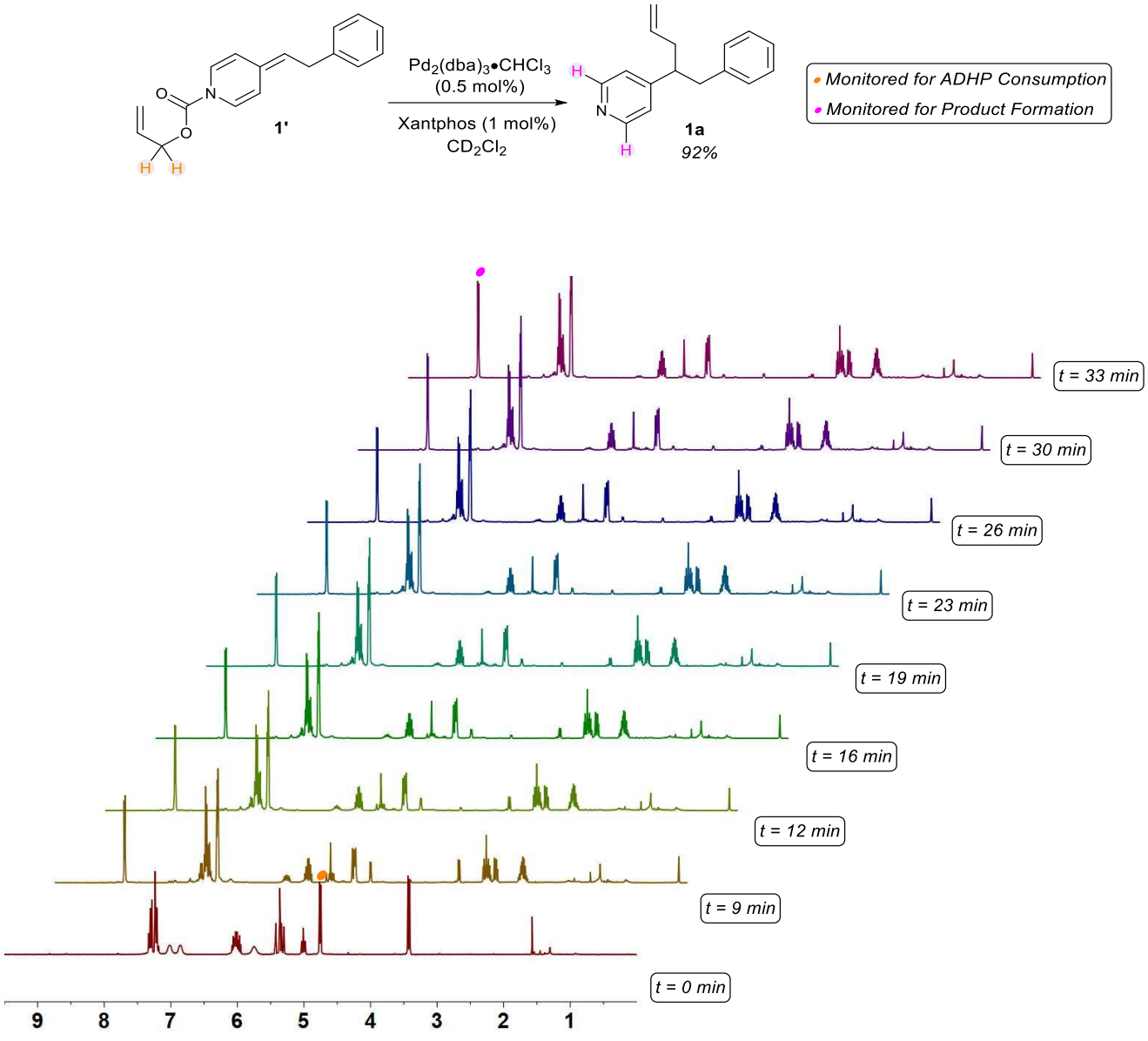

Note: Product yield was determined by quantitative ^{1}H NMR after reaction completion using1,4-bis(trichloromethyl)benzene as an internal standard.

NMR reaction progress experiment – [(Xantphos)Pd(η3-allyl)]OTf Catalytic System

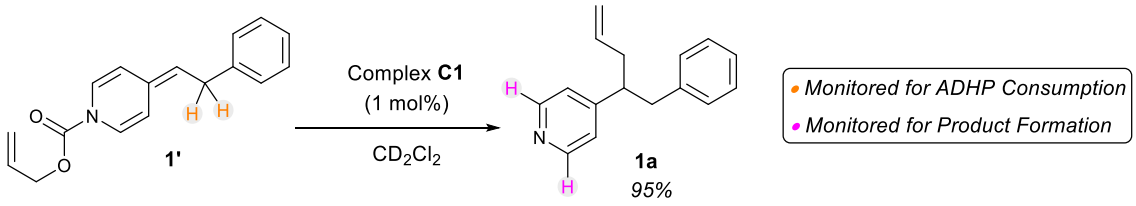

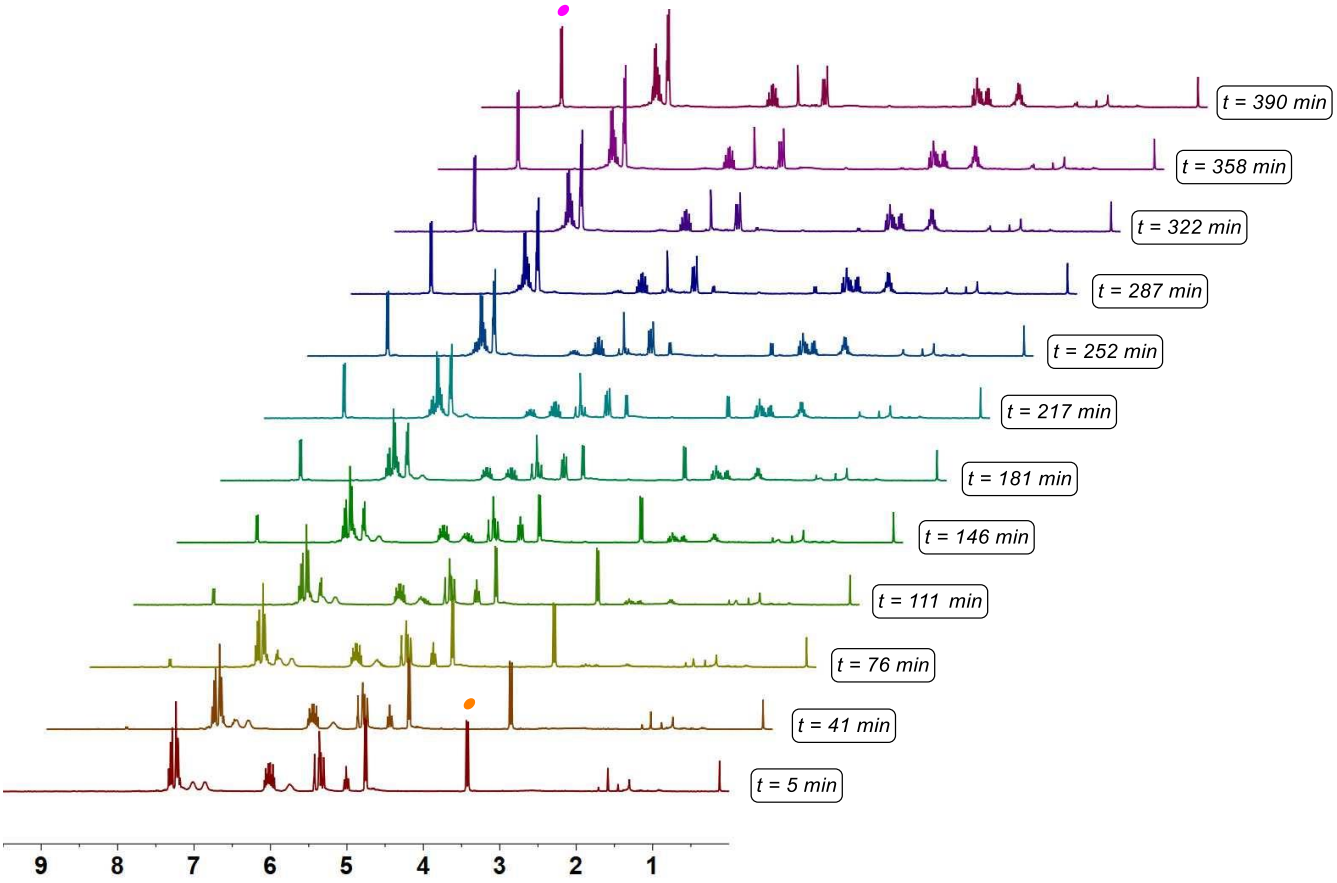

Note: Product yield was determined by using the integration values of the ADHP in the first scan as an internal standard.

Comparison of the reaction progress profiles for the Allylation of **1'** Using Pd-Xantphos and [(Xantphos)Pd(η3-allyl)]OTf (**C1**) Catalytic Systems

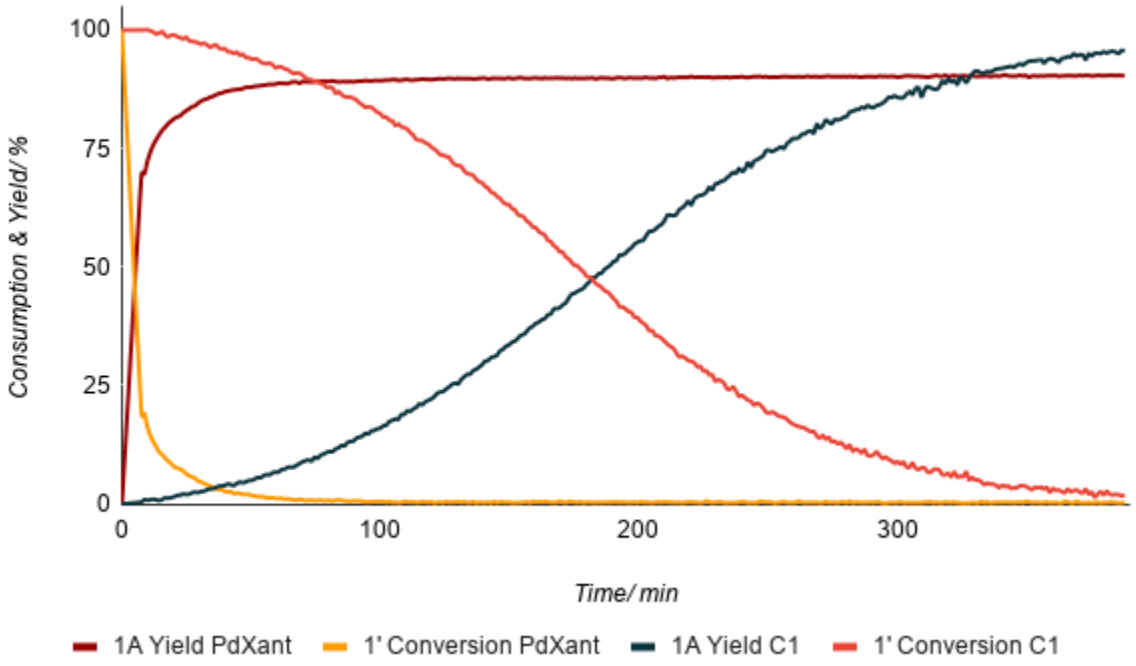

REFERENCES

1) Gomtsyan, A. *Chem. Heterocycl. Compd*. **2012**, 48 (1), 7-10.
2) Fuentes, A. V.; Pineda, M. D.; Venkatam, K. C. N. *Pharmacy* **2018**, 6(2), 43-53.
3) Vitaku, E.; Smith, D. T.; Njardarson, J. T. *J. Med. Chem.* **2014**, 57 (24), 10257-10274.
4) Taylor, R. D.; MacCoss, M.; Lawson, A. D. *J. Med. Chem*. **2014**, 57 (14), 5845-5859.
5) Ma, Z.; Lin, D, C.-H.; Sharma, R.; Liu, J.; Zhu, L.; Li, A.-R.; Kohn, T.; Wang, Y.; Liu, J.; Bartberger, M. D.; Medina, J. C.; Zhuang, R.; Li, F.; Zhang, J.; Luo, J.; Wong, S.; Tonn, G. R.; Houze, J. B. *Bioorg. Med. Chem. Lett*. **2016**, 26, 15-20.
6) (a) Perry, M. J.; O'Connell, J.; Walker, C.; Crabbe, T.; Baldock, D.; Russel, A.; Lumb, S.; Huang, Z.; Howat, D.; Allen, R.; Merriman, M.; Walls, J.; Daniels, T.; Hughes, B.; Laliberte, F.; Higgs, G. A.; Owens, R. J. *Cell Biochem. Biophys.* **1998**, 29, 113-132, (b) Houpis, I.; Molina, A.; Dorziotis, I.; Reamer, R. A.; Volante, R. P.; Reider, P. J. *Tet. Lett.* **1997**, 38, 7131-7134, (c) Lynch, J. E.; Choi, W.-B.; Churchill, H. R. O.; Volante, R. A.; Reamer, R. A.; Ball, R. G. *J. Org. Chem*. **1997**, 62, 9223-9228.
7) Campagnuolo, C.; Fattorusso, C.; Fattorusso, E.; Ianaro, A.; Pi-sano, B.; Taglialatela-Scafati, O. *Org. Lett.* **2003**, 5, 673-676.
8) Foley, D. J.; Nelson, A.; Marsden, S. P. *Angew. Chem. Int. Ed.* **2016**, 55 (44), 13650-13657.
9) Leach, A.; Jones, H.; Cosgrove, D.; Kenny, P.; Ruston, L.; MacFaul, P.; Wood, J.; Colclough, N.; Law, B. *J. Med. Chem*. **2006**, 49 (23), 6672-6682.
10) Hill, A. P.; Young, R. J. Drug Discovery Today 2010, 15 (15-16), 648-655.
11) Young, R. J.; Green, D. V.; Luscombe, C. N.; Hill, A. P., Drug Discovery Today **2011**, 16 (17-18), 822-830.
12) Nadin, A.; Hattotuwagama, C.; Churcher, I. *Angew. Chem. Int. Ed*. **2012**, 51, 1114-1122.
13) Murray, C. W.; Rees, D. C. *Angew.Chem. Int. Ed*. **2016**, 55,488–492.
14) Catalysis using endangered transition-metal not used in the synthesis of drug candidates: Roughley, S. D.; Jordan, A. M. *J. Med. Chem*. **2011**, 54 (10), 3451-3479.
15) Collins, K. D.; Glorius, F. *Nat. Chem.* **2013**, 5 (7), 597-601.
16) Collins, K. D.; Rühling, A.; Glorius, F. *Nat. Protoc.* **2014**, 9 (6), 1348-1353.
17) Gensch, T.; Teders, M.; Glorius, F. *J. Org. Chem.* **2017**, 82 (17), 9154-9159.

18) Lovering, F.; Bikker, J.; Humblet, C. *J. Med. Chem.* **2009**, 52 (21), 6752-6756.

19) Michaudel, Q.; Ishihara, Y.; Baran, P. S. *Acc. Chem. Res*. **2015**, 48, 712-721.

20) For reviews on asymmetric conjugate additions using transition-metal and organo-catalysis: a) Zheng, K.; Liu, X.; Feng, X. *Chem. Rev*. **2018**, 118, 7586-7656, b) Zhang, Y.; Wang, W. *Catal. Sci. Technol*. **2012**, 2, 42-53, c) Rossiter, B. E.; Swingle, N. M. *Chem. Rev*. **1992**, 92 (5), 771-806.

21) a) Hoffman, A.; Farlow, M. W.; Fuson, R. C. *J. Am. Chem. Soc*. **1933**, 55 (5), 2000-2004, b) Klumpp, D. A. *Synlett* **2012**, 1590−1604.

22) Best, D.; Lam, H. W. *J. Org. Chem*. **2014**, 79, 831-845.

23) Reactions with vinylpyridines: Liu, X.; Tan, Y.; Wang, X.; Xu, H.; Wang, Y.; Tian, P.; Lin, G. *Org. Lett.* **2020**, 22(10), 4038–4042.

24) a) Luo, C.; Bandar, J. S. *J. Am. Chem. Soc*. **2018**, 140, 3547-3550, b) Capaldo, L.; Fagnoni, M.; Ravelli, D. *Chem. Eur. J.* **2017**, 23, 6527-6530.

25) a) Lim, N.; Weiss, P.; Li, B. X.; McCulley, C. H.; Hare, S. R.; Bensema, B. L.; Palazzo, T. A.; Tantillo, D. J.; Zhang, H.; Gosselin, F. *Org. Lett.* **2017**, 19, 6212-6215, b) Hu, Q.; Jagusch, C.; Hille, U. E.; Haupenthal, J.; Hartmann, R. W. *J. Med. Chem*. **2010**, 53, 5749-5758, c) Hu, Q.; Yin, L.; Jagusch, C.; Hille, U. E.; Hartmann, R. W. *J. Med. Chem*. **2010**, 53, 5049-5053.

26) a) Wu, J.; Tang, W.; Pettman, A.; Xiaoa, J. *Adv. Synth. Catal.* **2013**, 355, 35-40, b) Martí-Centelles, R.; Murga, J.; Falomir, E.; Carda, M.; Marco, J. A. *Med. Chem. Commun*. **2015**, 6, 1809-1815.

27) a) Izawa, Y.; Pun. D.; Stahl, S. S. *Science* **2011**, 333, 209-213, b) Diao, T.; Wadzinski, T. J.; Stahl, S. S. *Chem. Sci.* **2012**, 3, 887-891, c) Izawa, Y.; Zheng, C.;Stahl, S. S. *Angew. Chem. Int. Ed*. **2013**, 52, 3672-3675, d) Diao, T.; Pun, D.; Stahl, S. S. *J. Am. Chem. Soc.* **2013**, 135, 8205-8212, e) Diao, T.; Pun, D.; Stahl, S. S. *J. Am. Chem. Soc.* **2013**, 135, 8213-8221.

28) a) Scewczyk, S. M.; Zhao, Y.; Sakai, H.; Dube, P.; Newhouse, T. R. *Tetrahedron* **2018**, 74, 3293-3300, b) Huang, D.; Zhao, Y.; Newhouse, T. R. *Org. Lett.* **2018**, 20, 684-687, c) Zhao, Y.; Chen, C.; Newhouse, T. R. *Angew. Chem. Int. Ed.* **2017**, 56, 13122-13125, d) Chen, Y.; Huang, D.; Zhao, Y.; Newhouse, T. R. *Angew. Chem. Int. Ed*. **2017**, 55, 8258-8262, e) Chen,

Y.; Turlik, A.; Newhouse, T. R. *J. Am. Chem. Soc.* **2016**, 138, 1166-1169. (f) Cheng, Y.; Romaire, J. P.; Newhouse, T. R. *J. Am. Chem. Soc*. **2015**, 137, 5875-5878.

29) Zhang, P.; Huang, D.; Newhouse, T. R. *J. Am. Chem. Soc.* **2020**, 142(4), 1757-1762.

30) a) Theissen, R. J. *J. Org. Chem*. **1971**, 36, 752-757, b) Bierling, B.; Kirschke, K.; Oberender, H.; Schulz, M. *J. Prakt. Chem*. **1972**, 314, 170-180, c) Wolff, S.; Agosta, W. C. *Synthesis* **1976**, 240-241.

31) Ito, Y.; Hirao, T.; Saegusa, T. *J. Org. Chem*. **1978**, 43 (5), 1011-1013.

32) Example of the use of the Saegusa oxidation in complex molecule synthesis: Uchida, K.; Yokoshima, S.; Kan, T.; Fukuyama, T. *Org. Lett*. **2006**, 8 (23), 5311-5313.

33) a) Minami, I.; Takahashi, K.; Shimizu, I.; Kimura, T.; Tsuji, J. *Tetrahedron* **1986**, 42, 2971-2977, b) Shimizu, I.; Tsuji, J. *J. Am. Chem. Soc*. **1982**, 104, 5844-5846 (c) Minami, I; Nisar, M.; Yuhara, M. Shimizu, I.; Tsuji, J. *Synthesis*, **1987**, 992-998.

34) Schonherr, H.; Cernak, T. *Angew. Chem. Int. Ed*. **2013**, 52 (47), 12256-12267.

35) a) Fisher, T. J.; Dussault, P. H. *Tetrahedron* **2017**, 73 (30), 4233-4258, b) Grigoropoulou, G.; Clark, J. H.; Elings, J. A. *Green Chem*. **2003**, 5 (1), 1-7, c) Crudden, C. M.; Edwards, D. *Eur. J. Org. Chem.* **2003**, 24, 4695-4712, d) Bataille, C. J. R.; Donohoe, T. *J. Chem. Soc. Rev.* **2011**, 40 (1), 114-128, e) Ogba, O. M.; Warner, N. C.; O'Leary, D. J.; Grubbs, R. H. *Chem. Soc. Rev.* **2018**, 47 (12), 4510-4544.

36) Zhang, Z.; Dwoskin, L. P.; Crooks, P. A. *Tet. Lett*. **2011**, 52, 2667-2669.

37) a) Trost, B. M.; Thaisrivongs, D. A. *J. Am. Chem. Soc*. **2008**, 130, 14092-14093, b) Trost, B. M.; Thaisrivongs D. A. *J. Am. Chem. Soc*. **2009**, 131, 12056-12057, c) Trost, B. M.; Thaisrivongs, J. Hartwig, D. A. *J. Am. Chem. Soc.* **2011**, 133, 12439-12441.

38) Liu, X. J.; You, S. L., *Angew. Chem. Int. Ed*. **2017**, 56 (14), 4002-4005.

39) Murakami, R.; Sano, K.; Iwai, T.; Taniguchi, T; Monde, M.; Sawamura, M. *Angew. Chem. Int. Ed*. **2018**, 57, 9465-9469.

40) a) Sha, S. C.; Zhang, J.; Carroll, P. J.; Walsh, P. J. *J. Am. Chem. Soc*. **2013**, 135, 17602-17609, b) Sha, S. C.; Jiang, H.; Mao, J.; Bellomo, A.; Jeong, S. A.; Walsh, P. J. *Angew. Chem. Int. Ed*. **2016**, 55, 1070-1074.

41) Waetzig, S. R.; Tunge, J. A. *J. Am. Chem. Soc*. **2007**, 129, 4138-4139.

42) Moon, P. J.; Wei, Z.; Lundgren, R. J. *J. Am. Chem. Soc.* **2018**, 42, 17418-17422.

43) Bordwell, F. *Acc. Chem. Res*. **1988**, 21, 456-463.

44) Uses of alkylidene dihydropyridine in the literature: a) Lansakara, A. I.; Mariappan, S. V.; Pigge, F. C. *J. Org. Chem.* **2016**, 81, 10266-10278, b) Joshi, M. S.; Pigge, F. C. *ACS Catal*. **2016**, 6, 4465-4469, c) Meanwell, M.; Nodwell, M. B.; Martin, R. E; Britton, R. *Angew. Chem. Int. Ed.* **2016**, 55, 13244-13248.

45) For an introduction to the concept of soft-enolization: Zhang, Z.; Collum, D. B. *J. Org. Chem*. **2017**, 82, 7595-7601.

46) Vinylpyridines are known to undergo radical polymerizations: Shimizu, S.; Watanabe, N.; Kataoka, T.; Shoji, T.; Abe, N.; Morishita, S.; Ichimura, H. Pyridine and Pyridine Derivatives. *Ullman's Encyclopedia of Industrial Chemistry* [online]; Wiley-VCH, Posted June 15, 2000. https://onlinelibrary.wiley.com/doi/abs/10.1002/14356007.a22_399 (accessed May 2, 2020).

47) Basha, A.; Lipton, M.; Weinreb, S. M. *Tet. Lett*. **1977**, 4171-4174.

48) Chen, Q.; Jourdin, X. M. D.; Knochel, P. *J. Am. Chem. Soc*. **2013**, 135(13), 4958-4961.

49) Louie, J.; Hartwig, J. F. *J. Am. Chem. Soc.* **1995**, 117, 11598-11599.

50) a) Kagawa, N.; Malerich, J. P.; Rawal, V. H. *Org. Lett*. **2008**, 10(12), 2381-2384, b) Zhu, Y.; Rawal, V. H. *J. Am. Chem. Soc*. **2012**, 134, 1, 111-114, c) Montgomery, T. D.; Zhu, Y.; Kagawa, N.; Rawal, V. H. *Org. Lett*. **2013**, 15(5), 1140–1143, d) Chen, J.; Cook, M. *J. Org. Lett.* **2013**, 15(5), 1088-1091.

51) Vranken, D. L.; Trost, B. M. *Chem. Rev*. **1996**, 96, 395-422.

52) Falciola, C. A.; Alexakis, A. *Eur. J. Org. Chem*. **2008**, 3765-3780.

53) Rössler, S. L.; Petrone, D. A.; Carreira, E. M. *Acc. Chem. Res*. **2019**, 52, 2657-2672.

54) a) Yin, L.; Kanai, M.; Shibasaki, M. *J. Am. Chem. Soc*. **2009**, 131, 9610-9611, b) Hara, N.; Nakamura, S.; Funahashi, Y.; Shibata, N. *Adv. Synth. Catal*. **2011**, 353, 2976-2980, c) Shibatomi, K.; Kitahara, K.; Sasaki, N.; Kawasaki, Y.; Fujisawa, I.; Iwasa, S. *Nat. Commun*. **2017**, 8, 15600, d) Grugel, C. P.; Breit, B. *Org. Lett*. **2018**, 20, 1066-1069.

55) Khanna, R. K.; Moore, M. H. *Spectrochimica Acta Part A*, **1999**, 55, 961-967.

56) Synthesis and isolation of the more stable β-keto carboxylate palladium complex was conducted under rigorous temperature control (−20 °C to −36 °C): Sherden, N. H.; Behenna, D. C.; Virgil, S. C.; Stoltz, B. M. *Angew. Chem. Int. Ed.* **2009**, 48, 6840-6843.

57) Huntington, K. M.; Yi, T.; Wei, Y.; Pei, D. *Biochemistry* **2000**, 39, 4543-4551.

58) Rideau, E.; You, H.; Sidera, M.; Claridge, T. D. W.; Fletcher, S. P. *J. Am. Chem. Soc.* **2017**, 139, 5614-5624.

59) Allyl chloroformates undergo S_N2' mediated decomposition releasing CO_2 and allyl chloride.

60) Johns, A. M.; Utsunomiya, M.; Incarvito, C. D.; Hartwig, J. F. *J. Am. Chem. Soc*. **2006**, 128 (6), 1828-1839

61) Still, W. C.; Kahn, M.; Mitra, A. *J. Org. Chem*. **1978**, 43 (14), 2923-2925.

62) Hoye, T. R.; Zhao, H. *J. Org. Chem*. **2002**, 67 (12), 4014-4016.

63) Schmaunz, C. E.; Pabel, J.; Wanner, K. T. *Synthesis* **2010**, 13, 2147-2160.

64) Zhang, X.; McNally, A. *ACS Catal*. **2019**, 9 (6), 4862-4866.

65) Lebel, H.; Davi, M.; Díez-González, S.; Nolan, S. P. *J. Org. Chem*. **2007**, 72 (1), 144-149.

66) Upadhyay, S. P.; Lupo, K. M.; Marquard, A. N.; Ng, J. D.; Bates, D. M.; Goldsmith, R. H. *J. Phys. Chem. C*. **2015**, 119, 19703-19714.

67) Kitbunnadaj, R.; Zuiderveld, O. P.; Christophe, B.; Hulscher, S.; Menge, W. M. P. B.; Gelens, E.; Snip, E.; Bakker, R. A.; Celanire, S.; Gillard, M.; Talaga, P.; Timmerman, H.; Leurs, R. *J. Med. Chem*. **2004**, 47 (10), 2414-2417.

68) Brundish, D.; Bull, A.; Donovan, V.; Fullerton, J. D.; Garman, S. M.; Hayler, J. F.; Janus, D.; Kane, P. D.; McDonnell, M.; Smith, G. P.; Wakeford, R.; Walker, C. V.; Howarth, G.; Hoyle, W.; Allen, M. C.; Ambler, J.; Butler, K.; Talbot, M. D. *J. Med. Chem*. **1999**, 42 (22), 4584-4603.

69) Parameswarappa, S. G.; Pigge, F. C. *J. Org. Chem*. **2012**, 77(18), 8038-8048.

70) Bonnet, V.; Mongin, F.; Trécourt, F.; Quéguiner, G. *J. Chem. Soc. Perkin Trans.* **2000**, 4245-4249.

71) Maekawa, H.; Nishiyama, Y. *Tetrahedron* **2015**, 71 (38), 6694-6700.

72) Kitbunnadaj, R.; Zuiderveld, O. P.; Christophe, B.; Hulscher, S.; Menge, W. M. P. B.; Gelens, E.; Snip, E.; Bakker, R. A.; Celanire, S.; Gillard, M.; Talaga, P.; Timmerman, H.; Leurs, R. *J. Med. Chem.* **2004**, 47, 2414-2417.

73) Kobayashi, Y.; Czechtizky, W.; Kishi, Y. *Org. Lett*. **2003**, 5 (1), 93-96.

74) Wu, H.; Yang, B.; Zhu, L.; Lu, R.; Li, G.; Lu, H. *Org. Lett*. **2016**, 18, 5804-5807.

^{1}H (400 MHz, $CDCl_3$) and ^{13}C (75 MHz, $CDCl_3$) – NMR spectra of **1**

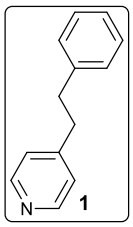

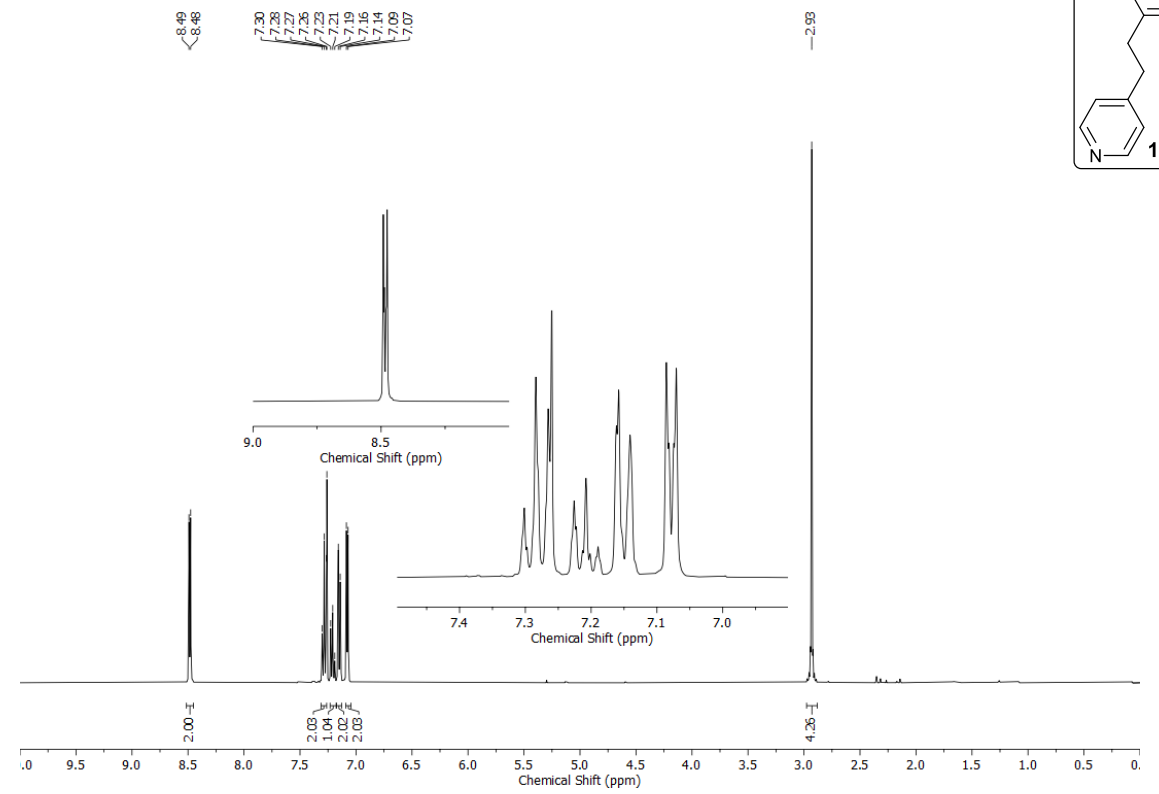

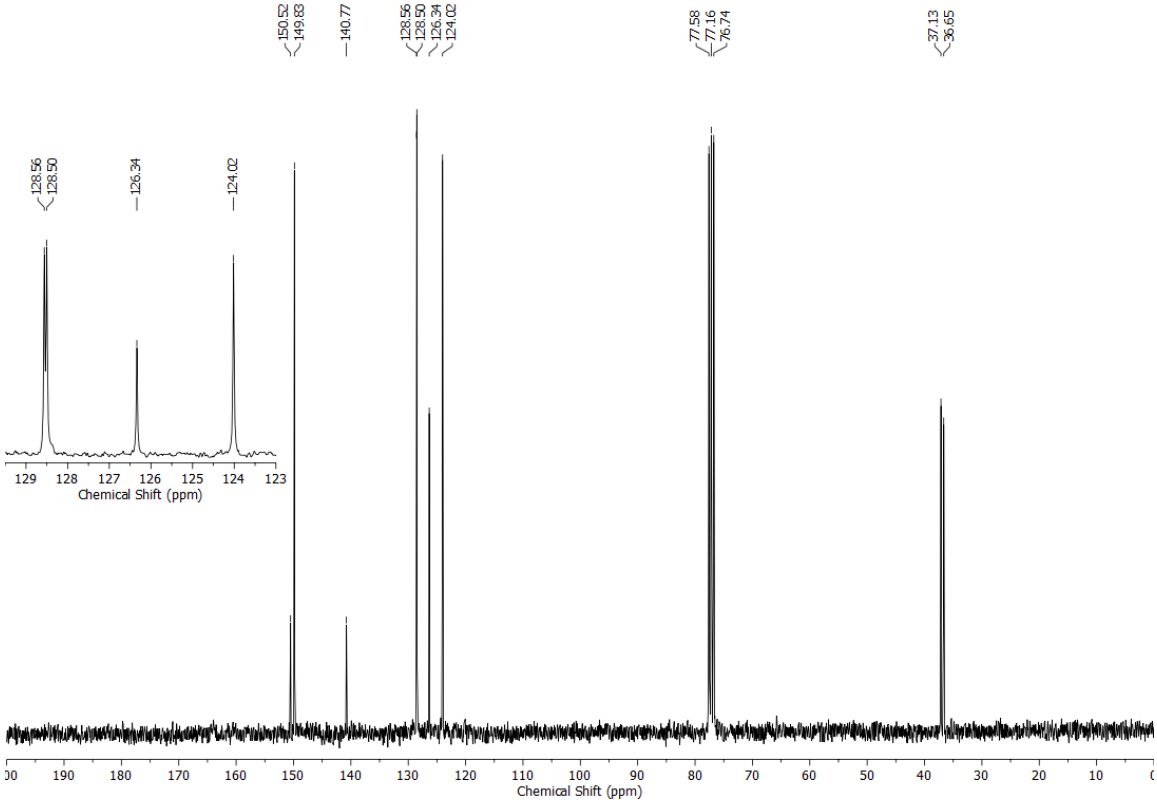

^{1}H (400 MHz, $CDCl_3$) and ^{13}C (101 MHz, $CDCl_3$) – NMR spectra of **2**

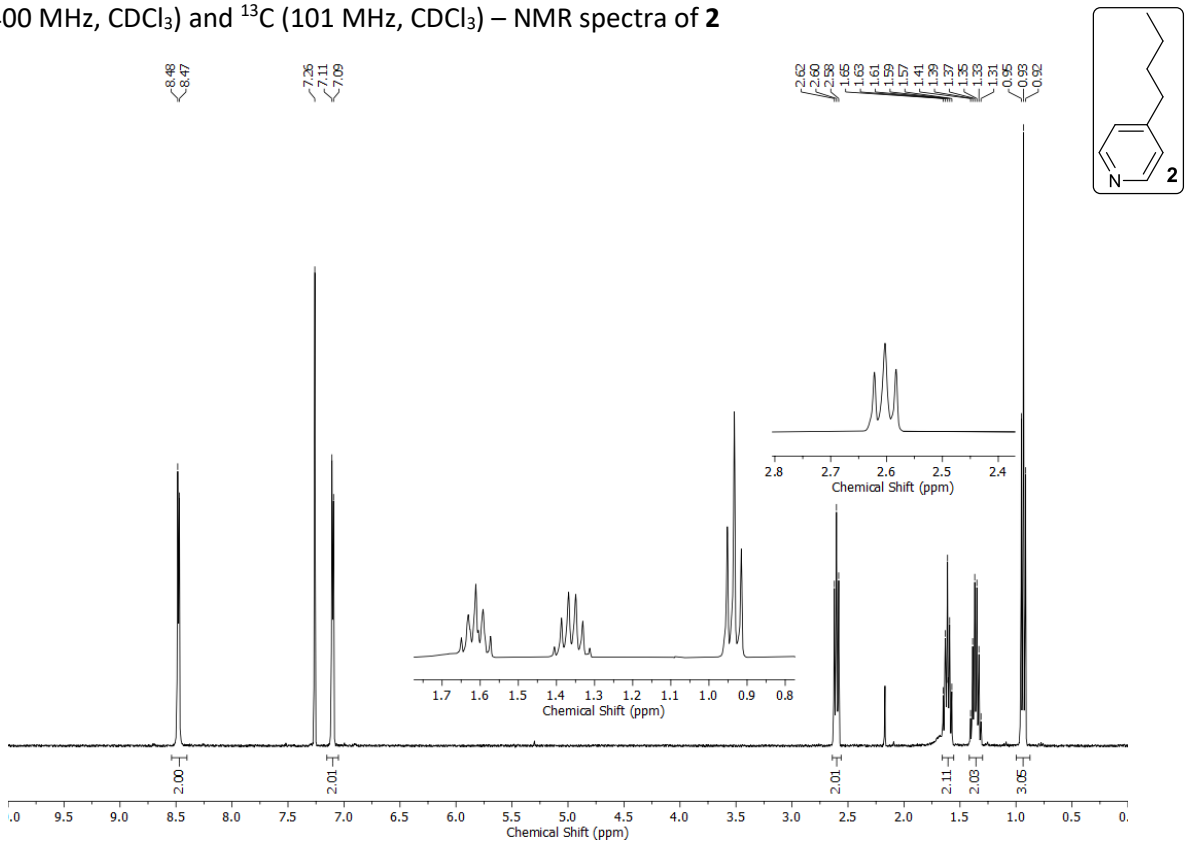

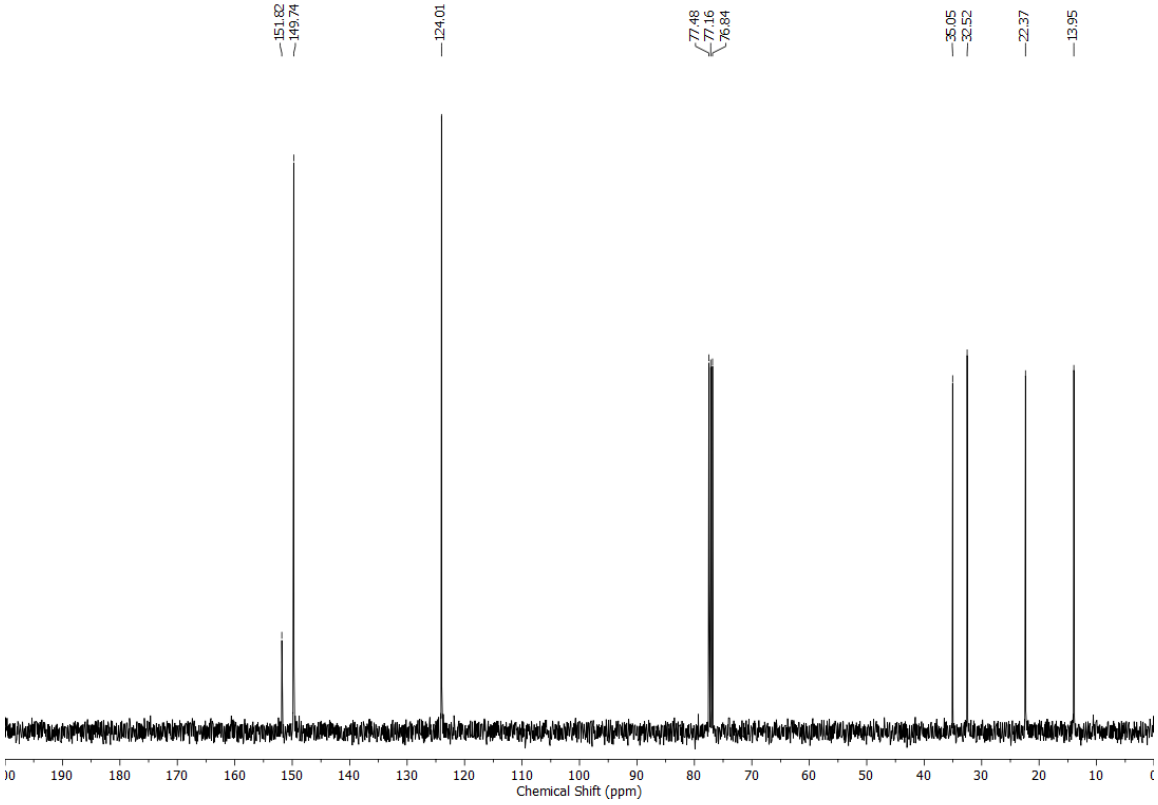

^{1}H (400 MHz, $CDCl_3$) and ^{13}C (101 MHz, $CDCl_3$) – NMR spectra of **3**

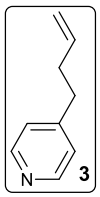

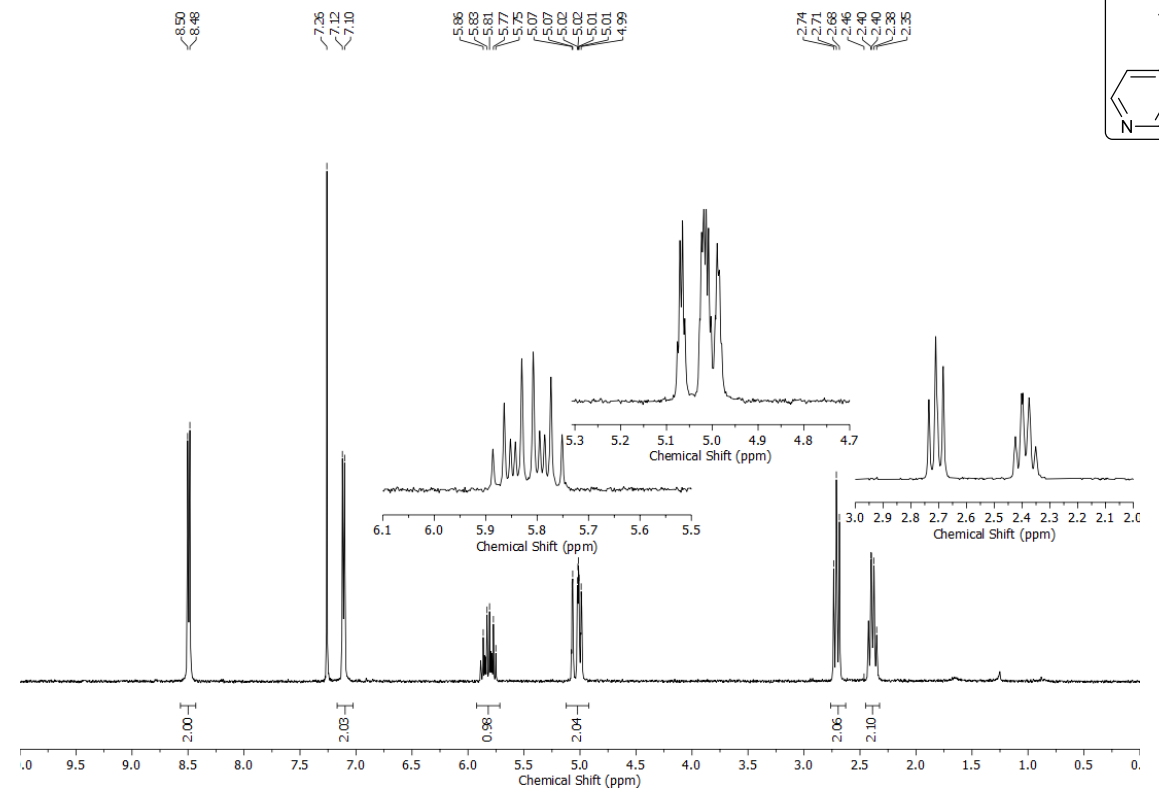

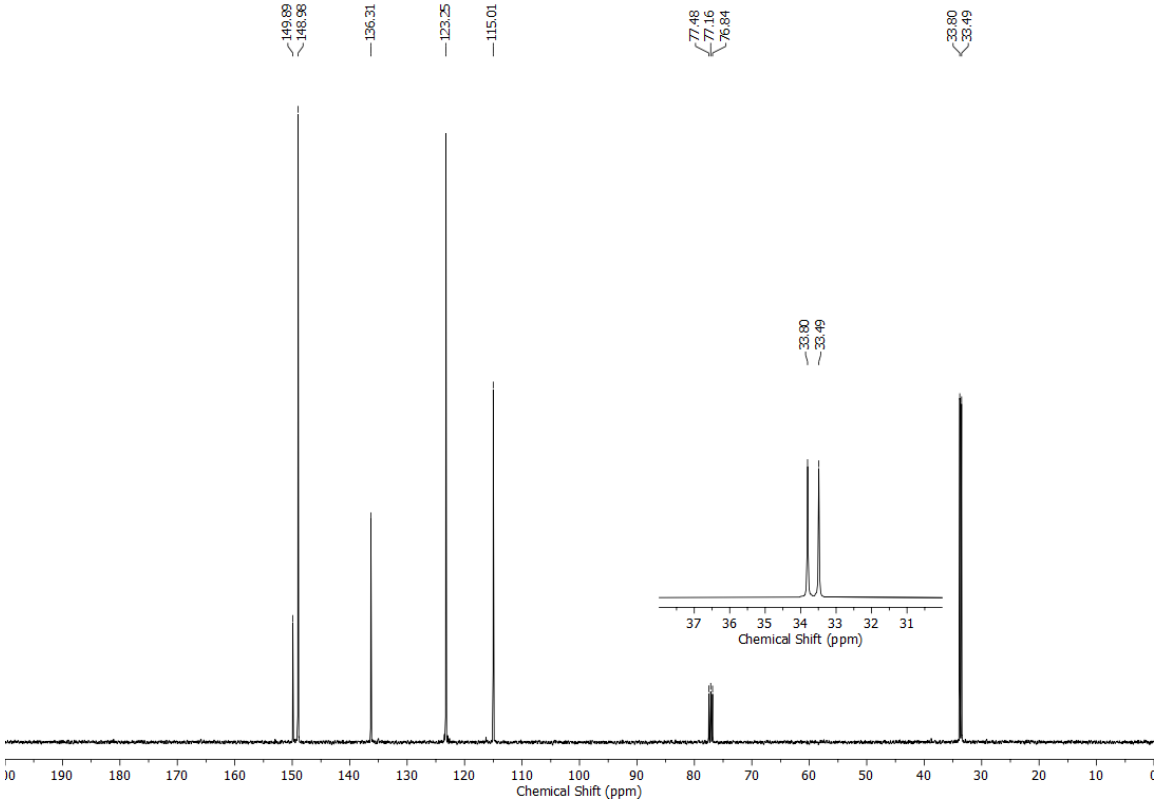

^{1}H (400 MHz, $CDCl_3$) and ^{13}C (101 MHz, $CDCl_3$) – NMR spectra of **4.1**

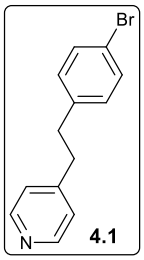

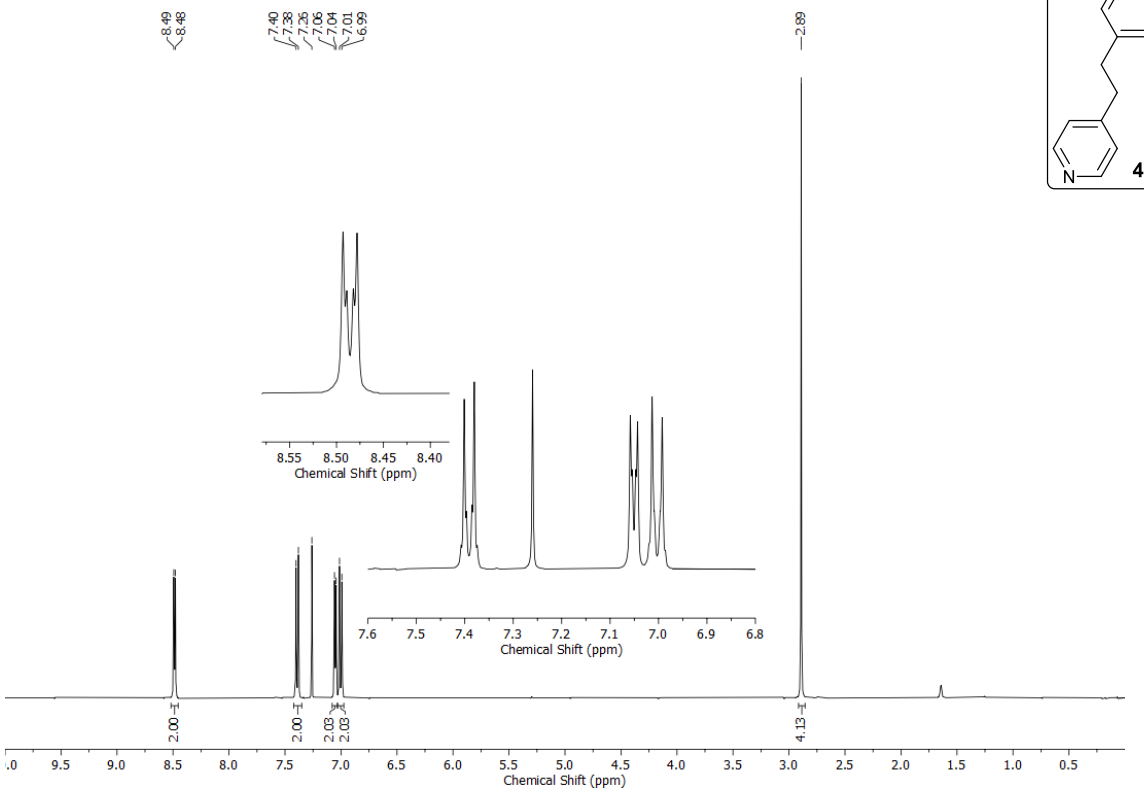

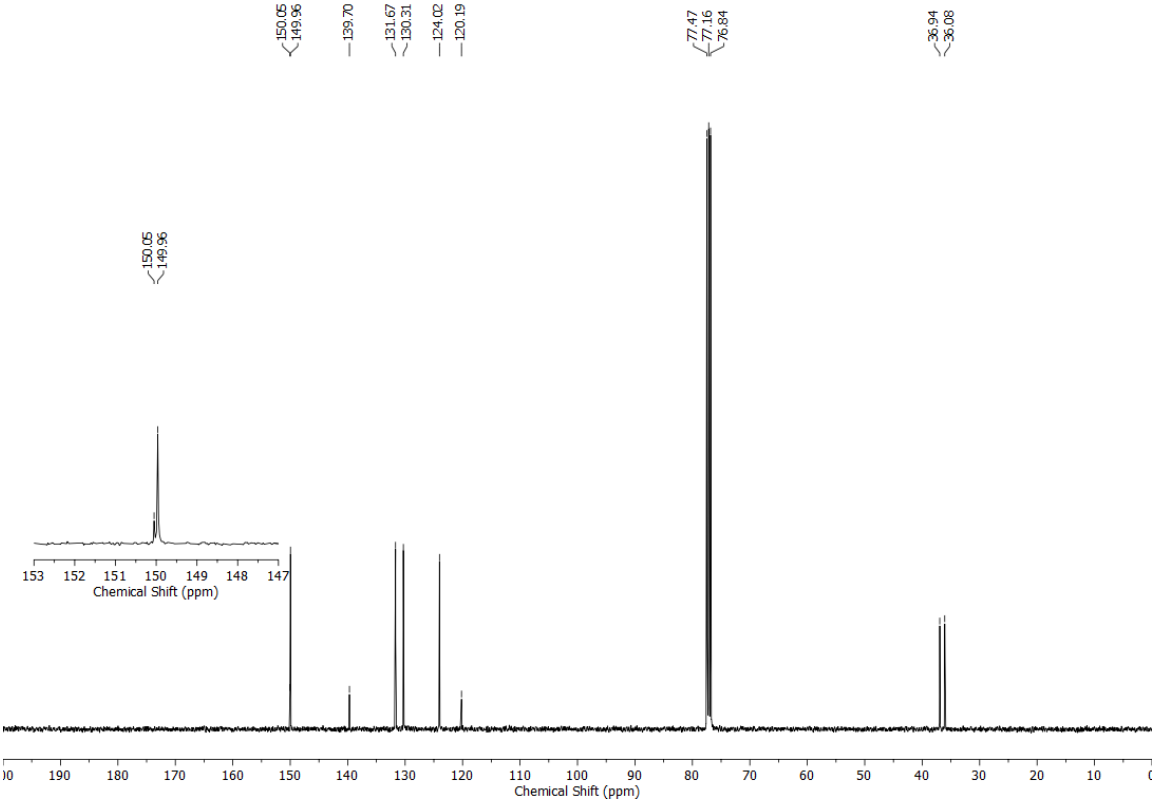

^{1}H (300 MHz, $CDCl_3$) and ^{13}C (101 MHz, $CDCl_3$) – NMR spectra of **4**

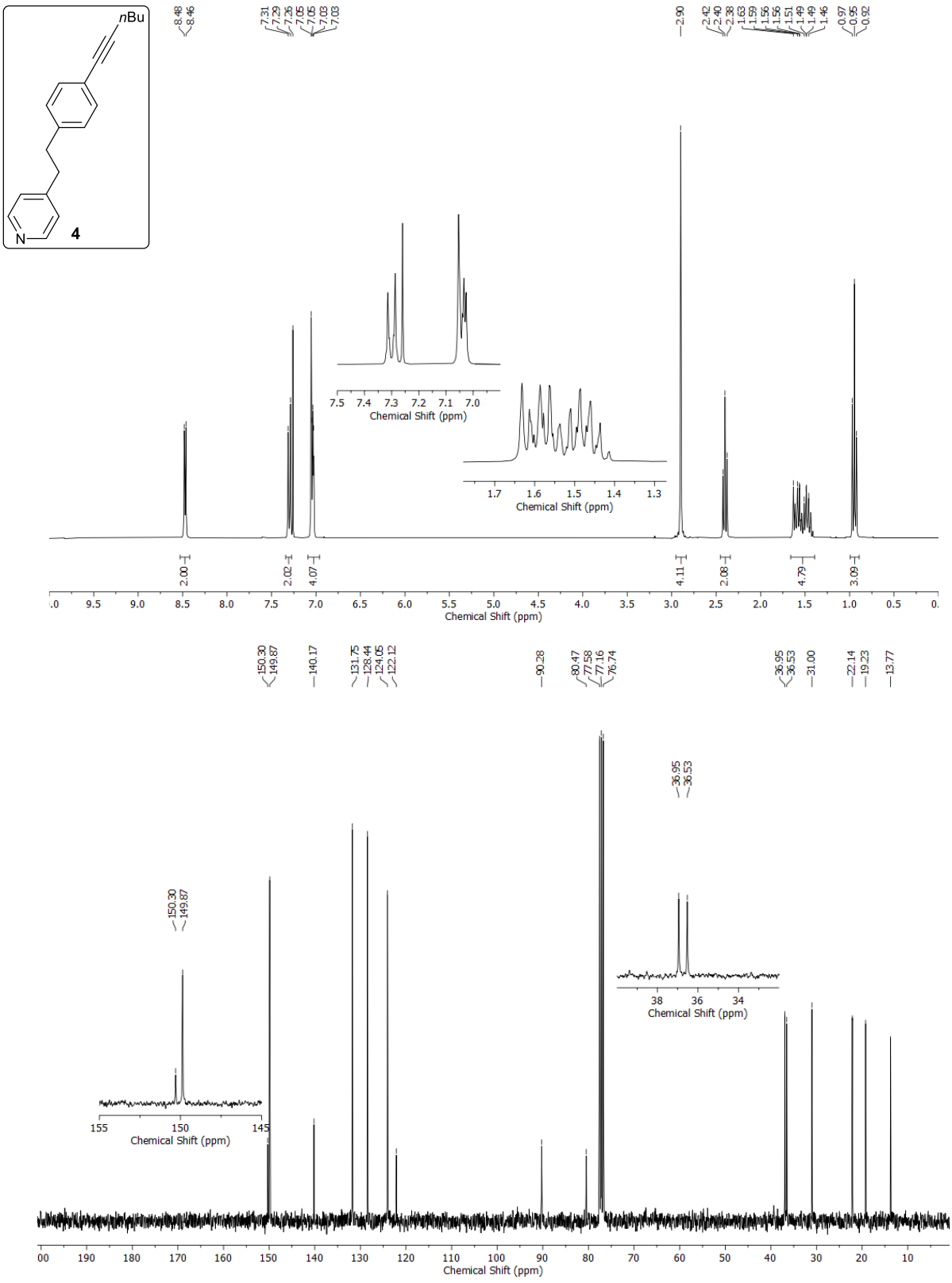

^{1}H (400 MHz, $CDCl_3$) and ^{13}C (101 MHz, $CDCl_3$) – NMR spectra of **5**

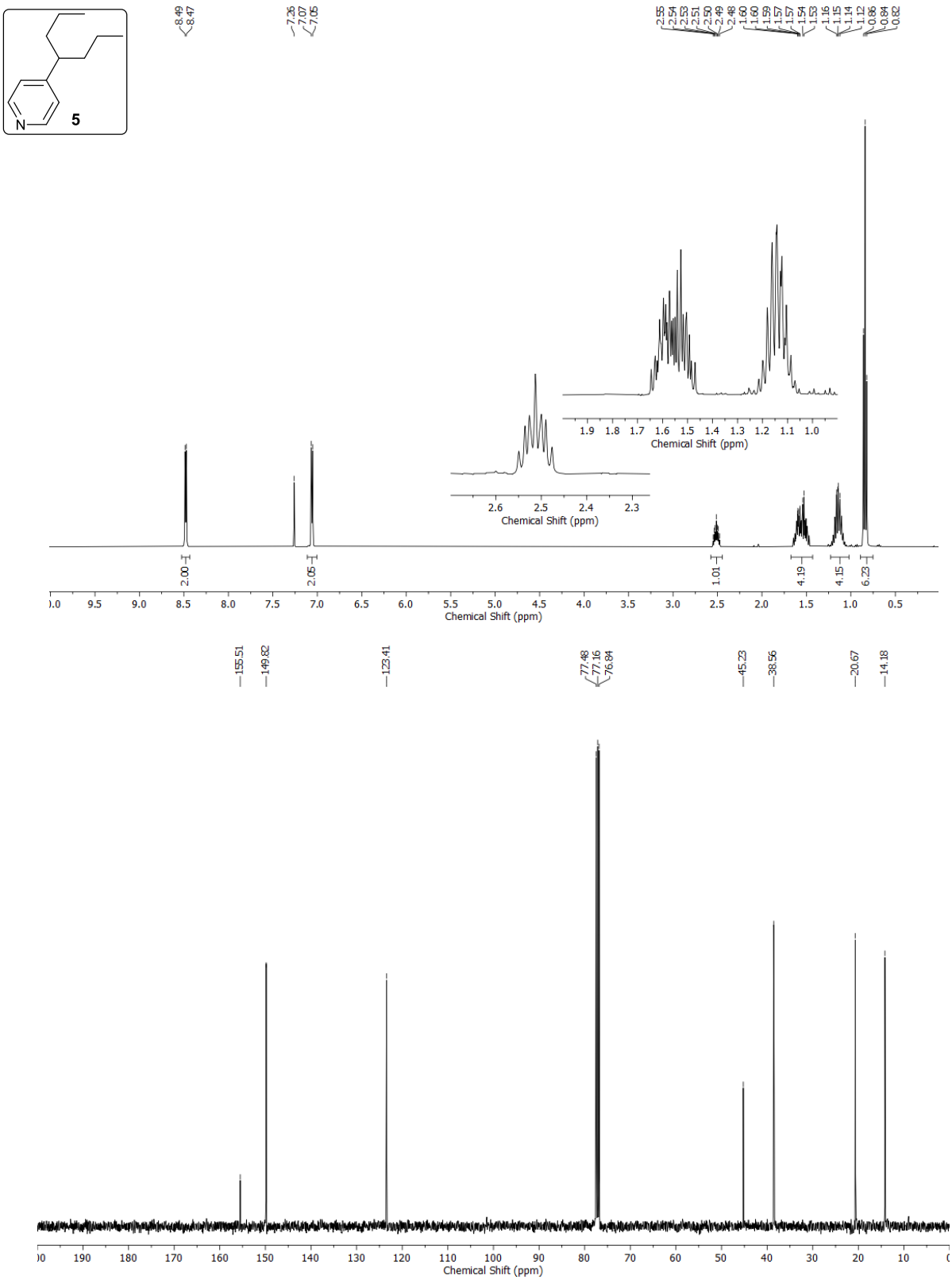

^{1}H (400 MHz, $CDCl_3$) and ^{13}C (101 MHz, $CDCl_3$) – NMR spectra of **6**

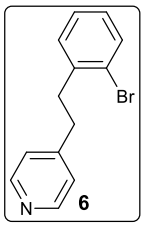

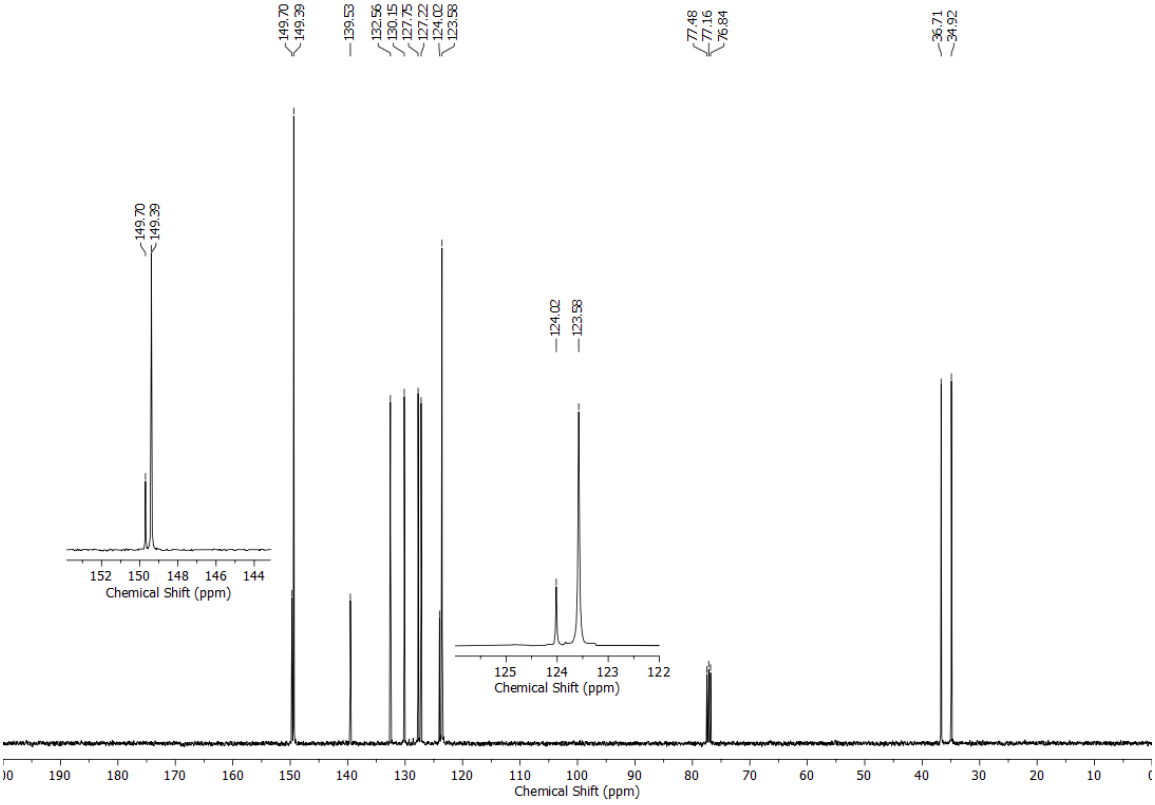

^{1}H (400 MHz, $CDCl_3$) and ^{13}C (75 MHz, $CDCl_3$) – NMR spectra of **7**

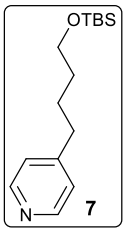

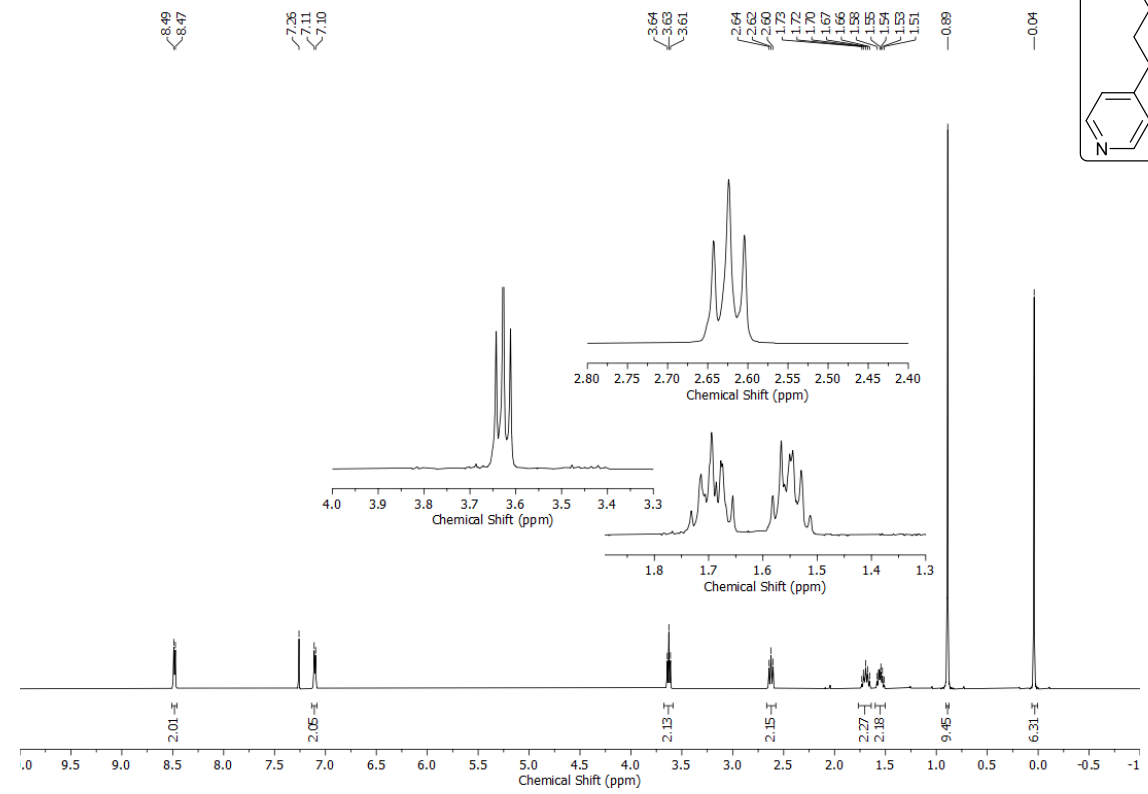

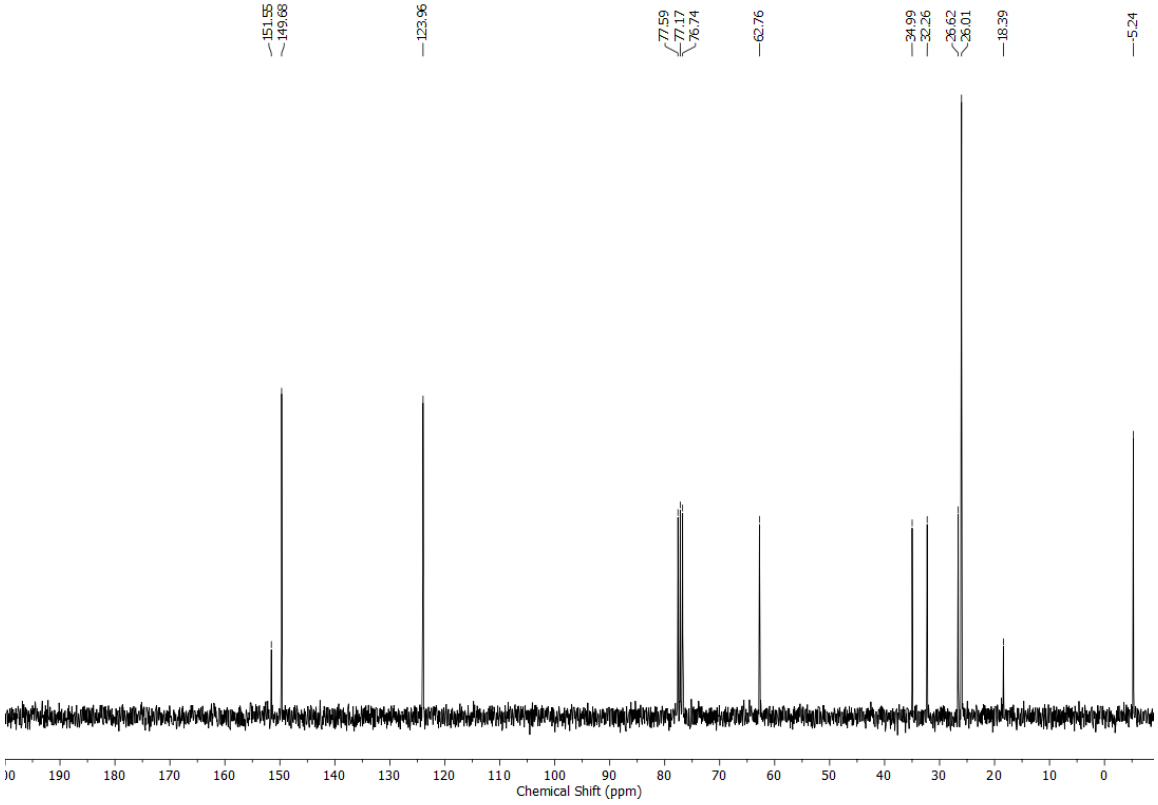

^{1}H (400 MHz, $CDCl_3$) and ^{13}C (101 MHz, $CDCl_3$) – NMR spectra of **8**

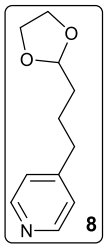

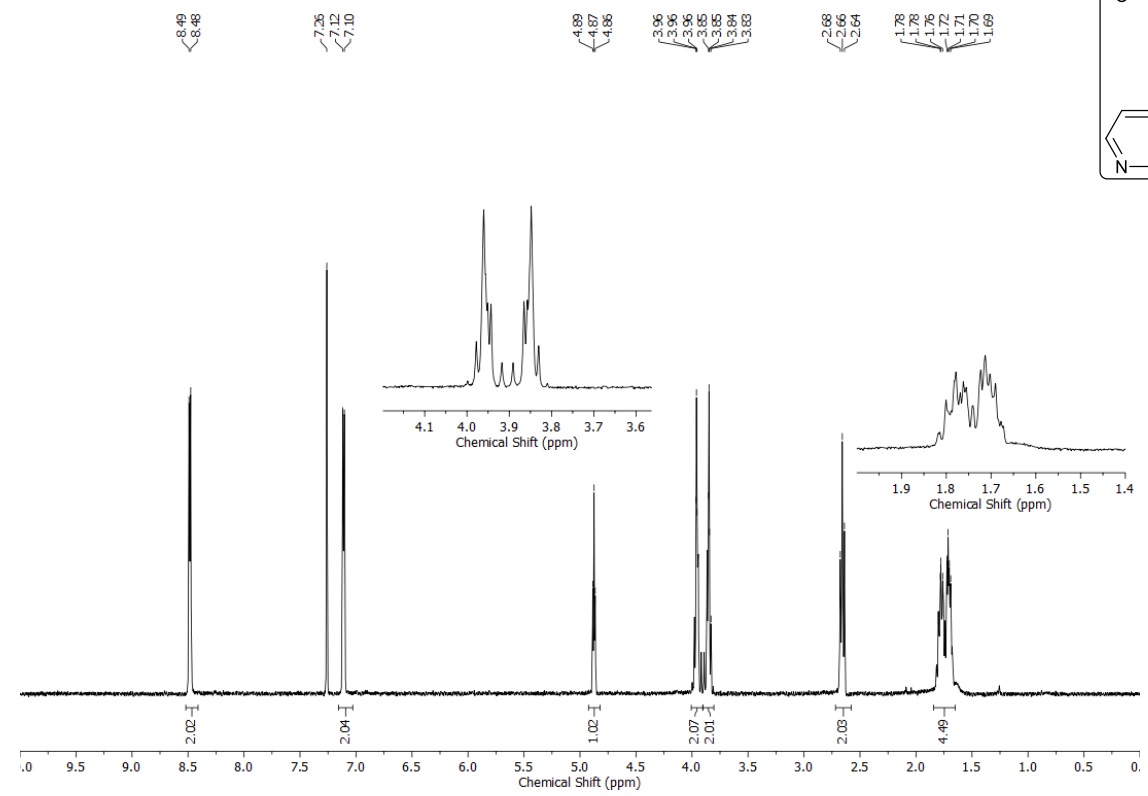

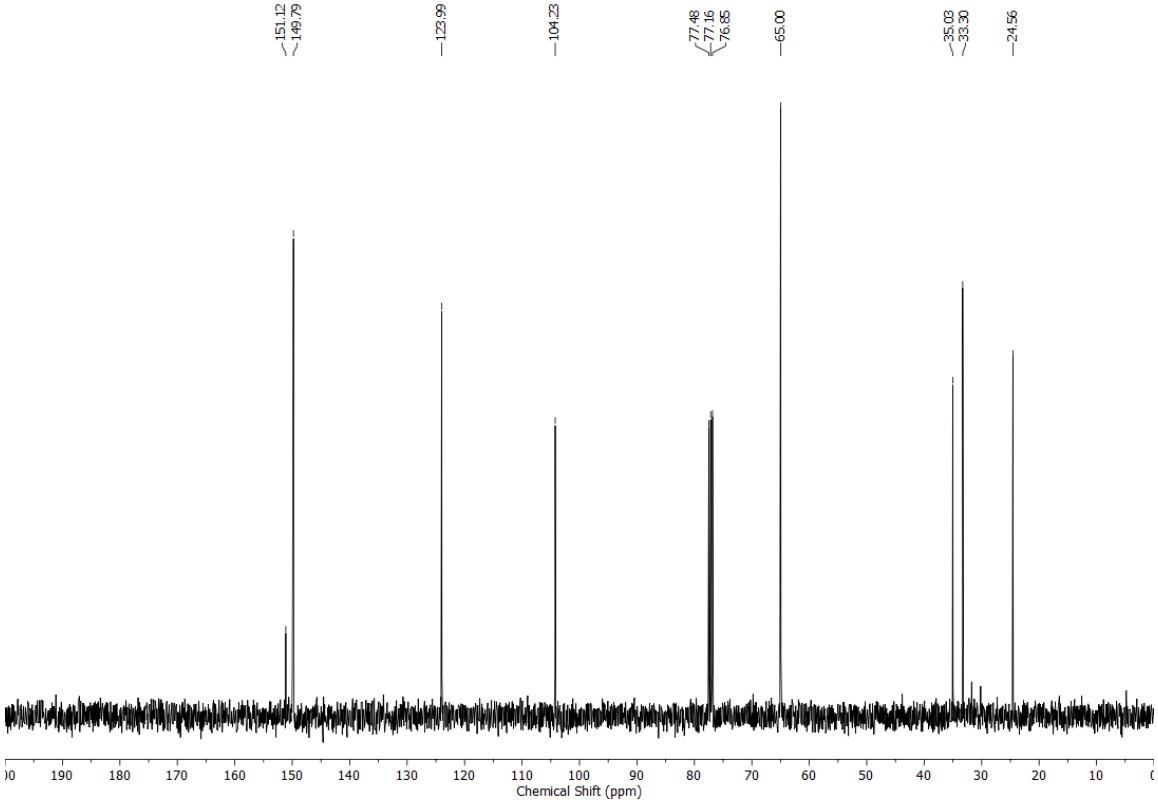

^{1}H (400 MHz, $CDCl_3$) and ^{13}C (101 MHz, $CDCl_3$) – NMR spectra of **9**

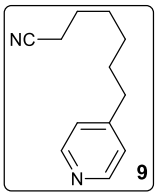

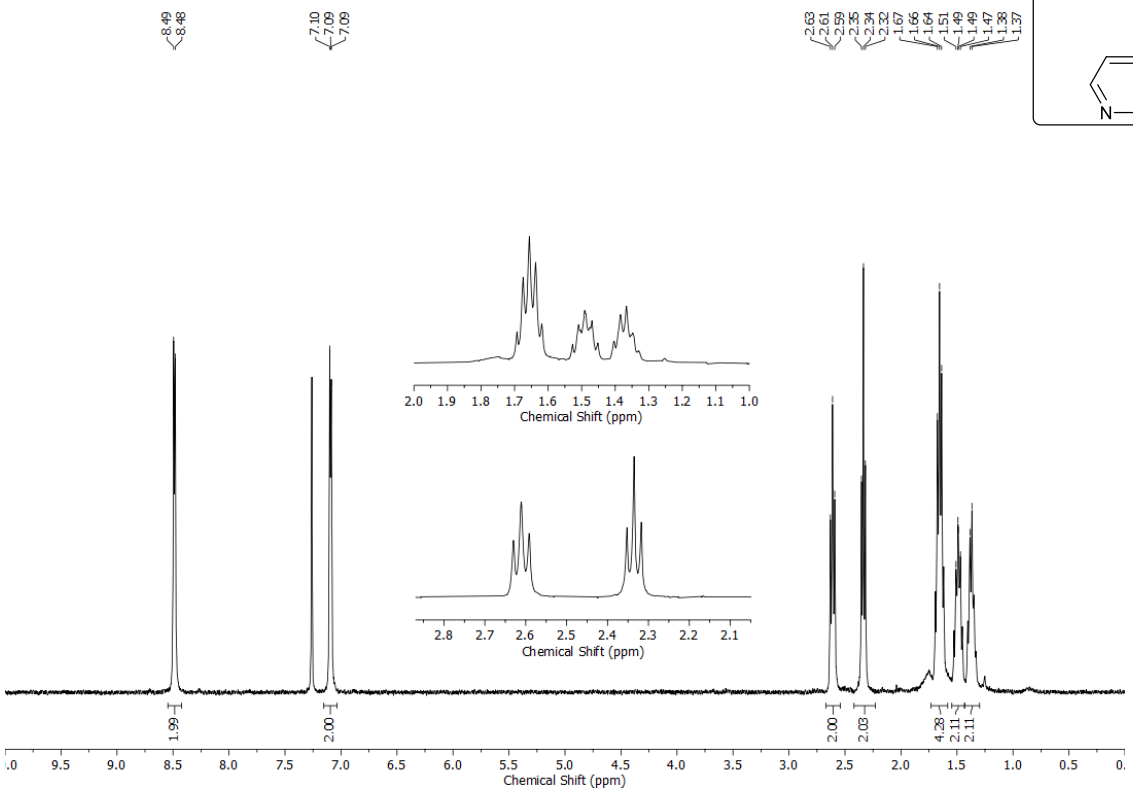

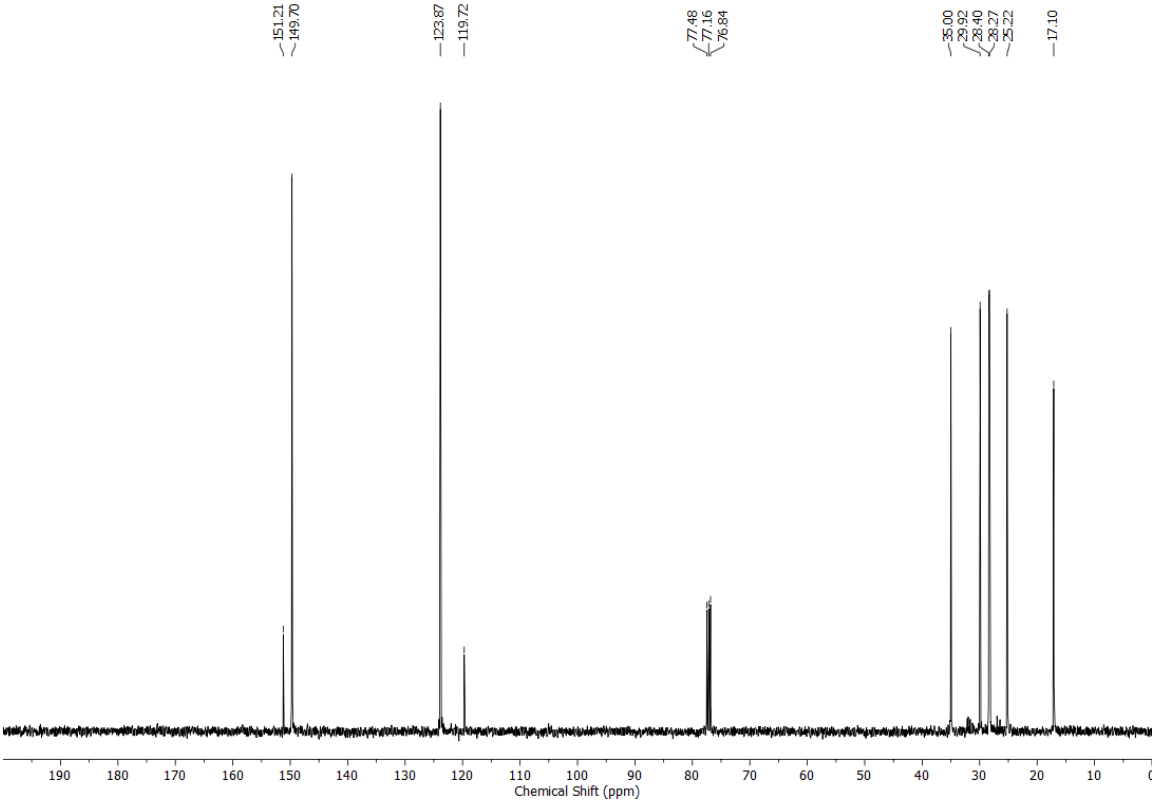

^{1}H (400 MHz, $CDCl_3$) and ^{13}C (101 MHz, $CDCl_3$) – NMR spectra of **10**

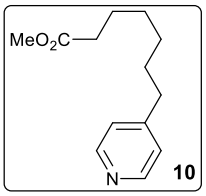

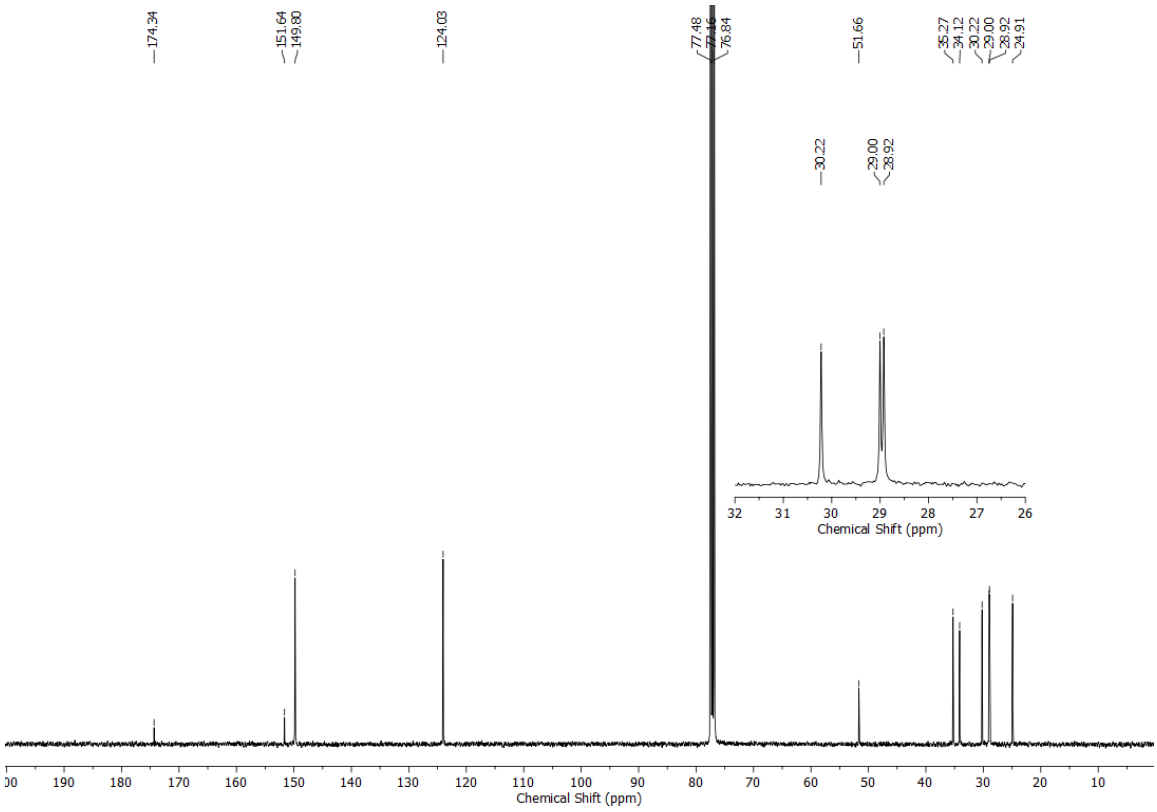

^{1}H (300 MHz, $CDCl_3$) and ^{13}C (75 MHz, $CDCl_3$) – NMR spectra of **11.1**

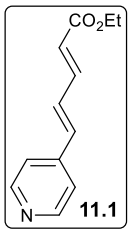

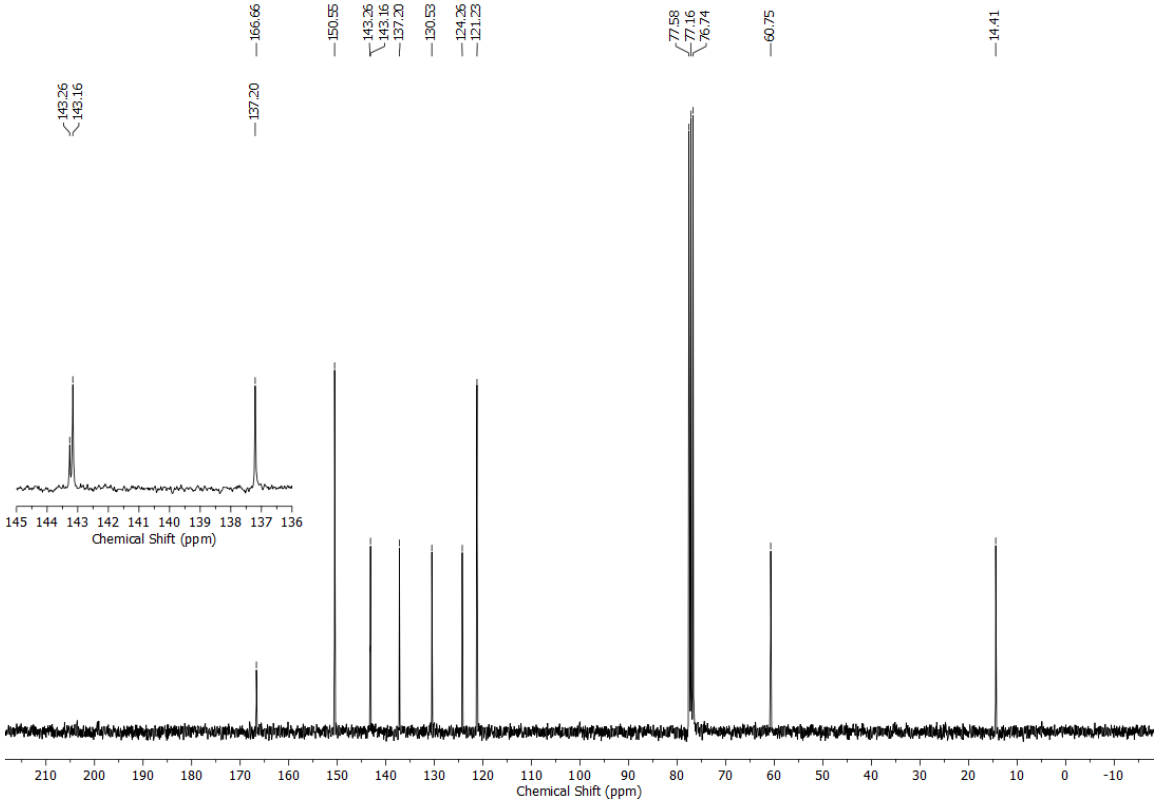

^{1}H (300 MHz, $CDCl_3$) and ^{13}C (75 MHz, $CDCl_3$) – NMR spectra of **11.2**

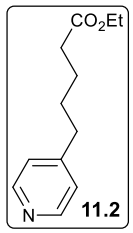

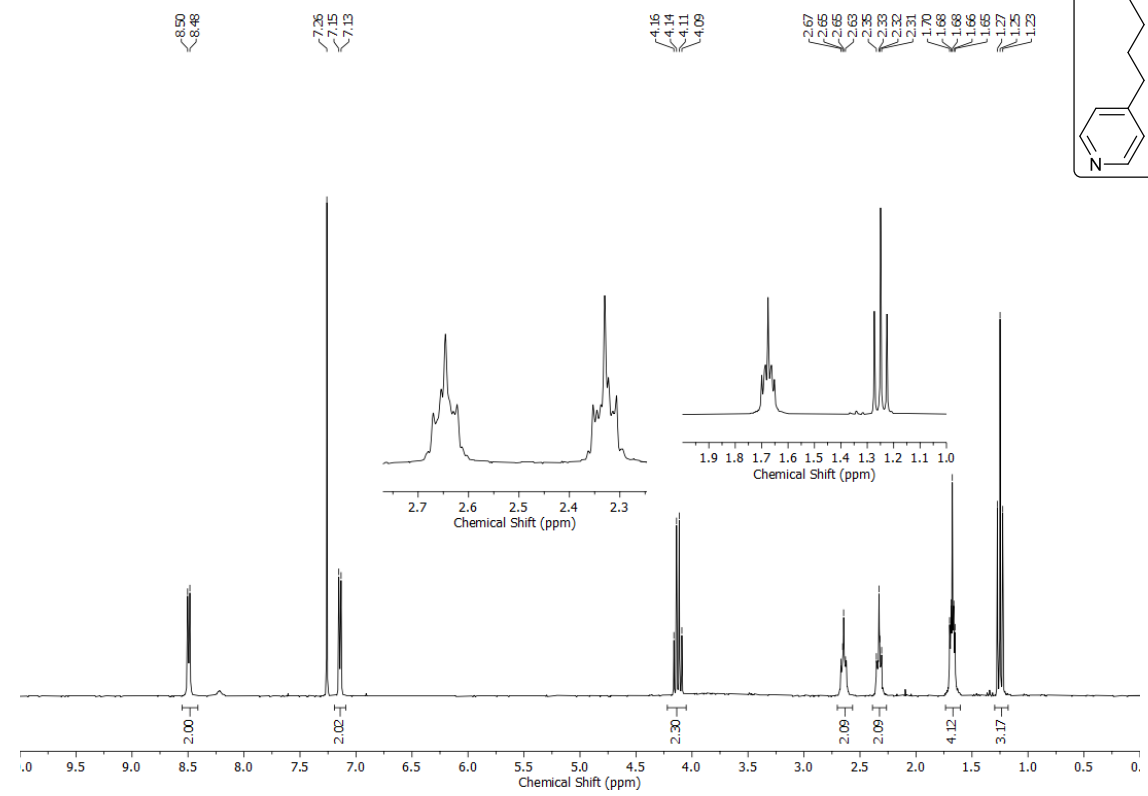

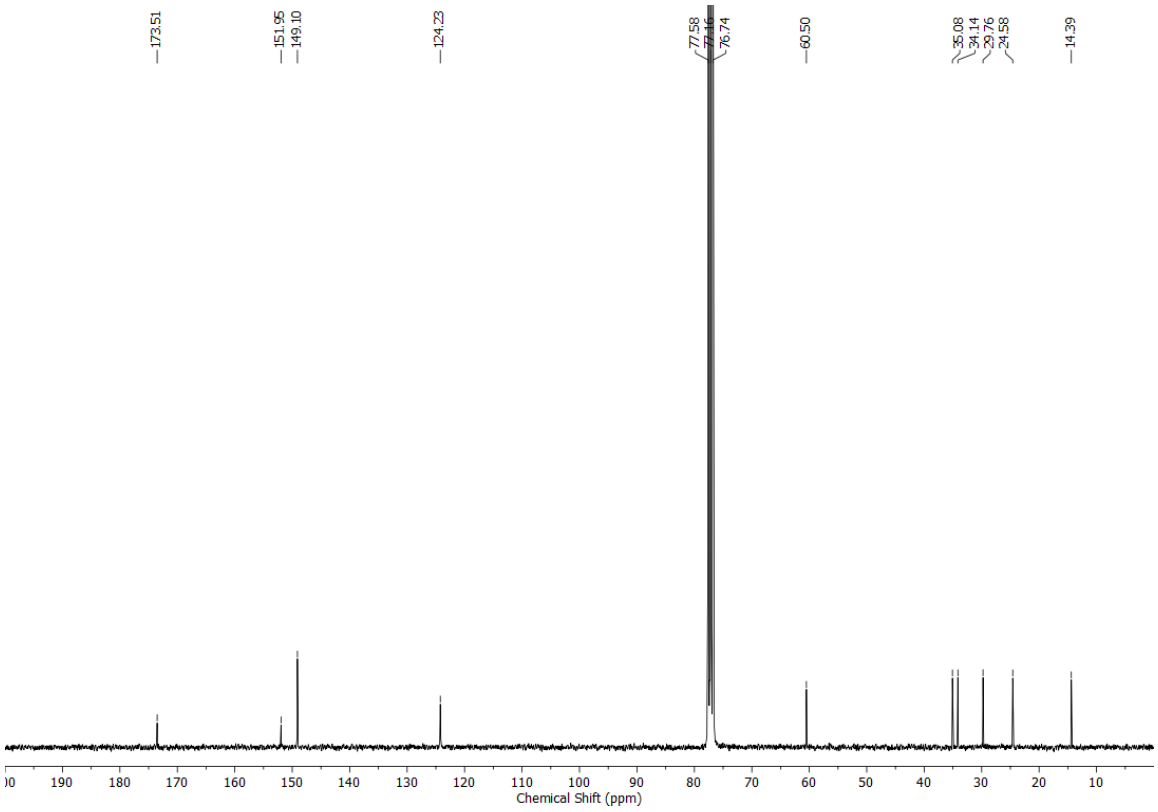

^{1}H (300 MHz, $CDCl_3$) and ^{13}C (75 MHz, $CDCl_3$) – NMR spectra of **11**

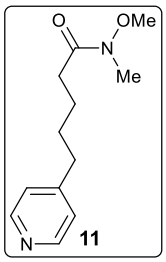

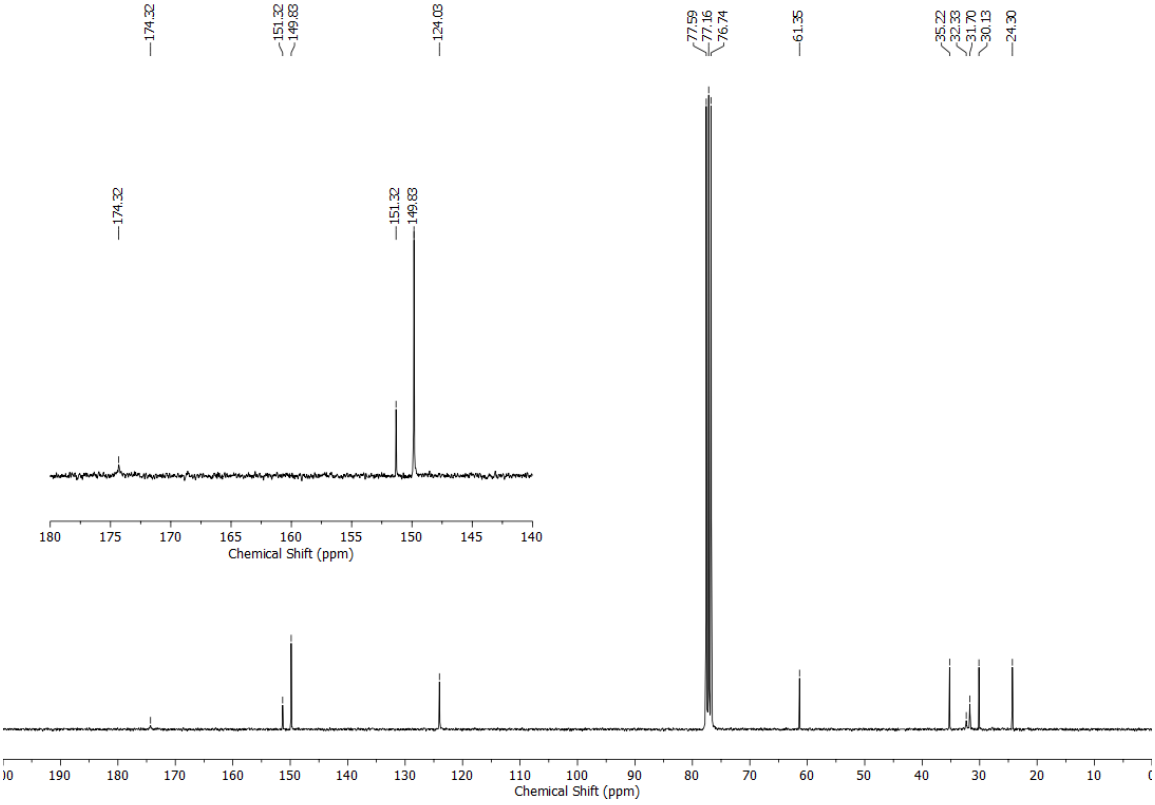

^{1}H (400 MHz, $CDCl_3$) and ^{13}C (101 MHz, $CDCl_3$) – NMR spectra of **12.1**

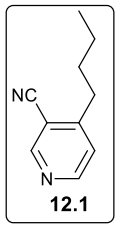

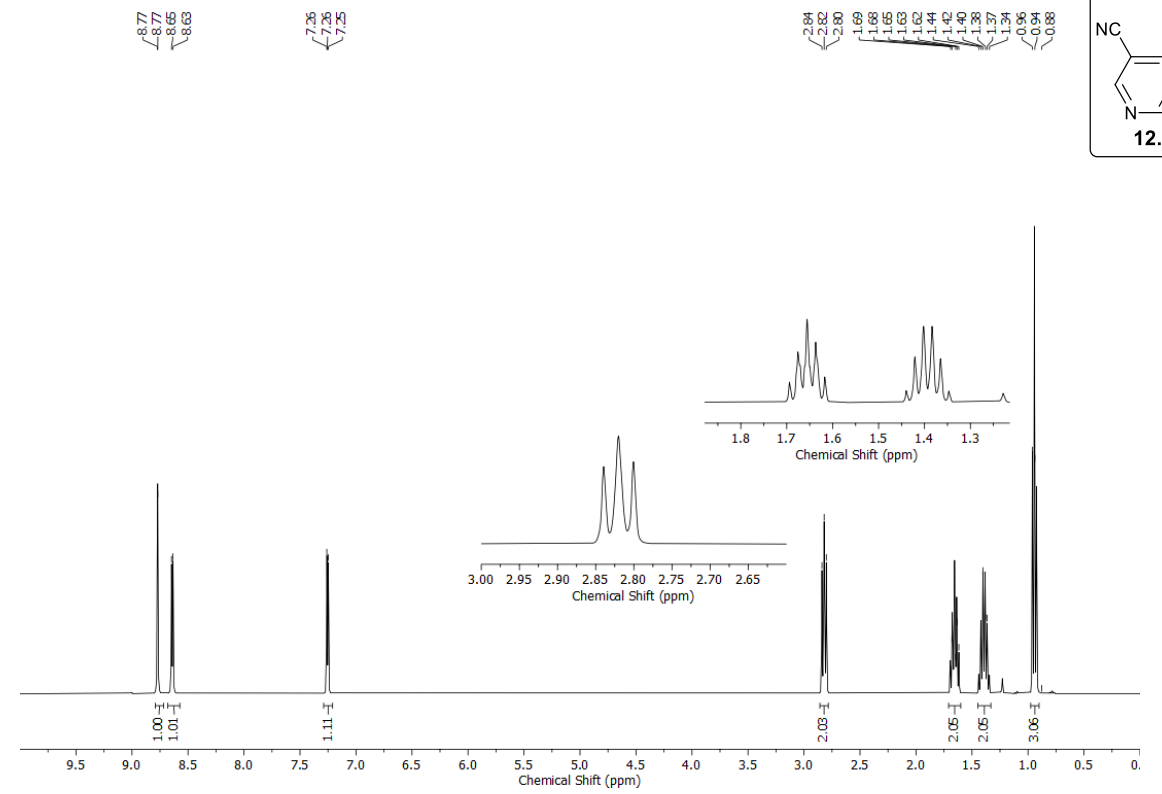

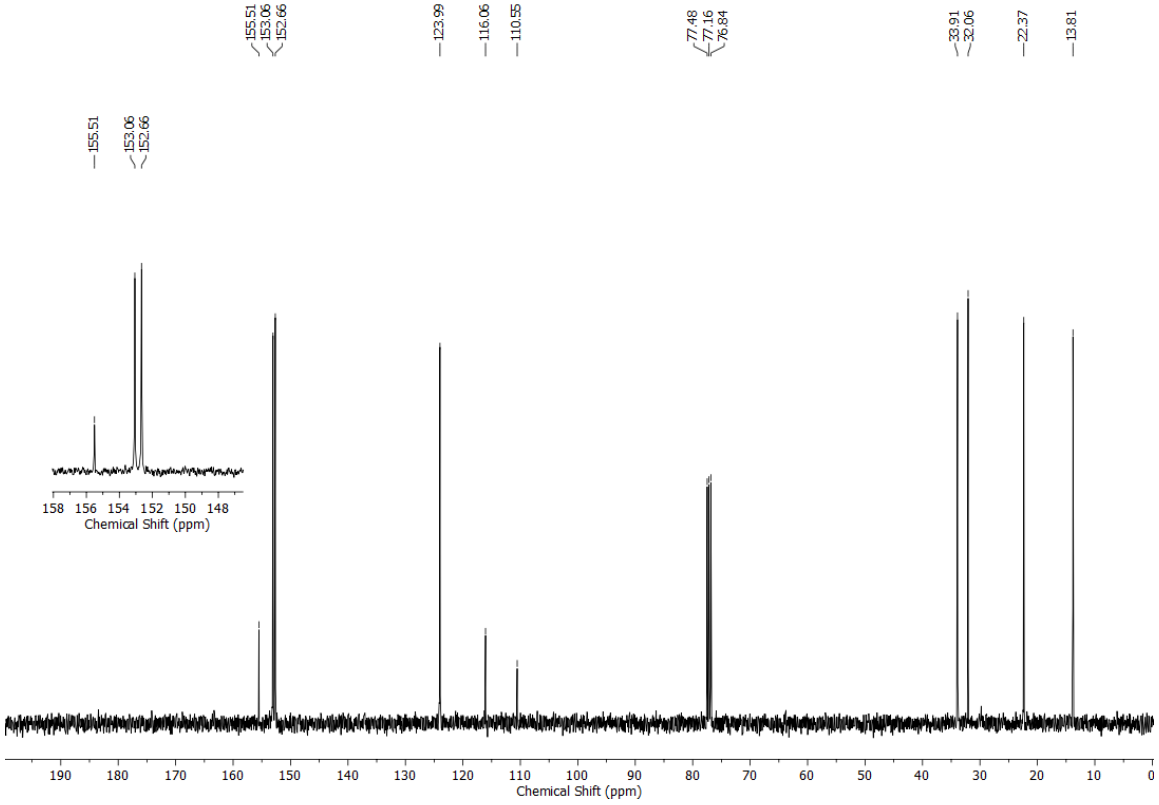

^{1}H (400 MHz, $CDCl_3$) and ^{13}C (101 MHz, $CDCl_3$) – NMR spectra of **12**

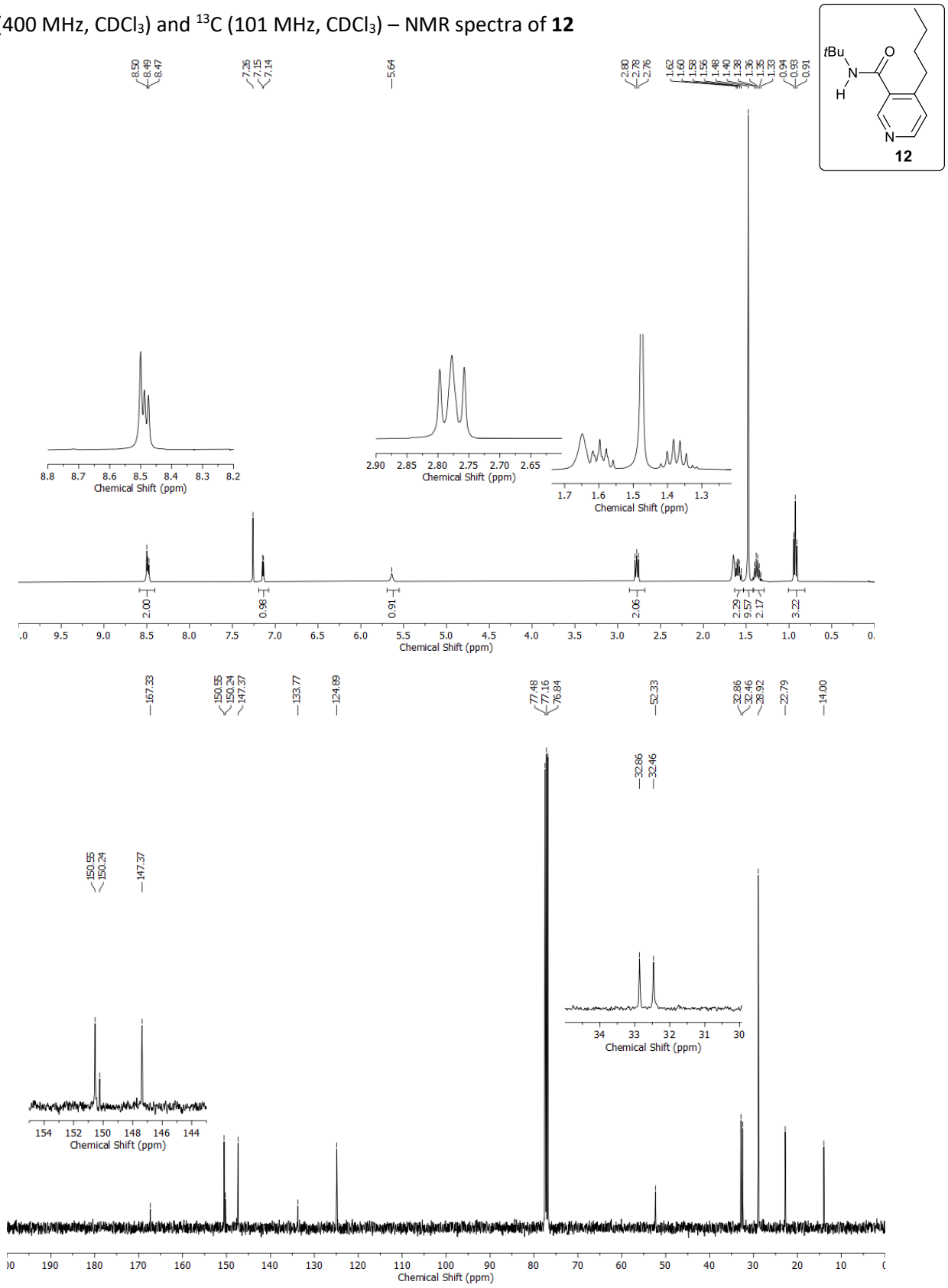

^{1}H (400 MHz, $CDCl_3$) and ^{13}C (101 MHz, $CDCl_3$) – NMR spectra of **13**

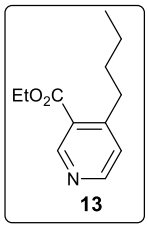

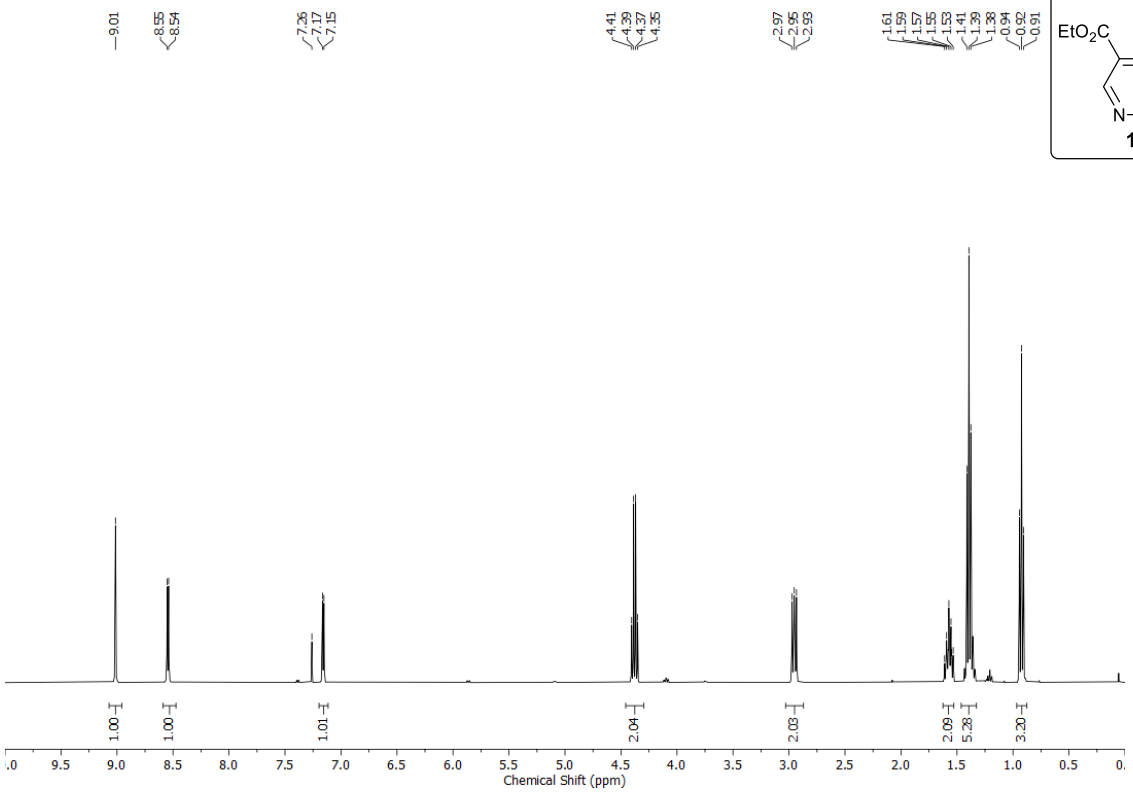

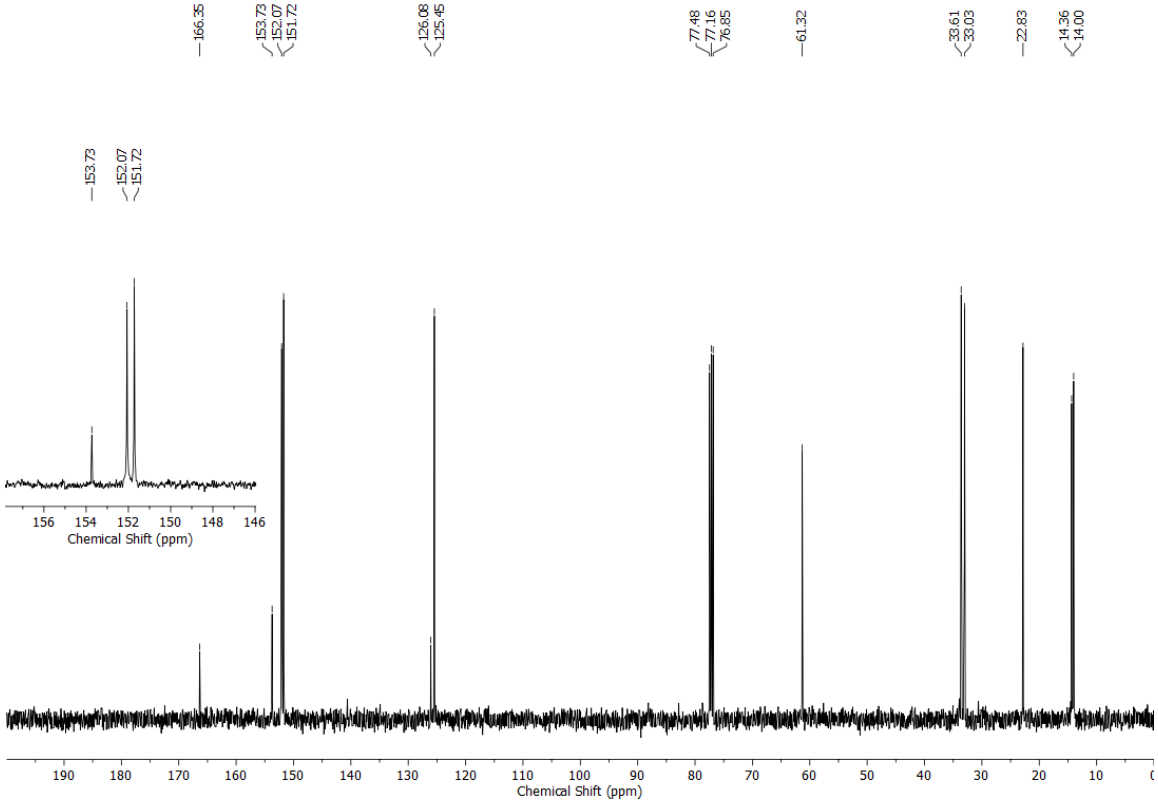

^{1}H (400 MHz, $CDCl_3$) and ^{13}C (101 MHz, $CDCl_3$) – NMR spectra of **15.1**

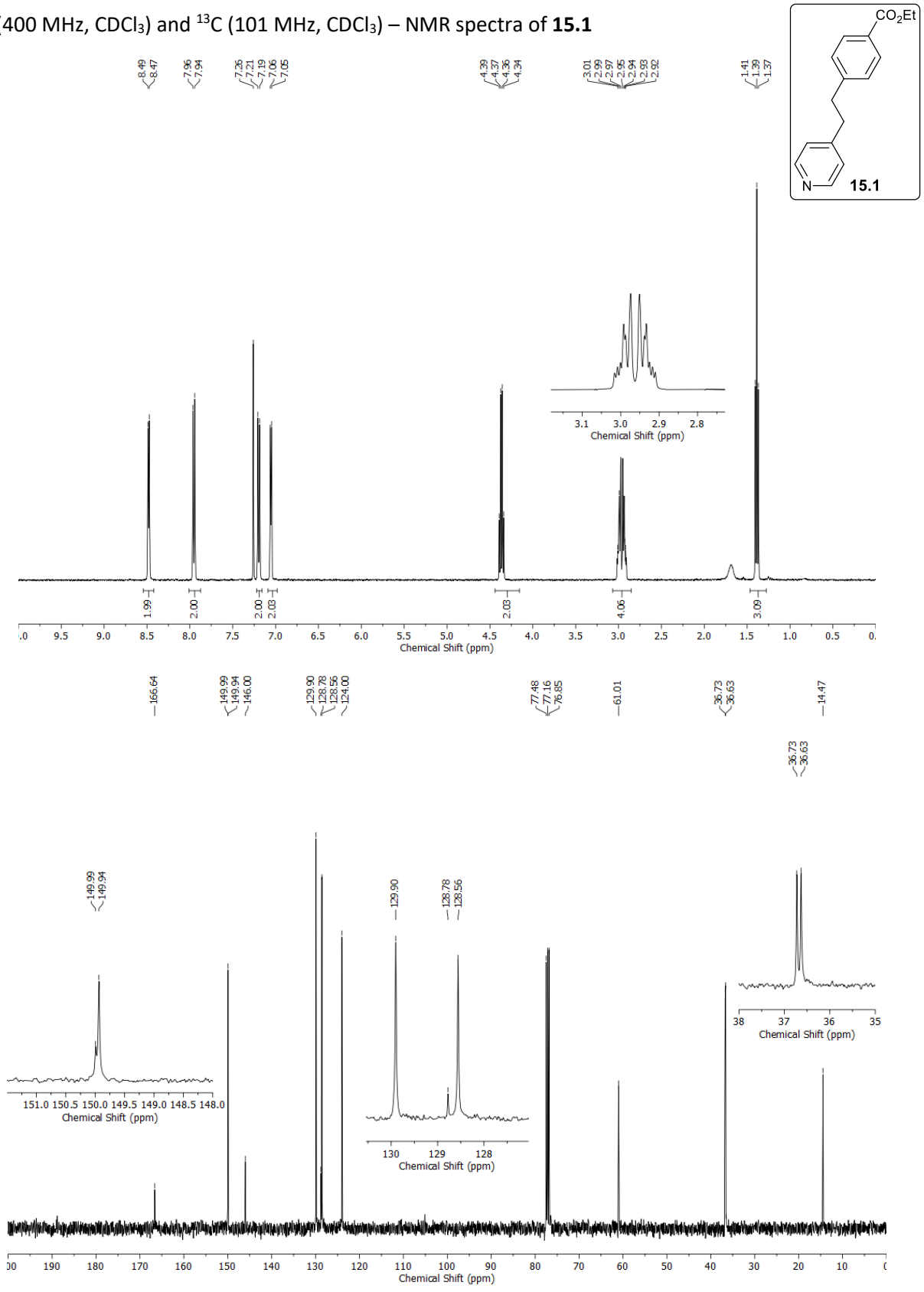

^{1}H (400 MHz, $CDCl_3$) and ^{13}C (101 MHz, $CDCl_3$) – NMR spectra of **15.2**

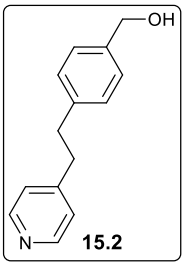

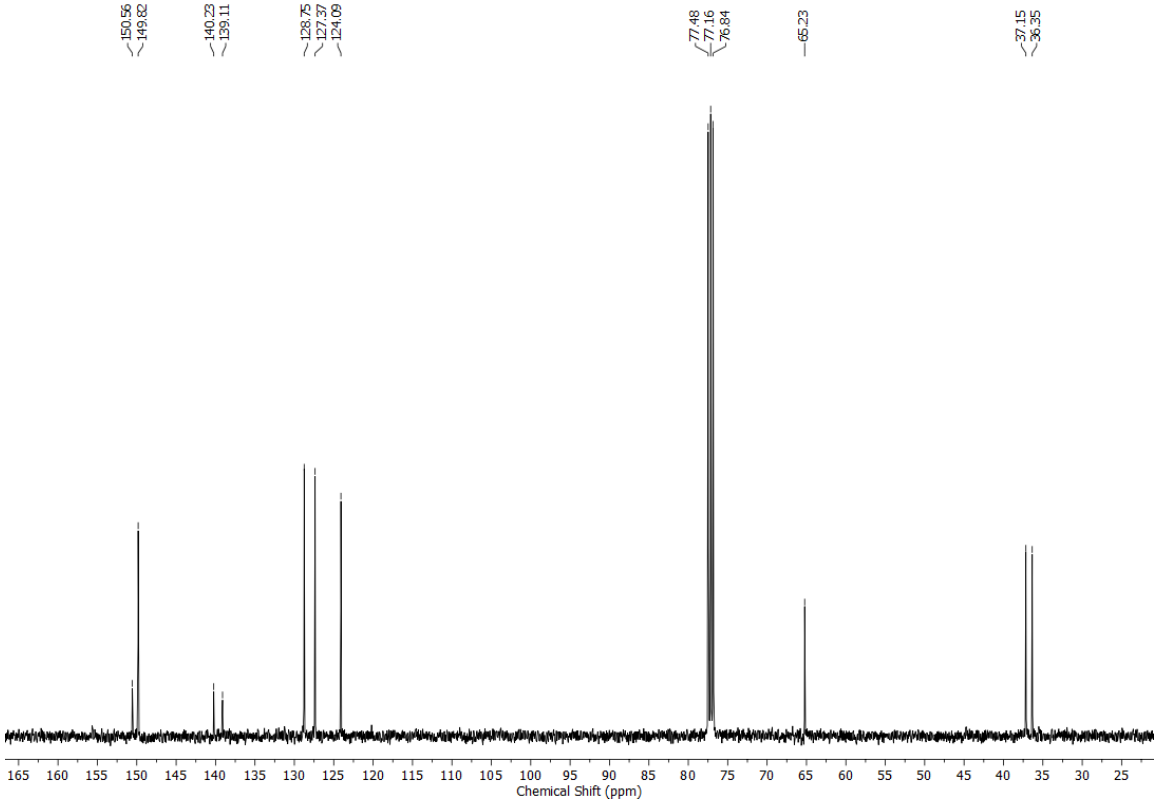

^{1}H (400 MHz, $CDCl_3$) and ^{13}C (101 MHz, $CDCl_3$) – NMR spectra of **15.3**

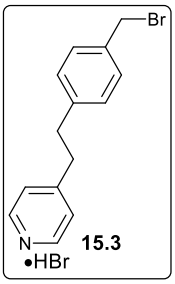

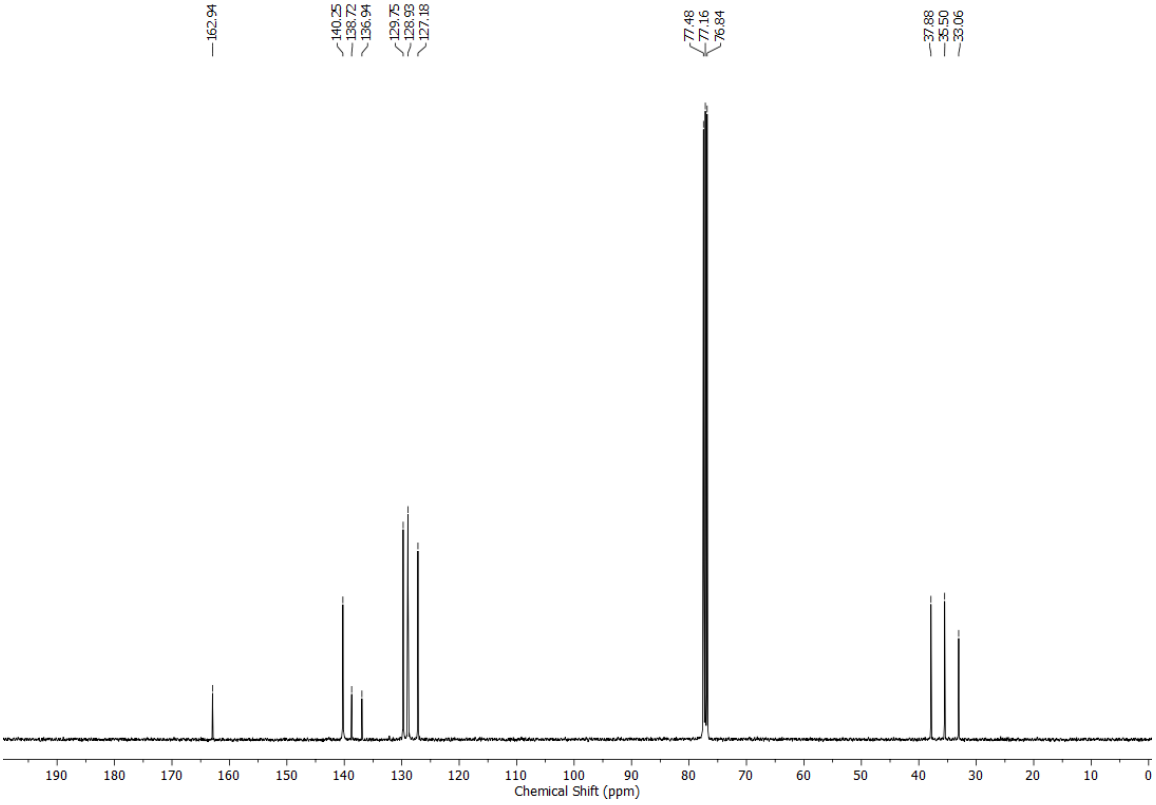

^{1}H (400 MHz, $CDCl_3$) and ^{13}C (101 MHz, $CDCl_3$) – NMR spectra of **15**

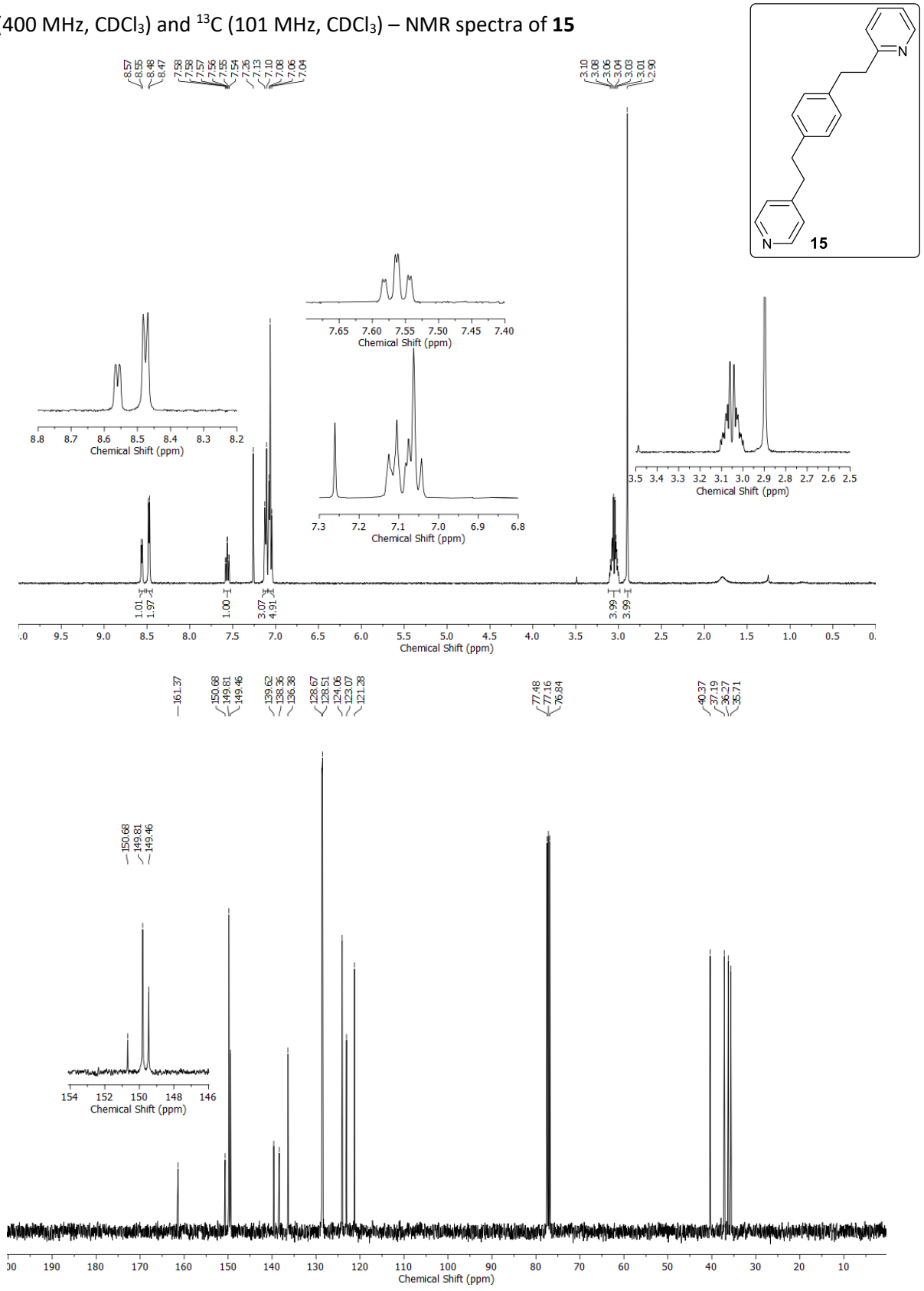

^{1}H (400 MHz, $CDCl_3$) and ^{13}C (101 MHz, DMSO) – NMR spectra of **1e**

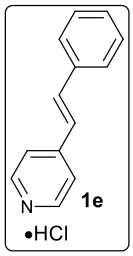

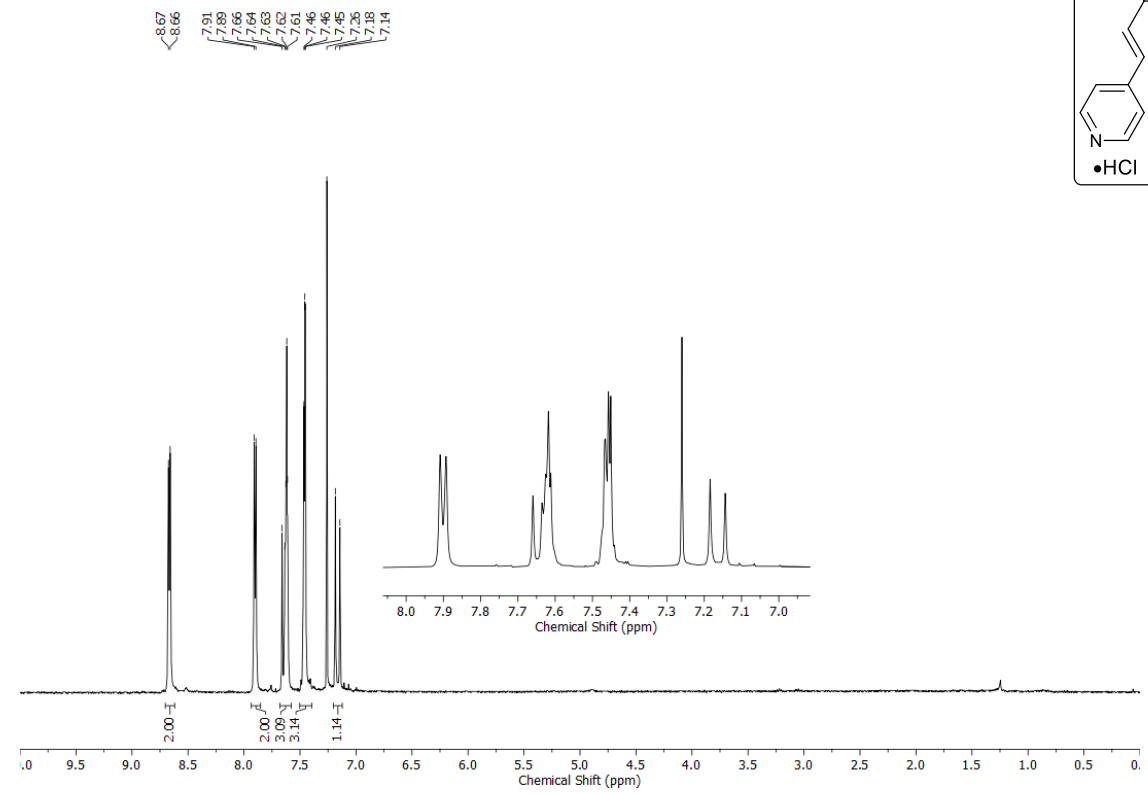

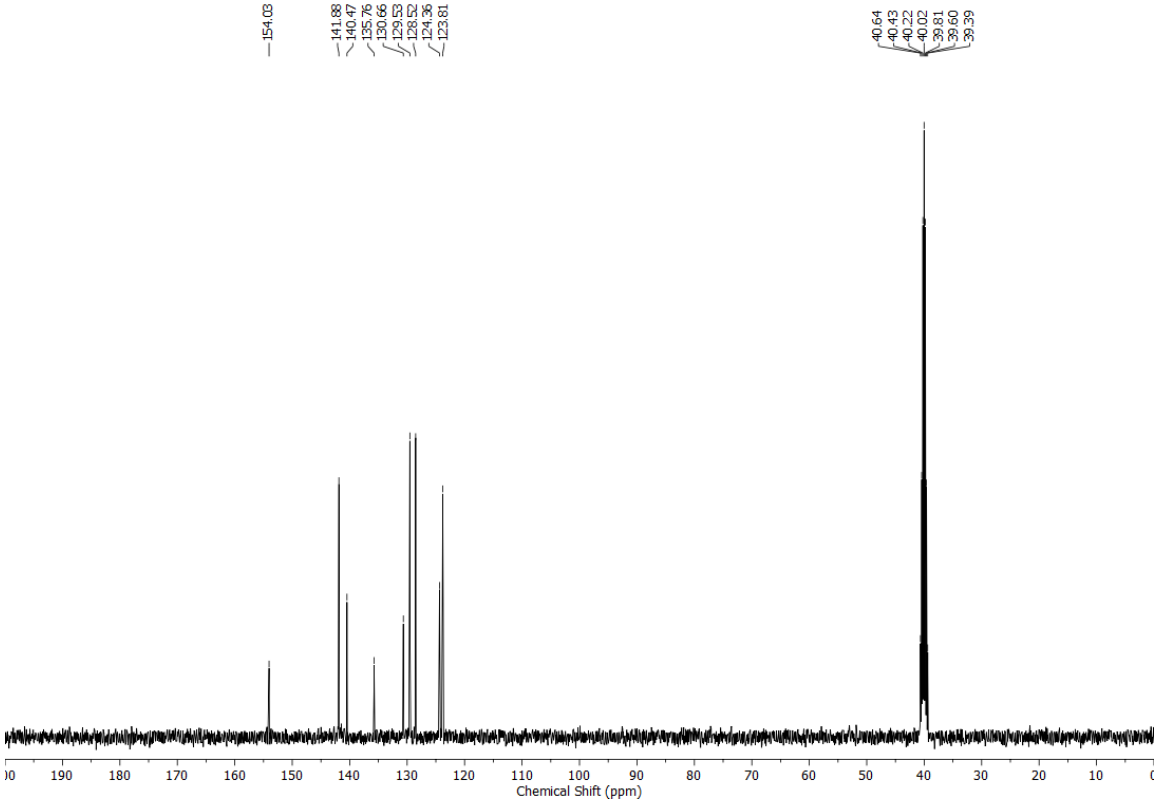

^{1}H (300 MHz, $CDCl_3$) and ^{13}C (75 MHz, $CDCl_3$) – NMR spectra of **2e**

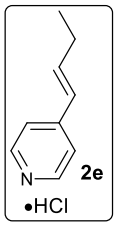

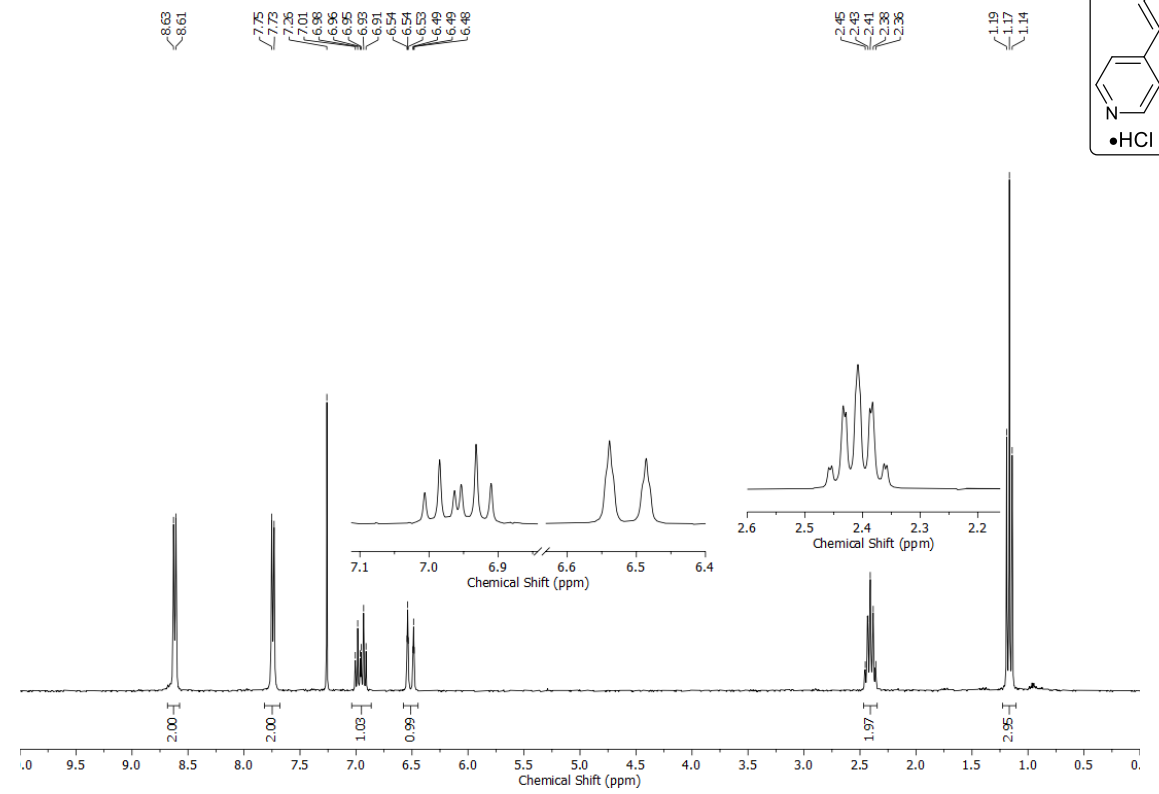

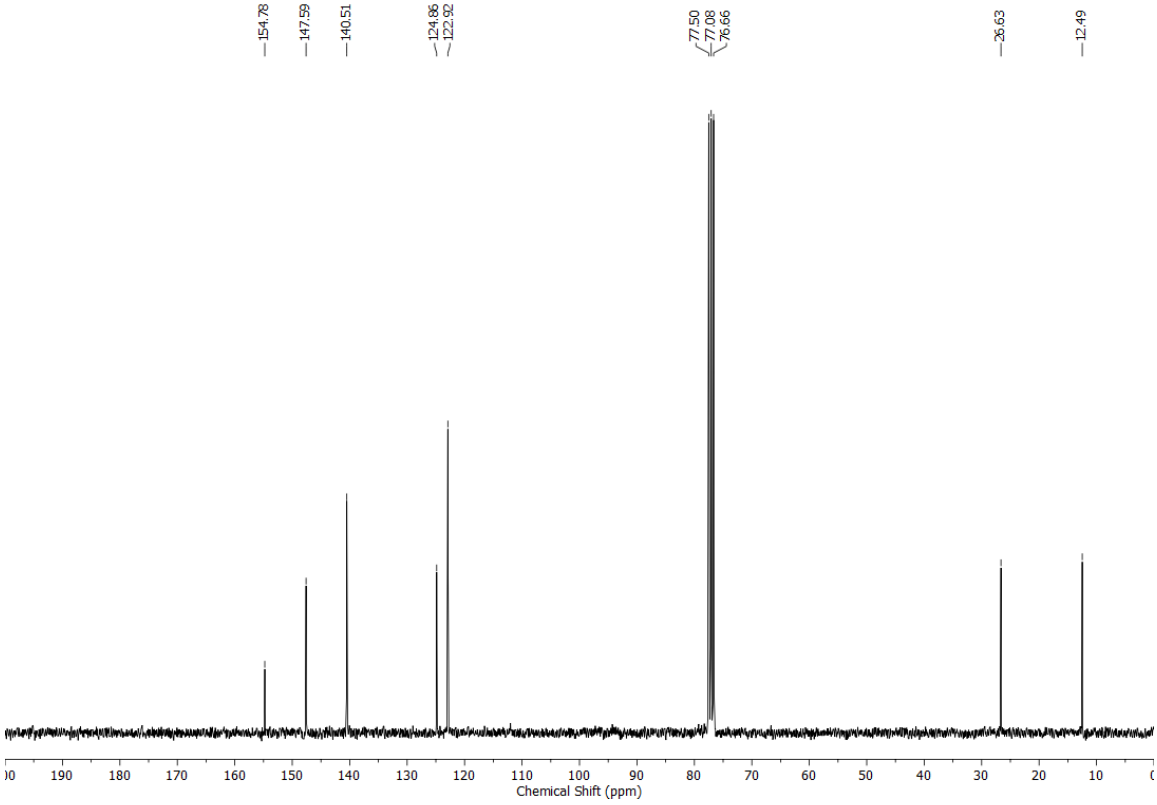

^{1}H (300 MHz, $CDCl_3$) and ^{13}C (101 MHz, $CDCl_3$) – NMR spectra of **3e**–HCl

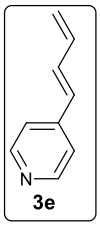

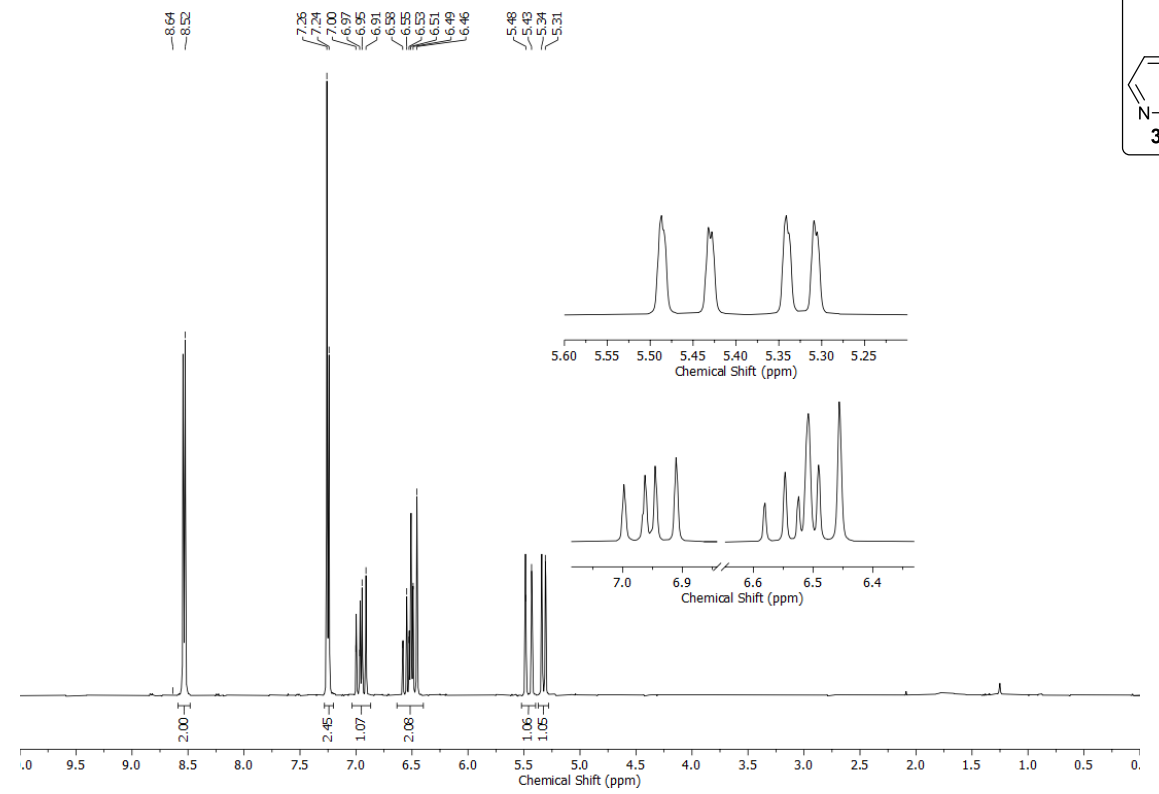

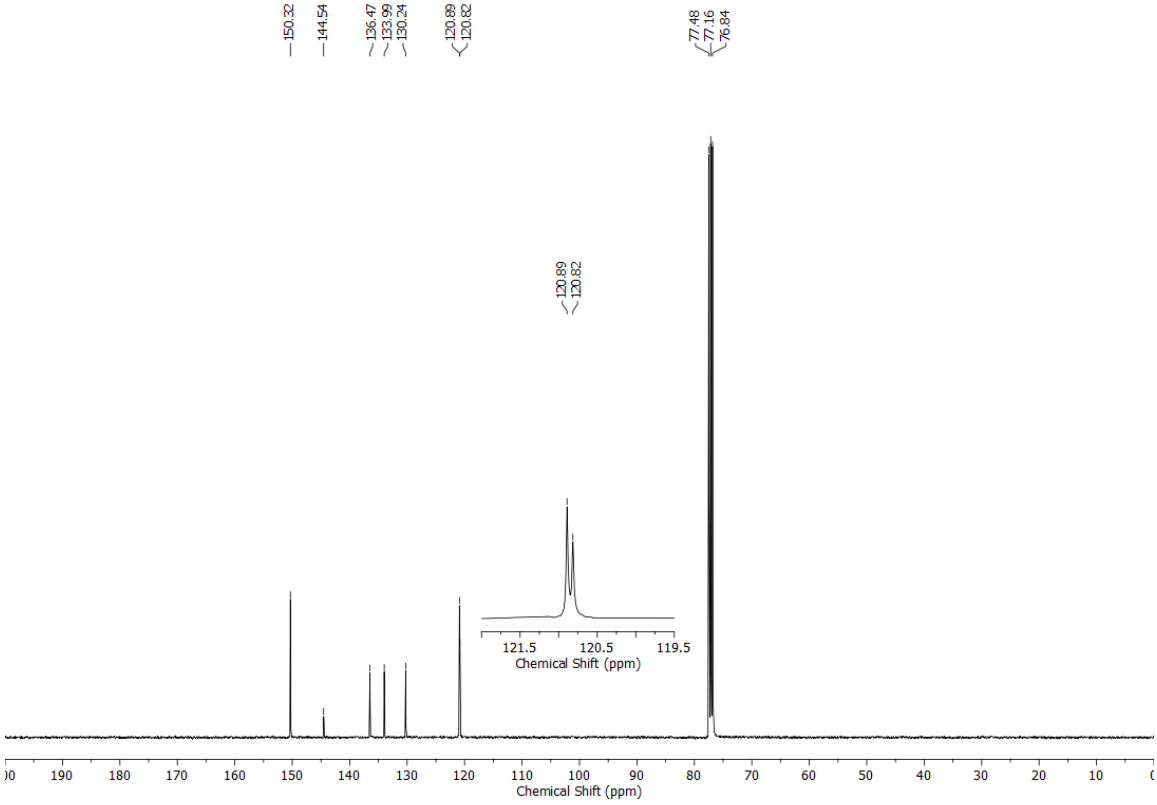

^{1}H (300 MHz, DMSO) and ^{13}C (101 MHz, $CDCl_3$) – NMR spectra of **4e**

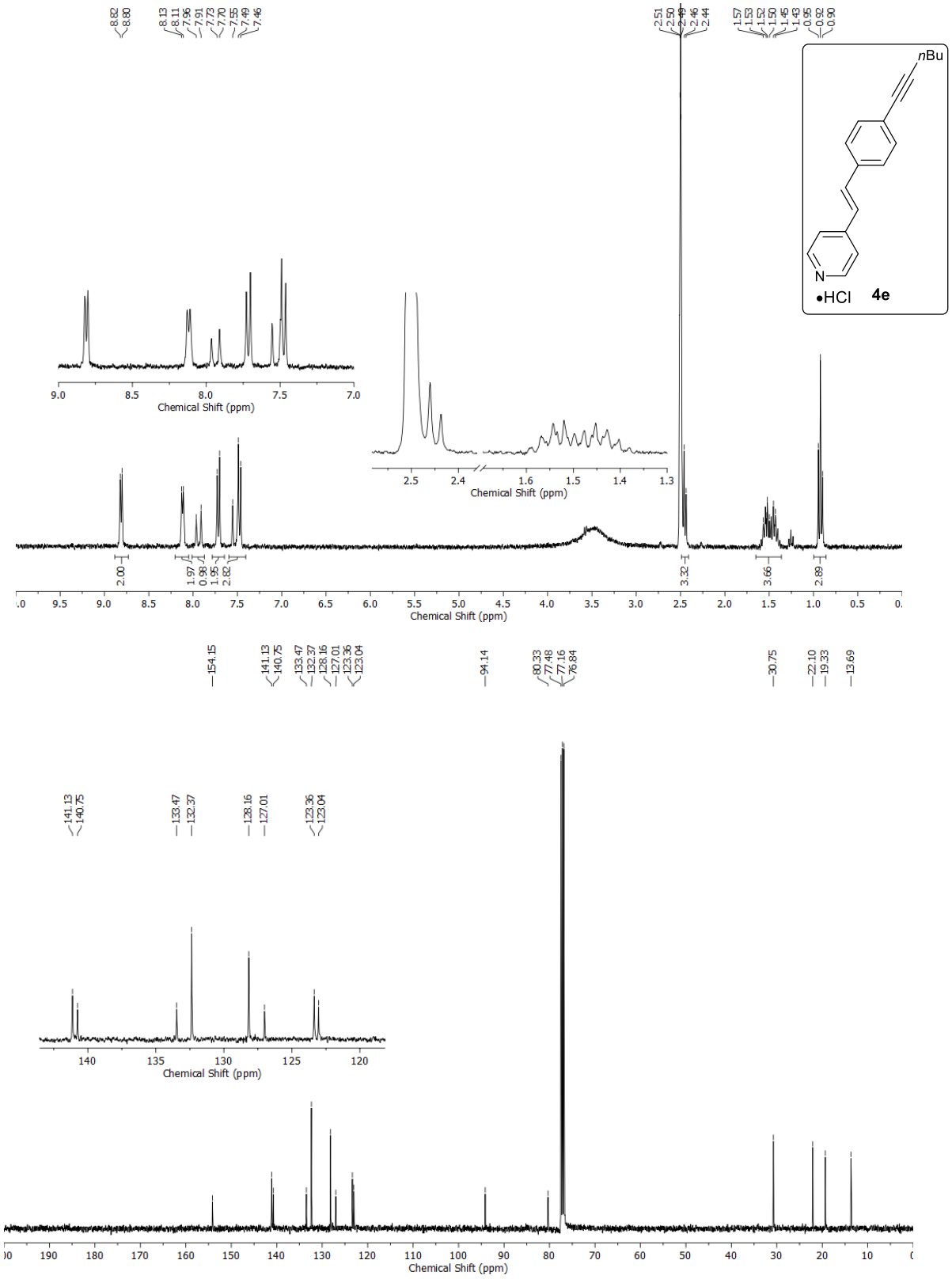

^{1}H (400 MHz, $CDCl_3$) and ^{13}C (101 MHz, $CDCl_3$) – NMR spectra of **5e**

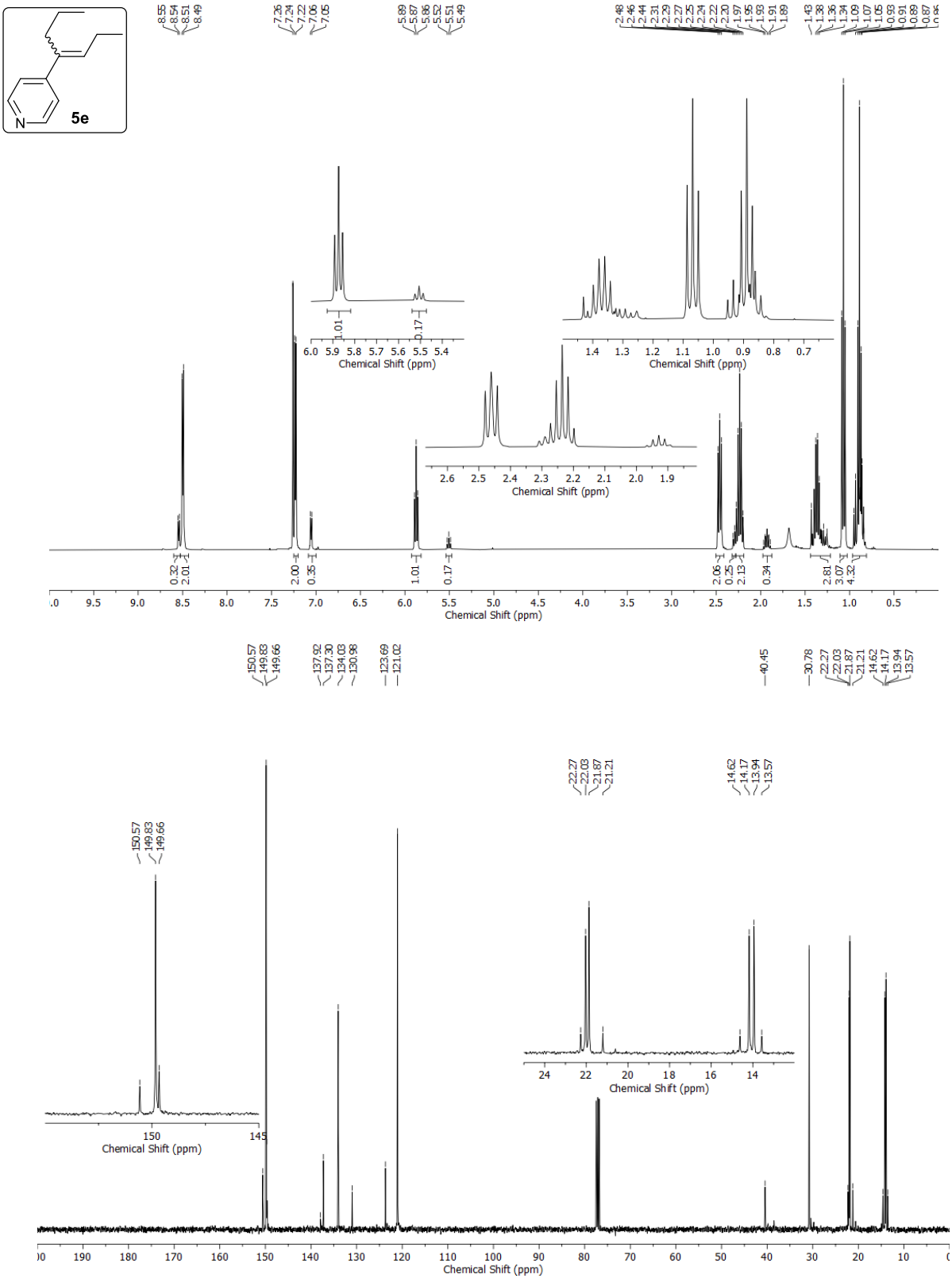

^{1}H (300 MHz, $CDCl_3$) and ^{13}C (75 MHz, $CDCl_3$) – NMR spectra of **6e**–HCl

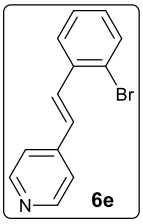

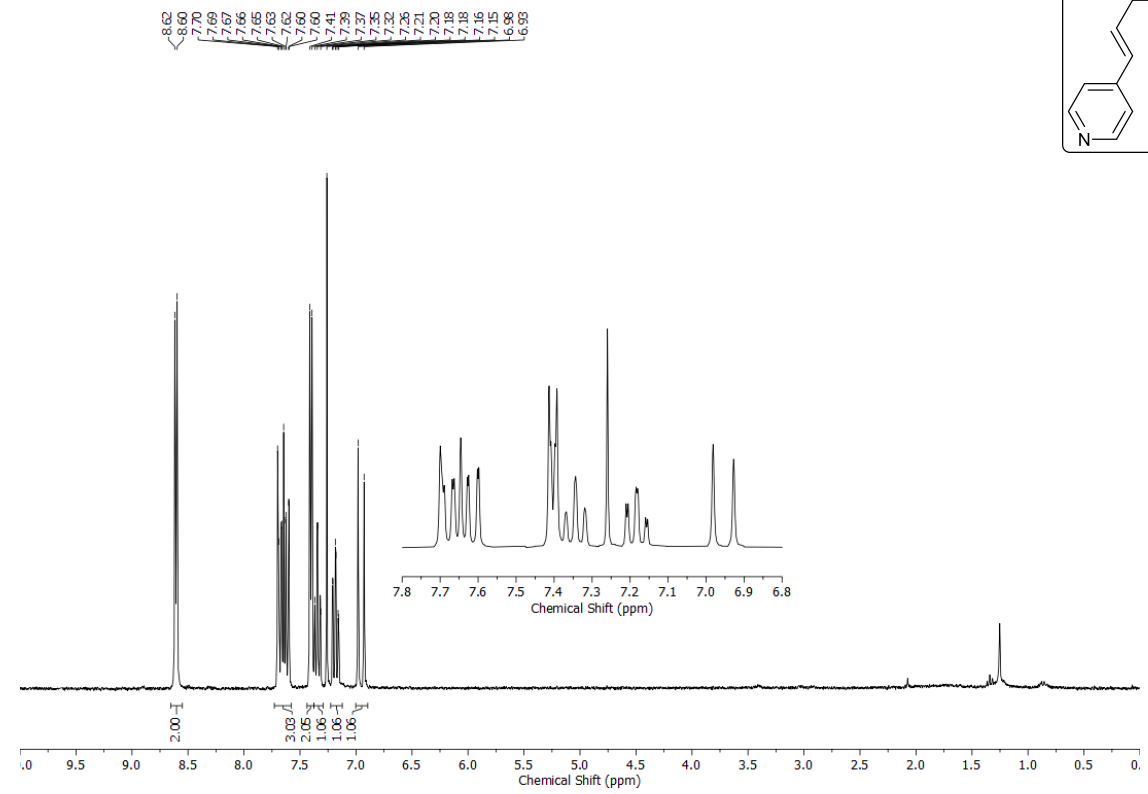

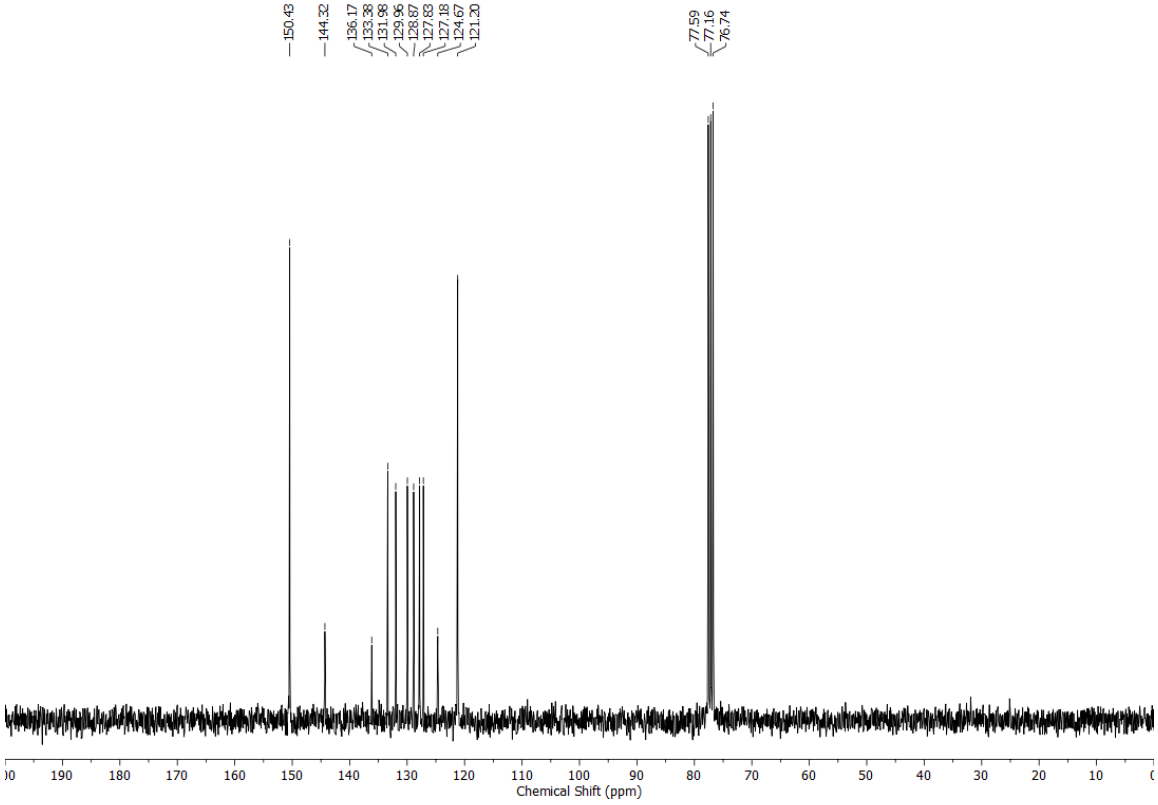

^{1}H (300 MHz, $CDCl_3$) and ^{13}C (75 MHz, $CDCl_3$) – NMR spectra of **7e**

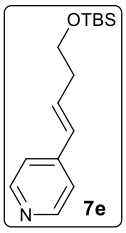

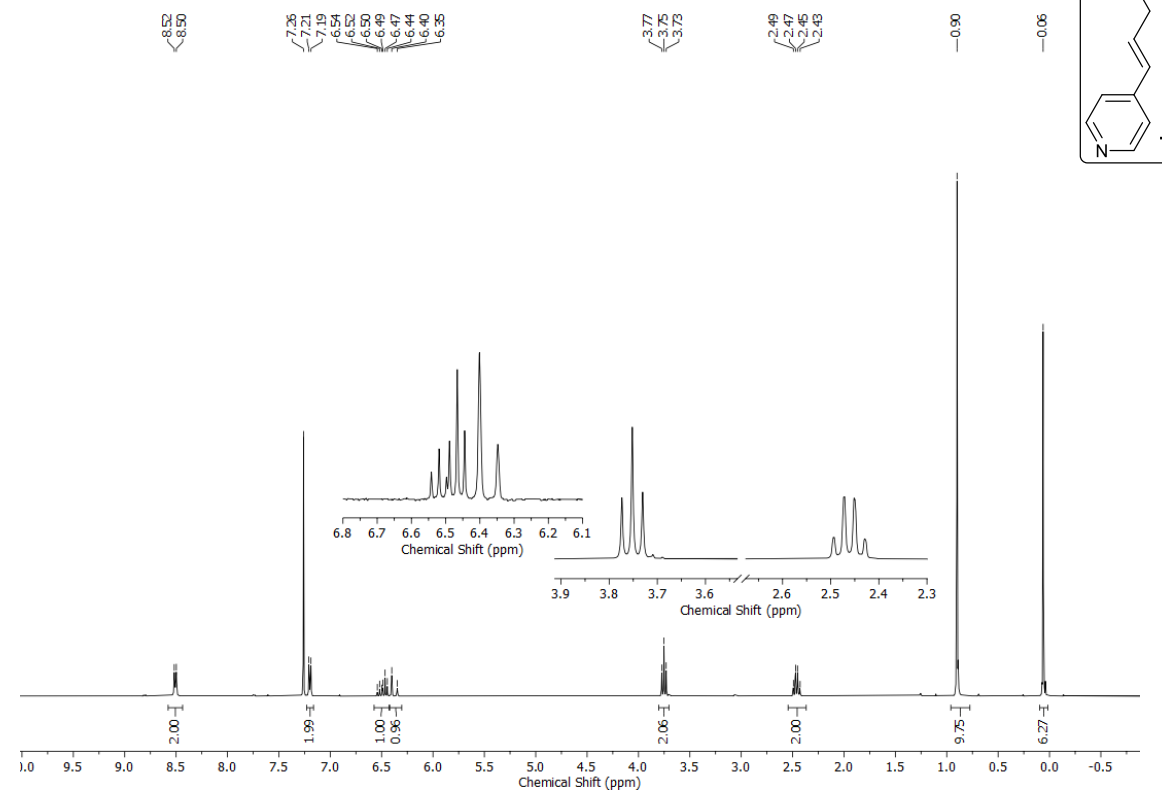

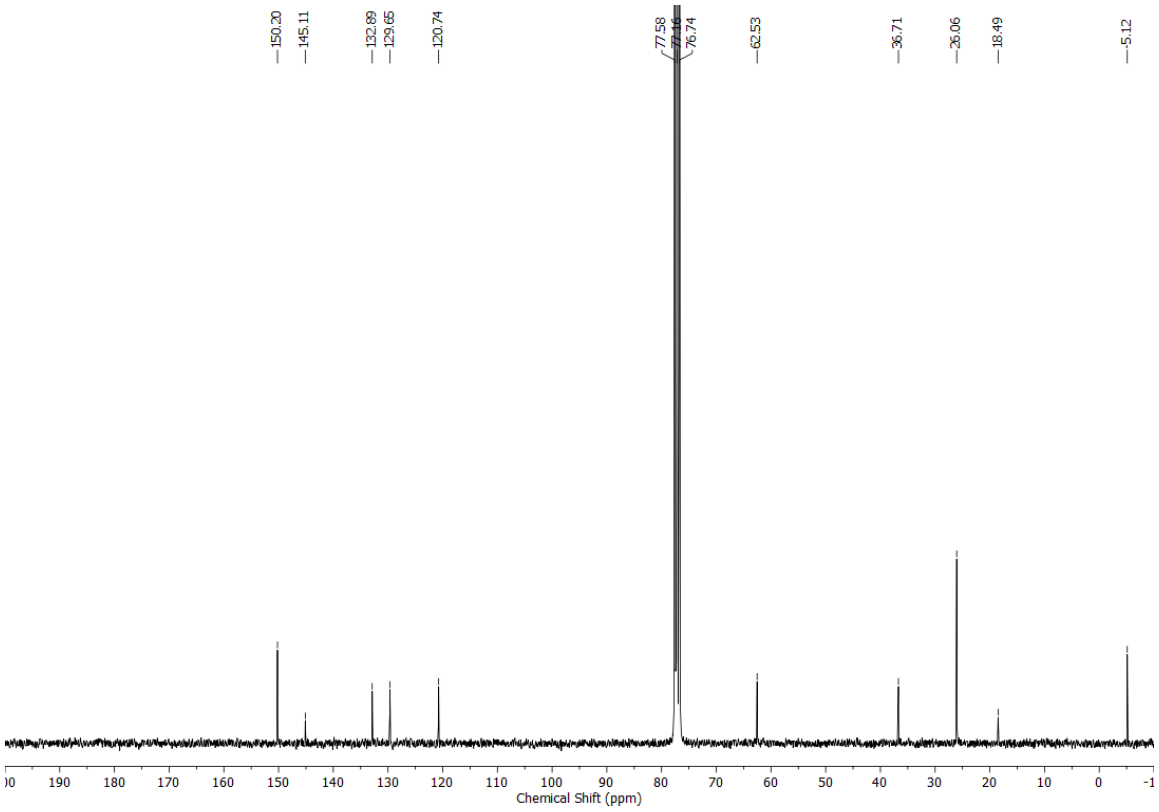

^{1}H (300 MHz, $CDCl_3$) and ^{13}C (101 MHz, $CDCl_3$) – NMR spectra of **8e**

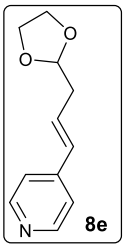

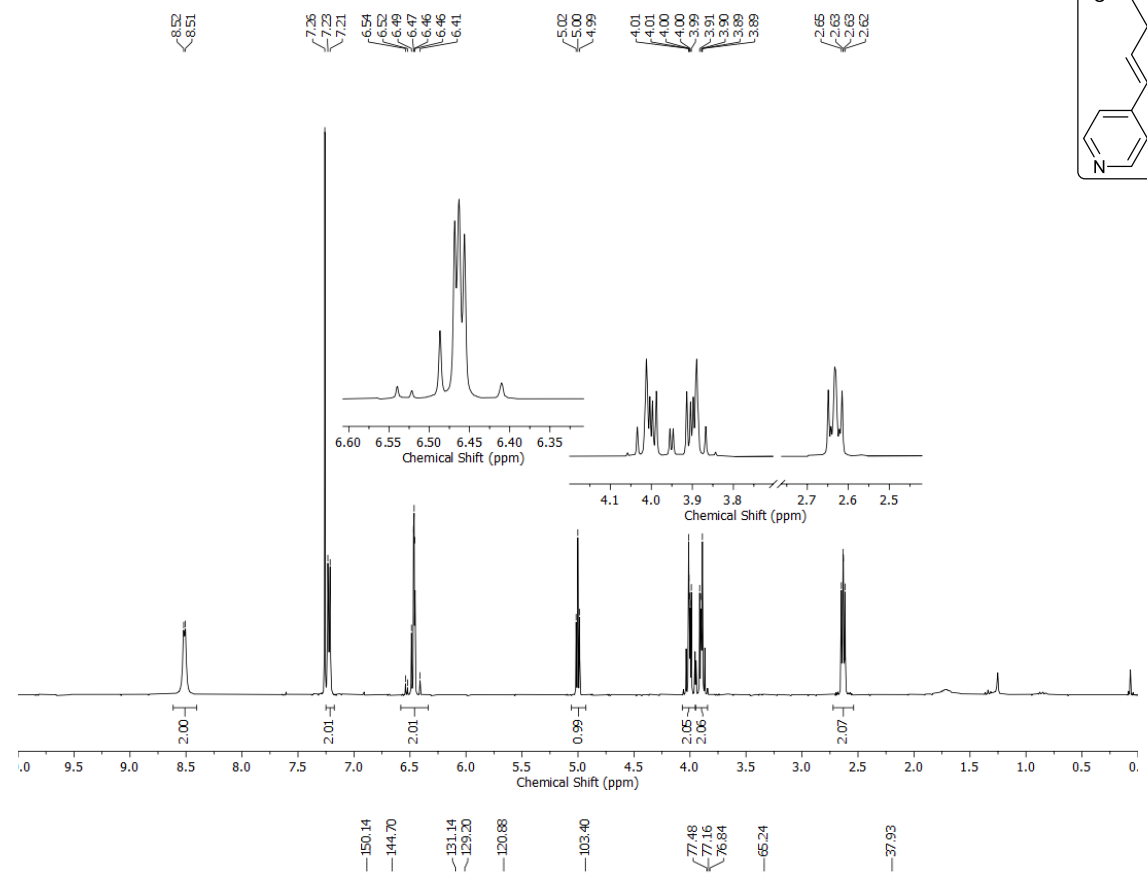

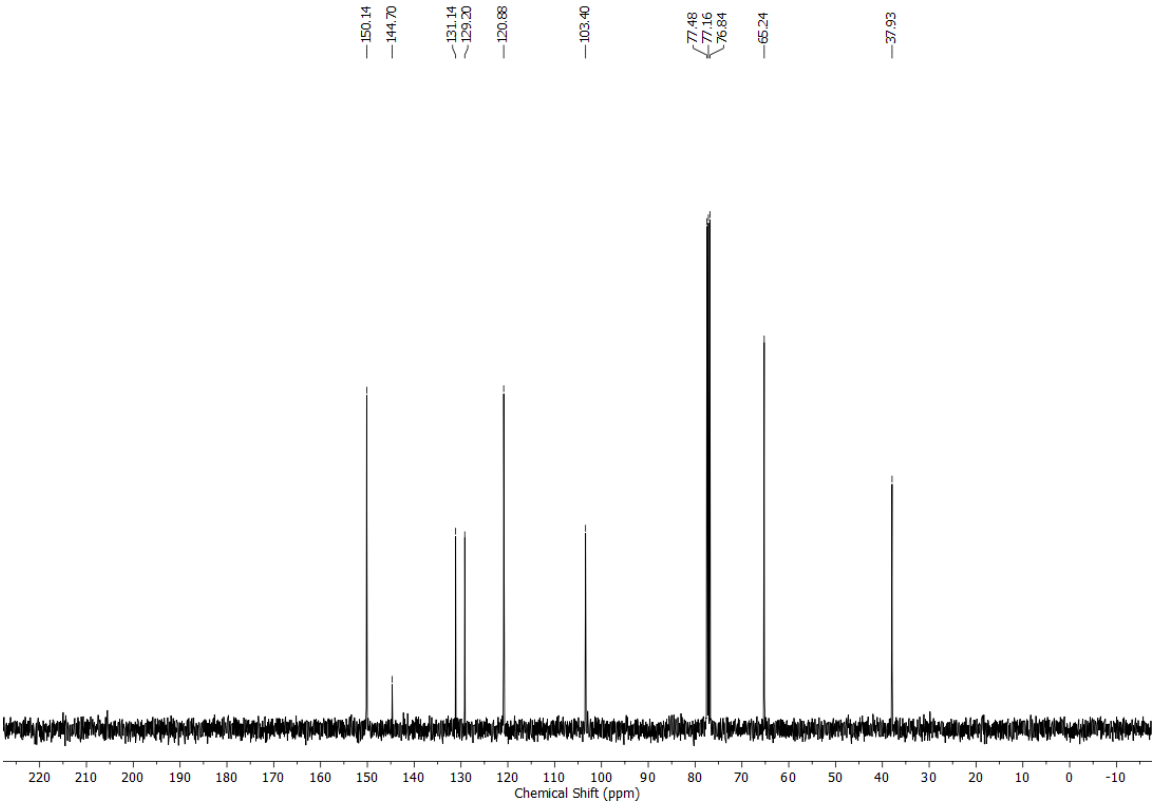

^{1}H (400 MHz, $CDCl_3$) and ^{13}C (101 MHz, $CDCl_3$) – NMR spectra of **9e**

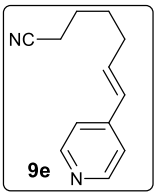

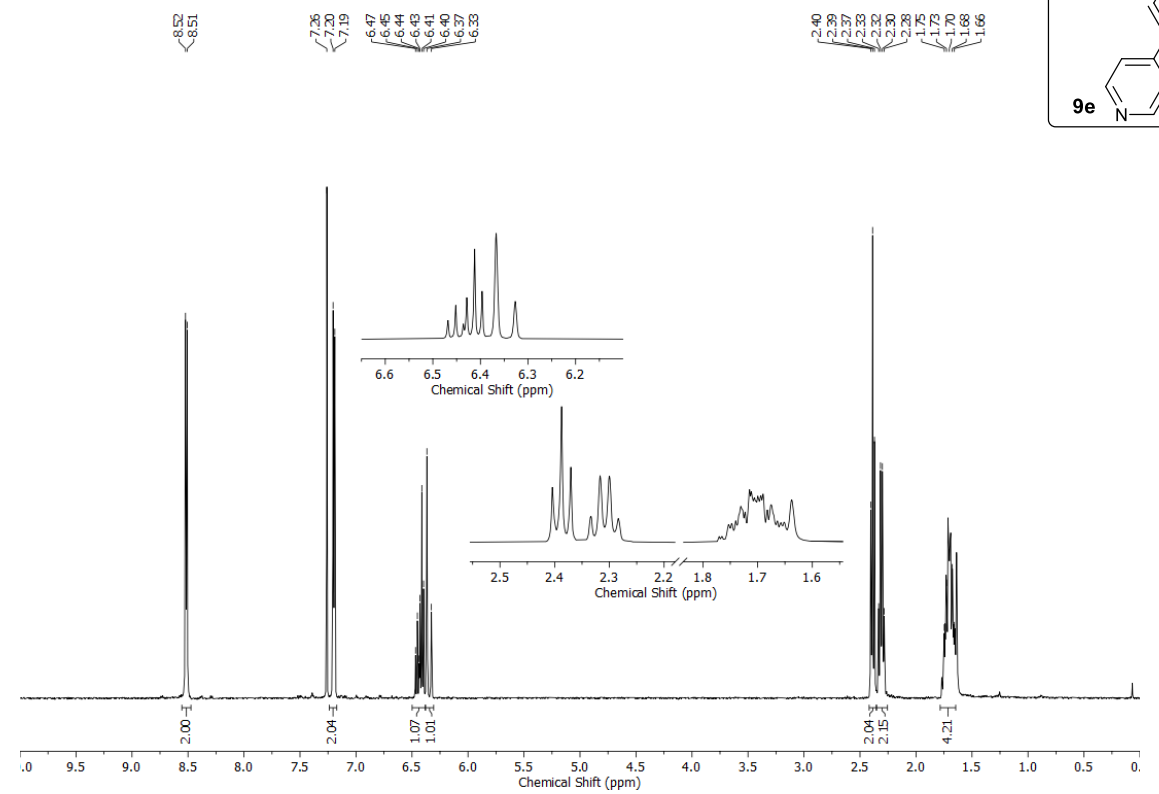

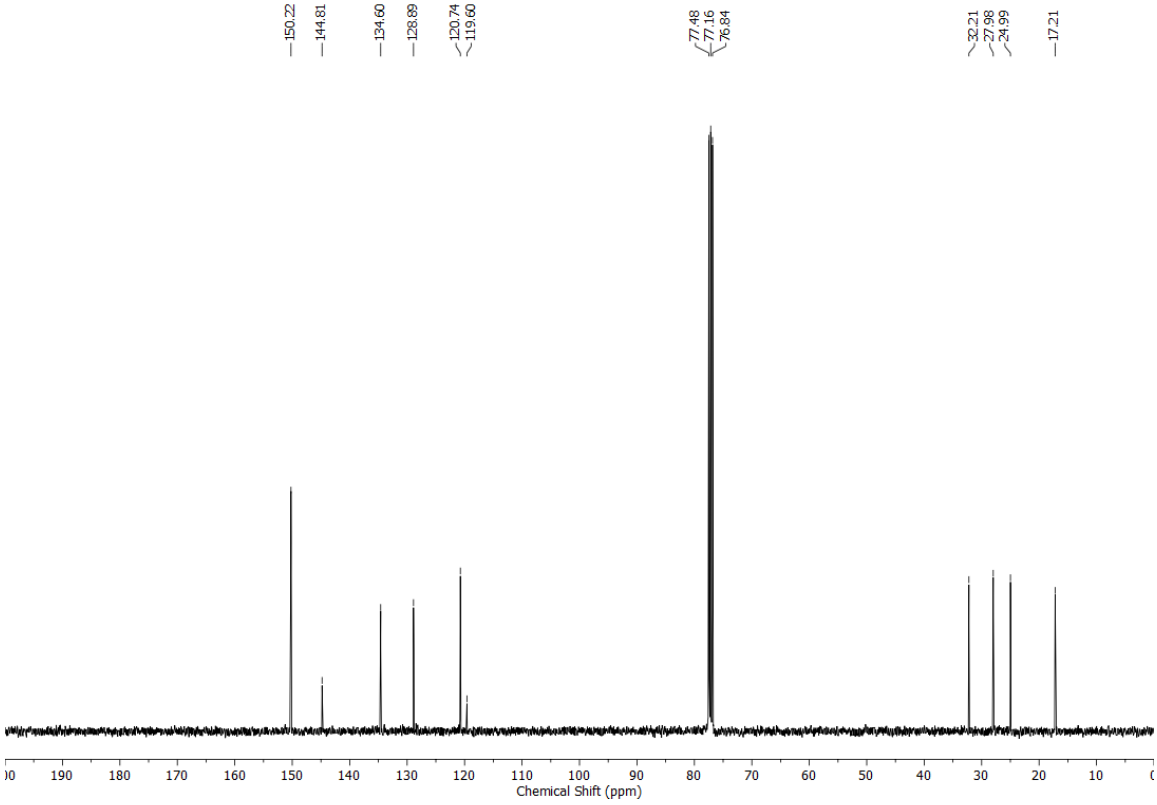

^{1}H (400 MHz, $CDCl_3$) and ^{13}C (101 MHz, $CDCl_3$) – NMR spectra of **10e**

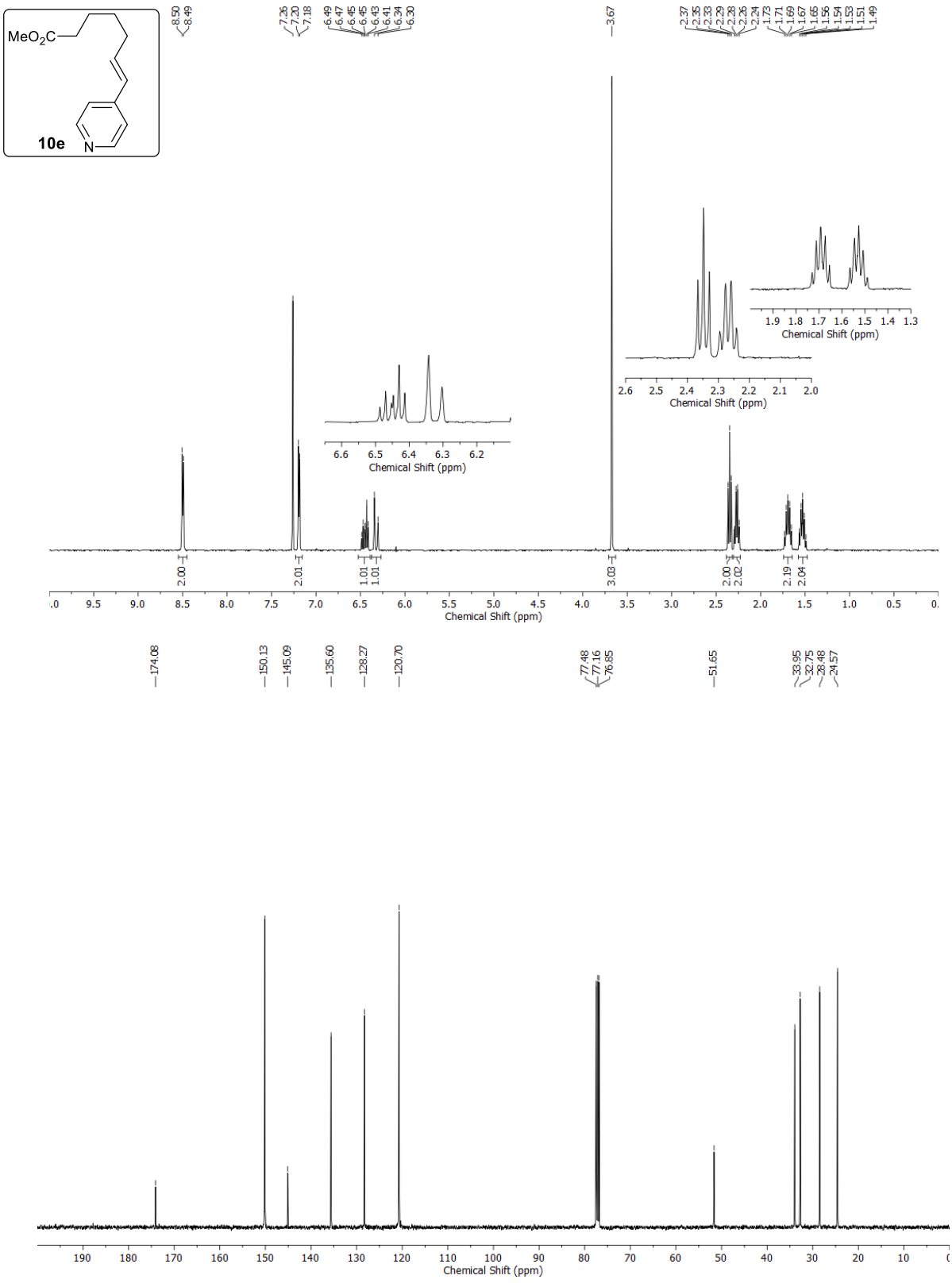

^{1}H (300 MHz, $CDCl_3$) and ^{13}C (75 MHz, $CDCl_3$) – NMR spectra of **11e**

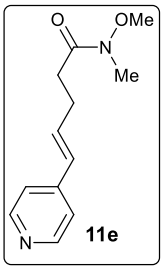

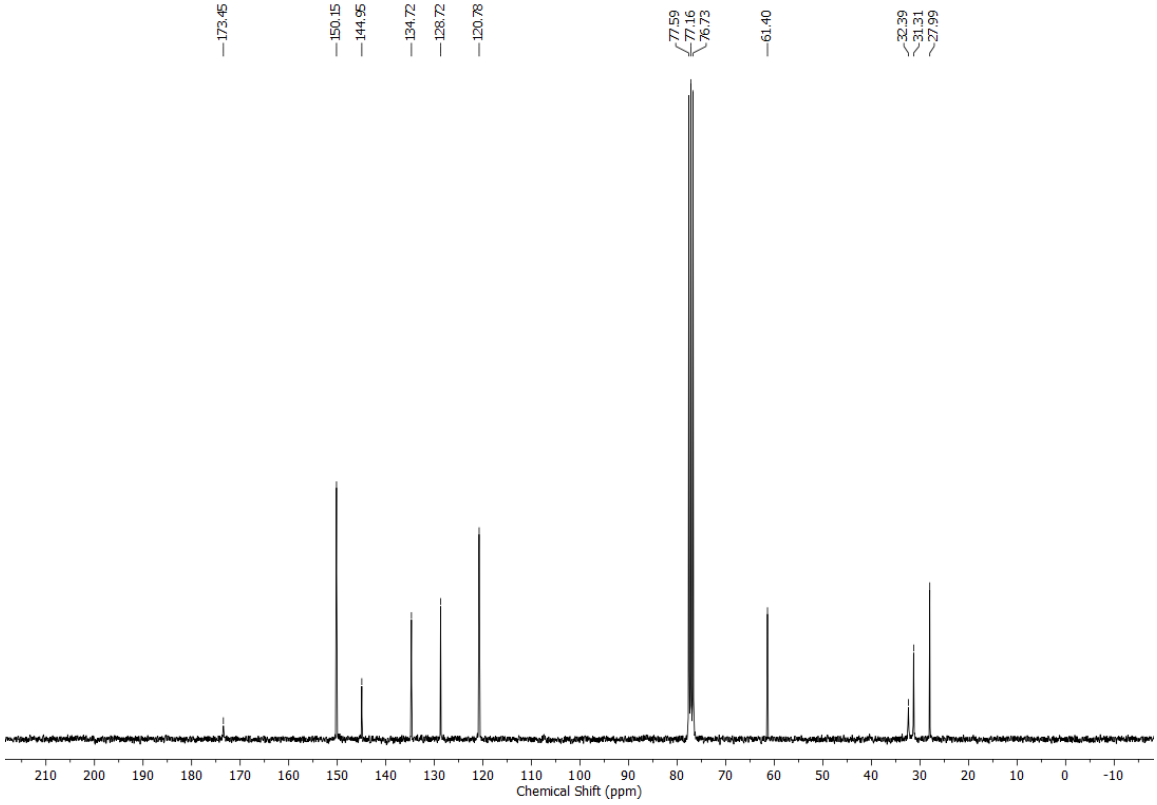

^{1}H (300 MHz, $CDCl_3$) and ^{13}C (75 MHz, $CDCl_3$) – NMR spectra of **12e**

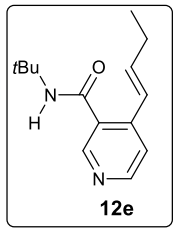

^{1}H (300 MHz, $CDCl_3$) and ^{13}C (75 MHz, $CDCl_3$) – NMR spectra of **13e**

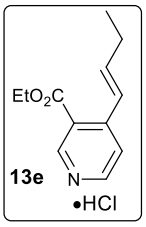

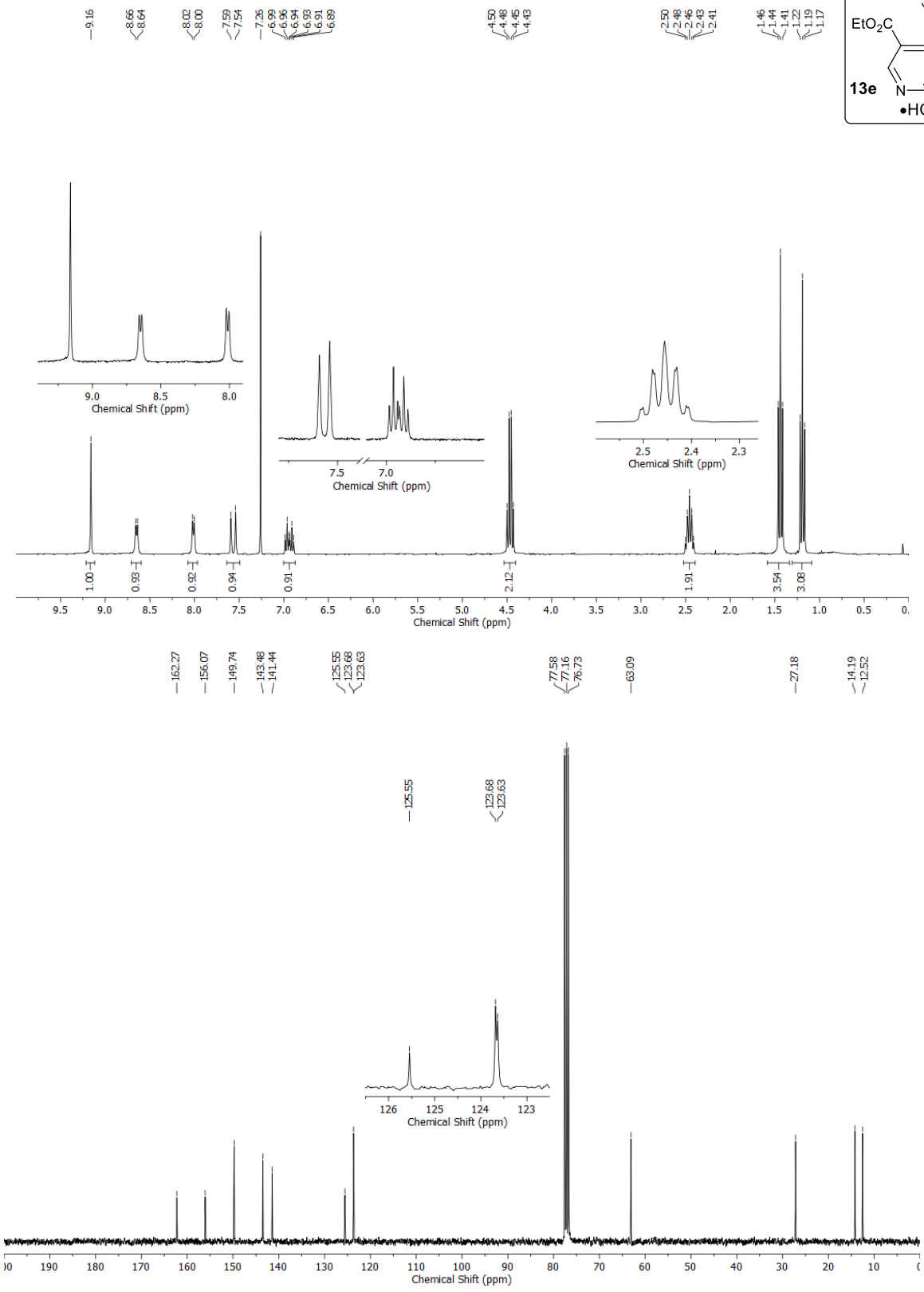

^{1}H (300 MHz, $CDCl_3$) and ^{13}C (101 MHz, $CDCl_3$) – NMR spectra of **14e**

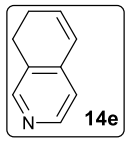

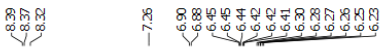

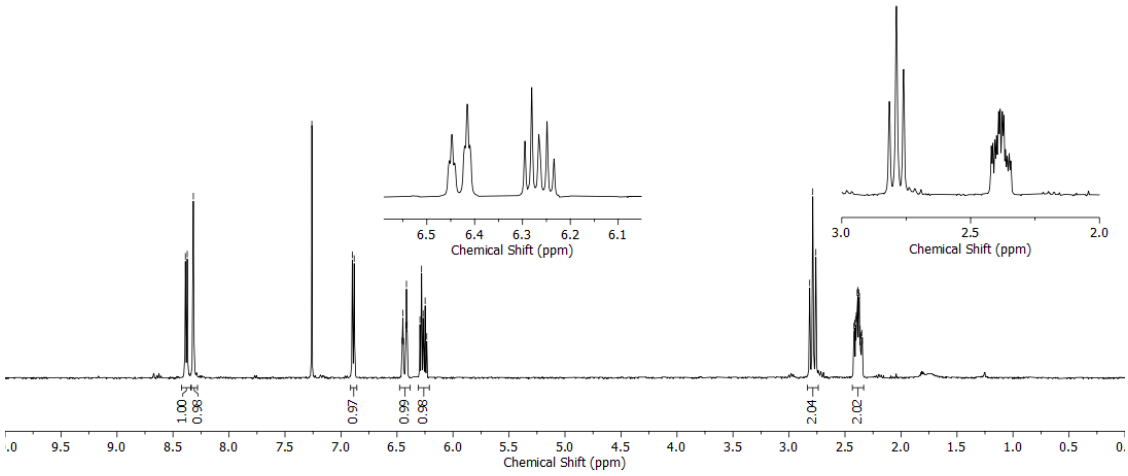

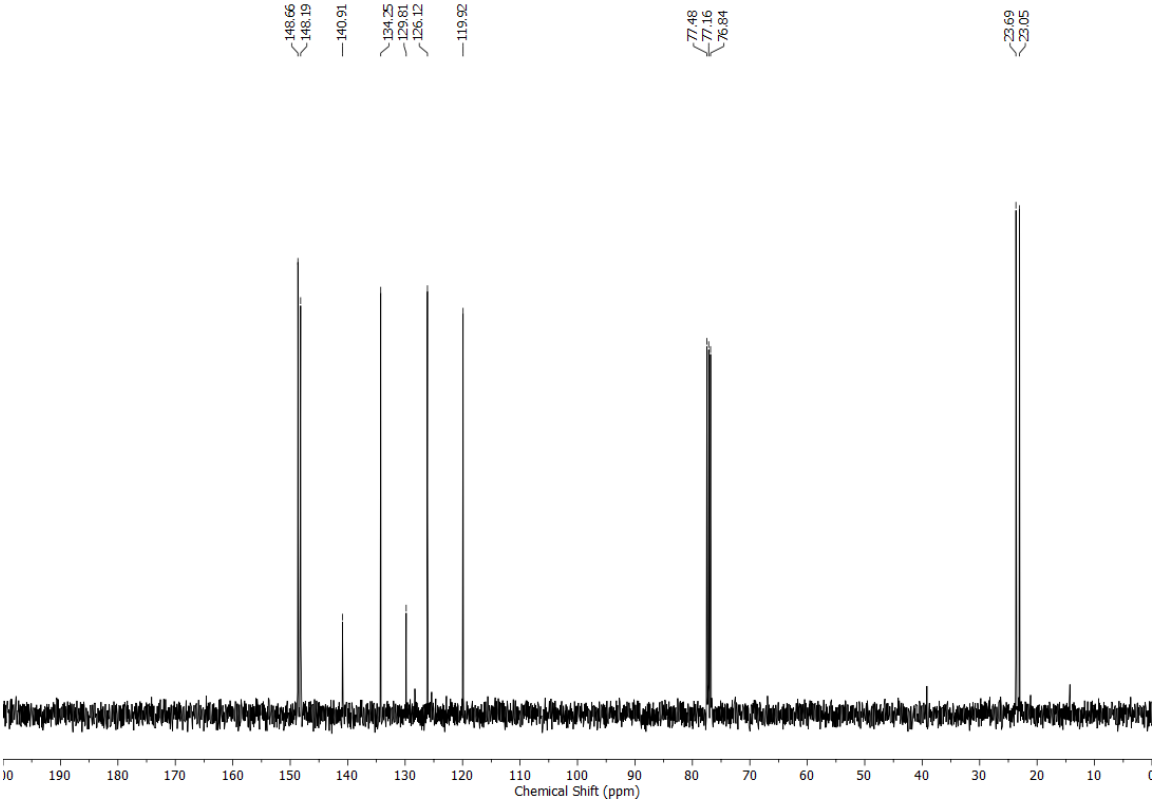

^{1}H (400 MHz, $CDCl_3$) and ^{13}C (101 MHz, $CDCl_3$) – NMR spectra of **15e**

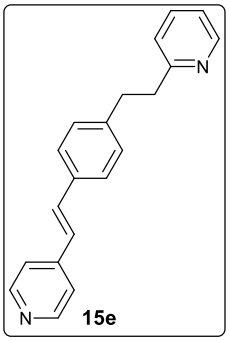

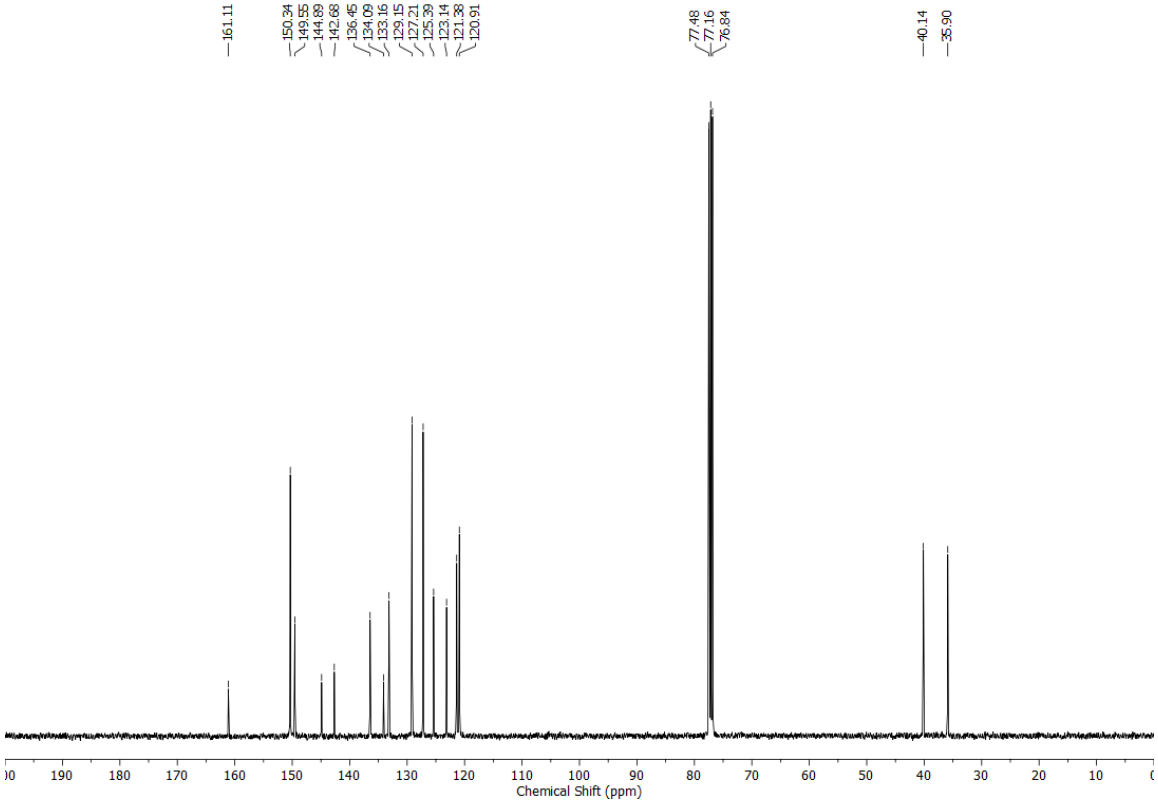

2D-HMBC (400 MHz, $CDCl_3$) – NMR spectra of **15e**

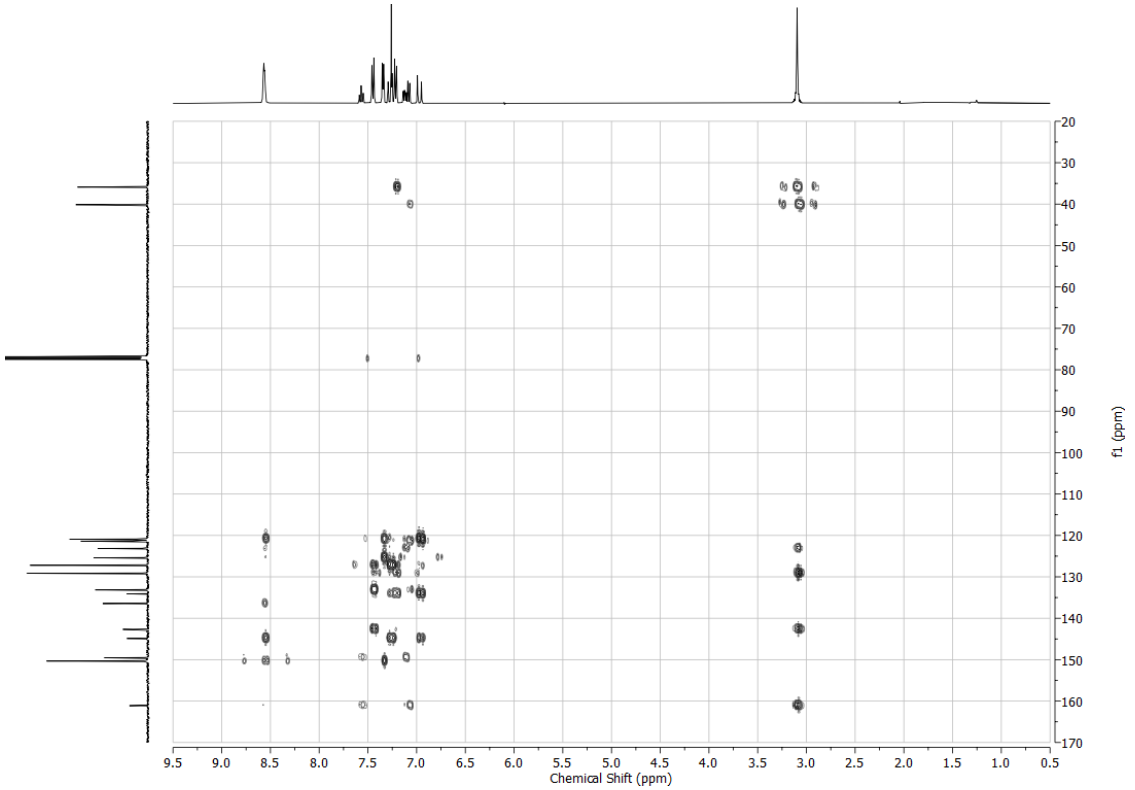

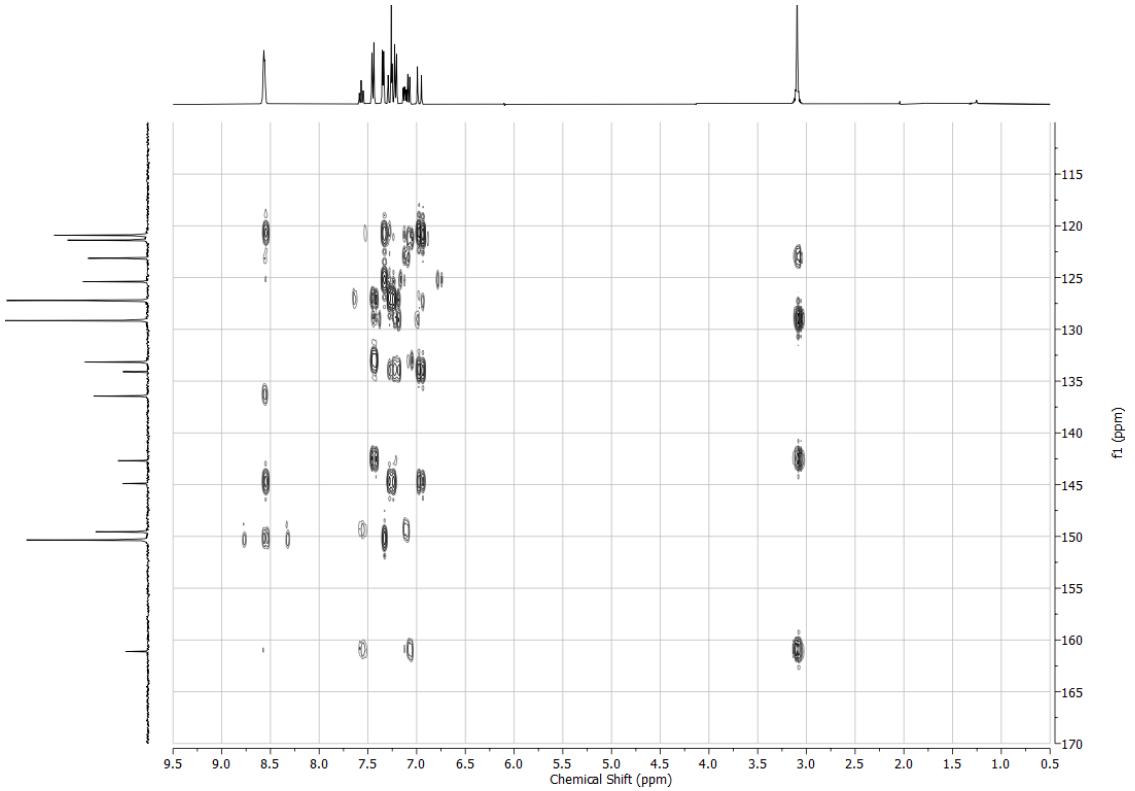

^{1}H (400 MHz, $CDCl_3$) and ^{13}C (101 MHz, $CDCl_3$) – NMR spectra of **16.1**

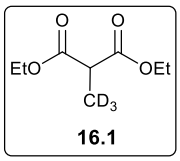

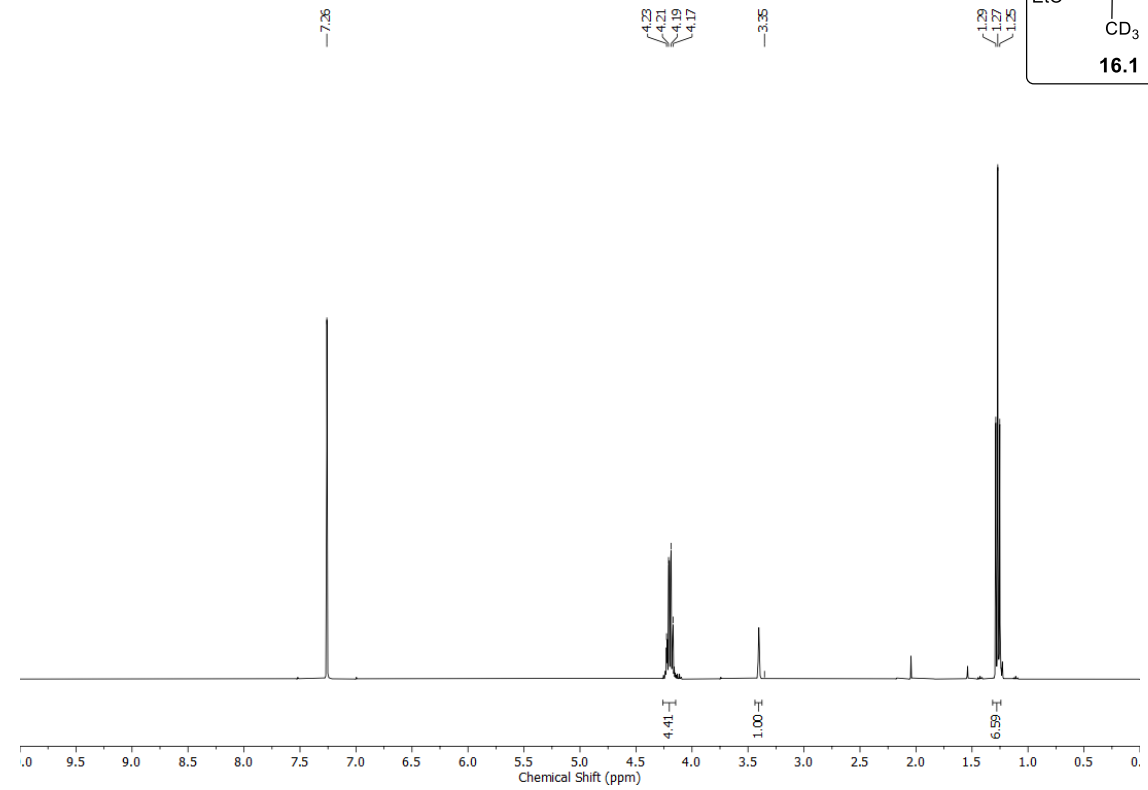

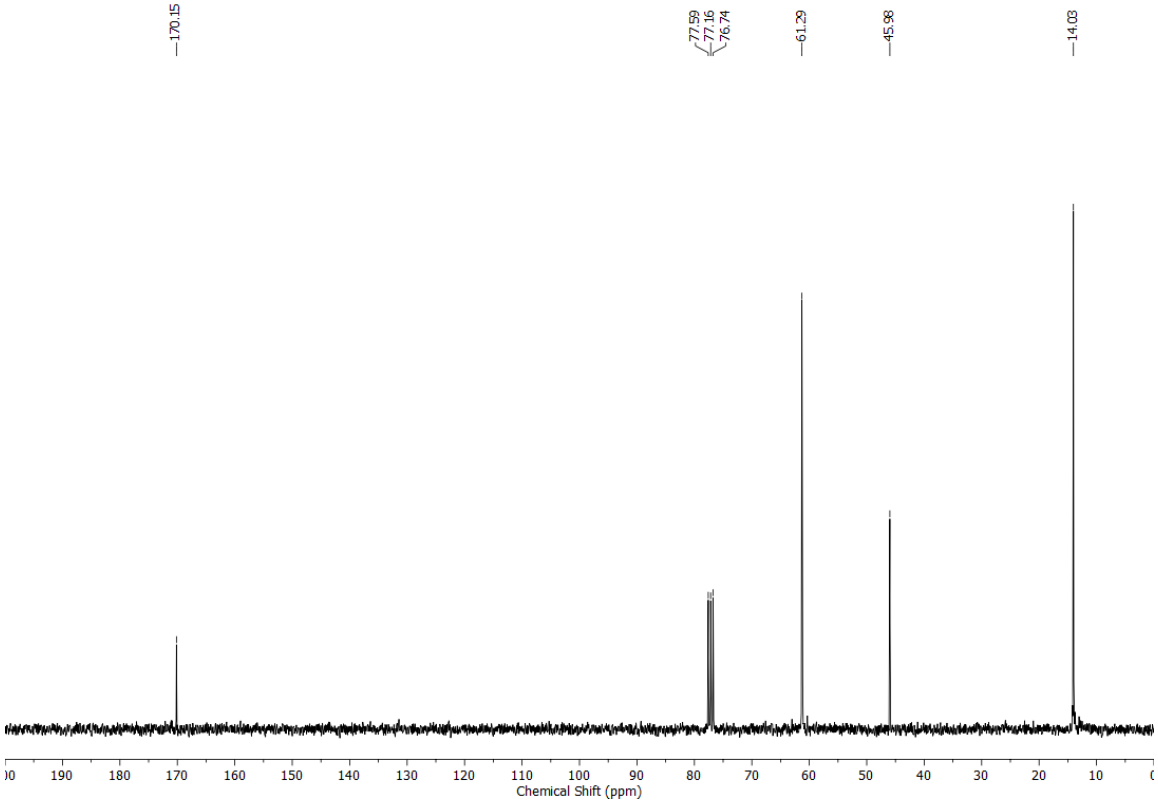

^{1}H (400 MHz, $CDCl_3$) and ^{13}C (101 MHz, $CDCl_3$) – NMR spectra of **16**

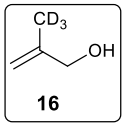

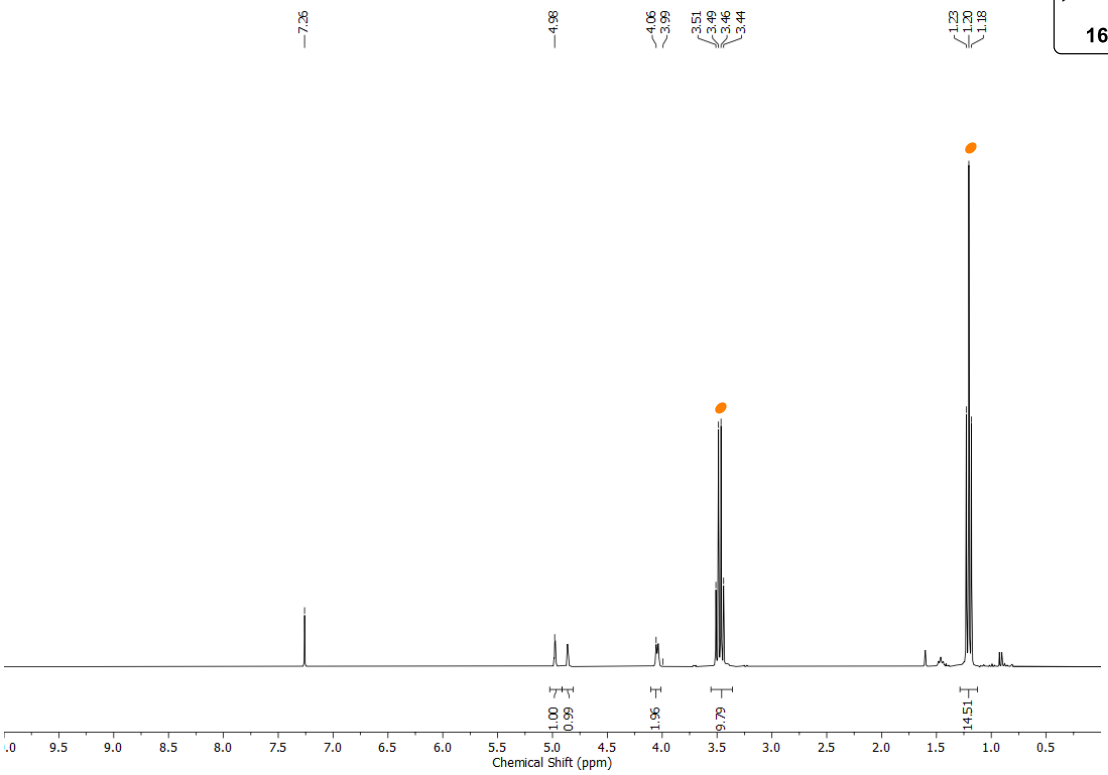

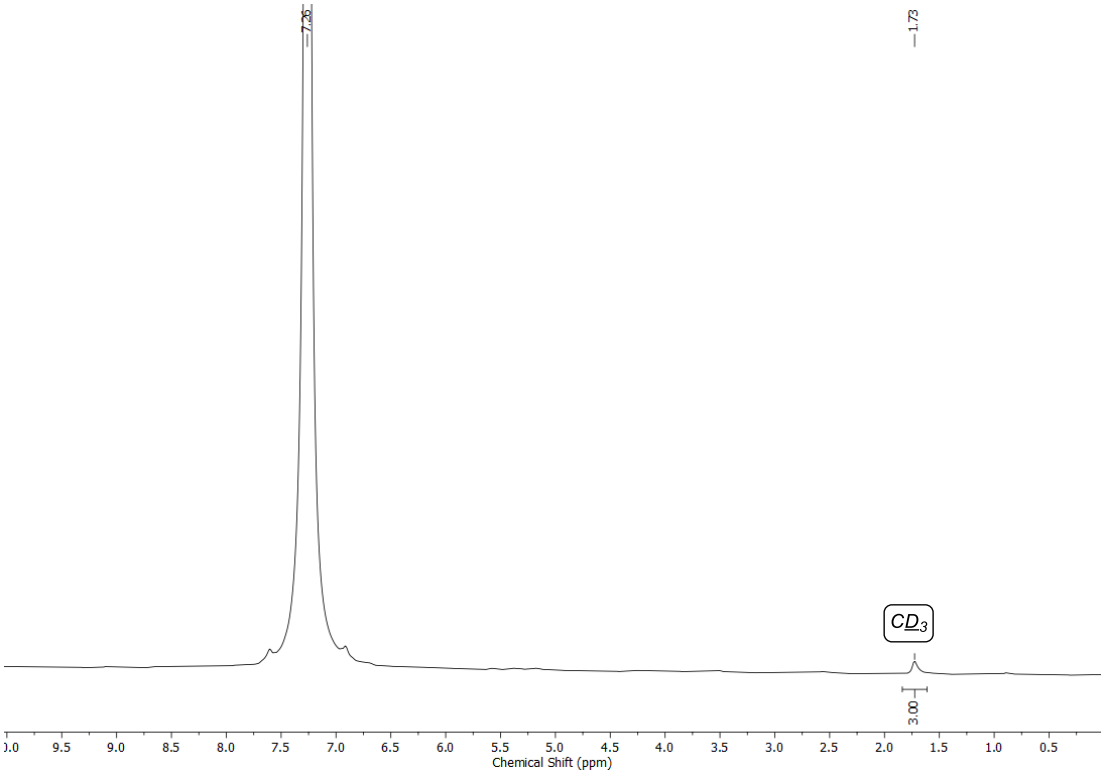

- Diethyl ether peaks

^{13}C (101 MHz, $CDCl_3$) – NMR spectra of **16**

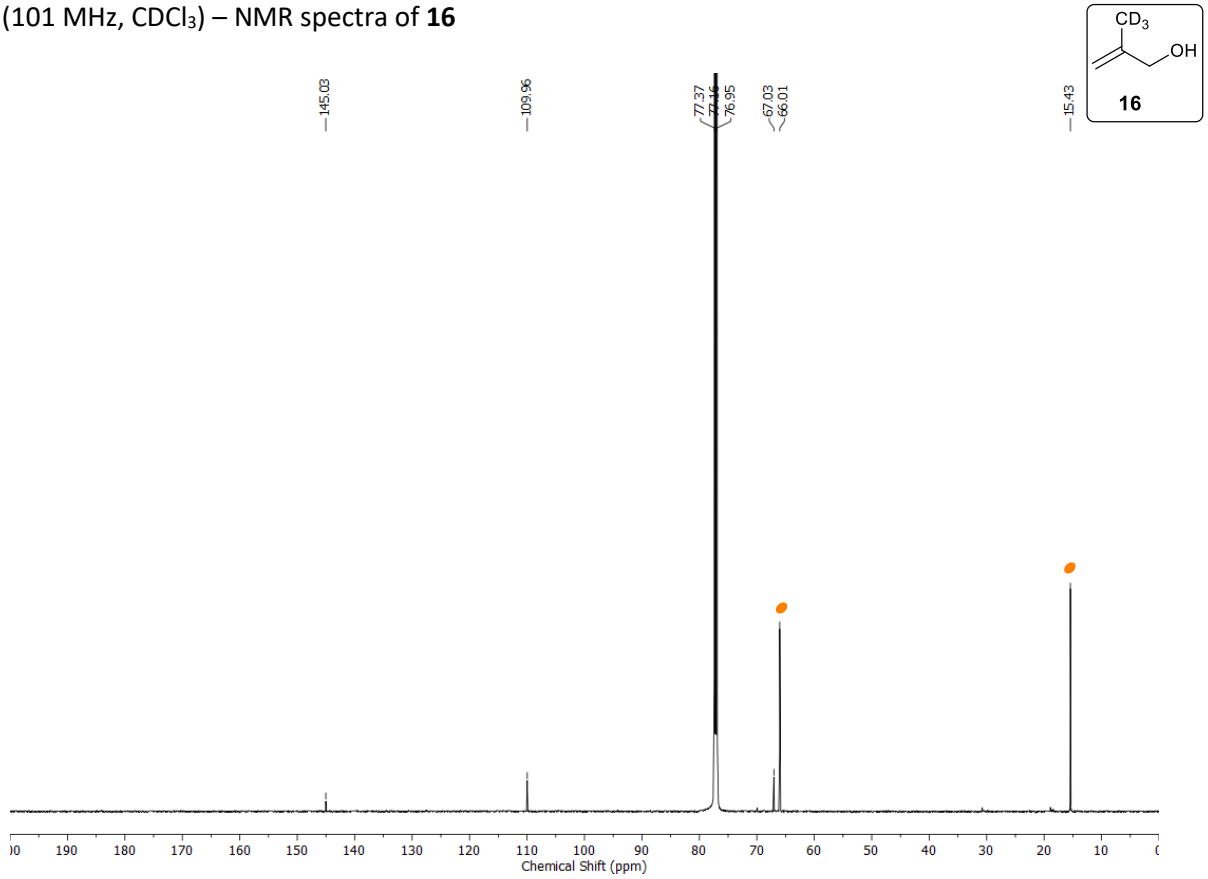

- Diethyl ether peaks

2D-HMBC (600 MHz, $CDCl_3$) – NMR spectra of **16** as a solution in Et_2O

The <u>C</u>D₃ signal at 18.3 ppm correlated with the allyl & vinyl protons as shown by HMBC.

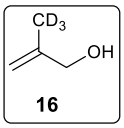

16

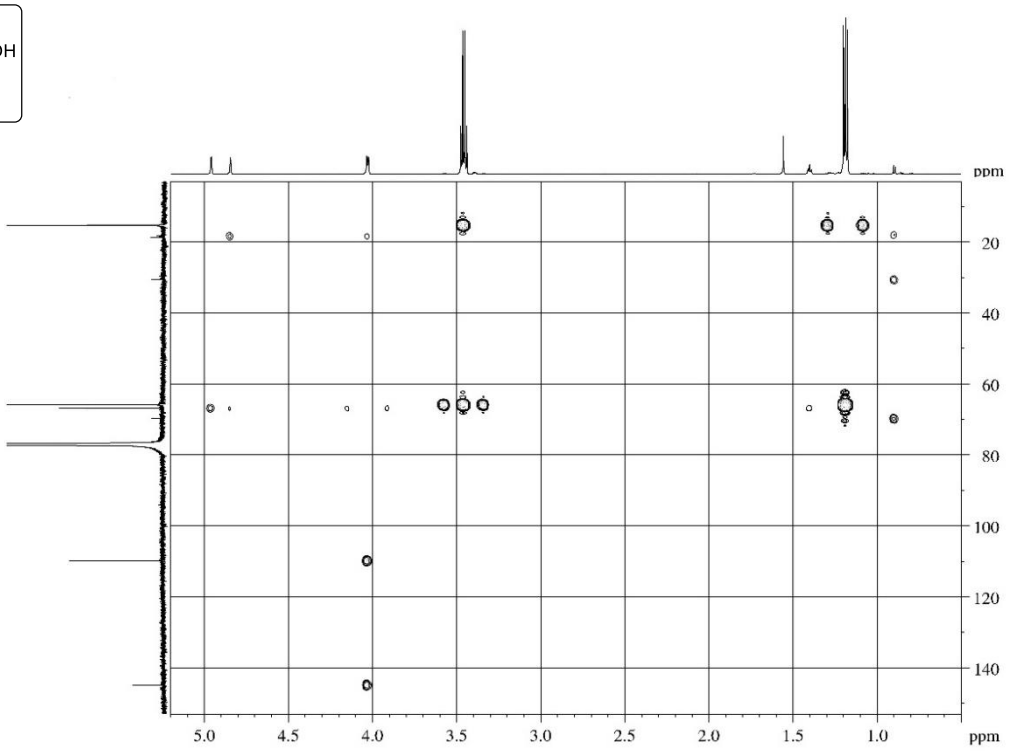

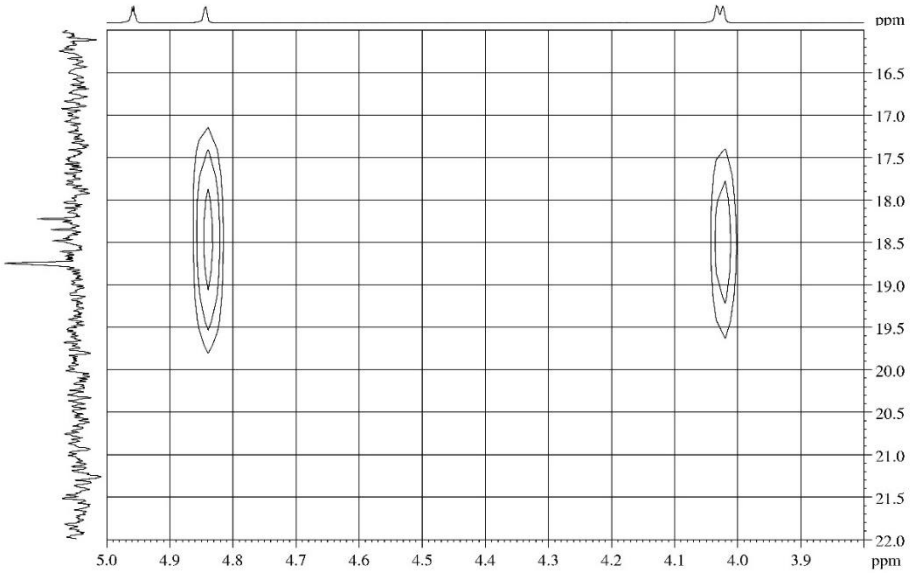

^{1}H (400 MHz, $CDCl_3$) and ^{13}C (101 MHz, $CDCl_3$) – NMR spectra of **1a(CH_3)**

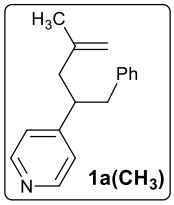

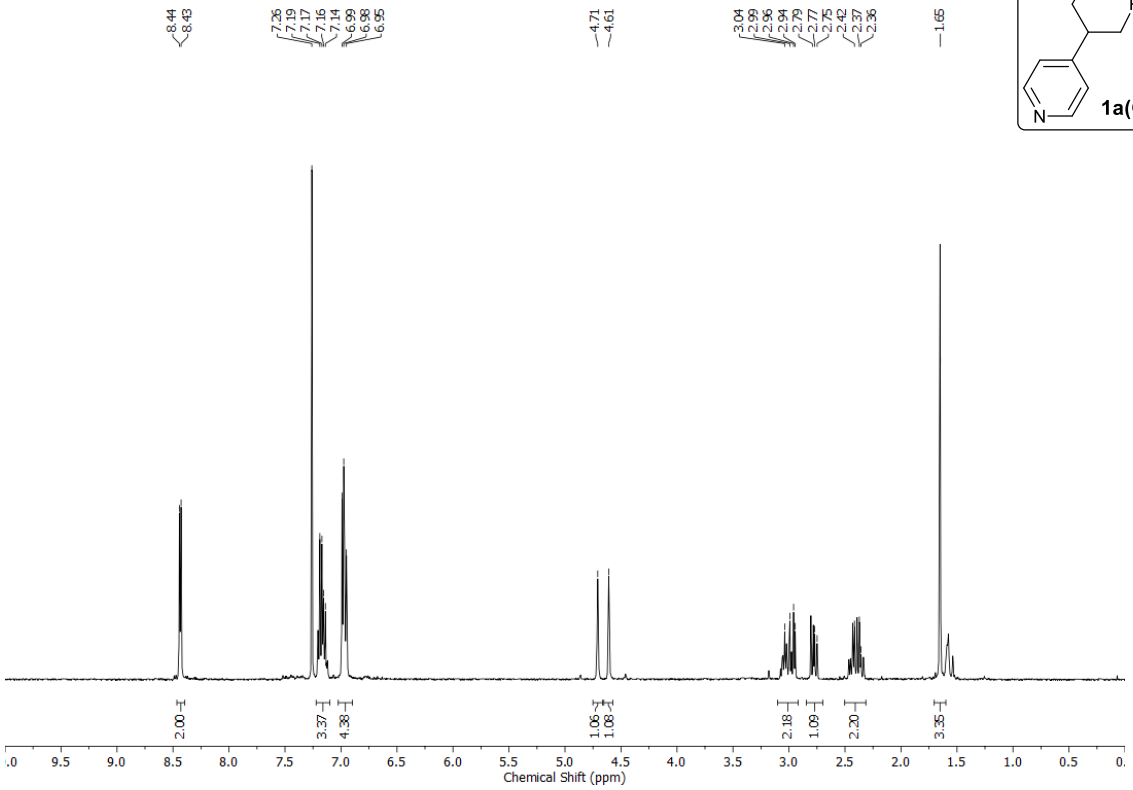

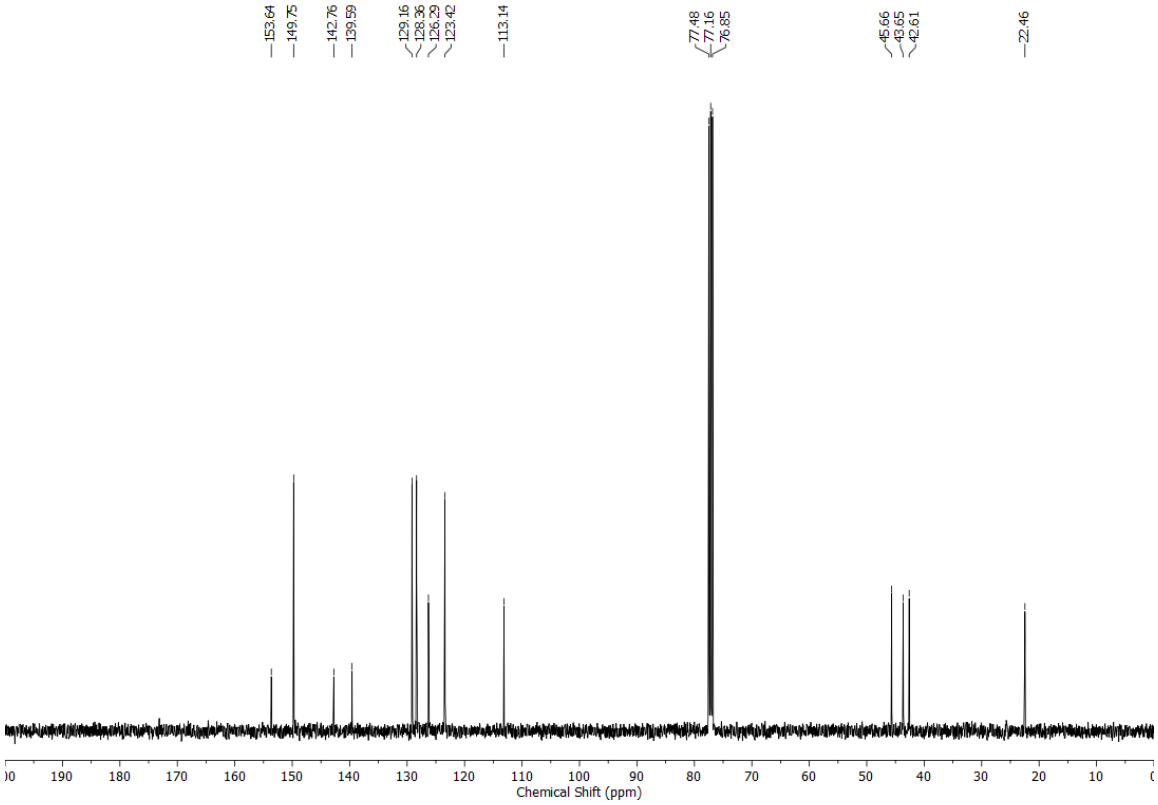

^{1}H (400 MHz, $CDCl_3$) and ^{13}C (101 MHz, $CDCl_3$) – NMR spectra of **1a(CD_3)**

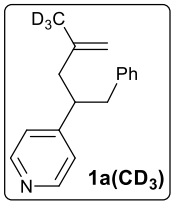

$\underline{CD}_3$ observed as a singlet in ^{2}H NMR at 1.63 ppm.

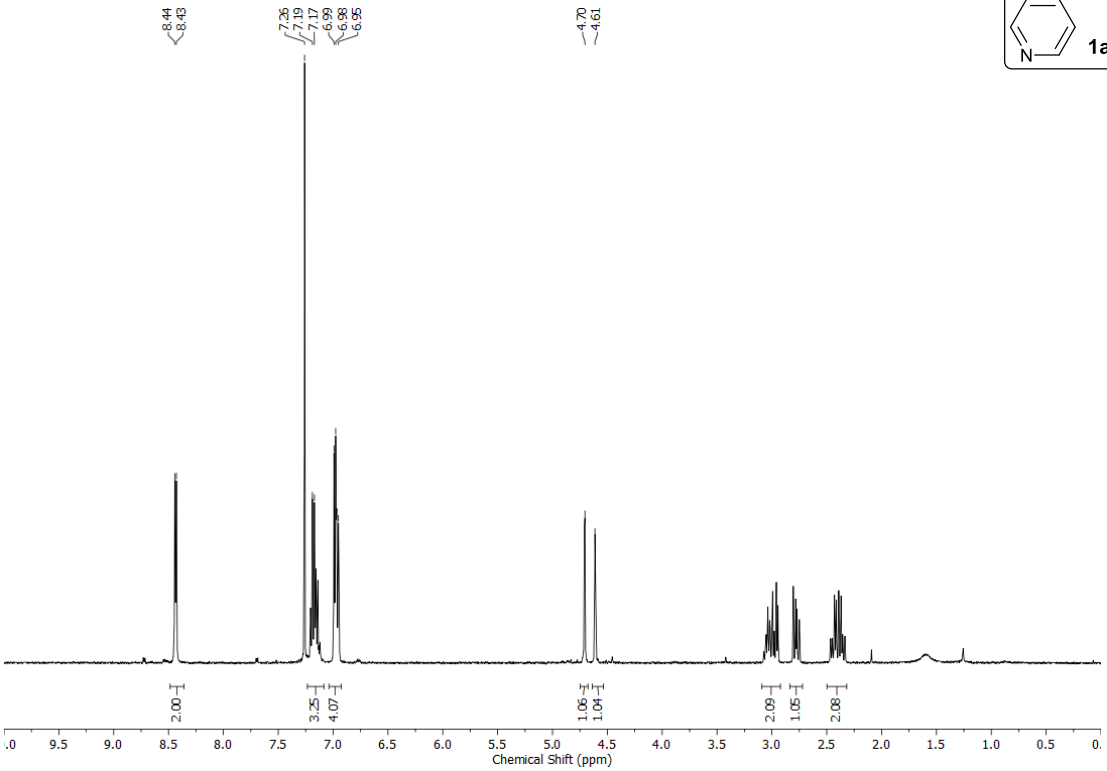

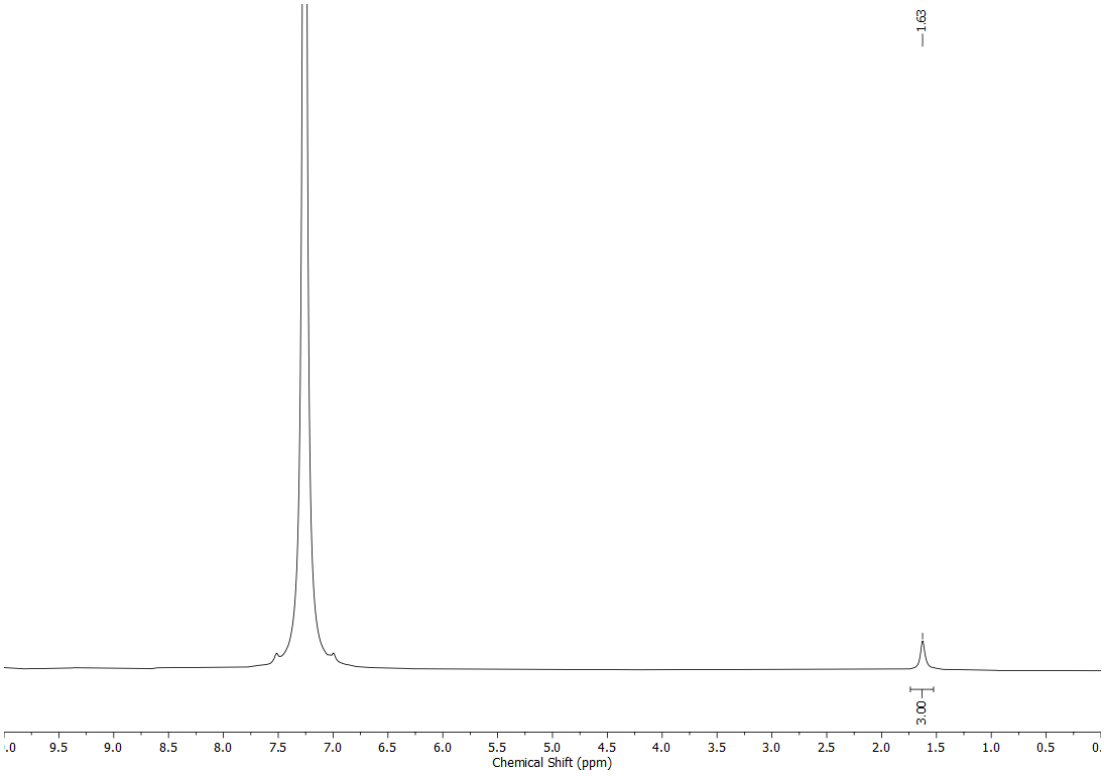

^{13}C (101 MHz, $CDCl_3$) – NMR spectra of **1a(CD_3)**

<u>C</u>D₃ observed as a septet at 21.6 ppm with a coupling constant *J* = 18.1 Hz.

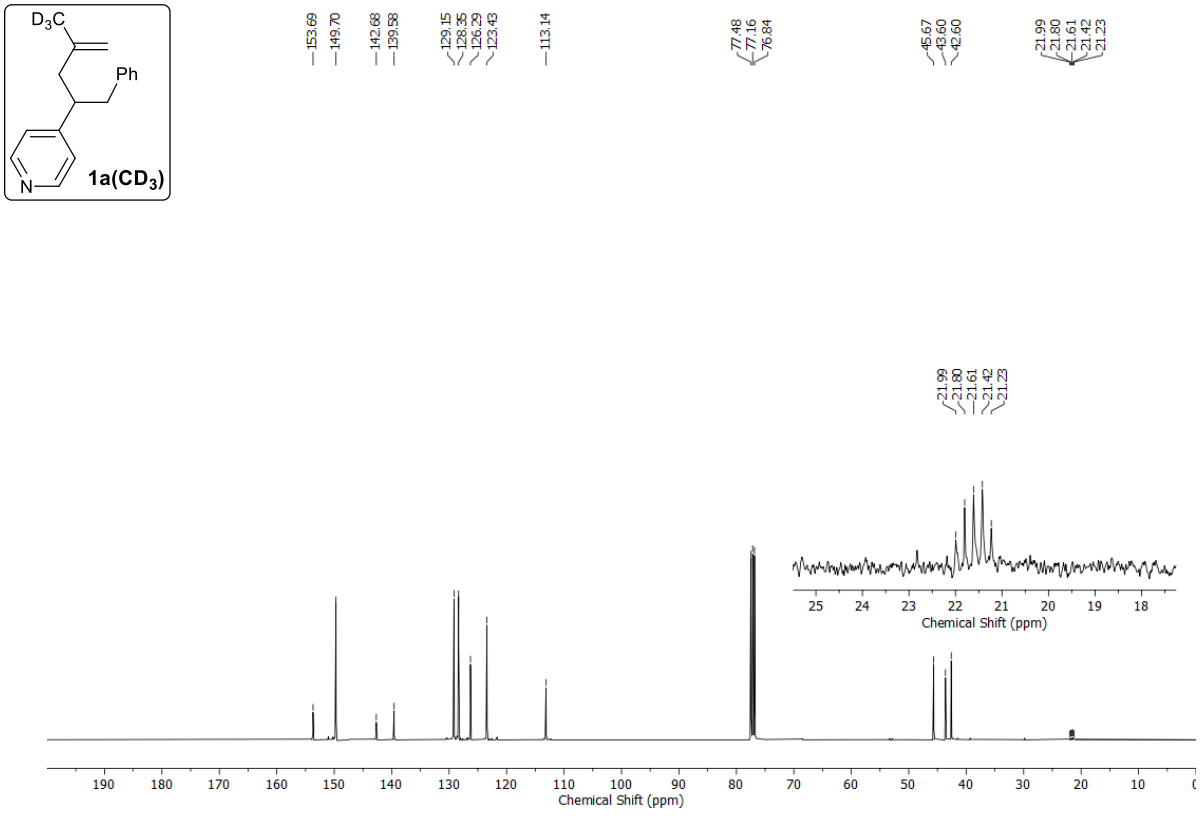

2D HMBC (600 MHz, $CDCl_3$) – NMR spectra of **1a(CD_3)**

The *CD_3* peak at 21.6 ppm correlated to the allylic & vinylic protons as shown by HMBC.

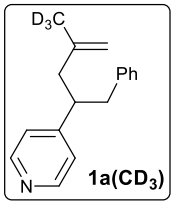

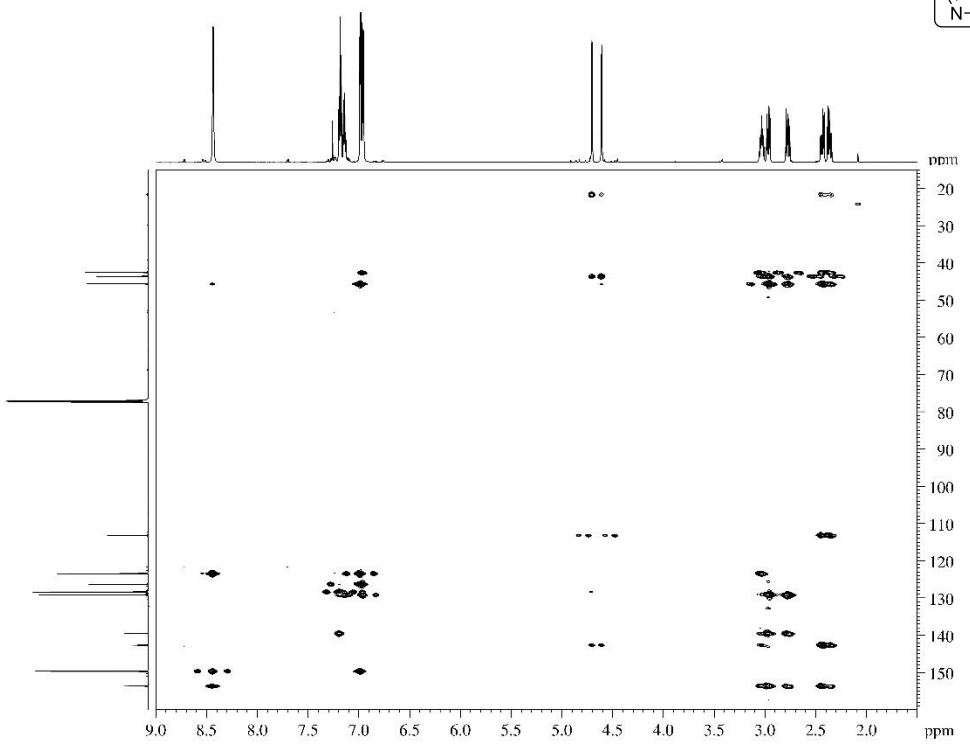

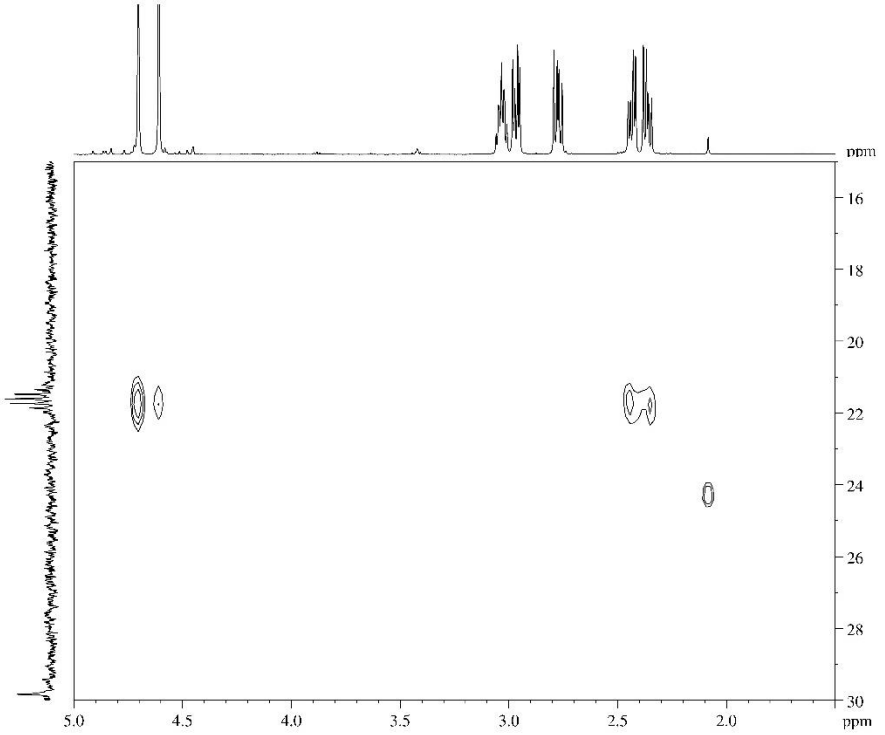

^{1}H (400 MHz, $CDCl_3$) and ^{13}C (101 MHz, $CDCl_3$) – NMR spectra of **17a(CH_3)**

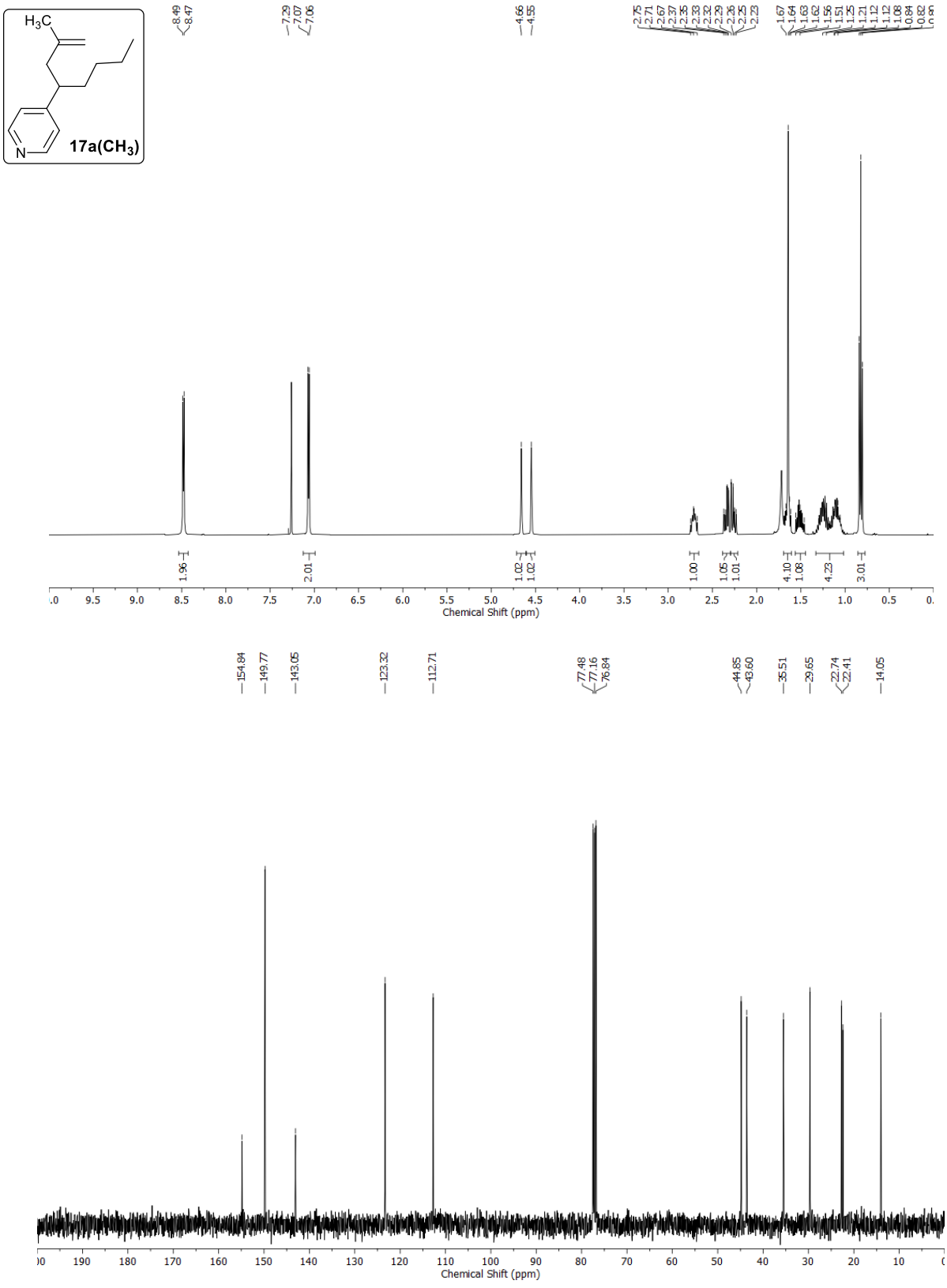

^{1}H (400 MHz, $CDCl_3$) and ^{13}C (101 MHz, $CDCl_3$) – NMR spectra of **17a(CD3)**

$\underline{CD}_3$ observed as a singlet in ^{2}H NMR at 1.62 ppm.

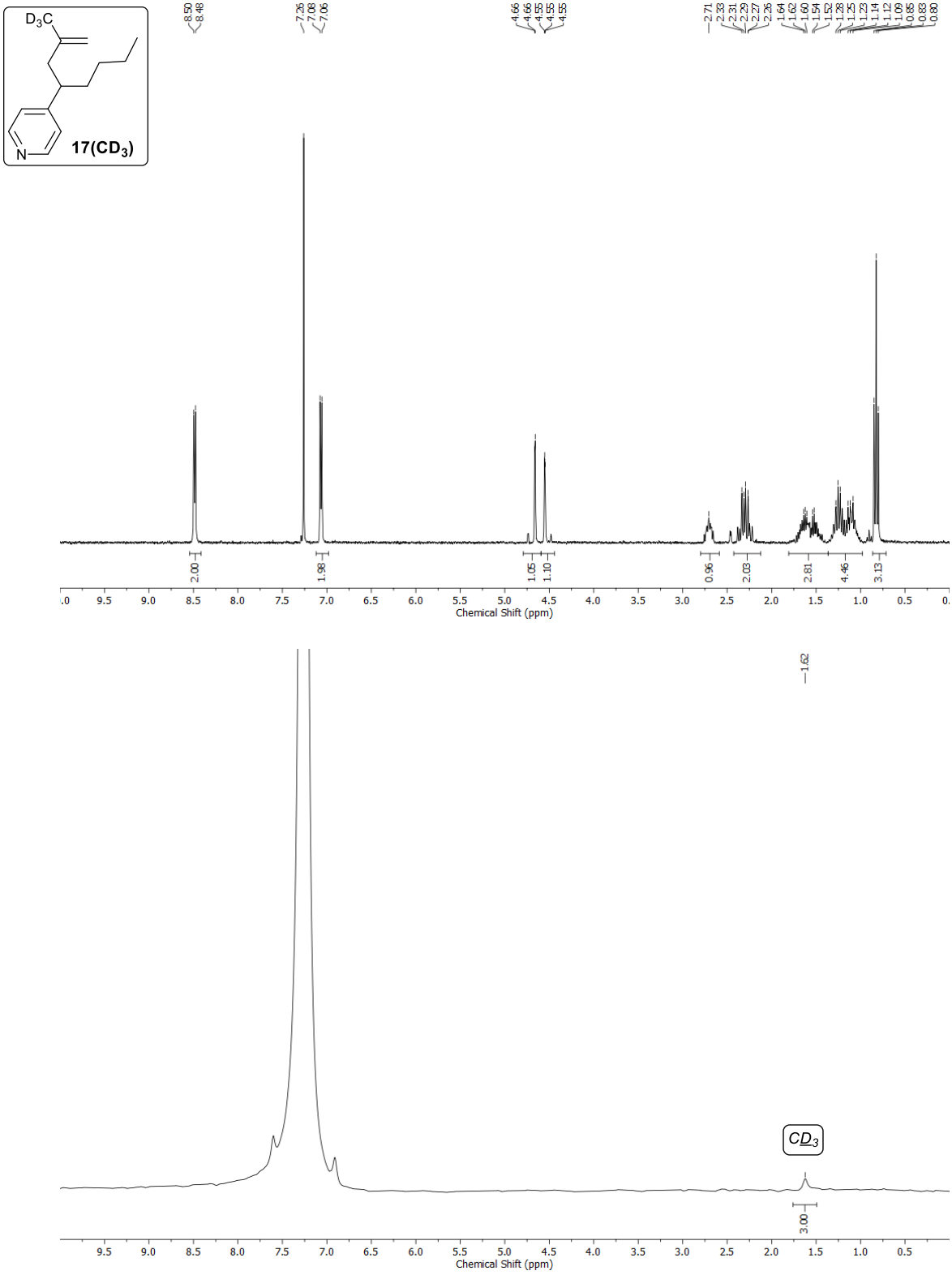

^{13}C (101 MHz, $CDCl_3$) – NMR spectra of **17a(CD3)**

CD₃ observed as a septet at 21.8 ppm with a coupling constant *J* = 19.6 Hz.

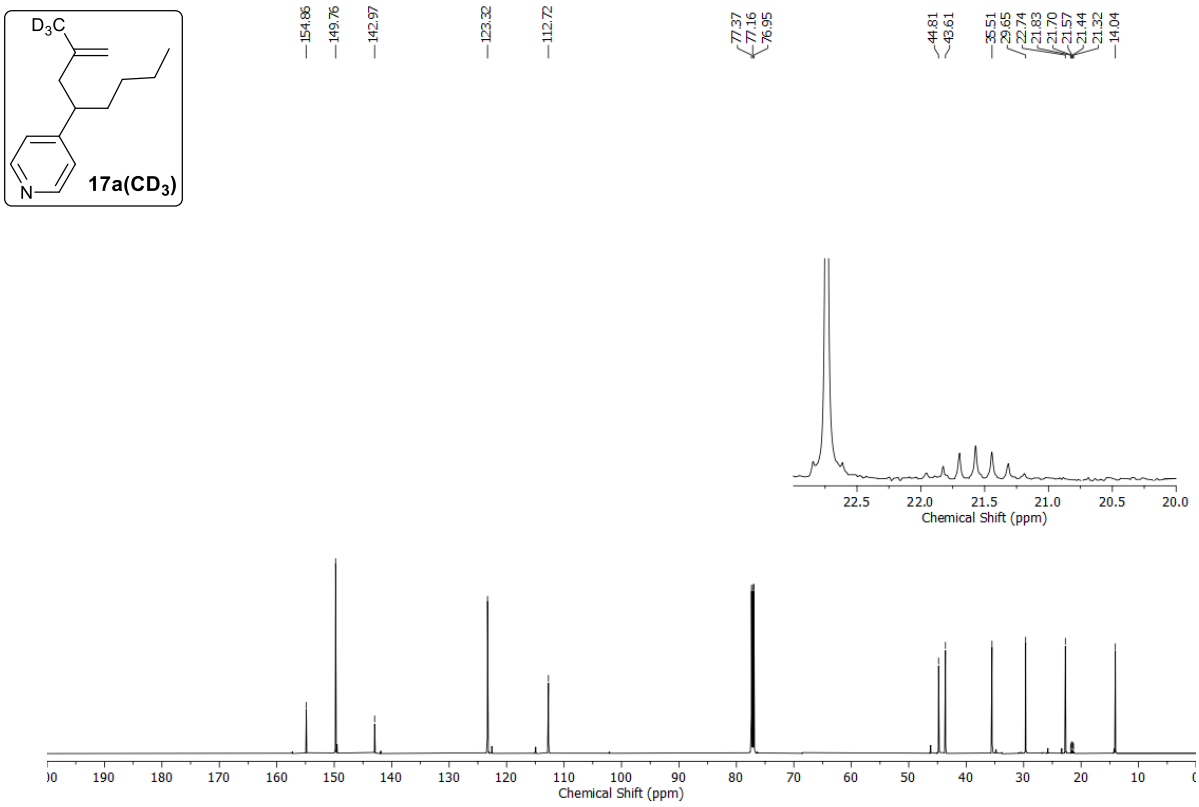

2D HMBC (600 MHz, $CDCl_3$) – NMR spectra of **17a (CD_3)**

The *$\underline{C}D_3$* peak at 21.8 ppm correlated to the allylic & vinylic protons as shown by HMBC.

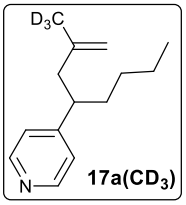

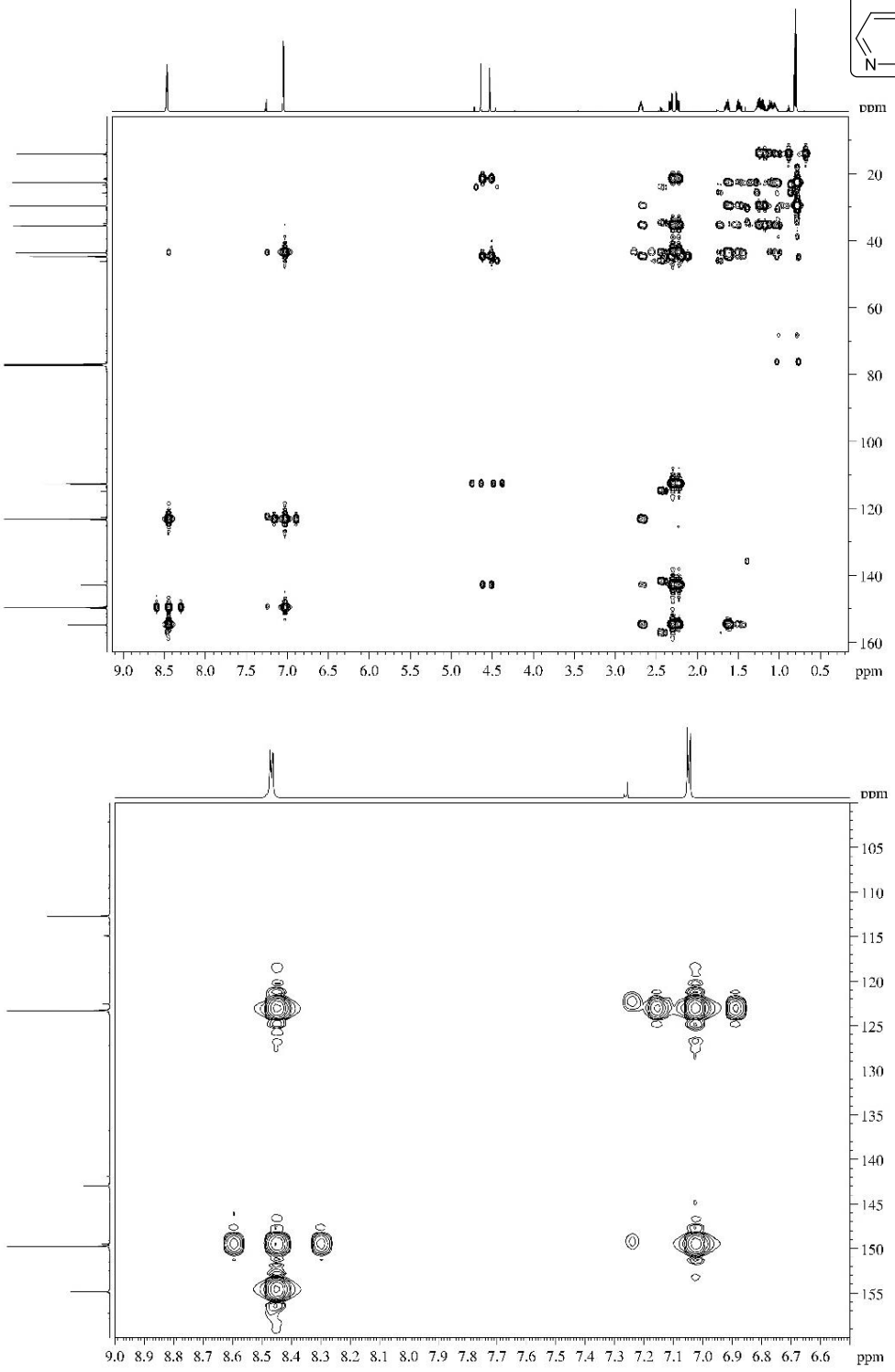

2D HMBC (600 MHz, $CDCl_3$) – NMR spectra of **17a (CD_3)**

The *$\underline{C}D_3$* peak at 21.8 ppm correlated to the allylic & vinylic protons as shown by HMBC.

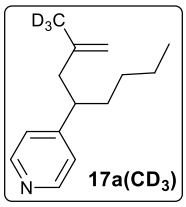

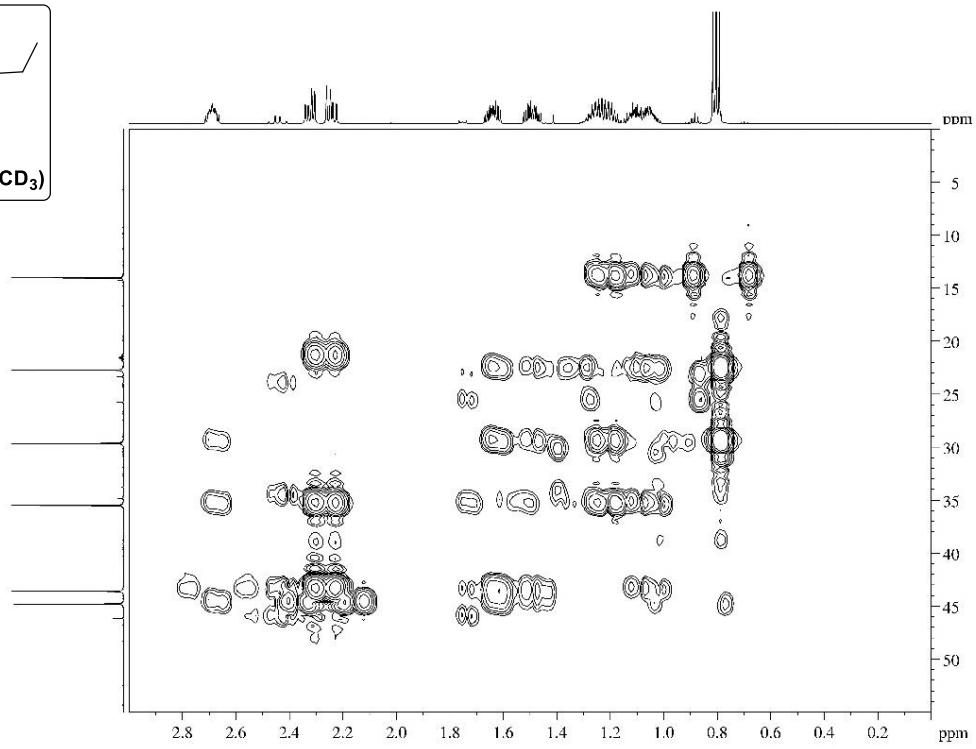

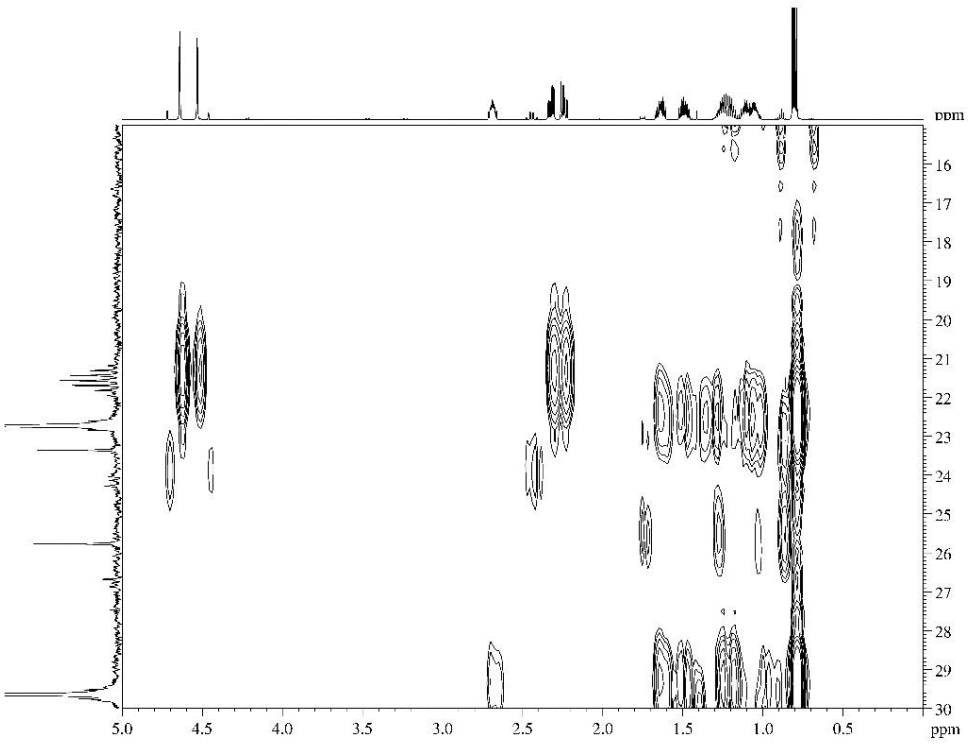

^{1}H (400 MHz, $CDCl_3$) and ^{2}H (61 MHz, $CDCl_3$) – NMR spectra of the cross-over products **1a(CH_3)+1a(CD_3)**

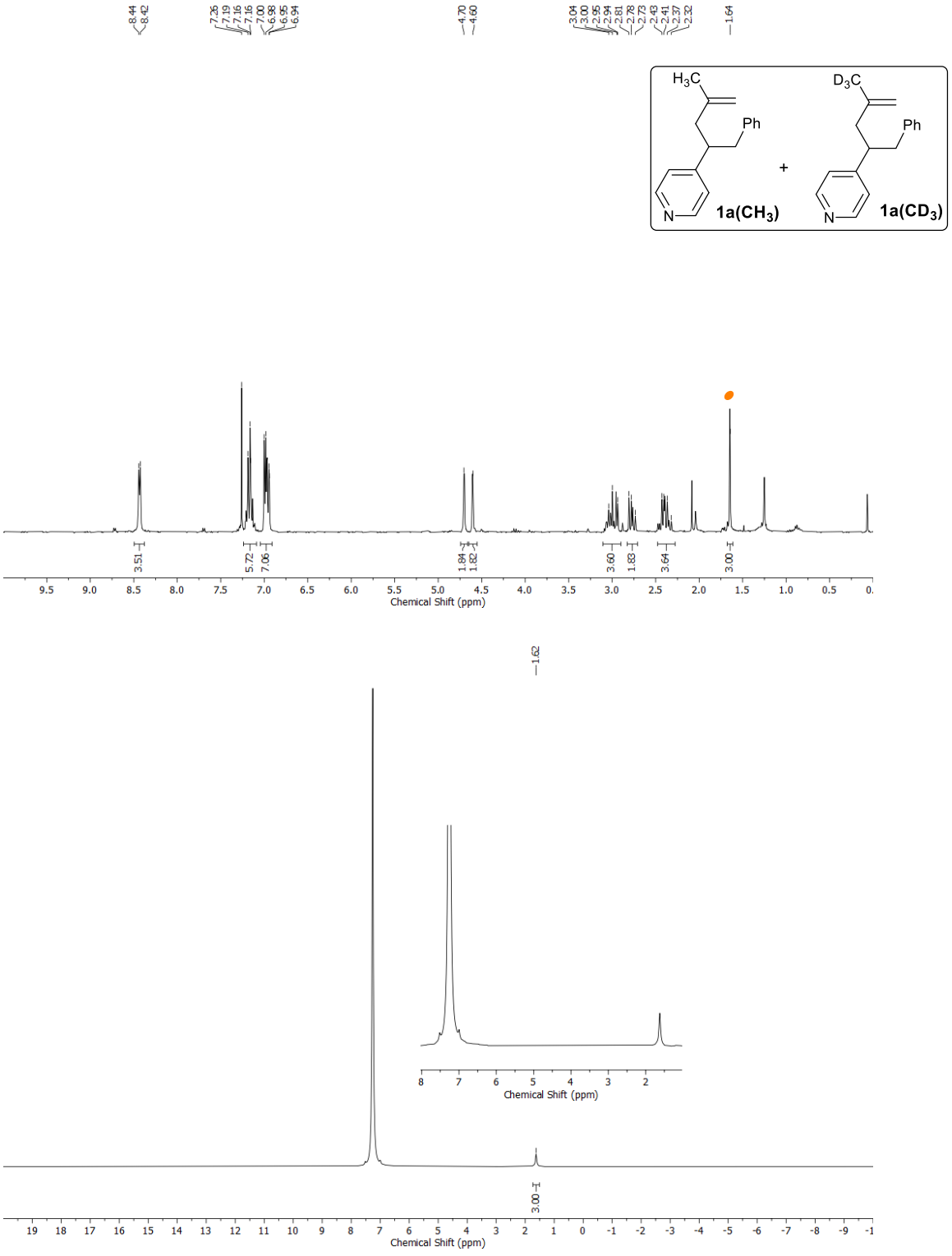

- CH_3 peak integration used to determine product ratio.

^{1}H (400 MHz, $CDCl_3$) and ^{2}H (61 MHz, $CDCl_3$) – NMR spectra of the cross-over products **17a (CH_3)** + **17a (CD_3)**. By integrating the *$\underline{CD}_3$* peak at 1.62 ppm in ^{2}H NMR relative to a known amount of $C\underline{D}_3CN$, the relative amounts of **17a (CD_3)** was established.

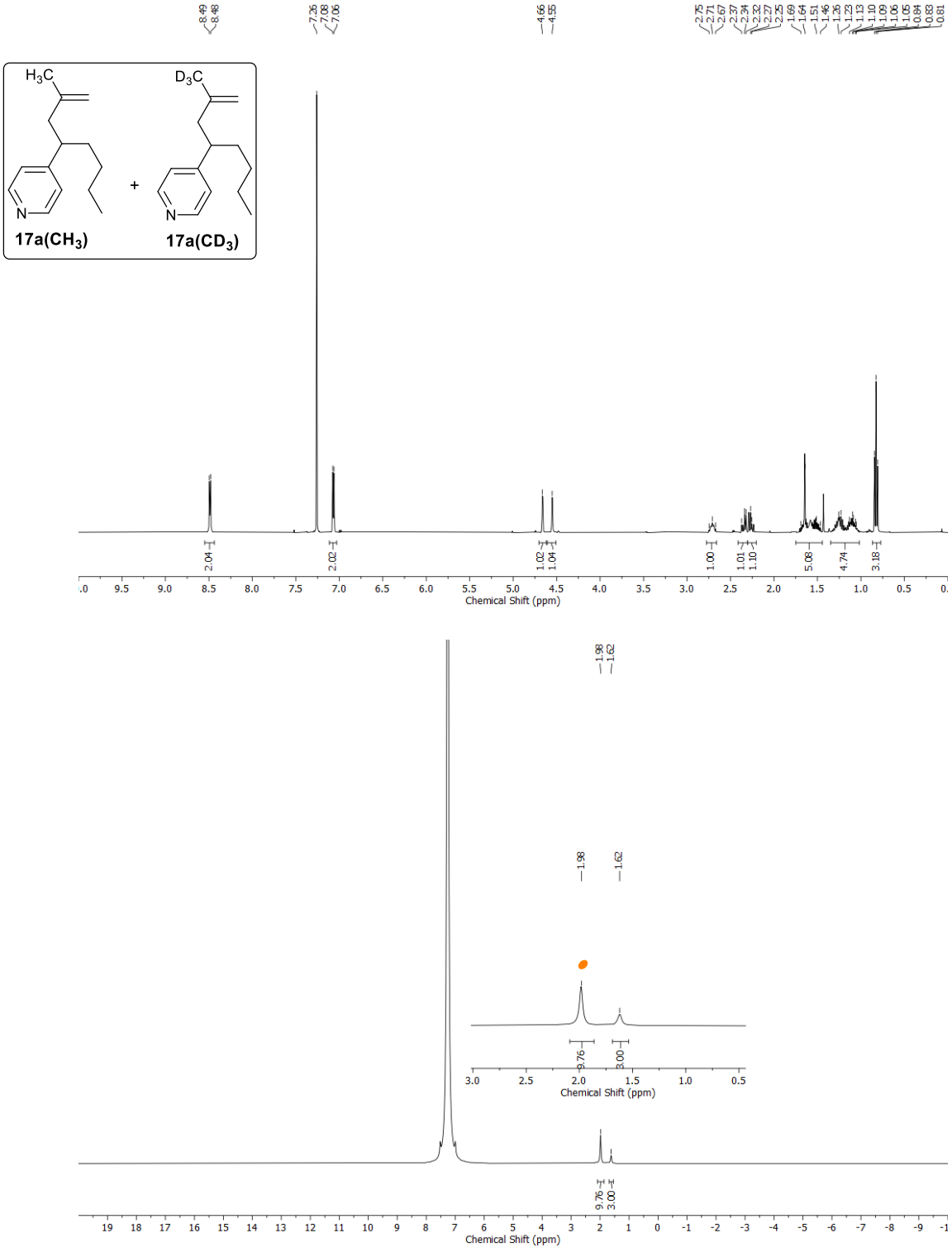

- CD_3CN used as internal standard.

^{1}H (400 MHz, $CDCl_3$) and ^{13}C (101 MHz, $CDCl_3$) – NMR spectra of **18**

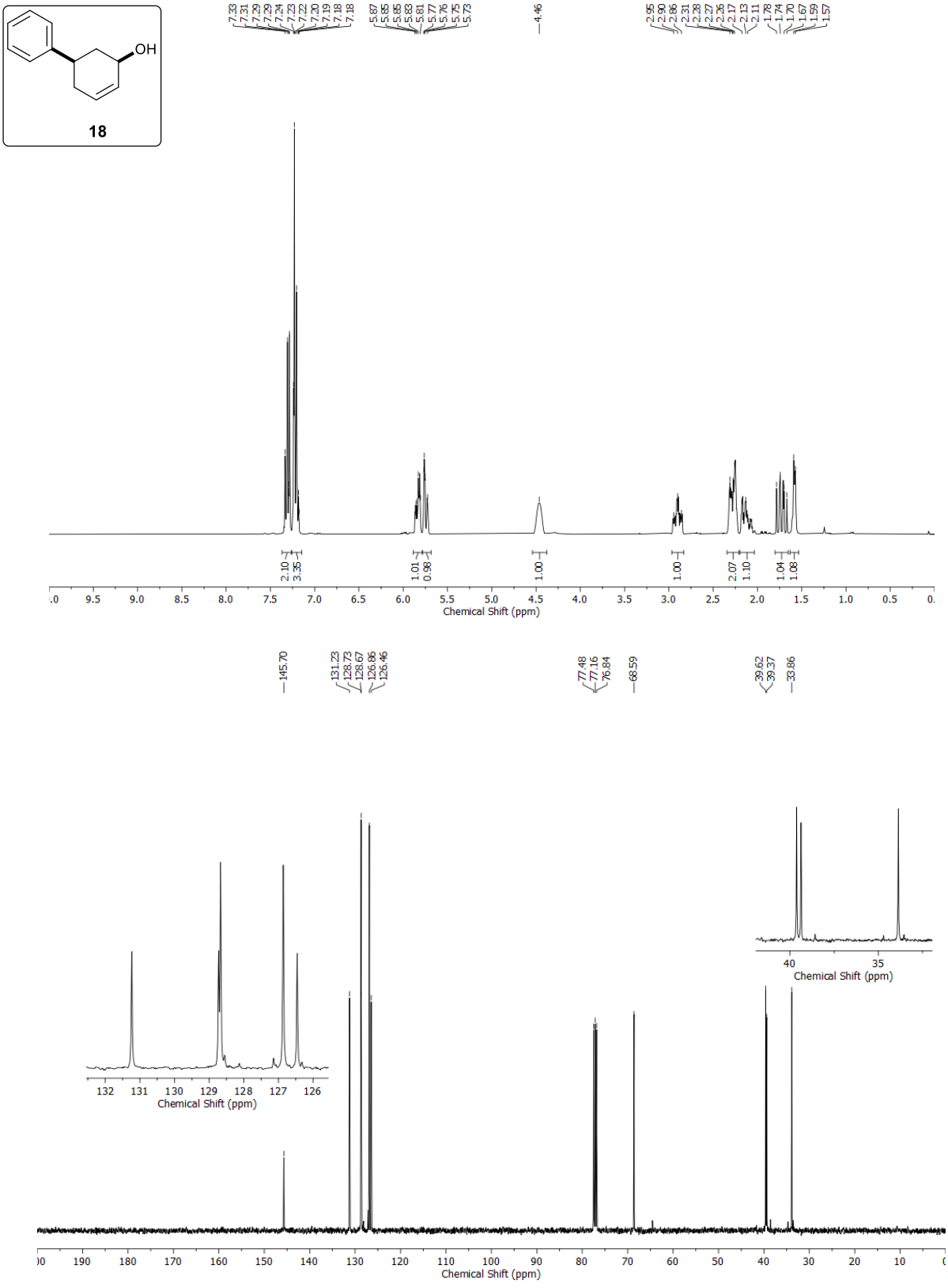

2D COSY (600 MHz, $CDCl_3$) – NMR spectra of **18**

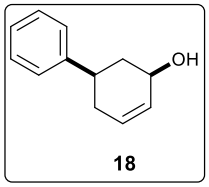

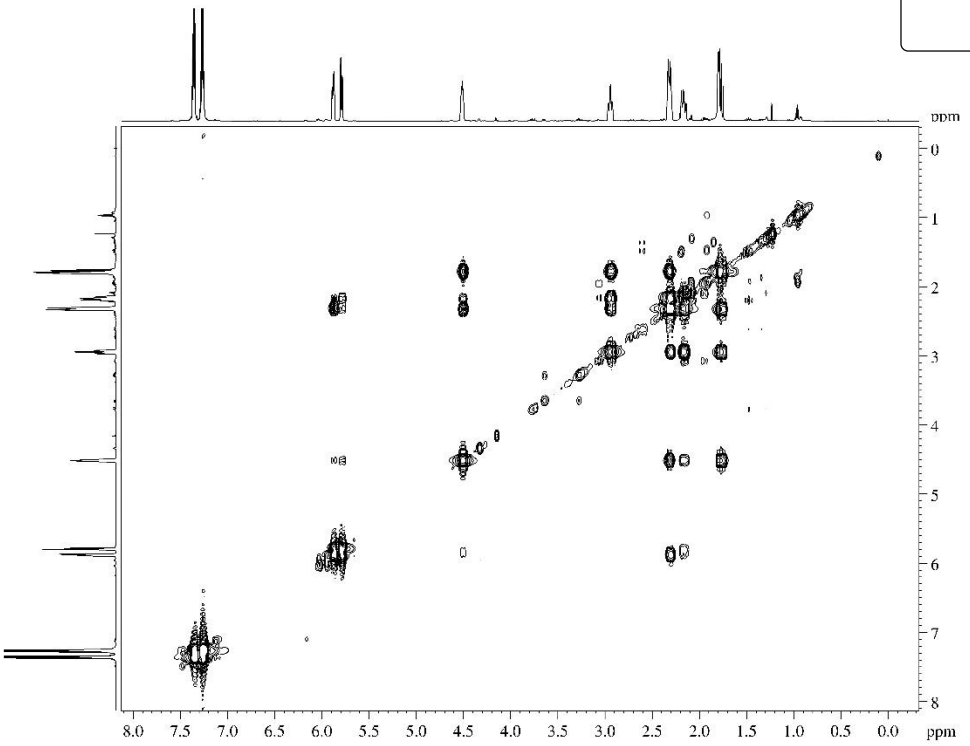

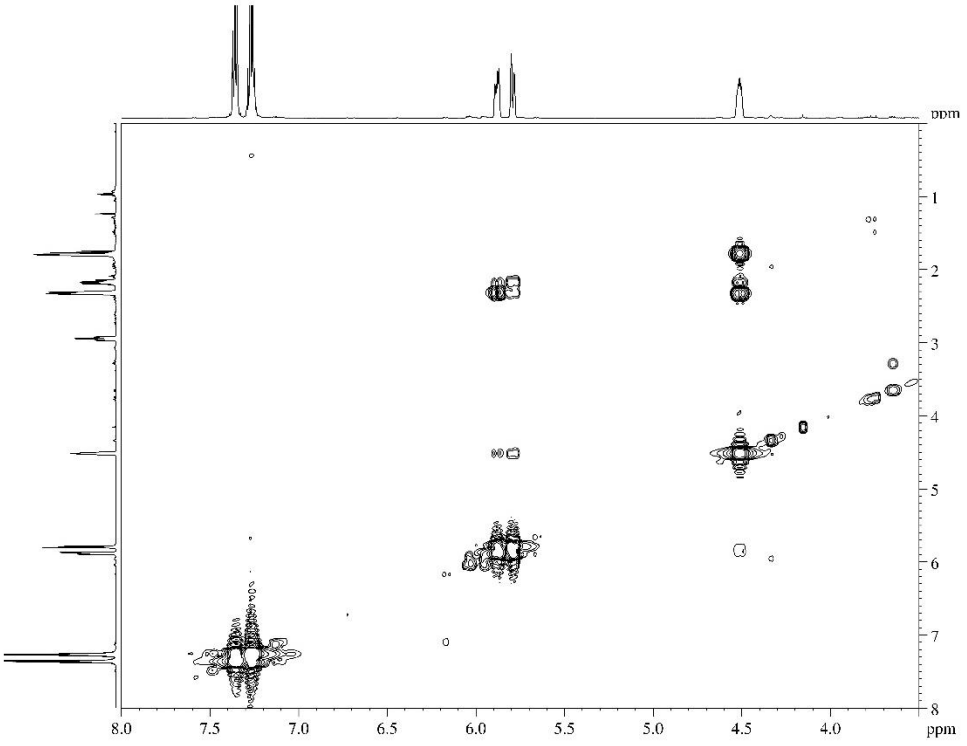

2D NOESY (600 MHz, $CDCl_3$) – NMR spectra of **18**

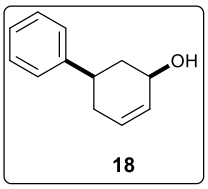

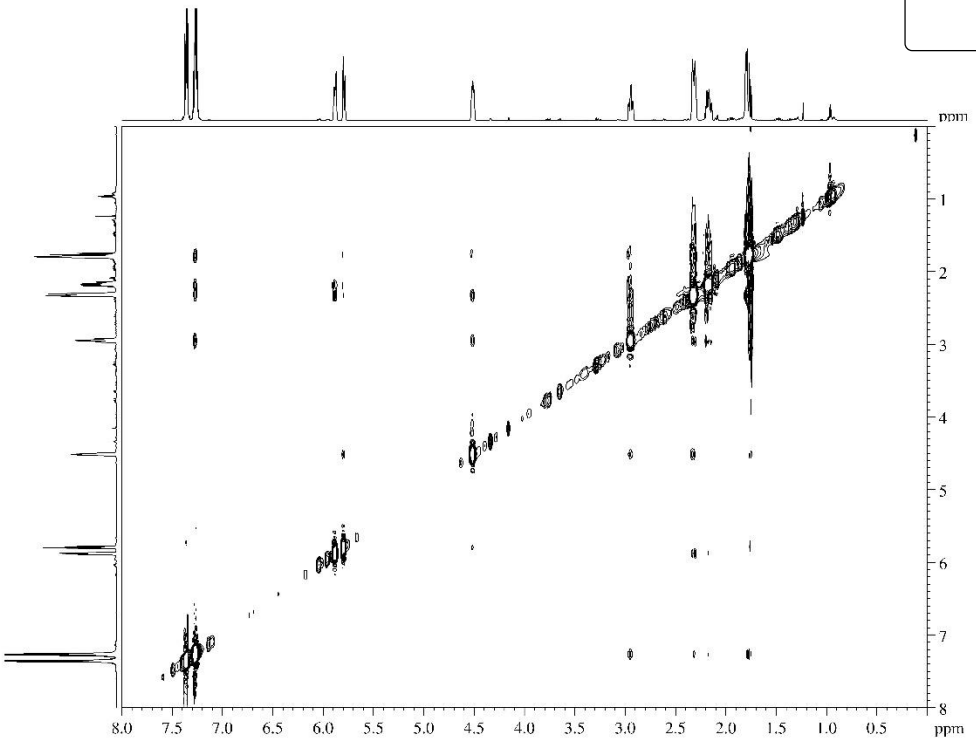

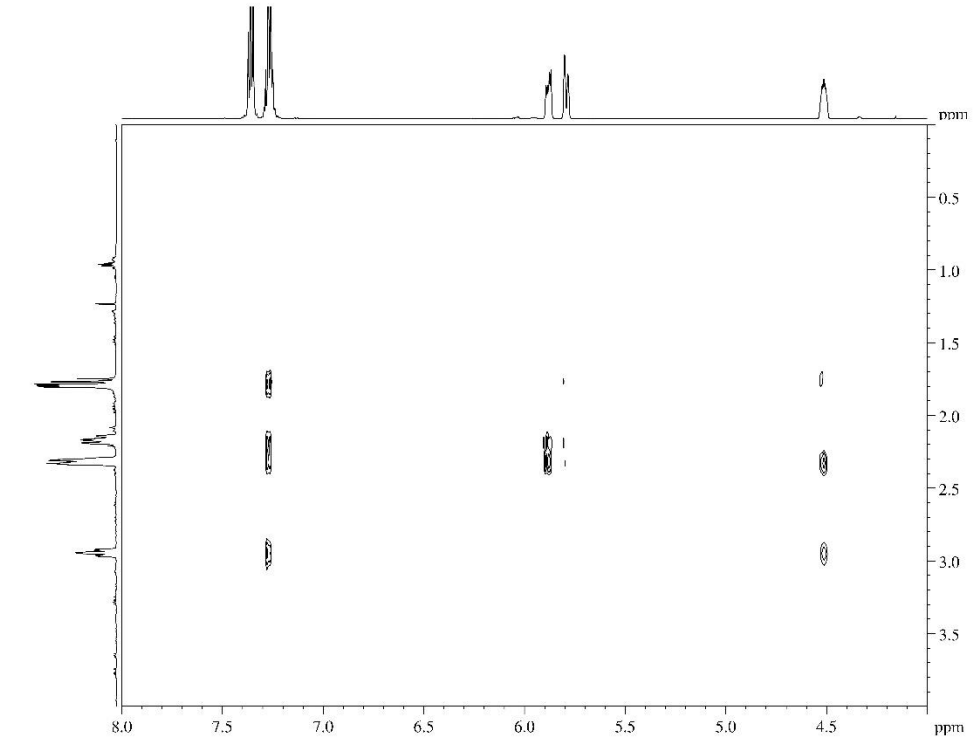

^{1}H (400 MHz, $CDCl_3$) and ^{13}C (101 MHz, $CDCl_3$) – NMR spectra of **19a**

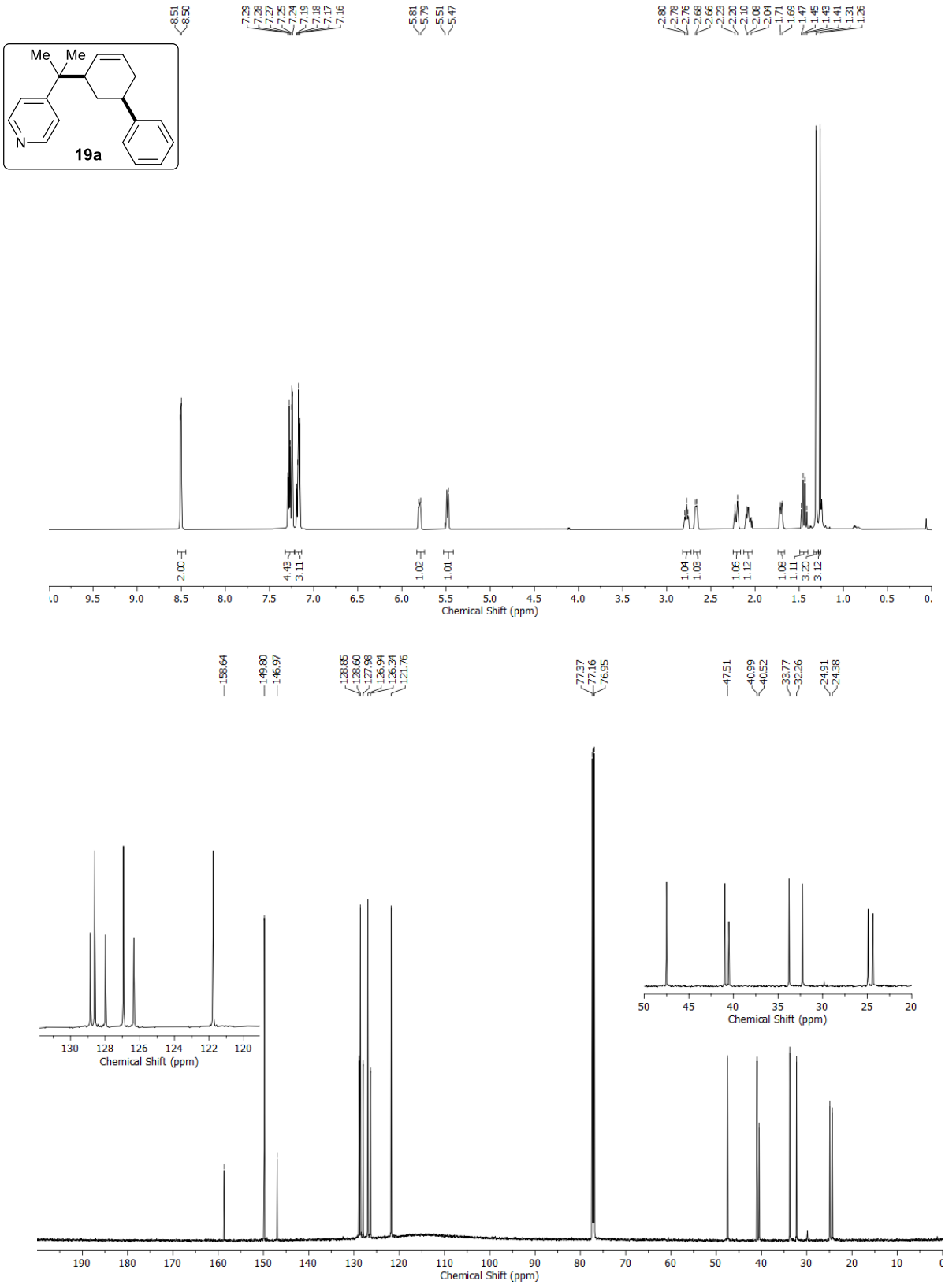

2D-COSY (600 MHz, $CDCl_3$) – NMR spectra of **19a**

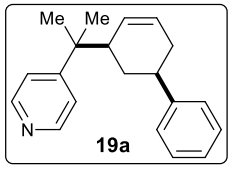

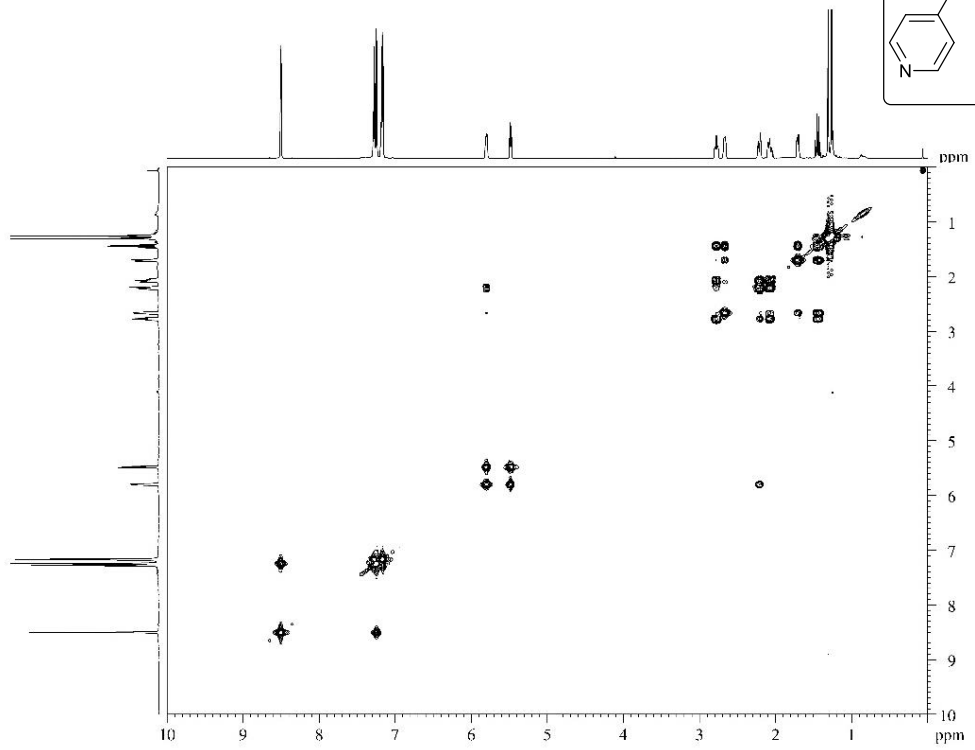

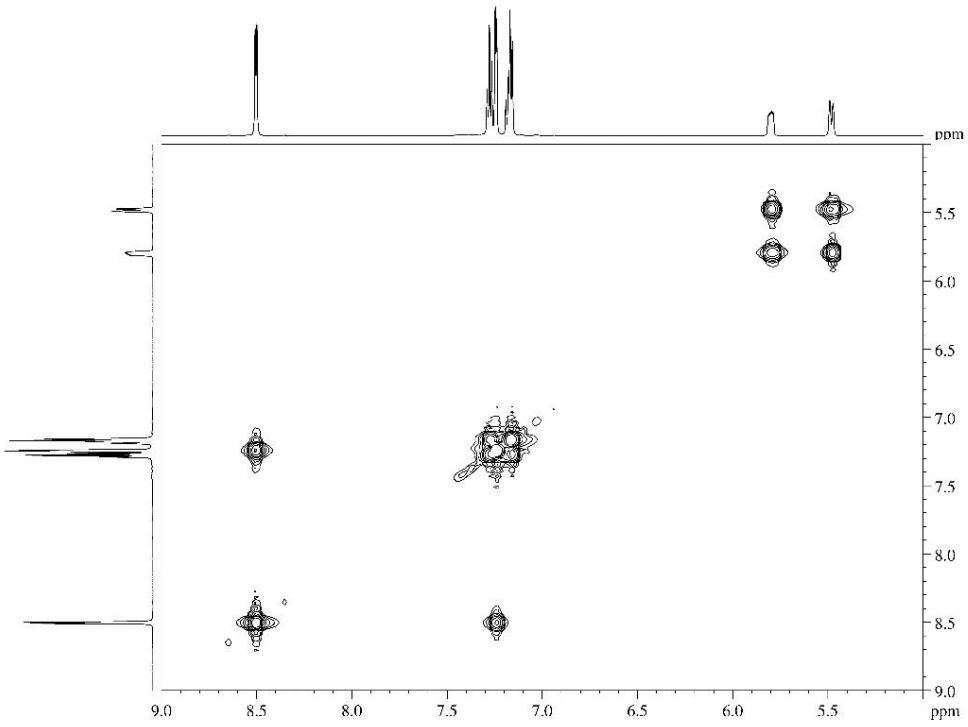

2D-COSY (600 MHz, $CDCl_3$) – NMR spectra of **19a**

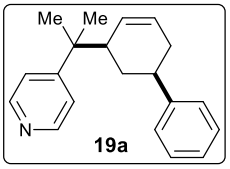

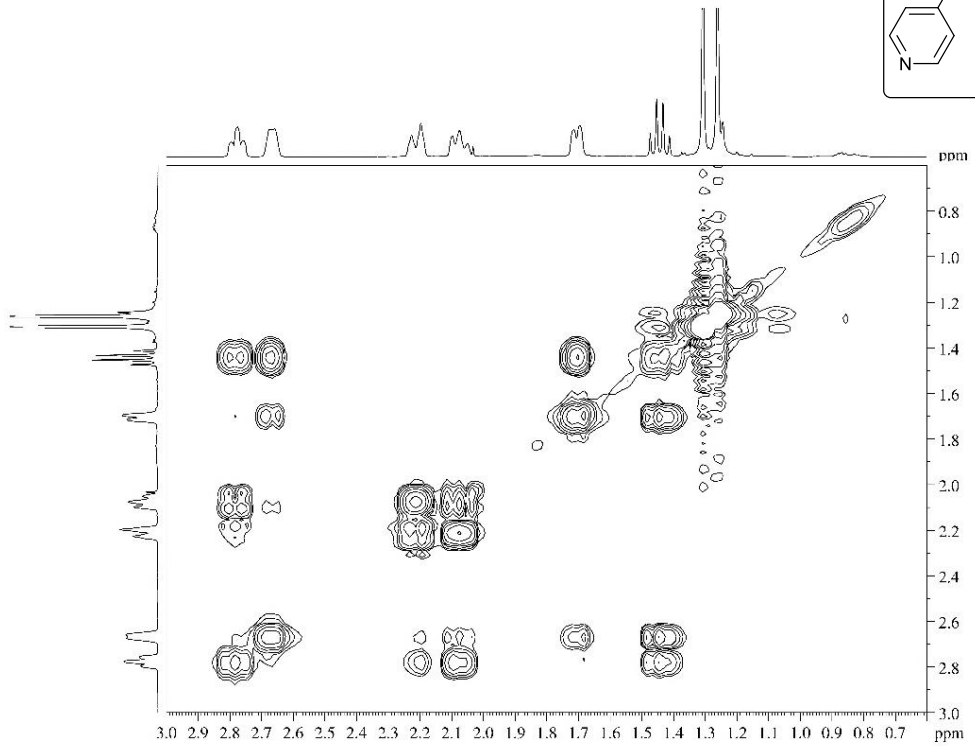

2D-HMBC (600 MHz, $CDCl_3$) – NMR spectra of **19a**

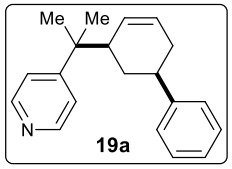

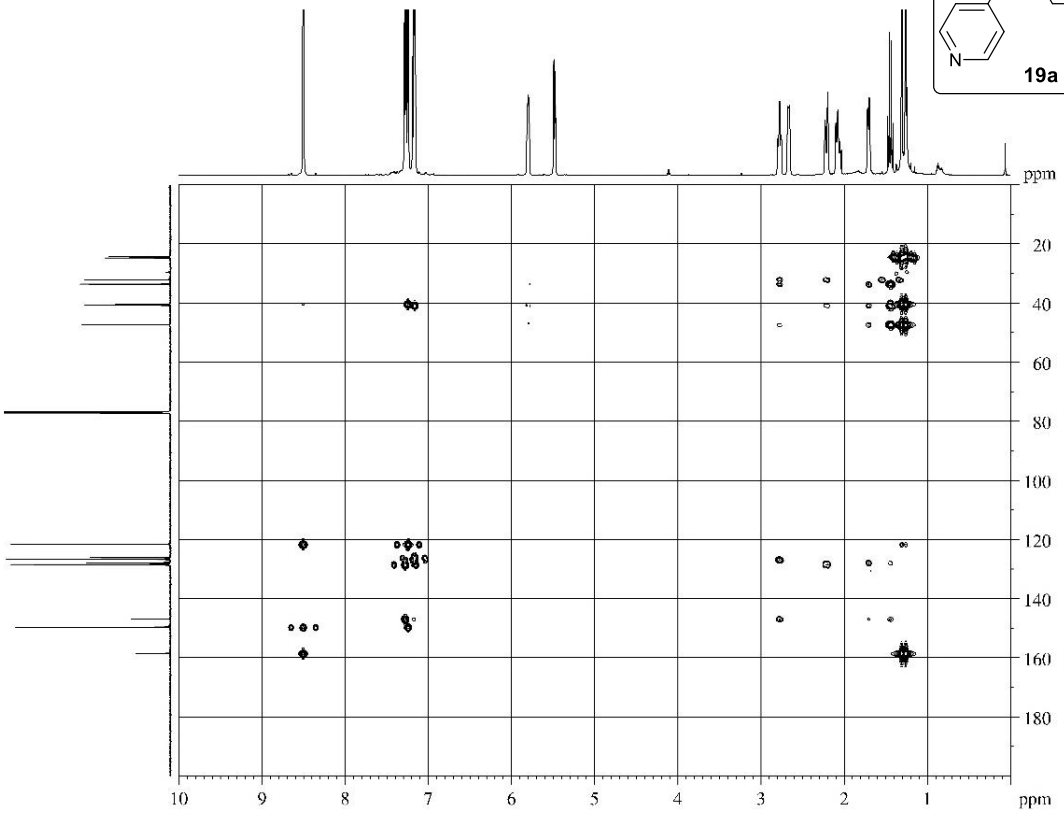

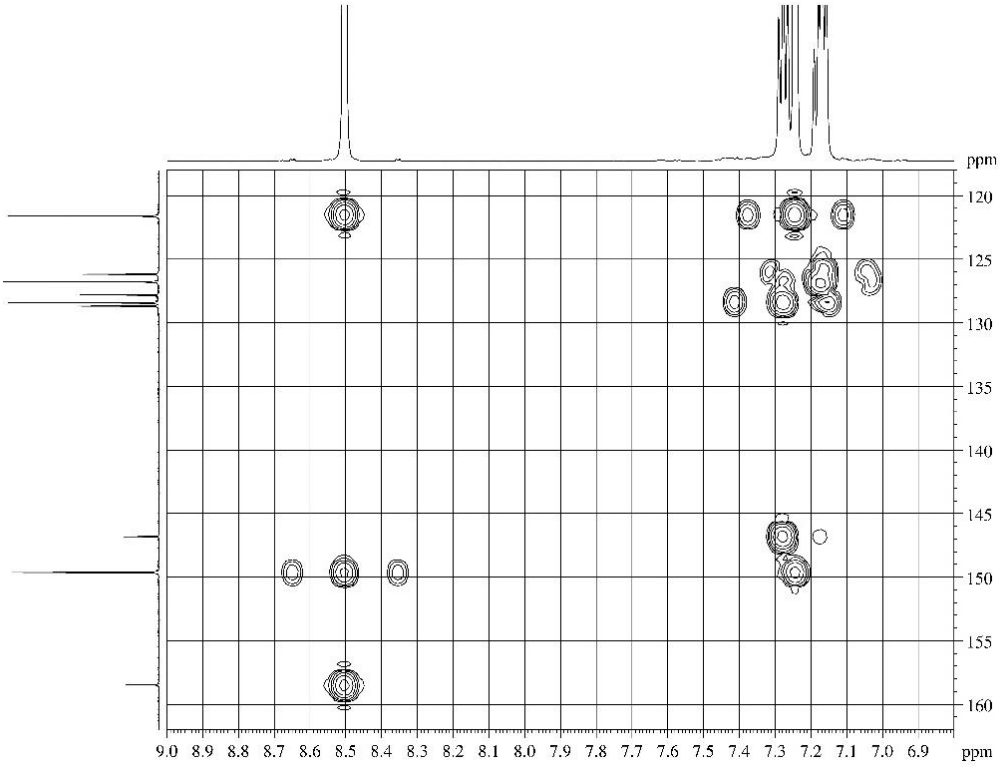

2D-HMBC (600 MHz, $CDCl_3$) – NMR spectra of **19a**

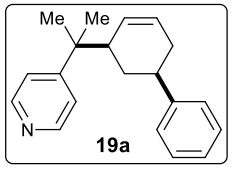

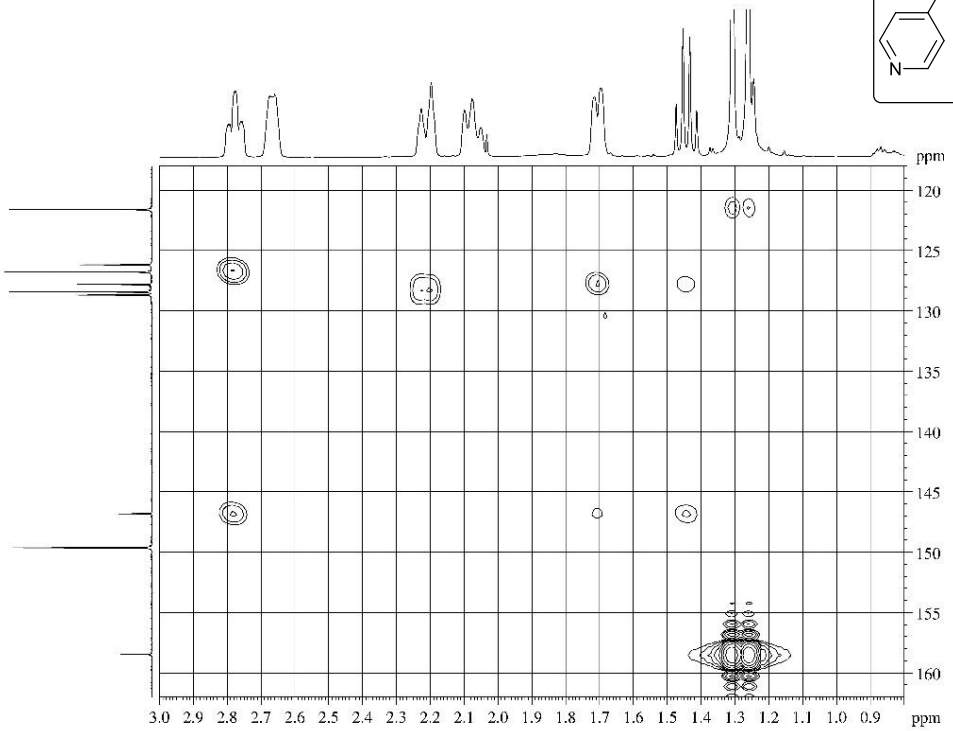

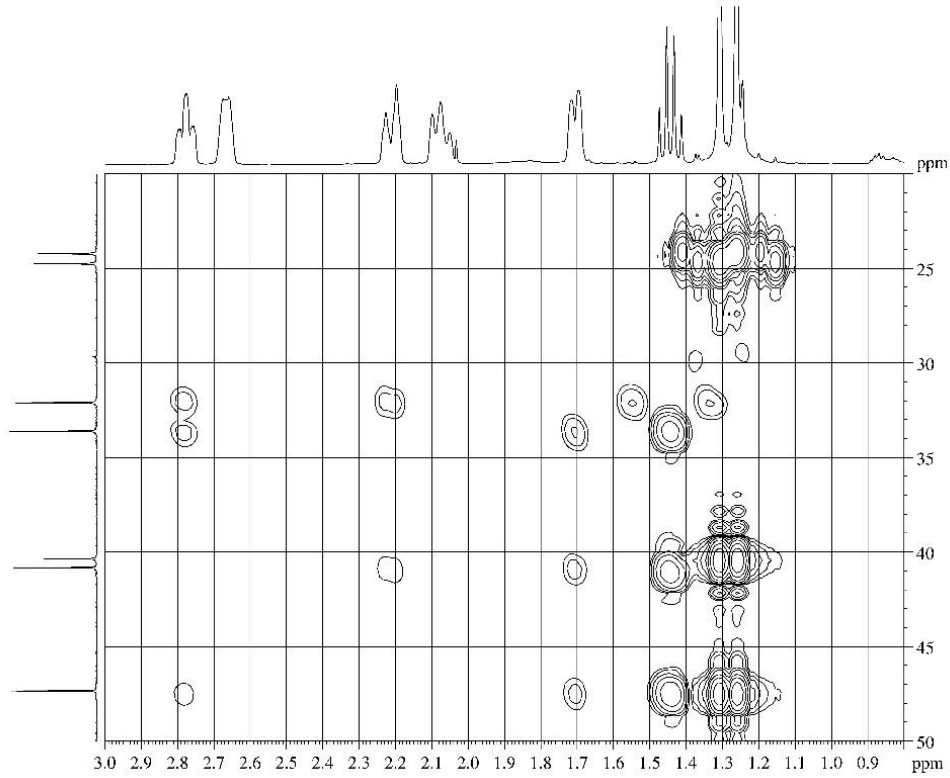

2D-NOESY (600 MHz, $CDCl_3$) – NMR spectra of **19a**

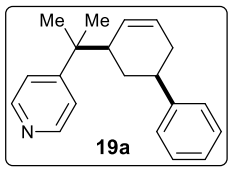

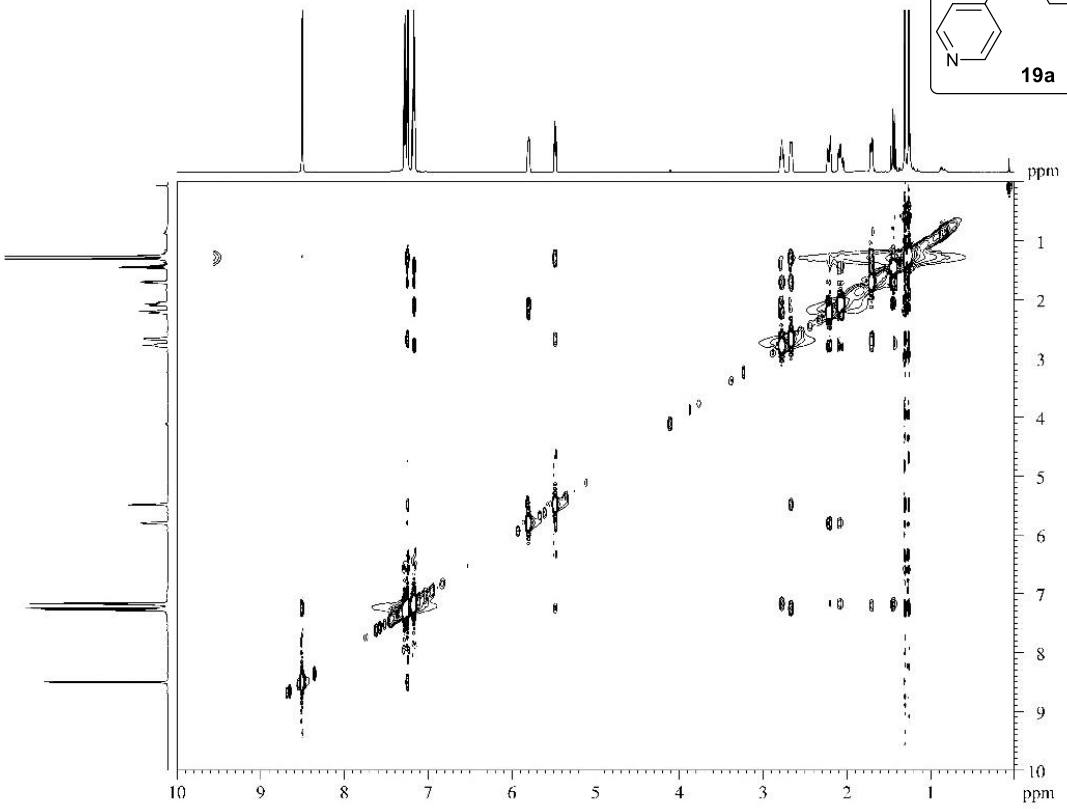

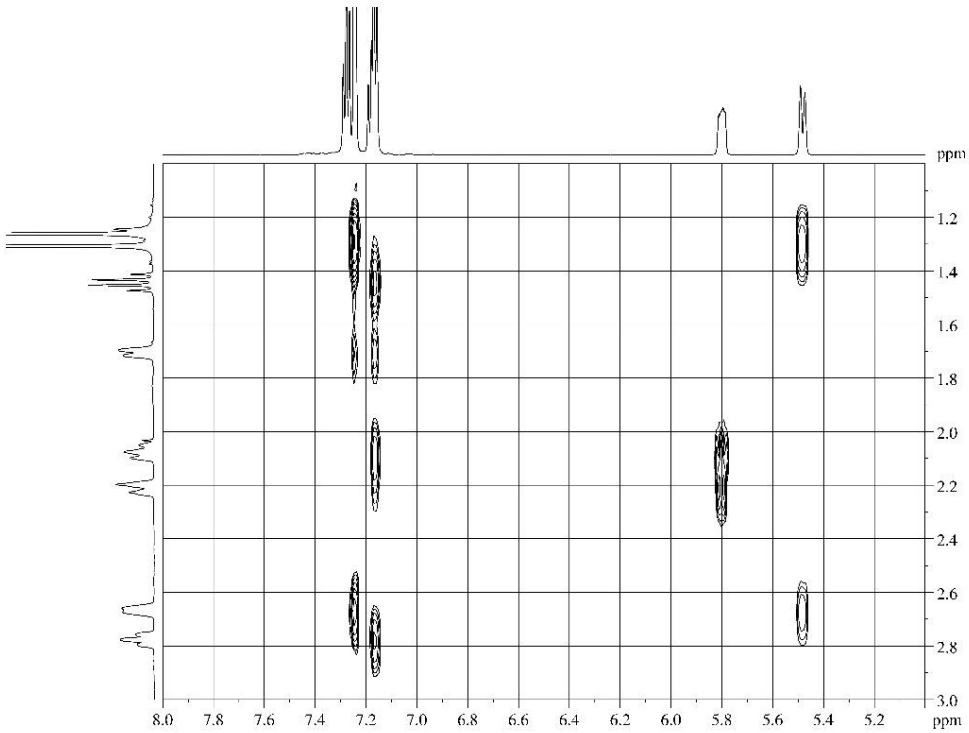

2D-NOESY (600 MHz, $CDCl_3$) – NMR spectra of **19a**

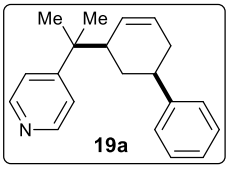

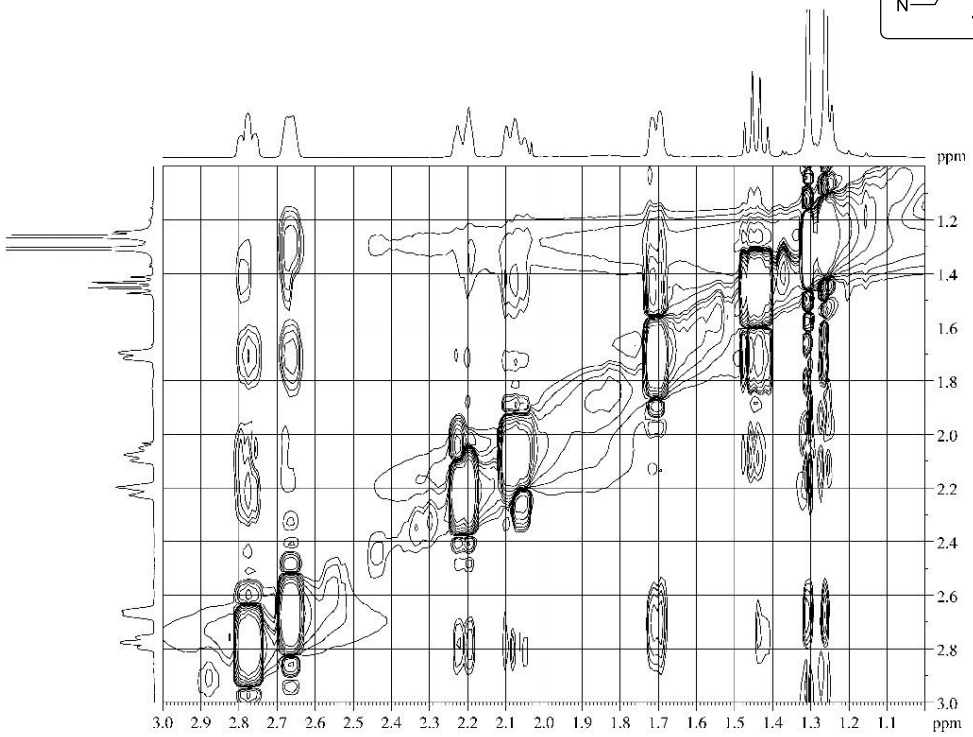

^{1}H (400 MHz, $CDCl_3$) and ^{13}C (101 MHz, $CDCl_3$) – NMR spectra of **C1**

[XantphosPd(η3-allyl)]OTf
C1

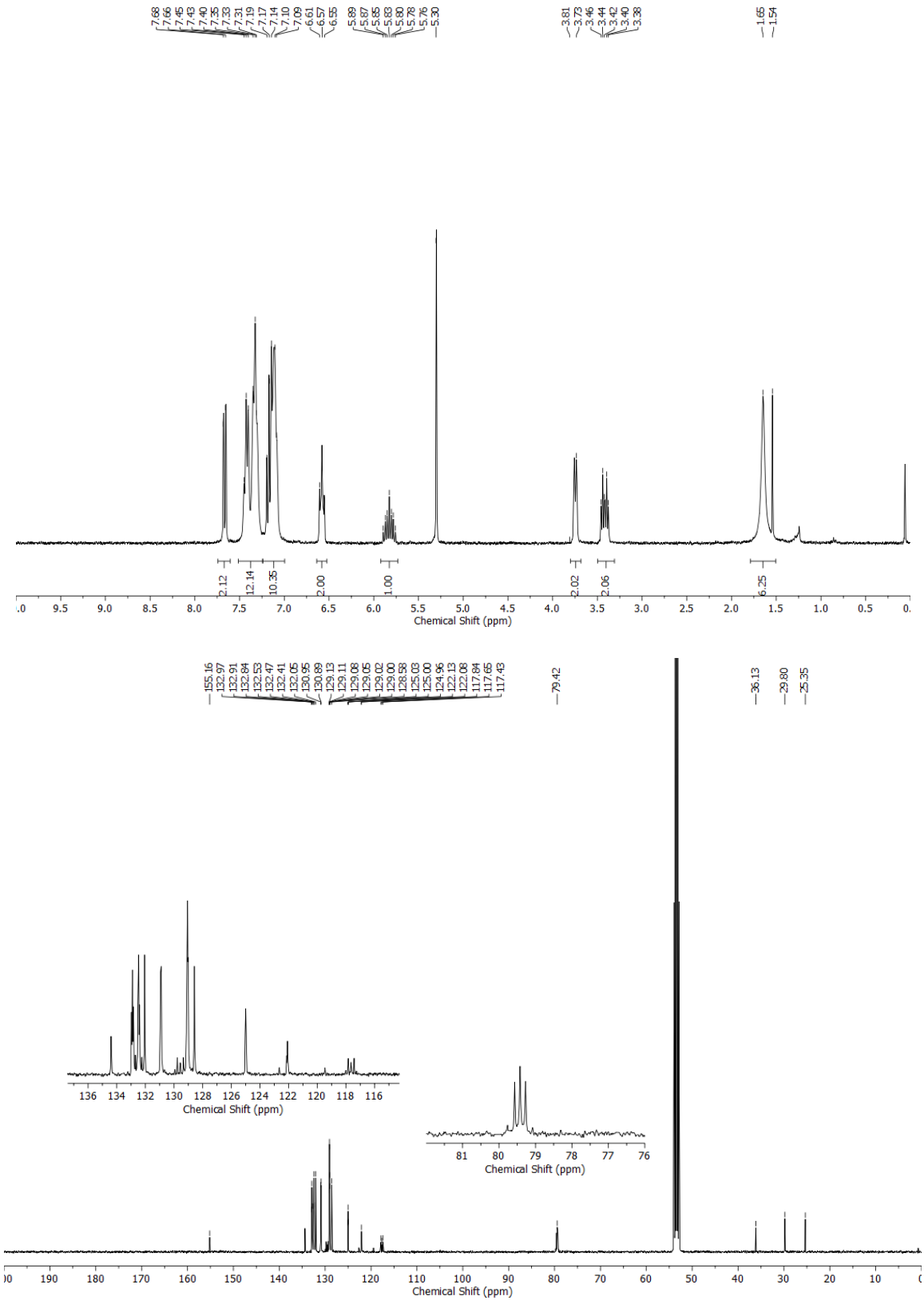

^{31}P (121 MHz, CD_2Cl_2) – NMR spectra of **C1**

[XantphosPd(η3-allyl)]OTf
C1